VOLUME 41 / NUMBER 1 / 1999

Radiocarbon

An International Journal of Cosmogenic Isotope Research

rtment of Geosciences
University of Arizona
East Ft. Lowell Road
on, Arizona 85712-1201 USA

ISSN: 0033-8222

RADIOCARBON
An International Journal of Cosmogenic Isotope Research

Editor: AUSTIN LONG
Consulting Editor: A J T JULL
Managing Editor Emerita: RENEE S KRA
Managing Editor: DAVID R SEWELL
Assistant Editor: KIMBERLEY TANNER ELLIOTT
Published by
Department of Geosciences
The University of Arizona

Published three times a year at The University of Arizona, Tucson, AZ 85712-1201 USA.

Subscription rate (1999): $120.00 (for institutions), $65.00 (for individuals). Foreign postage is extra. A complete price list, including Proceedings of International Conferences, special publications and back issues, appears on the inside back cover of this issue.

Missing issues will be replaced without charge only if claim is made within three months (six months for India, New Zealand and Australia) after the publication date. Claims for missing issues will not be honored if non-delivery results from failure by the subscriber to notify the Journal of an address change.

Authors: See our "Information for Authors" document at `http://www.radiocarbon.org/Authors/` for guidelines concerning manuscript submission and format. All correspondence and manuscripts should be addressed to the Managing Editor, *RADIOCARBON*, Department of Geosciences, The University of Arizona, 4717 East Ft. Lowell Road, Tucson, AZ 85712-1201 USA. Tel.: +1 520 881-0857; Fax: +1 520 881-0554; Internet: `editor@radiocarbon.org`

List of laboratories. Our comprehensive list of laboratories is published annually, and is also available on the WWW at `http://www.radiocarbon.org/Info/lablist.html`. We ask all laboratory directors to provide their laboratory code designation, as well as current telephone and fax numbers, and e-mail addresses. Changes in names or addresses, additions or deletions should be reported to the Managing Editor. Conventional and AMS laboratories are now arranged in alphabetical order by country and we include laboratories listed by code designation.

RADIOCARBON on the World Wide Web: `http://www.radiocarbon.org/`

RADIOCARBON is indexed and/or abstracted by the following sources: *Anthropological Index; Anthropological Literature; Art and Archaeology Technical Abstracts; Bibliography and Index of Geology* (GeoRef); *British Archaeological Bibliography; Chemical Abstracts; Chemistry Citation Index; Current Advances in Ecological and Environmental Sciences; Current Contents* (ISI); FRANCIS (Institut de l'Information Scientifique et Technique – CNRS); *Geographical Abstracts; Geological Abstracts; Oceanographic Literature Review; Science Citation Index; Social Sciences Citation Index.*

Vol 41, Nr 1 **Radiocarbon** 1999

CONTENTS

RADIOCARBON wishes to acknowledge the generosity of John Southon of the Lawrence Livermore Laboratory, California, in making a personal donation to help subsidize the printing of this issue.

FROM THE MANAGING EDITOR

Attentive readers of *RADIOCARBON* will notice some differences in the format of this issue. Beginning with Volume 41, we have decided to base our journal style on the current edition of the CBE Manual (CBE 1994) issued by the Council of Biology Editors.

In so doing, we hope to make life a bit simpler for authors, readers, and editors alike. Mastering intricate and idiosyncratic "instructions for authors" documents that differ widely from journal to journal must rank close behind writing grant applications as a bane of the scientist's existence. (And when authors simply ignore the instructions and use whatever conventions they are most familiar with, they become a bane of the editor's existence.) Although no general-purpose publication manual will cover every single requirement of a specialized journal like *RADIOCARBON,* we hope to collaborate in standardizing scientific communication where we can. In the words of the CBE Manual:

> Many minor differences in style among scientific disciplines seem pointless. The scientific world needs to take more steps toward a uniform and complete international system of scientific nomenclature and symbols.

We chose the CBE Manual for several reasons. First, because *RADIOCARBON* is an interdisciplinary journal, we wanted a guidebook that would represent the shared practices of the scientific community rather than of a single field. The CBE Manual originated in 1960 as a style guide for journals in life sciences and medicine, but the 6th edition aims to cover all disciplines in experimental and observational science. (To whatever extent that it retains its roots in biosciences, it occupies a safe neutral ground between our 2 major groups of contributors, archaeologists and physical scientists.) Second, the CBE Manual anchors its recommendations in internationally adopted standards documents wherever possible, and synthesizes usages from the entire English-speaking scientific world. Finally, the CBE Manual is issued by a major university press with worldwide distribution, and is readily available through local libraries and bookstores or Internet vendors.

Our new "Information for Authors" document is published on our website at the following URL:

`http://www.radiocarbon.org/Authors/`

In addition to presenting the new style guidelines and special conventions for reporting ^{14}C dates and formatting date lists, it outlines the scope of the journal and our publication process in general. It will be updated and extended from time to time as necessary. We welcome feedback on the document to help us keep it as useful as possible to our readers and contributors.

David R Sewell

REFERENCE

[CBE] Council of Biology Editors, Style Manual Committee. 1994. *Scientific style and format: the CBE manual for authors, editors, and publishers.* 6th ed. Cambridge: Cambridge University Press. 825 p.

RADIOCARBON Vol 41, Nr 1, 1999, p 1–8

A SIMPLE METHOD TO SEPARATE POLLEN FOR AMS RADIOCARBON DATING AND ITS APPLICATION TO LACUSTRINE AND MARINE SEDIMENTS

Scott A Mensing

Department of Geography, University of Nevada, Reno, Nevada 89507 USA

John R Southon

Center for Accelerator Mass Spectrometry, Lawrence Livermore National Laboratory, Livermore, California 94551 USA

ABSTRACT. We present a simple method for manually separating pollen concentrates for radiocarbon accelerator mass spectrometry (AMS) dating using a mouth pipetting system. The required equipment is readily available from scientific equipment supply houses at minimal cost. Pollen samples from lake sediments required about 4 h of hand picking, whereas samples from marine sediments required about 8 h labor. Pollen dates from marine sediments were much older than expected. We are attempting to resolve whether this is due to contamination of the pollen or the presence of significant quantities of old reworked pollen. Pollen dates from lake sediments associated with Mazama Ash were consistent with other published ages; however, replicate dates on pollen samples from above the ash were consistently older than the surrounding sediment. Our results suggest that caution must be used when interpreting pollen dates if the potential for sediment reworking is present.

INTRODUCTION

The ability to obtain reliable radiocarbon dates from pollen using accelerator mass spectrometry (AMS) is well established (Brown et al. 1989, 1992). A number of methods have been developed to concentrate pollen samples for AMS ^{14}C analysis. In the first published work on the topic, Brown et al. (1989) obtained pollen concentrates from lake sediments using a variation of the standard palynological pretreatment of samples (Faegri and Iversen 1975) followed by repeated bleaching and sieving. Brown et al. (1989) dated bulk sediments and pollen concentrates from samples associated with previously dated horizons, including the Mazama Ash. Pollen dates were younger than bulk sediment dates, but were consistent with the range of commonly cited dates for the Mazama Ash. In a later paper, Brown et al. (1992) tested a set of modified preparation procedures on 6 samples from peat deposits associated with the Mazama Ash. The procedures were sufficient to remove nearly all non-pollen materials and the dates again were consistent with other published dates for the Mazama Ash.

Efforts to concentrate pure pollen samples from sites in other regions have generally found that the procedures developed by Brown et al. (1989) did not remove sufficient organic materials to produce a datable sample (Long et al. 1992; Regnell 1992). New methods have been developed to improve the removal of chemically resistant organic matter from peats (Richardson and Hall 1994) and hard-water lakes (Long et al. 1992; Regnell 1992). These methods include the use of strong acids such as H_2SO_4 (Regnell 1992), microbiological degradation (Richardson and Hall 1994), centrifugation (Regnell and Everitt 1996), and manual separation with a micromanipulator (Long et al. 1992). Although each of these new procedures has resulted in some improvements, they typically required purchase of expensive specialized equipment and materials (Long et al. 1992; Regnell and Everitt 1996), or were not able to completely remove contaminants (Regnell 1992; Richardson and Hall 1994).

We have developed a simple, inexpensive method for manually separating pollen from detrital material for AMS dating. We have tested our procedures on lake sediments associated with Mazama Ash from the Sierra Nevada, California, and on varved marine sediments of known age from the Santa Barbara Basin, California.

METHODS

Lake sediment samples used in this study were from a 2-cm Livingstone core recovered from Lake Moran, California, USA (38°23′00″N, 120°07′45″W, elev. 2006 m), by Roger Byrne and Eric Edlund, University of California, Berkeley. The lake lies in a granitic basin dammed by a terminal moraine on the western slope of the Sierra Nevada. Mazama Ash is present as a 3-cm thick layer at a depth of 229–232 cm and has been identified as the Tsoyawata Ash bed (Llao Rock event) that was a precursor to the climactic Mazama eruption (Byrne, personal communication). At Osgood Swamp (38°50′45″N, 120°02′30″W), about 50 km northeast of Lake Moran near the crest of the Sierra Nevada, tephra was also identified as the Tsoyawata Ash (Davis 1978; Bacon 1983; Hallett et al. 1997). In this region, the climactic Mazama Ash bed has been found only at sites east of the Sierra Nevada (Davis 1978). The climactic Mazama Ash and the Tsoyawata Ash have been found together at several localities in the Lahontan Basin (Davis 1978) and in Mono Lake (Davis forthcoming).

One-cm thick samples were obtained from immediately above and below the ash. The annual pollen accumulation rate for Lake Moran exceeds 50,000 grains cm^{-2} yr^{-1}, with pine representing 50% of the pollen sum; consequently only a small sample (3–5 g wet weight) was processed.

Marine sediments were obtained from box cores recovered from the Santa Barbara Basin, California, USA (34°15′N, 119°52′W), by Tim Baumgartner, Scripps Institute for Oceanography. Anoxic conditions in the basin support virtually no benthic life and support the preservation of annually laminated varves. Varve thickness averages 2.0 mm per pair of laminae (Hulsemann and Emery 1961), or 5 yr per centimeter, a rapid sedimentation rate that allows for high-resolution sampling. The annual nature of the Santa Barbara sediments has been confirmed by ^{14}C age determination (Emery 1960), ^{210}Pb measurements (Koide, Soutar and Goldberg 1972; Krishnaswami et al. 1973; Bruland 1974), correlation with precipitation records and tree-ring indices (Soutar and Crill 1977), and through correlation with fluctuations in microfossil assemblages associated with strong El Niño events (Schimmelmann et al. 1990). Average annual pollen accumulation rate in the Santa Barbara Basin is only 3500 grains cm^{-2} yr^{-1}, (Mensing 1993), and pine represents only 10% of the pollen sum; therefore, relatively large samples (45–65 g wet weight) were required for processing. Three consecutive 5-yr sediment samples from 1963–1977 and 4 additional 10–30-yr samples from 1860–1950 were treated for pollen extraction.

Pollen extraction generally followed Brown et al. (1989). Carbonates were removed with 10% HCl. Sediments were then boiled in KOH for 20 min to remove humic acids. Silicates were digested with 49% HF in a hot bath for a minimum of 1 h, followed by 10% HCl in a boiling bath for 10 min. Following treatment with 2%–3% NaOCl, samples were sieved with 38 μm and 74 μm mesh to concentrate pine pollen, the largest common pollen type in our study areas. The >74 μm and <38 μm fractions were decanted into vials for dating. Visual analysis of both size fractions revealed that they contained primarily non-pollen material. The 38–74 μm fraction was then treated with NaOCl twice more, followed by sieving after each treatment. The 2nd and 3rd bleach/sieve treatments eliminated significant amounts of amorphous organic material while preserving most of the pollen. Experiments with more than 3 sieving treatments showed that the additional sieving removed only marginal amounts of detrital material. However, the treated extract still contained a significant quantity of non-pollen material that needed removal prior to dating.

Pollen separation used a simple manually operated mouth pipetting system (Fig. 1). Components include a polystyrene mouthpiece, latex tubing (ca. 5 mm o.d., 3 mm i.d.), a disposable universal pipette tip, and a 9-inch borosilicate glass Pasteur pipette. The materials are very inexpensive and are readily available from any scientific equipment supplier. Tubing was cut to a comfortable work-

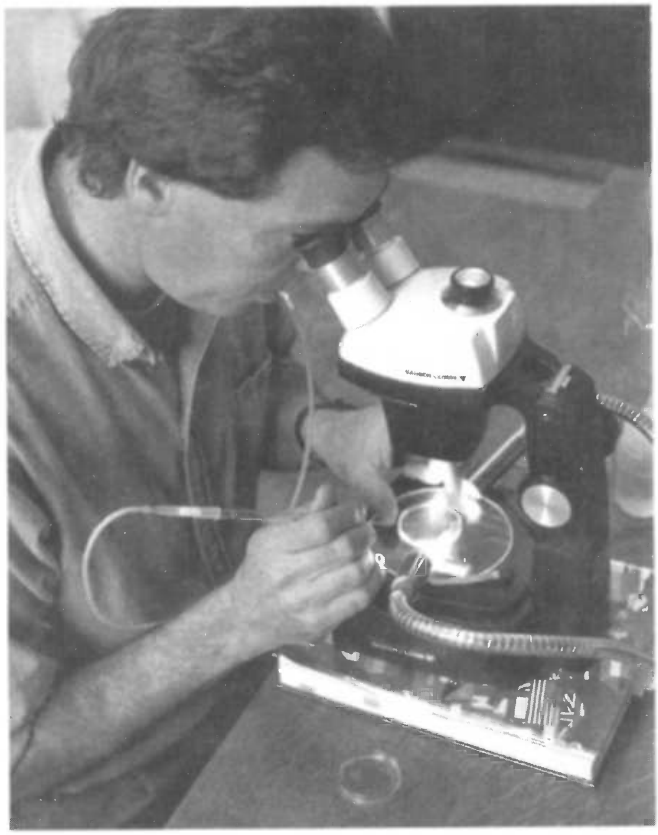

Figure 1 Photograph of the mouth pipetting apparatus in operation

ing length (ca. 60 cm) with one end fitted to the mouthpiece and the other end placed on the taper of the disposable pipette tip. A small swab of cotton was placed inside the disposable pipette tip to absorb moisture. The Pasteur pipette was prepared by heating over a flame and drawing out to an approximately 100-µm orifice. This was then inserted into the large opening of the plastic disposable pipette.

A small (ca. 0.1 mL) sample of pollen concentrate was ejected into a petri dish and flooded with deionized water to disperse the material. Pollen and other organic material quickly settled to the bottom. Pollen in the 38–74 µm fraction was easily identified for picking using a zoom binocular microscope in the range of 30–45× magnification under a fiber optic light source. The bleached pollen shows up clearly against a dark background. Pollen was aspirated into the Pasteur pipette. The small pipette orifice draws in the material through capillary action, and with gentle, periodic suction on the mouth pipette, one can rapidly vacuum pollen grains. This can be controlled to the extent that one can easily pick up a grain of pollen without also drawing in detritus that lies immediately adjacent. At this low magnification, we never found it difficult to hold the apparatus steady and guide the orifice to individual pollen grains. Generally 100–200 grains were collected in the pipette before ejecting the pollen directly into a vial for storage.

Samples were pipetted from the vials directly into quartz combustion tubes, and dried in a vacuum centrifuge. An excess of CuO oxidizer was added together with several mg of Ag powder, the tubes were flame-sealed under vacuum, and samples were combusted at 900 °C. The resulting CO_2 ali-

quots (typically 25–70 μg of carbon) were cryogenically purified and then converted to graphite by a hydrogen reduction with an Fe or Co catalyst, and ^{14}C was measured by AMS. Ultra-small samples such as these are sensitive not only to contamination of the samples by trace quantities of contemporary carbon (most likely adsorbed CO_2), but also to contamination by "dead" carbon and/or to fractionation effects (Brown and Southon 1997; Kirner et al. 1997; van der Borg et al. 1997; Pearson et al. 1998). Numerous small aliquots of ^{14}C-free coal and a Modern ^{14}C standard (HOxI) were used as process blanks to monitor the combustion and graphitization process, and results from these test samples were used to correct the measured pollen data (Donahue et al. 1990; Brown and Southon 1997). Dates were calculated according to Stuiver and Polach (1977).

RESULTS AND DISCUSSION

Brown et al. (1989) suggested that only 200–500 spruce pollen grains should be sufficient to obtain an AMS date. We found that due to the smaller size of pine pollen compared with spruce, and the difficulty in graphitizing very small samples, a sample of about 10,000 grains (ca. 70 μg of carbon) was necessary for reliable AMS dating. Manual picking of pollen grains averaged 1000–2500 grains per hour depending on the sample material. Separating a 10,000-grain sample from Lake Moran required only 4 h labor, whereas the Santa Barbara Basin material averaged 8 h per sample because pollen was less abundant and chemically resistant organic material in the 38–74 μm fraction was more abundant. However, even for pollen-poor sites, isolation of a sufficient quantity of nearly pure pollen for AMS dating required only one day of additional labor after the chemical extraction procedures. For all samples, manual separation of pollen produced a nearly pure concentrate (Fig. 2).

The Lake Moran pollen sample from below the ash (LM 232-233) produced a date of 6880 ± 175 BP (Table 1). The LM 232-233 38–74 μm fraction received the same preparation treatment, except that pollen was not separated from the non-pollen matrix. This sample produced an identical date. The LM 232-233 >74 μm fraction, which contained no pollen but did include some charcoal, produced a date of 7000 ± 60 BP, which is not inconsistent with the other 2 dates. The 38–74 μm and >74 μm fractions from above the ash (LM 228-229) give nearly identical dates, both younger than published Mazama Ash dates. However, pollen sample LM 228-229, from above the ash, returned a date of 7120 ± 150 BP, our oldest Lake Moran date. Another pollen sample was picked from the same preparation and the date on this sample (7040 ± 80 BP) confirmed the earlier results.

Unlike the climactic Mazama Ash, the Tsoyawata Ash has few published dates and no AMS dates. Bulk sediment from below the ash at Osgood Swamp in California dated 6990 ± 300 BP (Haynes et al. 1967). Carbonized twig fragments from the upper 1 cm of a soil directly below the ash at a site near Crater Lake, Oregon, produced a date of 7015 ± 45 BP. At Wildcat Lake, Washington State, Blinman, Mehringer and Sheppard (1979) found both ashes and obtained a date of 6940 ± 120 BP on bulk sediment below the lower ash and a date of 6750 ± 90 BP on bulk sediment between the 2 ashes. They used a complex process derived from upper core pollen accumulation rates to calculate the time between the 2 ash falls to be approximately 140 yr. Other authors have suggested that a period of <200 yr separates the 2 ash falls (Bacon 1983; Young 1989).

Many efforts have been made to accurately date the climactic Mazama event (see Hallett et al. 1997 for a recent review). New AMS dates on charcoal and twig fragments from Mazama air-fall deposits suggest a weighted mean age of 6730 ± 40 BP (Hallett et al. 1997). Adding the estimated time between the 2 ashes to this date gives an approximate age of 6870–6930 ± 40 BP for the Tsoyawata event. Each of our pollen dates falls within this range of potential dates; however, the pollen dates from above the ash are older than the sedimentary matrix of the same strata. Previous studies have

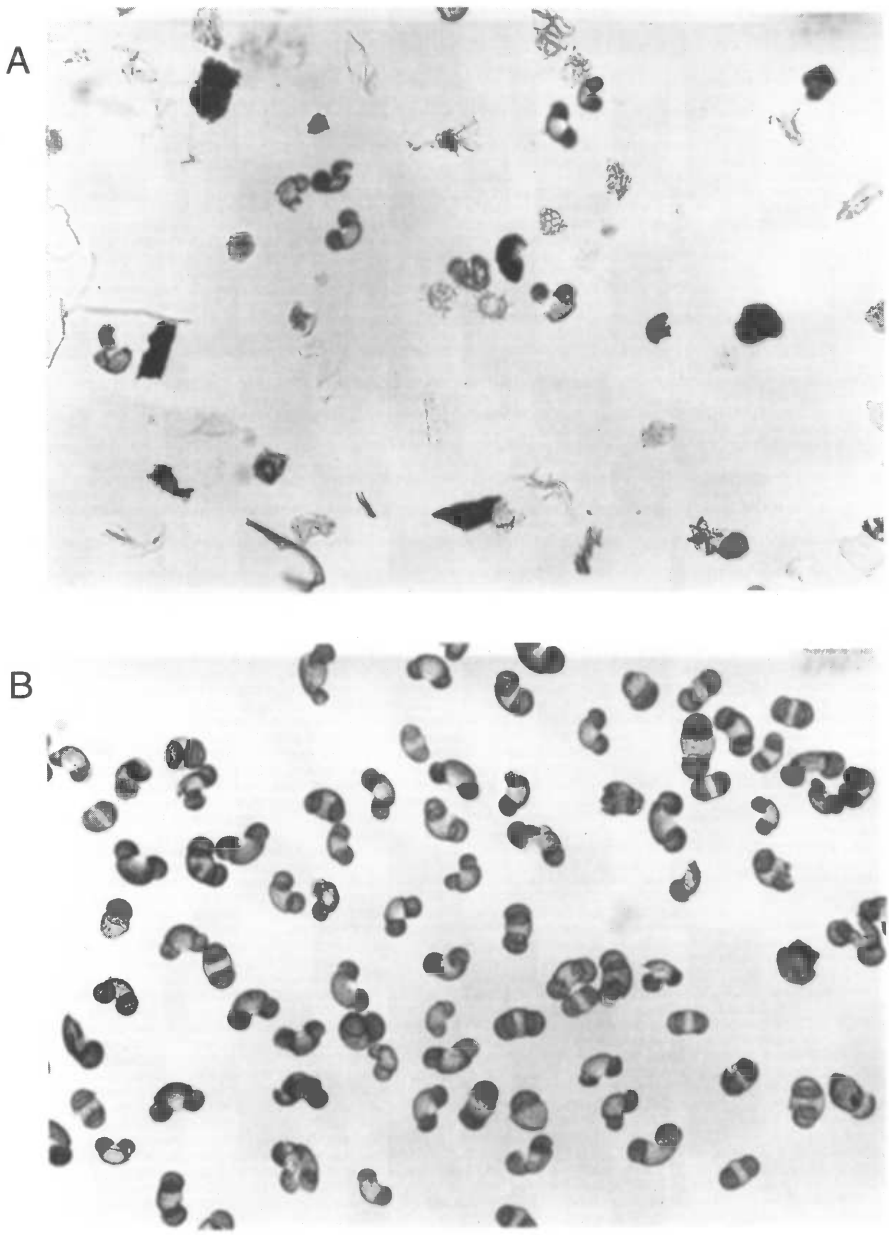

Figure 2 Photomicrographs showing samples before and after manual purification of the 38–74 μm fraction. 2A. Before separating pollen; note the presence of organic matter, unknown algal bodies and charcoal fragments. 2B. Pure concentrate remaining after separation of pine pollen.

consistently found pollen dates to be younger than the surrounding sediment, suggesting that the pollen represented a more accurate chronological indicator than the bulk sediment (Long et al. 1992; Regnell 1992). Although in general we would agree with this reasoning, our results suggest that the presence of reworked pollen in a sample could potentially provide a date older than sediment from the same strata. Mazama Ash may have altered soil infiltration rates, channeling runoff and leading

to localized downcutting. Palynological evidence for this period shows high percentages of oak pollen, suggesting conditions drier than today, and possibly lowered lake levels. As lake levels fluctuate, pollen eroded from near-shore sediments can be redeposited in the central basin. This is more likely to occur at times of rapid climate change, precisely the periods for which paleoecologists desire accurate dates.

For the Santa Barbara Basin samples, the exact calendar age for each sample was known from varve counts (Tim Baumgartner, personal communication 1993). We dated pollen from strata prior to and associated with the ^{14}C spike caused by nuclear testing in the 1950s and 1960s. The 3 pollen samples between 1963 and 1977 dated above modern as expected (Table 1), whereas the fraction modern averages 67% of the atmospheric value for this period, suggesting either that as much as 33% of the material is intrusive dead carbon, or that a large fraction of pre-bomb pollen is in the sample. Dates for the 4 pollen samples prior to the bomb peak were much older than expected, which suggests that any intrusive component must be quite old. We can suggest 2 possible reasons for these results; the pollen could be contaminated with residual old carbon, or a large contribution of old reworked pollen is in the sample. Similar arguments may also apply to charcoal in the Santa Barbara Basin since our 2 charcoal samples gave comparable or older dates than pollen. We are currently attempting to resolve this question, since it may have important implications for interpretation of pollen diagrams from the Santa Barbara Basin.

The <38 μm fractions produced very old dates. This is not simply due to the presence of marine organics, because the reservoir age for the Santa Barbara Basin is only 825 yr (Ingram and Kennett 1995). These ages could be due to the presence of petroleum seeps or black carbon (Masiello and

Table 1 Dates obtained for samples from Lake Moran (LM) and the Santa Barbara Basin (SBB). All dates were determined at the Lawrence Livermore National Laboratory Center for Accelerator Mass Spectrometry (CAMS). Lake Moran samples are depth in cm down the core and Santa Barbara Basin samples represent calendar years AD.

CAMS #	Location	Sample	Material	^{14}C age (BP)	Fraction modern
42474	LM	228–229	Pollen	7120 ± 150	
46338	LM	228–229	Pollen	7040 ± 80	
29051	LM	228–229	38–74 μm bulk fraction	6620 ± 60	
29052	LM	228–229	>74 μm bulk fraction	6650 ± 50	
29053	LM	232–233	Pollen	6880 ± 170	
29054	LM	232–233	38–74 μm bulk fraction	6880 ± 60	
29055	LM	232–233	>74 μm bulk fraction	7000 ± 60	
26573	SBB	1963–1967	Pollen	>Modern	1.1998
26574	SBB	1968–1972	Pollen	>Modern	1.1453
26575	SBB	1973–1977	Pollen	>Modern	1.0725
26580	SBB	1963–1967	<38 μm bulk fraction	4450 ± 60	
26579	SBB	1968–1972	<38 μm bulk fraction	7400 ± 60	
26578	SBB	1973–1977	<38 μm bulk fraction	4760 ± 50	
39879	SBB	1860–1890	Pollen	1080 ± 140	
39880	SBB	1890–1920	Pollen	1210 ± 140	
39881	SBB	1920–1950	Pollen	860 ± 140	
39882	SBB	1933–1942	Pollen	1760 ± 240	
26577	SBB	1963–1967	Charcoal	>Modern	1.0793
26576	SBB	1968–1972	Charcoal	1060 ± 100	

Druffel 1998). However, neither of these explanations seems reasonable for explaining the old pollen dates given the chemical treatment and appearance of the pollen.

CONCLUSION

We have developed a simple and inexpensive method for separating pure pollen samples for AMS ^{14}C dating. The equipment and method require virtually no investment. The only expensive equipment necessary, a binocular microscope capable of about 35× magnification, is commonly present in most pollen labs. We have demonstrated that samples sufficiently large for AMS dating (50–100 μg) can be efficiently extracted even from pollen-poor sediments. We are continuing to test samples from the Santa Barbara Basin to better understand dating pollen from the marine environment. The pollen dates from Lake Moran are consistent with other published dates for the Tsoyawata/Mazama Ash; however, our results raise the possibility that pollen present in sediments above the ash may include some percentage of old pollen that has been reworked and redeposited. Our results suggest that bulk sediment dates for a particular stratum do not necessarily indicate when the pollen was deposited; direct dating of pollen provides a more accurate date.

ACKNOWLEDGMENTS

We thank Roger Byrne of the University of California, Berkeley, for assistance in developing our methodology and discussion of results, Tim Baumgartner of Scripps Institute for Oceanography for supplying sediment samples from the Santa Barbara Basin, and Eric Edlund for supplying sediment from Lake Moran. Michaele Kashgarian of the Center for Accelerator Mass Spectrometry, LLNL, provided assistance with the analysis, Lara Rozzell provided photomicrography and helped in pollen separation and Marie Allen and Jeremy Smith also assisted in pollen separation. Bob Karlin of the University of Nevada, Reno, provided laboratory facilities during the initial phase of the research. This research was supported by a grant from the Center for Accelerator Mass Spectrometry, Lawrence Livermore National Laboratory. This work was supported by the NOAA Paleoclimatology program (NA36GP0418) and by DOE (W-7405-Eng-48).

REFERENCES

Bacon CR. 1983. Eruptive history of Mount Mazama and Crater Lake Caldera, Cascade Range, USA. *Journal of Volcanology and Geothermal Research* 18:57–115.

Blinman E, Mehringer PJ Jr, Sheppard JC. 1979. Pollen influx and the deposition of Mazama and Glacier Peak tephra. In: Sheets PD, Grayson DK, editors. *Volcanic activity and human ecology*. New York: Academic Press. p 393–425.

Brown TA, Farwell GW, Grootes PM, Schmidt FH. 1992. Radiocarbon dating of pollen extracted from peat samples. *Radiocarbon* 34(3):550–6.

Brown TA, Nelson DE, Mathewes RW, Vogel JS, Southon JR. 1989. Radiocarbon dating of pollen by accelerator mass spectrometry. *Quaternary Research* 32: 205–12.

Brown TA, Southon JR. 1997. Corrections for contamination background in AMS ^{14}C measurements. *Nuclear Instruments and Methods in Physics Research* B123:208–13.

Bruland KW. 1974. Pb-210 geochronology in the coastal environment. [PhD dissertation]. San Diego: University of California.

Davis JO. 1978. Quaternary tephrochronology of the Lake Lahontan area, Nevada and California. Nevada Archeological Survey, Research Paper Number 7. Reno (NV): 137 p.

Davis OK. Pollen analysis of a Holocene late-glacial sediment core from Mono Lake, Mono County, CA. *Quaternary Research*. Forthcoming.

Donahue DJ, Linick TW, Jull AJT 1990 Isotope-ratio and background corrections for accelerator mass spectrometry radiocarbon measurements. *Radiocarbon* 32(2):135–42.

Emery KO. 1960. *The sea off southern California, a modern habitat of petroleum*. New York: John Wiley & Sons. 366 p.

Faegri K, Iversen J. 1989. *Textbook of pollen analysis*. 4th ed. Chichester: John Wiley & Sons. 328 p.

Hallet DJ, Hills LV, Clague JJ. 1997. New accelerator mass spectrometry radiocarbon ages for the Mazama tephra layer from Kootenay National Park, British Columbia, Canada. *Canadian Journal of Earth Science*

34:1202–9.

Haynes CV Jr, Grey DC, Damon PE, Bennett R. 1967. Arizona radiocarbon dates VII. *Radiocarbon* 9:1–14.

Hulsemann J, Emery KO. 1961. Stratification in recent sediments of Santa Barbara Basin as controlled by organisms and water character. *Journal of Geology* 69: 229–90.

Ingram BL, Kennet JP. 1995. Radiocarbon chronology and planktonic-benthic foraminiferal ^{14}C age differences in Santa Barbara Basin sediments, Hole 893A. In: Kennett JP, Baldwin JO, Lyle M, editors. *Proceedings of the ocean drilling program scientific results* 146: 19–27.

Kirner DL, Burky R, Taylor RE, Southon JR. 1997. Radiocarbon dating organic residues at the microgram level. *Nuclear Instruments and Methods in Physics Research* B123:214–7.

Koide MA, Soutar A, Goldberg ED. 1972. Marine geochronology with Pb-210. *Earth and Planetary Science Letters* 14:442–6.

Krishnaswami S, Lal D, Amin BS, Soutar, A. 1973. Geochronological studies in Santa Barbara Basin. *Limnology and Oceanography* 18:763–70.

Long A, Davis OK, DeLanois J. 1992. Separation and ^{14}C dating of pure pollen from lake sediments: nanofossil AMS dating. *Radiocarbon* 34(3):557–60.

Masiello CA, Druffel ERM. 1998. Black carbon in deep-sea sediments. *Science* 280:1911–3.

Mensing SA. 1993. The impact of European settlement on oak woodlands and fire: pollen and charcoal evidence from the Transverse Ranges, California. [PhD dissertation]. Berkeley: University of California. 216 p.

Pearson A, McNichol AP, Schneider R J, Van Reden KF. 1998. Microscale AMS ^{14}C measurements at NOSAMS. *Radiocarbon* 40(1): 61–75.

Regnell J. 1992. Preparing pollen concentrates for AMS dating: a methodological study from a hard-water lake in southern Sweden. *Boreas* 21:373–7.

Regnell J, Everitt E. 1996. Preparative centrifugation: a new method for preparing concentrates suitable for radiocarbon dating by AMS. *Vegetation History and Archaeobotany* 5:201–5.

Richardson F, Hall, VA. 1994. Pollen concentrate from highly organic Holocene peat and lake deposits for AMS dating. *Radiocarbon* 36(3):407–12.

Schimmelmann A, Lange CB and Berger WH. 1990. Climatically controlled marker layers in Santa Barbara Basin sediments, and fine-scale core-to-core correlation. *Limnology and Oceanography* 35:165–73.

Soutar A, Crill PA. 1977. Sedimentation and climatic patterns in the Santa Barbara Basin during the 19th and 20th centuries. *Geological Society of America Bulletin* 88:1161–72.

Stuiver M, Polach HA. 1977. Discussion: reporting of ^{14}C data. *Radiocarbon* 19(3):355–63.

van der Borg K, Alderliesten C, de Jong AFM, van den Brink A, de Hass AP, Kersemaekers HJH, Raaymakers, JEMJ. 1997. Precision and mass fractionation in ^{14}C analysis by AMS. *Nuclear Instruments and Methods in Physics Research* B123:97–101.

Young SR. 1989. Holocene eruptions at Mount Mazama, Oregon: characteristics and distribution of plinian airfall deposits. *Continental Magmatism Abstracts.* New Mexico Bureau of Mines and Mineral Resources, Bulletin 131. Socorro: 302 p.

RADIOCARBON, Vol 41, Nr 1, 1999, p 9–15

A 23-YEAR RETROSPECTIVE BLIND CHECK OF ACCURACY OF THE COPENHAGEN RADIOCARBON DATING SYSTEM

Kaare L Rasmussen[1] • Henrik Tauber[1] • Niels Bonde[2] • Kjeld Christensen[2] • Páll Theodórsson[3]

ABSTRACT. A 23-yr record of the measuring accuracy of the Copenhagen radiocarbon dating laboratory has retrospectively been provided through a true blind test. A total of 92 samples of oak from old tree trunks were dated in the period 1971 to 1993 and their dendrochronological age determined independently. The ^{14}C activity of the dendrochronological samples measured in the Copenhagen radiocarbon laboratory was compared to the activity of the tree rings of the same age measured by Stuiver and Pearson (1993) for calibration purposes. The average difference was found to be 54 ± 72 ^{14}C yr. The results further indicate that the actual standard deviation is only 7% higher than that quoted by the laboratory. The investigation has shown a long-term stability of laboratory accuracy with no systematic laboratory variations either with respect to sample age or to the time of measurement from 1971 to 1993.

INTRODUCTION

Quality assurance is vital for a sustained confidence in radiocarbon dates. This was clearly displayed by the results of the International Collective Study conducted by ^{14}C-dating laboratories, which demonstrated the importance of a constant attention to factors influencing the general accuracy of ^{14}C measurements and to the danger of laboratory bias (Long 1990; Scott et al. 1998). Quality control is the responsibility of the individual ^{14}C laboratory, which should engage in a formal quality program in order to dispel the doubts and distrust that are sometimes voiced against the method, for example by Pilcher (1993), who somewhat belligerently concluded that ^{14}C dates should rather be considered as "reasonable estimates of the nearest half millennium in which the sample falls". The present investigation shows that ordinary laboratory ^{14}C dating, if properly performed and controlled, can be much better than that.

One means of quality control in the ^{14}C laboratory is measuring samples that can later be dated by independent methods. This was realized already by Tauber (1977), when the first 12 samples of oak (*Quercus* sp.) were dated in the Copenhagen ^{14}C laboratory. Altogether, 92 such samples have been dated here in order to facilitate the building of a Danish dendrochronological master chronology. When found, oak samples judged suitable for contributing to the master chronology were sent to the laboratory in order to provide an approximate age for the dendrochronologists. Once the specimen was dendrochronologically dated and the dendrochronological series had been firmly connected to the present, an absolute age could be assigned to the ^{14}C-dated sample. The absolute age was thus unknown to the ^{14}C laboratory at the time of dating, and the final dendrochronological age provided a check on the overall precision of the laboratory.

The standard deviation of a ^{14}C age is estimated from the counting statistics of the sample, the background, and the modern sample; together, these are called the combined counting statistics. This figure does not, however, include all types of variability introduced in the various steps of the dating process, according to the proposed quality assurance protocol for ^{14}C-dating laboratories (Long 1990).

A comparison between the abovementioned ^{14}C ages and the corresponding dendrochronological ages provides a good measure of the total analytical precision of a ^{14}C dating laboratory, and the

[1]Carbon-14 Dating Laboratory, National Museum and Geological Survey of Denmark, Ny Vestergade 11, DK-1471 Copenhagen K, Denmark
[2]Environmental Archaeology and Archaeometry, National Museum, Ny Vestergade 11, DK-1471 Copenhagen, Denmark
[3]Science Institute, University of Iceland, Dunhaga 3, IS-107 Reykjavík, Iceland

fairly regularly performed datings of such samples thus give a reasonable estimate of the total analytical precision of the Copenhagen radiocarbon laboratory for the last 23 yr. No oak sample that has been dated by both the ^{14}C method and by dendrochronology in Copenhagen has been left out of the present study.

THE ^{14}C METHOD

The Copenhagen ^{14}C laboratory utilizes a 2.0 L conventional gas-proportional counter now equipped with a gas-proportional guard counter. Until 1991, however, the guard system consisted of 17 Geiger counters in an overlapping half-circle geometry. The change from 180° Geiger counters to a 360° proportional counter took place in January 1991. Prior to moving the laboratory in 1989, the background count rate in the Copenhagen ^{14}C laboratory was ca. 3.1 cpm; after the counting equipment was moved to a new location in a smaller and less massive building, the background count rate with the Geiger counters went up to ca. 3.7 cpm. Installing the 360° gas proportional guard counter resulted in a background count rate of ca. 3.1 cpm. Thus the background count rate is presently, and has for the bulk of the time been, ca. 3.1 cpm.

The activity of 0.95 times that of HOxI, corrected for background has been approximately 17 cpm in this system.

Wood samples are normally subjected to the standard A-A-A treatment prior to analysis in our laboratory. Slight modifications to the procedure are used for more decomposed samples, very few of which are in the present data set. The samples are burned to CO_2 in 6 atmospheres of pure oxygen in a Phonon bomb (manufactured by BJ Precision Engineering Co., Norfolk, England). The water is separated, and the sample is dissolved in NH_4OH and later precipitated with $CaCl_2$ and washed on a filter with hot water to remove soluble carbonates and excess of hydroxide. The carbonate is kept precipitated in water in sealed flasks for at least 3 weeks in order to let the bulk of possible ^{222}Rn decay (ca. 6 half-lives). The samples are then converted to CO_2 again and admitted to our preparation line. Here they are purified in an oven with CaO prepared from pure Icelandic double spar. Memory effects are avoided by baking the CaO-oven for several hours at elevated temperatures between each purification. After purification, the sample is transferred to the counter.

A total of about 1.5 g of carbon is counted. The counting pressures of samples, blanks, and oxalic acids are always kept between 1098 and 1102 mm Hg, and monitored and corrected to within an accuracy of ±0.1 mm Hg. Before and after the counting of each sample, a sealed ^{60}Co source with a known activity is introduced at a fixed position near the counter and the count rate measured for 5 min at an interval of 50 V. This gives both the plateau and the proper working voltage. A precalculated count rate from the ^{60}Co source is selected 500 V below the plateau, where the count rate versus high tension curve is most sensitive. The working voltage is then set to this value plus 500 V and adjusted to within ±5 V. Any contamination of the sample from electronegative gases (e.g., H_2O, O_2, SO_2 or NO) is detected here and if a sample is contaminated, it is taken back in the preparation line for further purification. The samples are counted for at least 20 h in the 2.0 L 1100 mm Hg conventional proportional counter. The air pressure, temperature and humidity are measured throughout the operation, and small corrections due to variations in these values are applied to the date. After amplification, discrimination and pulse-shaping, the pulses from both the central counter and the guard counter are registered on a data acquisition board in a computer. The total number of anticoincidence, coincidence and total guard counter counts is stored each hour. At the end of the measurement these totals are plotted, and visual inspection performed to verify that no systematic errors have occurred, in other words, that the variations in counting rate are in agreement with the expected

statistical bounds. Prior to the installation of data collection hardware, control was ensured by taking frequent readings during working hours.

Blanks are prepared from large single crystals of Icelandic double spar, which are etched in HCl to 80% of their initial weight in order to remove any surface contamination. Blanks are measured for 1 day every second week, and so are the NIST oxalic acid samples (HOxI, 1950). Our HOxI samples are prepared in strict accordance with the recommendations in Valastro et al. (1977), and $\delta^{13}C$ values of the oxalic acid samples over the 3 years 1992–1993 average to $-19.9 \pm 0.5‰$ VPDB, which is very close to what is expected (−19.1‰) according to Valastro et al. (1977). We still use oxalic acid from the original NBS 5-pound jar.

Stable isotope values ($\delta^{13}C$) have been measured on all samples dated from 1975 onwards. The accuracy of the mass spectroscopic measurements is now better than ±0.03‰ VPDB, and has in the past probably been better than 0.1‰ VPDB. Dates are corrected to $\delta^{13}C = -25‰$ VPDB. Dates produced prior to 1975, when stable isotope fractionation was not measured, are assigned an extra uncertainty, and the uncertainties on these samples were never quoted as less than ±100 yr. The average $\delta^{13}C$ of the oak samples turns out to be $-24.9 \pm 1.0‰$ VPDB, which is also in full agreement with what is expected from rather well-preserved wood samples. Once in the preparation line the dendrochronological samples, the oxalic acid samples and the blank samples are treated identically. The same 2 laboratory assistants prepared all samples included in the present study.

Calibration of conventional ages is performed with the University of Washington program CALIB version 3.0.3C using the 20-yr averaged atmospheric curve, and we have used intervals of calibrated ages at $\pm 1\sigma$ calculated by method A (Stuiver and Reimer 1993; Stuiver and Pearson 1993; Pearson and Stuiver 1993).

THE DENDROCHRONOLOGICAL METHOD

The dendrochronological dates are based on the assumption that trees that grew under the same environmental conditions over the same period of time contain similar tree-ring width patterns.

A master chronology for oak (*Quercus* sp.) has been established in Denmark for dating purposes back to around 100 BC (Bonde et al. 1994). For the older periods 2 Danish chronologies relevant to the present study were dated absolutely by comparison with German master chronologies, the Danish chronologies covering the periods 2955–2483 BC and 2069–401 BC (Christensen 1997). All samples are measured with a binocular microscope at magnifications of 10–40×. The tree-ring series are measured twice, preferably on different radii. The measured tree-ring width patterns are plotted for visual inspection and an average of the 2 curves is used for dating. The tree-ring patterns are compared to the established tree-ring chronology using various standard computer programs such as CROSS (Baillie and Pilcher 1973), CATRAS (Aniol 1983), and DENDRO (Tyers 1997). The samples submitted for ^{14}C dating usually consisted of 20–30 tree rings.

The reported dendrochronological dates in this paper are the dates of the middle tree ring submitted for ^{14}C dating. The curvature of the tree rings in the wood samples will lead to a slight overweighting of material from juvenile rings. With the typical sizes of oak trees in question and typical distances from the center of the tree, this error will normally be < 1 yr.

RESULTS AND DISCUSSION

Because of irregular wiggles in the calibration curves, there is no simple, unique way of comparing the calibrated ^{14}C dates with the corresponding dendrochronological midpoint dates.

One way to get an approximate measure of the difference between the 2 data sets is to compare the dendrochronological midpoint ages with ages of the midpoints of the ± 1σ intervals of the calibrated ^{14}C dates. Calculated this way, the average difference between the 2 data sets is 52 ± 85 calendar years, the ^{14}C ages being younger than the dendrochronological ages. The mean difference of 52 yr is well within the ± 1σ interval. As the ± 1σ intervals for the calibrated ^{14}C dates are often asymmetrically distributed, differences calculated in this way may tend to be slightly exaggerated. Even so, 55% of the 92 dendrochronological midpoint ages lie within the ± 1σ interval of the calibrated ^{14}C age, and 90% within the ± 2σ interval, which is close to the expected values.

Another, more direct, way of establishing the difference between the 2 data sets is to compare uncalibrated ^{14}C ages. With a known dendrochronological age for each sample, the conventional ^{14}C age determined in the Copenhagen laboratory can be directly compared to the conventional ^{14}C age of the dendrochronological sample of the same age measured by Stuiver and Pearson (1993) in the construction of the bidecadal calibration curve. In Figure 1 the conventional ages measured in the Copenhagen laboratory are shown as a function of the corresponding conventional ages measured by Stuiver and Pearson (1993). The line of identical ages is also shown. The agreement is good throughout the entire age span covered by the investigation.

We have calculated the differences by subtracting the Danish dates from the selected calibration curve dates, and calculated the standard deviation of each difference as the square root of the sum of

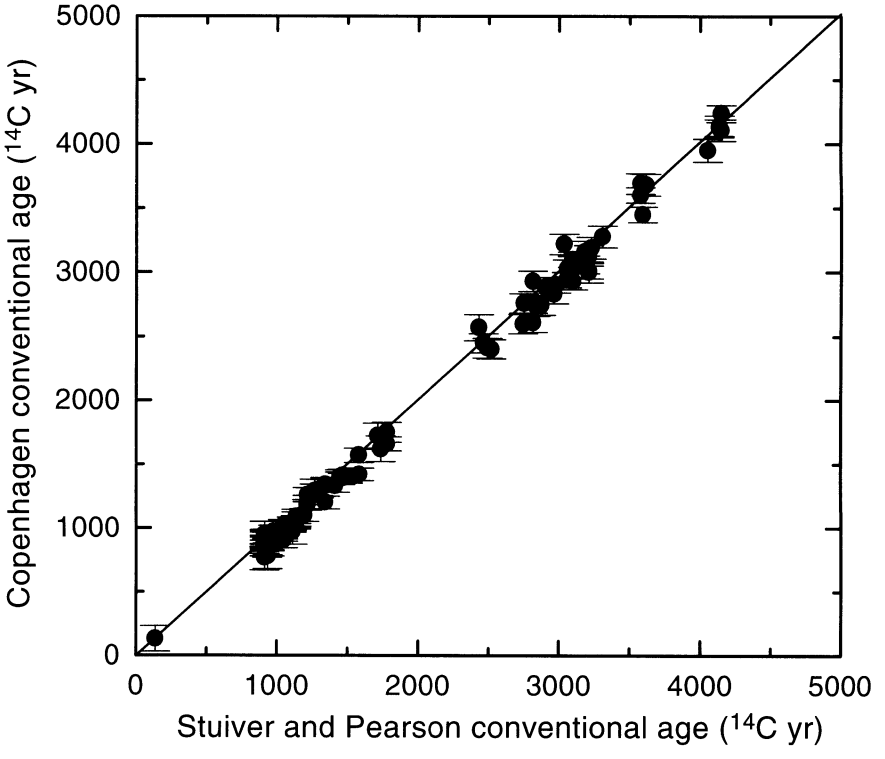

Figure 1 Conventional ^{14}C ages measured in the Copenhagen radiocarbon laboratory as a function of conventional ^{14}C ages of dendrochronologically dated samples of the same age selected from the Stuiver and Pearson (1993) bidecadal calibration curve. The straight line shows identical ages.

squares of the 2 standard deviations. The average standard deviation is ± 12 ^{14}C yr for the calibration curve dates, and ± 67 ^{14}C yr for the Copenhagen dates. The average difference between the 2 data sets is 54 ± 72 ^{14}C yr, the Copenhagen dates being younger than the calibration curve dates. Again the average difference of 54 ^{14}C yr is well within the ± 1σ interval. The distribution of the differences is shown in Figure 2.

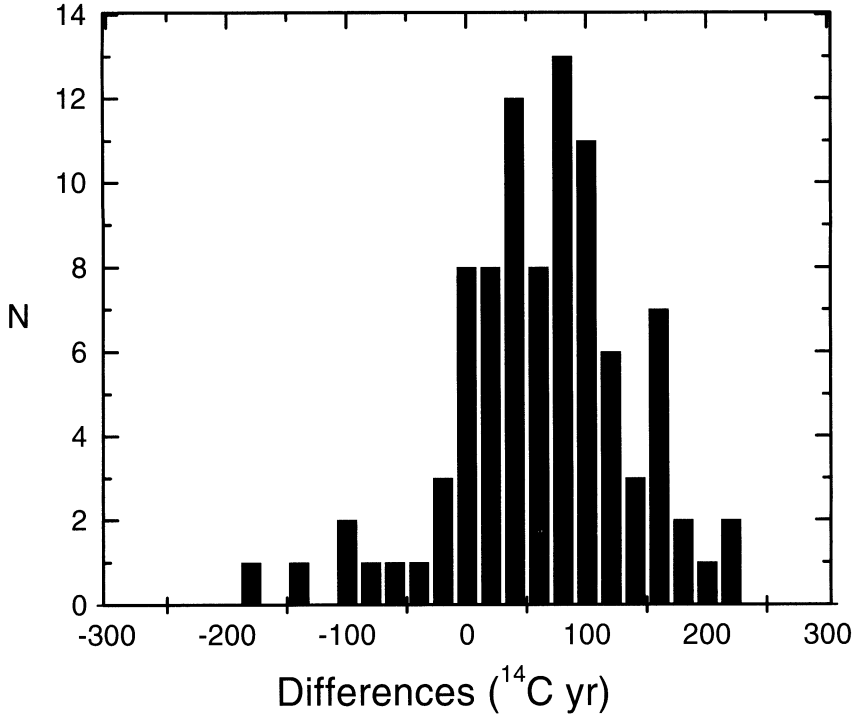

Figure 2 The distribution of the differences between conventional ^{14}C ages of dendrochronologically dated samples selected from the bidecadal calibration curve of Stuiver and Pearson (1993) and conventional ^{14}C ages of samples of the same dendrochronological age measured by the Copenhagen laboratory.

The average standard deviation of the uncalibrated ^{14}C dates measured in Copenhagen of ± 67 ^{14}C yr is very close to the value of ± 72 ^{14}C yr found from the differences. The ratio K of the actual mean standard deviation (72 ^{14}C yr) divided by the quoted mean standard deviation (67 ^{14}C yr) is a convenient measure of the degree to which the quoted standard deviation is representative of the overall uncertainty in a ^{14}C date. From the present study, the K-value of the 92 ^{14}C dates made by the Copenhagen laboratory is found to be 1.07, which means that the quoted standard deviations have, on average, been only 7% too low throughout the period covered by the investigation.

In 1990, an intensified scheme of measuring blanks and oxalic acids was introduced in the laboratory procedure. At about the same time a proportional gas guard counter and computerized data collection were installed. Although based on only 11 samples, the measured differences relative to Stuiver and Pearson (1993) for the following period were only 10 ± 95 ^{14}C yr, which suggests that the possible bias has been considerably reduced or has disappeared following these improvements. As a quality assurance program we will further monitor our system in the future, utilizing dendro-

chronologically dated samples and other samples of known ages, and hope in this way to continue improving its precision.

An important question is whether the differences between uncalibrated ^{14}C ages of corresponding samples measured in the Copenhagen laboratory and by Stuiver and Pearson (1993) show systematic variations with respect to the time at which the ^{14}C dating was performed in the Copenhagen laboratory. In Figure 3 the differences are shown as a function of the time of measurement in the Copenhagen laboratory. Although the dating activity of dendrochronological samples has not been constant throughout the period of analysis, Figure 3 shows no systematic increase or decrease during the 23 yr covered by this investigation. One might speculate whether there are small jumps at around days 1800 and 7000. If the time series is divided up into 3 subseries, from 0–1776, 1813–6807 and 7071–8188, the average differences become 49 ± 76, 62 ± 62 and 9 ± 95 ^{14}C yr. If, however, the lowest point in the first subseries is removed, the average difference here becomes 61 ± 62 ^{14}C yr, or exactly the same as in the second subseries. So we can conclude that there is no significant jump at day 1800. Even if it is not statistically significant, the jump at day 7000 seems more substantial, and as noted above it is probably due to the introduction of the gas guard counter system and the intensified scheme of measuring standards.

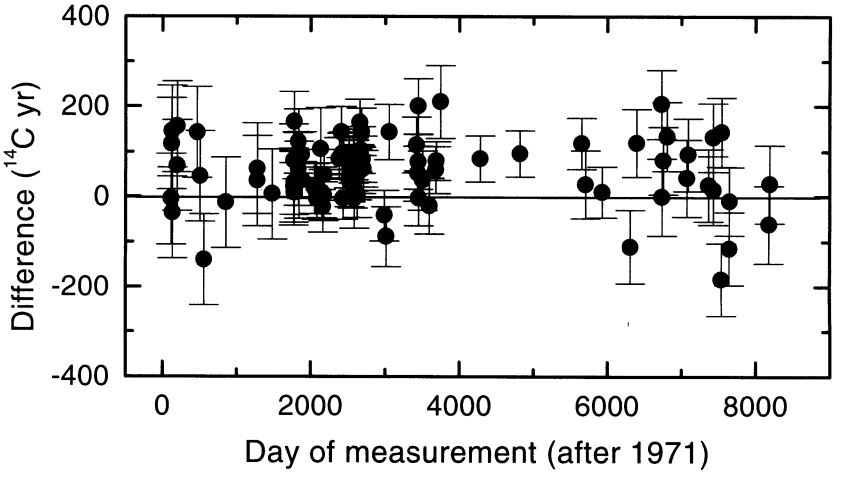

Figure 3 The differences between conventional ^{14}C ages selected from the bidecadal calibration curve of Stuiver and Pearson (1993) and conventional ^{14}C ages of samples of the same dendrochronological age measured in Copenhagen, shown as a function of time of measurement in the Copenhagen laboratory. Combined uncertainties are shown as ±1σ. No systematic variations are discernible with respect to measuring time.

CONCLUSION

Ninety-two oak samples dated in the Copenhagen ^{14}C laboratory have subsequently been dendrochronologically dated. The average difference between the dendrochronological midpoint dates and the mean ages of the ± 1σ intervals of the calibrated ^{14}C dates was 52 ± 85 calendar years. The average difference between the conventional ages measured in Copenhagen and the conventional ages of the dendrochronologically dated samples of the same age measured by Stuiver and Pearson (1993) for their calibration curve was found to be 54 ± 72 ^{14}C yr. Both comparisons show a good agreement, well within ± 1σ, between ^{14}C measurements made in Copenhagen and the Stuiver and Pearson (1993) calibration curve measurements. The standard deviation of 72 yr is very close to the aver-

age standard deviation of the conventional ^{14}C dates of 67 yr, the ratio K being 1.07. No systematic laboratory variations in the ^{14}C dates have been detected, either as a function of sample age or as a function of time of measurement from 1971 to 1993.

It should be stressed that the 92 oak samples dated in the Copenhagen ^{14}C laboratory were not sampled for the purpose of monitoring the accuracy of the laboratory, but were received by the laboratory over the last 23 yr for the specific purpose of establishing a master chronology for oak for the Danish area. So these randomly selected samples are in all respects ordinary samples from different periods treated according to the normal procedures in the laboratory. This demonstrates that good accuracy can be obtained in ^{14}C dating if constant and thorough effort is practiced in the ^{14}C laboratory.

ACKNOWLEDGMENTS

Karen Skov, Birgit Rønne, and Mogens Jacobsen are thanked for technical assistance. Austin Long and David Sewell are thanked for constructive criticism. This work was supported by The Danish National Science Research Council, the Carlsberg Foundation, Statens Museumsnævn, and The National Bank of Denmark.

REFERENCES

Aniol RW. 1983. Tree-ring analysis using CATRAS. *Dendrochronologia* 1: 45–53.

Baillie MGL, Pilcher JR. 1973. A simple crossdating program for tree-ring research. *Tree-Ring Bulletin* 33: 7–14.

Bonde N, Bartholin T, Christensen K, Eriksen OH. 1994. Dendrokronologiske dateringsresultater på Nationalmuseet 1993. *Arkæologiske Udgravninger i Danmark* 1993: 305–21.

Christensen K. 1997. Oak trunks from the Halsskov Fjord. In: Pedersen L, Fischer A, Aaby B, editors. *The Danish Storebælt since the Ice Age: man, sea and forest.* Copenhagen: A/S Storebæltsforbindelsen. 339 p.

Long A. 1990. A quality assurance protocol for radiocarbon laboratories. *Radiocarbon* 32(3):393–7.

Pearson GW, Stuiver M. 1993. High-precision bidecadal calibration of the radiocarbon time scale, 500–2500 BC. *Radiocarbon* 35(1):25–34.

Pilcher JR. 1993. Radiocarbon dating and the palynologist: a realistic approach to precision and accuracy. In: Chambers FM, editor. *Climate change and human impact on the landscape.* Chapter 3. London: Chapman and Hall. p 23–32.

Scott EM, Harkness DD and Cook GT. 1998. Interlaboratory comparisons: lessons learned. *Radiocarbon* 40(1):331–40.

Stuiver M, Pearson GW. 1993. High-precision bidecadal calibration of the radiocarbon time scale, AD 1950–500 BC and 2500–6000 BC. *Radiocarbon* 35(1):1–24.

Stuiver M, Reimer PJ. 1993. Extended ^{14}C data base and revised CALIB 3.0 ^{14}C age calibration program. In: Stuiver M, Long A, Kra RS, editors. Calibration 1993. *Radiocarbon* 35(1):215–30.

Tauber H. 1977. An assessment of the C-14 dating method. The Nordic Conference on thermoluminescence dating and other archaeometric methods. Uppsala University, Sweden, November 1976. Roskilde: Risø National Laboratory. p 5–24.

Tyers IG. 1997. Dendro for windows program guide [computer documentation]. ARCUS Report 340. Department of Archaeology, University of Sheffield.

Valastro S, Land LS, Varela AG. 1977. An improved procedure for wet oxidation of the ^{14}C NBS Oxalic acid and standard. *Radiocarbon* 19(3):375–82.

RADIOCARBON, Vol 41, Nr 1, 1999, p 17–24

THE RELIABILITY OF AMS RADIOCARBON DATING OF SHELLS FROM CHINA

Weijian Zhou[1] • M J Head[1] • Fubao Wang[2] • D J Donahue[3] • A J T Jull[3]

ABSTRACT. We tested the feasibility of dating freshwater and terrestrial molluscs from the semiarid and arid zone in China, since these types of shell material deposit only aragonite to form their shell structure, and shell integrity can be easily observed using X-ray diffraction. We also tested the possibility of estimating microenvironmental changes from shell $\delta^{13}C$ values, but variations within shell populations preclude the use of these values as a reliable indicator. Reservoir ages were calculated for living shells of the same species as fossil shells by using their measured ^{14}C ages, which were recalculated using an average value of atmospheric ^{14}C activity for the years spanning their time of collection as the modern standard. The results indicate that freshwater and terrestrial shells are potentially useful as dating material, provided extreme care is taken in their collection and other datable material (in this case wood and pollen) is within the profile to act as a comparison.

INTRODUCTION

Freshwater and terrestrial mollusc shells are likely to have incorporated older limestone-derived bicarbonate into their shell structures. Shells from estuarine, lacustrine or river systems can either have relatively large apparent ages, or be living in equilibrium with the atmosphere, depending on the source and flow rate of the water (Head 1991; Spennemann and Head 1996). Often, the living environment of these shells may be determined by $\delta^{13}C$ values, though if the source of the water is variable or mixed, these values may provide little information. Land snails ingest calcium carbonate, which is digested to form CO_2 and subsequently incorporated into their shells (Goodfriend 1987).

Freshwater and terrestrial species produce shells consisting of aragonite with a coating of calcite if recrystallization has occurred. The aragonite and calcite can be distinguished visually and separated using a small drill and grinding wheel, or with selective use of a dilute HCl solution. The aragonite can be verified by X-ray diffraction or Fourier transform infrared spectrometry. If postdepositional recrystallization has occurred, calcite is the favored form of the reworked calcium carbonate.

Snail shell fossils are quite common within loess–palaeosol sequences throughout the Loess Plateau in China. Different combinations of species have been found in different layers, reflecting slightly different natural environments. The snails can be regarded as a type of indicator for the paleoenvironments in which the loess–paleosol sequences were formed (Liu et al. 1985). Species reflecting warmer, wetter conditions are predominant in paleosols, but these gradually decrease in number, giving way to drought-enduring and cold-resistant *Cathaica* assemblages in loess. In the paleosol sequences, fossil snail species are similar to the species assemblages currently found. One of the predominant species is *Metodontia* (Liu et al. 1985).

SAMPLE TREATMENT AND METHODS

X-ray diffraction patterns were run on shell samples at both Nanjing Normal University and the University of Arizona in order to determine the presence of calcite in the shell crystalline structure. Calcite would indicate either secondary deposition or recrystallization, since both lacustrine and terrestrial shells are normally composed mainly of aragonite. The shells were cleaned for 30 min with distilled water in an ultrasonic bath, then dried in an oven at approximately 60 °C. The shells were then treated with phosphoric acid for 5–7 min, rinsed with water several times, and dried in an oven again at about 60 °C. Portions of each shell sample were then treated with phosphoric acid in an acid

[1]State Key Laboratory of Loess and Quaternary Geology, Chinese Academy of Sciences, PO Box 17, Xi'an 710054, China
[2]Department of Geo and Ocean Sciences, Nanjing University, 22 Hankou Road, Nanjing 210093, China
[3]NSF AMS Facility, University of Arizona, PO Box 210081, Tucson, Arizona 85721 USA

evolution vessel to produce CO_2, which was reduced to graphite for ^{14}C AMS determinations (Slota et al. 1987). This work was carried out at the NSF AMS Facility at the University of Arizona. A portion of the CO_2 from each sample was taken for $\delta^{13}C$ determinations.

In 1993, live samples were collected from each of the sites involved in this study. The molluscs were boiled in water to facilitate the removal of flesh and outer protein material. They were then oven-dried, treated with hydrogen peroxide to remove the bulk of organic material, rinsed with distilled water and dried again. Further treatment was as described for the fossil samples. X-ray diffraction patterns run on powdered portions of all the modern mollusc samples indicated that these shells consisted of 100% aragonite. Since nuclear explosions have increased the atmospheric ^{14}C concentration above natural levels, we calculated a percent Modern value of 1.1404 ± 0.0072 with respect to the ^{14}C modern standard, and this value was used instead of the normal modern standard to calculate an apparent age for the living shells. These apparent ages were then used to correct the conventional ^{14}C accelerator mass spectrometry (AMS) ages (Stuiver and Polach 1977) obtained for the fossil shell samples.

RESULTS AND DISCUSSION

In the present study we try to estimate the validity of ages obtained from freshwater and terrestrial snail shells in 4 ways: 1) by measuring and correlating the stable carbon isotopic composition of shells formed under different environmental conditions; 2) by measuring the ^{14}C composition of contemporary freshwater and terrestrial shell samples to gain an appreciation of the reservoir effect associated with the specific species of shells studied; 3) by using X-ray diffraction data to differentiate calcite from aragonite; and 4) by comparing ^{14}C ages of shells with those obtained from other datable materials (in this case, wood and pollen) collected from the same stratigraphic horizons. From the ^{14}C measurements of living shells collected in 1993 we calculated a modern standard using Southern Hemisphere monthly atmospheric ^{14}C concentration data for the period 1990–1993 (the average age of most of these shells is about 3 yr) kindly provided by JC Vogel, Quaternary Dating Research Unit, EMATEK-CSIR, Pretoria. Because Northern Hemisphere atmospheric data from the collection area are inadequate, only the Southern Hemisphere data were used. The consequent age differences would be no more than 40 yr, which is quite adequate for this type of study. From the living shell sample collected in 1993, an apparent age of 1260 ± 70 BP was calculated. This apparent age was then subtracted from the measured ^{14}C ages of the shells to give reservoir-corrected ^{14}C ages, which were then assessed as semiquantitative estimates by comparison with other dated material or by stratigraphic correlation.

Freshwater Shells

A series of freshwater mollusc samples (*Radix* spp.) were collected from cores taken from lake sediments in Ang Ren Lake, Tibet (29°25′N, 87°20′E). The sediments cover a range of 464 cm (Fig. 1), with a coarse gravel deposit overlying the top. From 0 cm down to 394 cm are layers of light gray to white diatomites containing shells. From 394 cm to 404 cm is a layer of peaty material containing wood branches. Below this is a layer of light yellow diatomite. X-ray diffraction studies on the mollusc samples indicated that these shells consisted only of aragonite. Table 1 shows $\delta^{13}C$ values and ^{14}C AMS results, together with the calculated reservoir-corrected ages.

To further evaluate the shell chronology, we dated cellulose extracted from wood branches collected at a depth of 398 cm (AA-16360, 9920 ± 80 BP). This age fits well with the onset of warmer conditions after the end of the Younger Dryas cold period. The wood cellulose age is significantly younger than the bottom shell AMS ^{14}C age (AA-16818, 392.6 cm, 10,530 ± 85 BP) by about 610 ^{14}C yr. It is also older than the shell reservoir-corrected age (9270 ± 100 BP) by 650 ^{14}C yr, indicating that the reservoir correction value used for this shell date may not be a true indicator of the

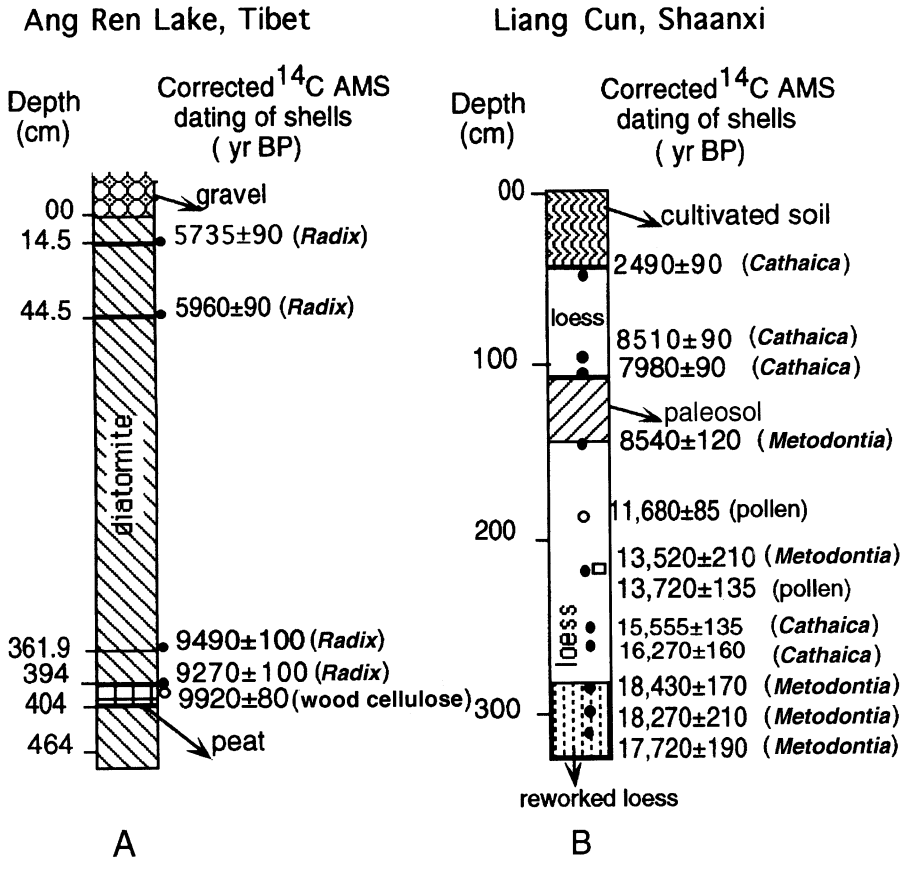

Figure 1 Stratigraphic columns of the selected localities. A. Diatomite profile of Ang Ren Lake, Tibet. B. Loess–paleosol sequence at Liang Cun. The symbols ●, ○, and □ represent shell, wood and pollen samples, respectively, as control points. Shell sample ages have been corrected using the reservoir-corrected modern shell age. The corrected AMS ^{14}C ages on the right side of 1B are considered to be the most reliable ages for the sequence.

Table 1 AMS dating of freshwater shells from Ang Ren Lake, Tibet

Lab code[a]	Depth (cm)	$\delta^{13}C$ (‰)	^{14}C age (yr BP)	Reservoir-corrected age
AA-16852[b]	Live	−1.3	205 ± 50	1260 ± 70
AA-16816	14	−0.5	6995 ± 75	5735 ± 90
AA-16817	43.7	0	7220 ± 70	5960 ± 90
AA-16819	361.4	−4.2	10,750 ± 85	9490 ± 100
AA-16818	392.6	−1.8	10,530 ± 85	9270 ± 100
AA-16360[c]	398	−27.4	9920 ± 80	

[a]AA is the laboratory code of the NSF AMS Facility, University of Arizona.

[b]Indicates the living shell sample collected to calculate a reservoir age to be subtracted from the other shell ages.

[c]Indicates the wood cellulose sample used as a check for the shell ages.

effect associated with this sample. The best explanation for this possible change in reservoir conditions is to postulate a relatively freshwater phase occurring after peat deposition, indicating a relatively gradual (ca. 100 yr) change from warm-wet to cold-wet to cold-dry conditions. A reservoir correction of about 700 ^{14}C yr would be indicated if the wood cellulose age is taken as a marker.

All $\delta^{13}C$ values for the shell samples are similar, except for the shell sample collected at 361.9 cm. The value of –4.2‰ differs significantly from the rest and could indicate continuance of this freshwater phase. However, an older reservoir correction would be more feasible to fit the age of the sample into the stratigraphic sequence. A hypothetical rate of deposition versus age plot was calculated using the wood cellulose age and the top shell reservoir-corrected age at 14 cm (AA-16816, 5735 ± 90 BP). Figure 2 shows the correlation between this plot and the reservoir-corrected ages of the other 2 shells. The only reservoir-corrected shell age that does not fit the sequence is that for sample AA-16818, which we have already associated with a freshwater phase directly above the peat layer.

The gravel layer can be associated with colder, drier conditions associated with periodic flooding. A hypothetical age of about 5500 BP fits in with the concept of cold conditions beginning at about 5500 BP elsewhere. The peat layer can be associated with the onset of warmer, wetter conditions after the Younger Dryas cold period. The wood cellulose age 9920 ± 80 BP fits the concept quite well (Table 1).

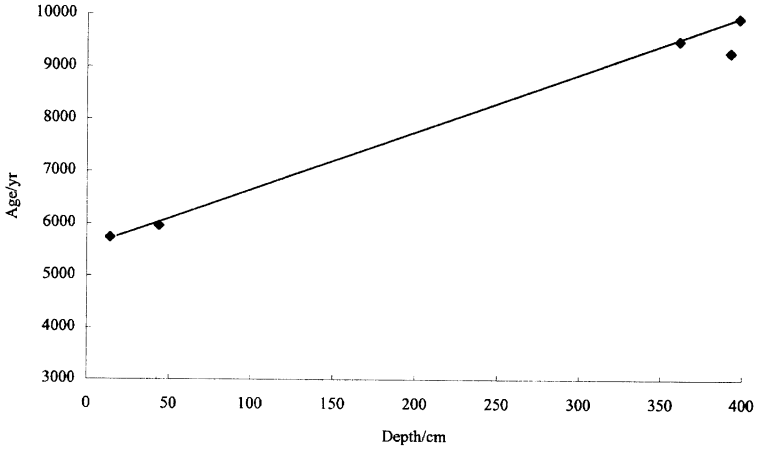

Figure 2 Ang Ren Lake, Tibet. A plot of reservoir-corrected AMS ^{14}C shell ages vs. depth compared with a hypothetical rate of deposition plot using a wood cellulose date from 398 cm and the corrected shell date at 14 cm as control points. We can see that all of the reservoir-corrected shell ages fall along the line except for sample AA-16818. This shows that the reservoir-corrected ages used for this profile are acceptable.

Terrestrial Shells

The Liang Cun loess–paleosol sequence profile is located at the second terrace of the north bank of the Bahe River, 40 km north of Xi'an City (34°28′N, 108°57′E), shown in Figure 1B. The profile is 3.3 m thick and consists of pale yellowish upper Malan Loess, containing snail shells (*Cathaica* sp.) from 330–140 cm below the surface. Evidence of slight reworking at around 185–190 cm and also at 225–230 cm indicates possible weak paleosol formation. A pale grayish-yellow weak pedogenic paleosol extends from 140–102 cm, a pale yellowish loess deposit from 102–49 cm, and cultivated soil between 49 cm and the surface. In the loess sections, the *Cathaica* species of snail shells predominates, while in the weak paleosol sections, the *Metodontia* species is also present (Liu et al. 1985).

Twenty fossil shell and 2 paleosol samples were collected for dating, as well as a living shell sample (*Cathaica*). X-ray diffraction patterns for those shells collected below 140 cm, and $\delta^{13}C$ values for all shell samples were obtained, together with AMS ^{14}C ages. An apparent age for the living shell sample (aragonite) was calculated as 2680 ± 60 BP. This value was subtracted from the AMS shell ages to give reservoir-corrected ages (Table 2). For this feasibility study we have assumed that since both species of snail shell occupy somewhat similar environments, then the apparent age of the shells would also be similar. The $\delta^{13}C$ values form 2 distinct groupings, –2.5 to –3.5‰ (*Metodontia*) and –5.8 to –9.9‰ (*Cathaica*). All samples whose crystal structure was examined using X-ray diffraction, and have $\delta^{13}C$ values between –5.8 and –9.9‰ also have calcite present in their crystal structures, except for the living shell sample. Therefore, the ^{14}C ages for these samples may be considered unreliable, though this may not necessarily be the case.

Table 2 ^{14}C AMS dating of terrestrial shells from the Liang Cun loess–paleosol sequence, Shaanxi Province, China

Lab code	Depth (cm)	$\delta^{13}C$ (‰)	^{14}C age (yr BP)	Reservoir-corrected age
AA-16578[a]	Live	–9.3	1625 ± 50	2680 ± 60
AA-12327	49	–7.2	5170 ± 80	2490 ± 90
AA-12328	62	–8.5	3710 ± 60	1030 ± 70
AA-12329	95	–7.2	11,190 ± 80	8510 ± 90
AA-12330	102	–7.8	10,660 ± 80	7980 ± 90
AA-12331	140	–3.5	11,220 ± 110	8540 ± 120
AA-12332	148	–8.4	10,490 ± 80	7810 ± 90
AA-12333	158	–8.3	8360 ± 70	5680 ± 80
AA-12334	177	–7.3	4770 ± 60	2090 ± 70
AA-12335	186	–7.5	13,680 ± 100	11,000 ± 110
AA-12336	193	–8.7	2710 ± 50	30 ± 60
AA-12337	197	–9.9	12,840 ± 125	10,160 ± 130
AA-12338	218	–5.8	11,880 ± 120	9200 ± 130
AA-12339	226	–2.8	16,200 ± 200	13,520 ± 210
AA-12340	243	–8.2	11,030 ± 90	8350 ± 100
AA-12341	252	–6.0	18,950 ± 150	16,270 ± 160
AA-12342	262	–6.0	18,235 ± 125	15,555 ± 135
AA-12343	267	–6.8	14,480 ± 130	11,800 ± 140
AA-12344	290	–2.8	21,110 ± 160	18,430 ± 170
AA-12345	300	–2.5	21,400 ± 200	18,720 ± 210
AA-12346	310	–3.3	20,400 ± 185	17,720 ± 190
AA-12309[b]	186	–25.8	11,680 ± 85	
AA-12310[b]	226	–26.2	13,725 ± 135	

[a]Indicates the living shell sample collected to calculate a reservoir age to be subtracted from the other shell ages.

[b]Indicates pollen samples separated from paleosol sequences to provide a check for the shell sample.

We concentrated pollen from the paleosol samples collected at 226 and 186 cm depth, and obtained ^{14}C AMS ages of 13,725 BP (AA-12307) and 11,680 BP (AA-12306), respectively. At 226 cm depth, the pollen age agrees quite well with the reservoir-corrected shell aragonite age (*Metodontia*) within one standard deviation, but the reservoir-corrected shell age (*Cathaica*) from 186 cm depth is about 700 yr younger than the pollen age. This shell sample contains some calcite, as indicated in X-ray diffraction patterns, and thus would be considered to give an unreliable age. Zhou et al. (1997)

pointed out that pollen is an ideal material for dating paleosols from the Loess Plateau when it is deposited under a stable environment. Hence, a rough estimate of the deposition rate within the profile could be obtained using these pollen ages. A value of about 62 yr per centimeter was calculated, and from this, a comparison could be made with the reservoir-corrected ages of the shells (Fig. 3). At 49 cm, the reservoir-corrected age of sample AA-12327 (2490 ± 90 BP, *Cathaica*) is about 500 yr younger than the hypothetical age from the linear rate of deposition plot, but this can be considered acceptable. The reservoir-corrected age for sample AA-12328 at 62 cm (1030 ± 70 BP, *Cathaica*) is significantly younger than the hypothetical rate of deposition plot. Since it contains calcite in the shell, this may explain the result, though the sample may also be intrusive.

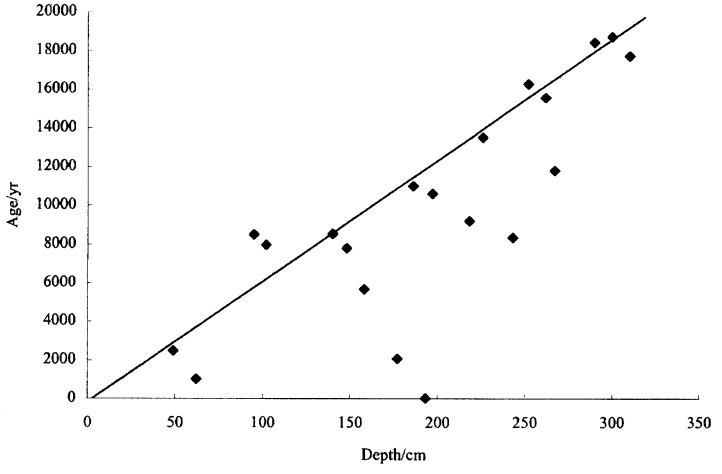

Figure 3 The Liang Cun loess-paleosol sequences. A plot of reservoir-corrected AMS ^{14}C shell ages vs. depth compared with a hypothetical rate of deposition plot using the 2 pollen dates from 186 and 226 cm, respectively. We can see that the majority of the reservoir-corrected shell ages are younger than the rate of deposition plot, but 9 are acceptable. These are indicated in Figure 1B. The majority of the acceptable reservoir-corrected shell ages are from the species *Metodontia.*

An approximate age of 8650 BP was obtained from the linear rate of deposition plot for the bottom of the paleosol at 140 cm, and 6300 BP for the top of the paleosol at 102 cm. Samples AA-12329 (95 cm, 8510 ± 90 BP, *Cathaica*), AA-12330 (102 cm, 7980 ± 90 BP, *Cathaica*) and AA-12331 (140 cm, 8510 ± 120 BP, *Metodontia*), all yield somewhat similar reservoir-corrected ages, giving the impression that some mixing caused by bioturbation may have occurred while the soil was being formed. At 95 cm, the hypothetical age from the deposition rate is approximately 5870 BP. This gives the impression that this paleosol may extend deeper than was previously thought (to 95 cm rather than 102 cm). It is interesting to note that the *Metodontia* species is found at 140 cm, while *Cathaica* species is found at the top of the paleosol, possibly indicating that warmer conditions were in place when the *Metodontia* shells were living, while the *Cathaica* species started populating the soil when the colder climate began to predominate. This possibly means that the onset of warmer conditions at this site predates the *Metodontia* shell age of 8540 ± 120 BP (reservoir corrected).

From 140 to 186 cm, samples AA-12332 (148 cm, 7810 ± 90 BP, *Cathaica*), AA-12333 (158 cm, 5680 ± 80 BP, *Cathaica*), and AA-12334 (177 cm, 2090 ± 70 BP, *Cathaica*) give reservoir-corrected ages that do not fit the hypothetical age from the rate of deposition plot, and are too young for the rest of the sequence. There is a strong possibility that these samples are intrusive. At 186 cm, a

weakly developed paleosol yields a shell reservoir-corrected age of 11,000 ± 110 BP (AA-12335, *Cathaica*), which is significantly younger (680 ^{14}C yr) than the pollen age from this depth, but calcite is in the shells, and recrystallization may explain this age discrepancy.

The samples at 193 cm (AA-12336, 30 ± 60 BP, *Cathaica*), 197 cm (AA-12337, 10,160 ± 130 BP, *Cathaica*), and 218 cm (AA-12338, 9200 ± 130 BP, *Cathaica*), all give reservoir-corrected ages that are far too young, and the samples could be considered to be intrusive to the profile, rather than being affected by recrystallization. At 226 cm, the shell sample AA-12339 gives a reservoir-corrected age (13,520 ± 210 BP, *Metodontia*) that is in close agreement with the pollen age from the same level (AA-12310, 13,725 ± 135 BP). The samples collected from 252 and 262 cm (AA-12341, 16,270 ± 160 BP, *Cathaica* and AA-12342, 15,555 ± 135 BP, *Cathaica*) give reservoir-corrected ages that straddle the hypothetical plot obtained from extrapolating the rate of deposition data obtained from the 2 pollen ages. The samples at 243 and 267 cm (*Cathaica*), give both AMS results and reservoir-corrected ages that seem too young.

The other 3 samples that could be considered to yield reliable ^{14}C ages from the reservoir-corrected values are AA-12344 (18,430 ± 170 BP, *Metodontia*), AA-12345 (18,720 ± 210 BP, *Metodontia*), and AA-12346 (17,720 ± 190 BP, *Metodontia*). Samples AA-12344 and AA-12345 were collected within 7 cm of each other, so the results may be reflecting bioturbation and mixing within the sediment. Also, from rough deposition rates, the loess at 300 cm depth gives an approximate age of 18,530 BP. At this level, possible bioturbation may indicate the presence of loess reworking. The presence of the Metodontia species of shells also possibly indicates the onset of warmer conditions, and the chronology suggests that this section of the profile represents warmer conditions occurring as climatic conditions become less harsh after the last Glacial maximum.

We cannot assume that the anomalous ages for many of the snail shell samples collected down the profile are caused purely by recrystallization effects, as age differences are far too great. Rat burrowing, much in evidence at the site, could have transported the snails into the profile. This phenomenon seems to be associated with the *Cathaica* species. Certainly, the shells seem to be intrusive, and no definite explanation is forthcoming at this stage. Since the living shell species used to calculate a shell reservoir age was *Cathaica*, and reservoir-corrected *Metodontia* ages seem to fit the hypothetical rate of deposition plot quite well, one of these showing good agreement with a pollen age from the same profile depth, it is reasonable to assume that the reservoir effect calculated for the *Cathaica* species also applies to the *Metodontia* species (Table 2).

CONCLUSION

Freshwater molluscs collected from Ang Ren Lake indicate that they can be considered to be viable dating materials, provided that only aragonite is used for dating. Living shell samples of the same species seem to provide a reasonable estimate of the possible apparent age of most of the fossil shells collected from this site when the ^{14}C atmospheric concentration for the period spanning the age range of the living shells, compared with the modern standard, is actually used as the modern standard. Certainly, a reservoir correction factor obtained in this way provides a more feasible chronology than the uncorrected conventional ^{14}C AMS ages, and they fit in a reasonable sequence with a wood cellulose age from material collected 398 cm down the profile.

The reservoir-corrected ages also provide a chronology that fits reasonably well with evidence of climatic changes obtained elsewhere. The age of the wood cellulose fits well with the accepted age of the onset of warmer conditions after the Younger Dryas period. The approximate age of 5500 BP for the bottom of the gravel layer at the top of the profile also fits well with a similar age found else-

where for the onset of cold, dry conditions. The only anomalous age for a shell sample in the sequence is directly above the peat layer, and can be related to it. Obviously, this sample has been associated with different climatic conditions, and a different reservoir correction would apply.

Dating terrestrial shells from a loess profile sequence such as Liang Cun possibly can be considered viable if modern shell ^{14}C data are available to estimate a reservoir effect, as indicated above, and if the shell consists only of aragonite. Ideally, only one species of shell should be used, but in this site, the reservoir age calculated for the *Cathaica* species seems to apply to the *Metodontia* species as well. The poor development of the paleosols within the sequence at this site could be the main reason that variable reservoir effects do not seem to occur for the different shell species. A representative number of reservoir-corrected ages for both species tentatively fit a hypothetical rate-of-deposition plot even though there are many outliers. Since the majority of the reservoir-corrected shell ages are too young, this fits the assumption that both recrystallization and intrusion into the profile have occurred.

The weakly developed paleosol at 102–140 cm seems to give reservoir-corrected ages that are younger than a paleosol sequence that should be of similar age from the nearby Bei Zhuang Cun profile (Head et al. 1989; Zhou et al. 1990). The bottom paleosol of the Bei Zhuang sequence dated from 9600 to 8000 BP. However, since the level at 102–140 cm at Liang Cun shows mixing and reworking, the indicated reservoir-corrected age of 8610 ± 120 BP for the bottom of the profile cannot be considered representative of the true age. The reservoir-corrected ages at around 300 cm seem to be associated with loess reworking, and since they are from the *Metodontia* species, may indicate a slight warming period. This ties in with the beginning of change from glacial conditions expected during this time range.

Reservoir-corrected ages from ^{14}C concentrations of living species of snail shells from the Loess Plateau seem to provide a working chronology for the site studied, provided that they can be checked against ^{14}C ages obtained from other materials. The *Metodontia* species apparently provides much more reliable dating material than the *Cathaica*, which seems more susceptible to recrystallization.

ACKNOWLEDGMENTS

This study was supported by NSFC, 49725308 and 49894170; CAS, KZ-951-A1-402 and KZ-952-S1-419; SSTC 95-40, and the US National Science Foundation (Grant EAR 95-08413). We thank an anonymous reviewer for providing constructive advice.

REFERENCES

Donahue DJ, Jull AJT, Toolin LJ. 1990. Radiocarbon measurements at the University of Arizona AMS Facility. *Nuclear Instruments and Methods in Physics Research* B52:224–8.

Goodfriend GA. 1987. Radiocarbon age anomalies in shell carbonate of land snails from semi-arid areas. *Radiocarbon* 29(2):159–68.

Head MJ. 1991. The radiocarbon dating of fresh water and marine shells. In: Gillespie R, editor. *Proceedings of the Quaternary Dating Workshop 1990.* Canberra: Australian National University. p 16–18.

Head MJ, Zhou W, Zhou M. 1989. Evaluation of the ^{14}C ages of organic fractions from loess–paleosol sequences near Xian, China. *Radiocarbon* 31(3):680–94.

Liu Tungsheng et al. 1985. *Loess and the environment.* Beijing: China Ocean Press. p 73–83.

Slota PJ Jr, Jull AJT, Linick TW, Toolin LJ. 1987. Preparation of small samples for ^{14}C accelerator targets by catalytic reduction of CO. *Radiocarbon* 29(2):303–6.

Spennemann DHR, Head MJ. 1996. Reservoir modification of radiocarbon signatures in coastal and nearshore waters of Eastern Australia: the state of play. *Quaternary Australasia* 14(1):32–9.

Stuiver M, Polach HA. 1977. Discussion: reporting of ^{14}C data. *Radiocarbon* 19(3):355–63.

Zhou WJ, Donahue DJ, Jull AJT. 1997. ^{14}C AMS dating of pollen from aeolian sand palaeosol and peat samples: implications for rapid climate change in the late Quaternary. *Radiocarbon* 39(1):19–26.

Zhou WJ, Zhou MF, Head MJ. 1990. ^{14}C chronology of Bei Zhuang Cun sedimentation sequences since 30,000 years BP. *Chinese Science Bulletin* 35(7):567–72.

RADIOCARBON, Vol 41, Nr 1, 1999, p 25–45

CHRONOLOGY OF VEGETATION AND PALEOCLIMATIC STAGES OF NORTHWESTERN RUSSIA DURING THE LATE GLACIAL AND HOLOCENE

Kh A Arslanov[1] • L A Saveljeva[1] • N A Gey[1] • V A Klimanov[2] • S B Chernov[1] • G M Chernova[3] G F Kuzmin[4] • T V Tertychnaya[1] • D A Subetto[5] • V P Denisenkov[3]

ABSTRACT. We have studied 6 reference sections of bog and lake sediments in the Leningrad and Novgorod provinces to develop a geochronological scale for vegetational and paleoclimatic changes in northwestern Russia during the Late Glacial and Holocene. Every 10-cm layer along the peat and gyttja sections (4–8.5 m thick) was investigated palynologically and the great majority of them were radiocarbon dated. Using the data obtained, standard palynological diagrams were plotted and vegetation history reconstructed. The palynozones indicated on the diagrams were related to the climatic periods and subperiods (phases) of the Blytt-Sernander scheme. On the basis of 230 ^{14}C dates obtained, we derived the geochronology of climatic periods and phases, as well as the chronology for the appearance and areal distribution of forest-forming tree species. The uppermost peat layers were dated by using the "bomb effect". We compared the stages of Holocene vegetation and paleoclimatic changes discovered for the Leningrad and Novgorod provinces with the those obtained for Karelia, which we had studied earlier using the same methodology.

INTRODUCTION

The climatic-geochronological division of the Holocene has been based on recognition of climatic periods and phases using the Blytt-Sernander scheme. This relative scale was originally linked with the absolute radiocarbon one only by means of ^{14}C dating of the borders between climatic periods and phases identified in the Ageröds Mosse bog sediments (Nilsson 1964). Later, similar, climatic-geochronological scales supported by ^{14}C dating were developed for many regions of Western Europe. The Holocene geochronological scale of northwestern Russia is also based on the Blytt-Sernander scheme, but the climatic periods and phases identified here are not correlated well enough with the ^{14}C scale, owing to a shortage of Holocene sections investigated in detail by palynological and geochronological methods. The basis of our research project has been to study thoroughly the Holocene sediments in continuous sequences and to relate the pollen zones discovered to the climatic periods and phases, and to the ^{14}C time scale. Another goal has been to reconstruct Late Glacial and Holocene climatic parameters based on palynological and geochronological data.

METHODS

The most appropriate natural objects for the reconstruction of Late Glacial and Holocene vegetation and paleoclimates are thick layers of raised bog and lake sediments that have accumulated continuously over time. The records from bog and lake organic sediments complement each other. The bog peat consists of organic carbon formed in situ. It also contains moss, plant fragments, and microfossils that are necessary for the study of paleovegetation and paleoclimates. However, the palynological spectra of bog sediments reflect the local, regional, and zonal components of vegetation while the palynological spectra of lake sediments reflect mostly the regional and zonal ones (Khomutova 1995). The lake sediments occasionally contain microfossils and old redeposited carbon or organic carbon produced in a hard-water medium, which makes comparison of lake and bog records difficult, as we will demonstrate below.

[1]Geographical Research Institute, St Petersburg State University, Sredny pr., 41, St Petersburg 199004 Russia
[2]Institute of Geography, Russian Academy of Sciences, Staromonetny Lane, 29, Moscow 109017 Russia
[3]Geographical and Geoecological Faculty, St Petersburg State University, 10th Line, 33, St Petersburg 199004 Russia
[4]All-Russian Research Institute of Peat Industry, Marsovo Pole, 5, St Petersburg 191065 Russia
[5]Institute of Limnology, Russian Academy of Sciences, Sevostianov's Str., 9, St Petersburg 196105 Russia

During the last 5 years, we have studied 5 reference sections of bogs and one of lake sediments located in the provinces of Leningrad and Novgorod. We previously studied 2 sections of bog sediments located in Karelia (Elina et al. 1996). We used the same methods for all sections under study: every 10–12 cm layer along the whole thickness was investigated palynologically and generally geochronologically (by the ^{14}C dating method). The botanical composition of bogs was also studied. The bog samples were taken using a hand drill, and the lake ones with a Livingstone piston sampler. In all, 320 ^{14}C dates (90 dates for the sections in Karelia) have been obtained at the geochronological laboratory at St Petersburg State University. For ^{14}C dating, we used the liquid scintillation method described in Arslanov et al. (1993). Peat samples were pretreated by heating in 1% HCl for 30 min and then by keeping them in 1% NaOH overnight at room temperature. Humus from lake sediment samples was extracted by a 5-h treatment in hot 2% NaOH (after first heating in 1% HCl and removing Ca^{++}). Li_2C_2 was synthesized from charcoal obtained by pyrolysis from the pretreated peat samples and humic acids. When the amounts of samples were small enough (<3 g), we carried out synthesis with excess of Li (in a ratio of 1 g humic acid to 2 g Li) without pyrolysis. To synthesize benzene from acetylene we used a $V_2O_5 \cdot Al_2O_3 \cdot SiO_2$ catalyst, which allowed us to obtain benzene of high purity (with 90%–95% yield). The reliability of the laboratory work was demonstrated by our results of dating 25 samples for the IAEA and TIRI programs (also the Wrangel mammoth dates); all dates were consistent with the control figures within the limit of 2σ (Arslanov et al. 1998; Scott et al. 1997).

We carried out precise dating of the upper layers of peat stratum formed during last 45 years by measuring the "bomb radiocarbon" content in layers 2 cm thick. To determine calendar years for these layers, the curve of ^{14}C content–peat depth was matched to the well-known curve of ^{14}C excess in the atmosphere (Broecker and Walton 1959; Levin et al. 1980; McNeely 1994).

Sample Treatment for Palynological Analysis

The peat samples were pretreated by boiling in 10% NaOH for 5 min and then washing with distilled water by centrifuging; the residue was then analyzed. The mineral samples were treated initially in 10% HCl at room temperature to fully dissolve the carbonates, then the residue was washed with distilled water. Thereafter the residue was treated by boiling in 10% NaOH for 5 min, followed by washing in distilled water. The organic and mineral fractions were separated by adding a heavy liquid (PD-6 or KK-2,6), the density of which was adjusted to 2.28–2.29, and then the mineral residue was separated by centrifuging. A small amount of water and a few drops of HCl were added to the suspension bearing pollen and sporae to separate them: the precipitate was finally divided by centrifuging. The percentages of pollen (AP and NAP) and spores (Sporae) were calculated taking the total pollen and spores sum as 100%; the percentage of pollen and spores of the AP, NAP, and Sporae groups was calculated by taking the pollen or spores sum as 100% for each group.

RESULTS

Figures 1–5 are chrono-palynological diagrams of the sections of bog and lake sediments which were studied, and run from south to north: the Nikokolsko-Lutinskoye bog, the Shirinsky Mokh bog, the Lammin-Suo bog, Vishnevskoye Lake and the Sakkala bog. The diagram of the northernmost section, the "Suo" bog, located near the city Priozersk in the Leningrad province, was recently published in Chernova et al. (1997) and is not presented here. Two sections, the Nilosko-Lutinskoye bog and the Vishnevskoye lake, were studied earlier but only a few ^{14}C dates were obtained for these sections at that time (Arslanov et al. 1992; Kuzmin et al. 1985).

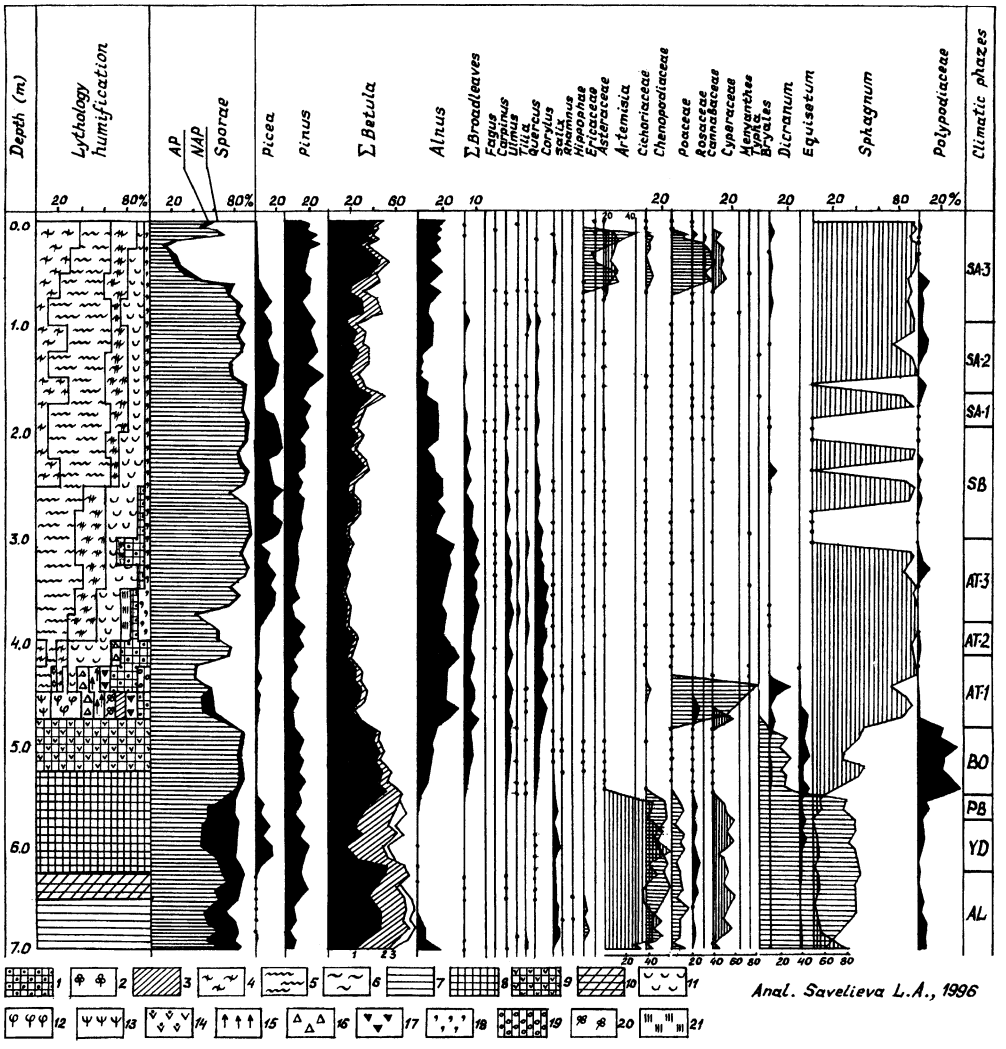

Figure 1 Chrono-palynological diagram of the Nikolsko-Lutinskoye raised bog sediments. Symbols: 1. *Pinus* peat; 2. *Menyanthes*; 3. *Carex* peat; 4. *Sphagnum fuscum*; 5. *S. magellanicum*; 6. *S. angustifolium*; 7. clay; 8. sapropel (gyttja); 9. peaty sapropel (gyttja); 10. clayey sapropel (gyttja); 11. *Eriophorum vaginatum*; 12. *Sphagnum platiphillum*; 13. *S. contortum*; 14. *S. terres*; 15. *Equistetum limosum*; 16. *Phragmites communis*; 17. herbaceous remains; 18. small shrubs; 19. *Betula pubescens*; 20. *Menyanthes trifoliata*; 21. *Scheuchzeria* peat.

Nikolsko-Lutinskoye Bog

The Nikolsko-Lutinskoye bog is located in the southwestern part of the Lake Ilmen shore lowland (depression) within the watershed of the Ljuta and Lemenka rivers and occupies an area of about 37.1 km^2. The section of peat (4.9 m thick) and sapropel (1.7 m thick) with clay (0.4 m thick) at the bottom was recovered by drilling to 7 m depth. We determined 11 stages of vegetation change beginning with the Allerød (AL) interstadial in this section. The pollen and ^{14}C data (Fig. 1; Table 1) show that sparse pine-birch forests with a small amount of spruce dominated during the Allerød interstadial (*Betula sect. Albae*: 30%–55%, *Pinus*: 5%–20%). Shrub and small shrub species of birch with willow were widespread (*Betula sect. Fruticosae*: 30%, *Betula nana*: 3%–5%, *Salix*: 2%–7%). *Artemisia* (25%–40%) and Chenopodiaceae (5%–15%) were the dominant herbaceous pollen types.

Table 1 ^{14}C dates of Nikolsko-Lutinskoye raised bog sediments

Depth (cm)	Lab code	$\delta^{14}C$ (‰) or ^{14}C age (yr BP)[a]	Calibrated age (AD/BC)
0–2	LU-3432	*102.3 ± 10.5*	1989 AD–1993 AD
4–6	LU-3433	*188.2 ± 9.8*	1980 AD–1984 AD
8–10	LU-3434	*287.9 ± 7.1*	1971 AD–1975 AD
12–14	LU-3436	*465.6 ± 7.1*	1962 AD–1966 AD
16–18	LU-3435	*56.4 ± 7.6*	1953 AD–1957 AD
20–22	LU-3437	*26.3 ± 5.9*	1944 AD–1948 AD
40–42	LU-3438	200 ± 60	1750 AD–1948 AD
50–52	LU-3440	160 ± 30	1750 AD–1948 AD
50–60	LU-3441	600 ± 50	1306 AD–1404 AD
80–90	LU-3444	720 ± 170	1060 AD–1420 AD
90–100	LU-3445	780 ± 70	1181 AD–1294 AD
110–120	LU-3447	880 ± 30	1062 AD–1219 AD
120–130	LU-3448	1170 ± 50	792 AD–959 AD
150–160	LU-3451	1350 ± 40	652 AD–760 AD
160–170	LU-3452	1380 ± 40	636 AD–680 AD
170–180	LU-3453	1520 ± 40	460 AD–614 AD
180–190	LU-3454	1580 ± 30	446 AD–534 AD
190–200	LU-3455	1700 ± 70	252 AD–424 AD
200–210	LU-3456	2140 ± 70	352 BC–48 BC
210–220	LU-3457	2090 ± 80	192 BC–6 AD
220–230	LU-3458	2320 ± 80	506 BC–202 BC
230–240	LU-3459	2200 ± 60	364 BC–184 BC
240–250	LU-3460	2570 ± 60	806 BC–548 BC
250–260	LU-3461	2510 ± 40	772 BC–536 BC
260–270	LU-3462	2780 ± 70	992 BC–838 BC
270–280	LU-3463	3050 ± 60	1396 BC–1214 BC
280–290	LU-3464	3300 ± 80	1678 BC–1462 BC
290–300	LU-3465	3680 ± 80	2184 BC–1936 BC
300–310	LU-3466	4320 ± 60	3032 BC–2880 BC
310–320	LU-3467	4350 ± 80	3090 BC–2884 BC
320–330	LU-3468	4520 ± 60	3342 BC–3104 BC
330–340	LU-3469	4710 ± 60	3620 BC–3376 BC
340–350	LU-3470	4970 ± 110	3940 BC–3650 BC
350–360	LU-3471	5070 ± 70	3950 BC–3796 BC
360–370	LU-3472	5250 ± 110	4230 BC–3970 BC
380–390	LU-3474	5710 ± 90	4682 BC–4460 BC
390–400	LU-3475	5730 ± 120	4760 BC–4460 BC
410–420	LU-3477	6140 ± 90	5210 BC–4946 BC
420–430	LU-3478	6450 ± 90	5440 BC–5284 BC
440–450	LU-3480	6620 ± 100	5580 BC–5440 BC
450–460	LU-3481	6760 ± 70	5676 BC–5531 BC
460–470	LU-3482	6920 ± 60	5814 BC–5688 BC
470–480	LU-3489	7060 ± 80	5968 BC–5812 BC
490–510	LU-3491	7900 ± 110	7000 BC–6600 BC
500–510	LU-3492	8250 ± 240	7530 BC–6790 BC
510–520	LU-3493	8130 ± 100	7300 BC–6820 BC
520–530	LU-3494	9040 ± 160	8330 BC–7935 BC
530–540	LU-3495	9040 ± 250	8400 BC–7710 BC
550–560	LU-3497	9650 ± 240	9120 BC–8400 BC
570–580	LU-3499	10,360 ± 140	10,525 BC–9975 BC
580–590	LU-3500	10,680 ± 120	10,775 BC–10,525 BC
590–600	LU-3501	11,300 ± 240	11,525 BC–11,025 BC
600–610	LU-3502	10,670 ± 140	10,800 BC–10,500 BC
630–640	LU-3505	12,030 ± 250	12,400 BC–11,775 BC

[a] $\delta^{14}C$ measurements in *italics*.

During the Younger Dryas (YD) the pine-birch forests were sharply reduced (*Betula sect. Albae* <15%) and shrubs and small shrub species of birch and willow occupied relatively large areas (*Betula sect. Fruticosae* 18%–38%, *Betula nana* 3%–7%; *Salix* 2%–7%). Also, xerophytes began to be widespread: *Artemisia* (40%–60%) and Chenopodiaceae (10%–20%).

An expansion of arborescent species of birch began in the Preboreal (PB): *Betula sect. Albae* 30%–55%; sparse birch forests, with some pine and spruce, dominated (*Pinus* 15%–20%, *Picea* 5%–10%). The share of steppe species such as *Artemisia* and Chenopodiaceae decreased sharply.

During the Boreal (BO), pine-birch forests were dominant (*Betula sect. Albae*: 45%–55%, *Pinus*: 13%–18%); alder (10%–14%) and hazel (5%–7%) appeared in shrub layers. Some broad-leaved tree species appeared at the same time, mostly elm.

Throughout the Atlantic (AT), pine-birch forests predominated with an admixture of broad-leaved trees. At the beginning of the Atlantic (AT-1) the proportion of birch in the forest community decreased and that of broad-leaved trees (7%–13%) such as elm, linden, and oak increased. Toward the middle of the Atlantic (AT-2) the share of broad-leaved trees decreased again to 5%–6%. Toward the end of pollen zone AT-2 beech appeared in the forests but conditions that suited the broad-leaved species only became established in pollen zone AT-3. During the whole period, alder forests with hazel in the undergrowth were widespread in areas with excess moisture.

During the Subboreal (SB), spruce expansion was maximal: spruce, together with birch, became the forest-forming species (*Picea* 12%–29%, *Betula sect. Albae* 20–40%). The proportion of the broad-leaved trees remained significant (5%–8%). In the wetter areas spruce was replaced by alder (*Alnus* 10%–20%).

During the Early Subatlantic (SA-1), birch, pine, and spruce continued to be the main forest-forming species, but the proportion of spruce decreased (*Picea* 6%–15%). Oak and elm predominated among broad-leaved species. Spruce-pine-birch forests were widespread from pollen zone SA-2, then pine-birch forests with an admixture of spruce. At the end of the zone, that is, the recent phase, pine-birch forests with a small proportion of spruce were predominant in the territory. The broad-leaved species were rare during the Subatlantic and the alder forests occupied only a limited area.

Shirinsky Mokh Bog

The Shirinsky Mokh bog is located in the basin of the Volkhov River, 25 km to the southeast of the town of Kirishy, in Leningrad province. The borehole was drilled to a depth of 7.1 m in the center of the bog and uncovered a peat stratum (6.65 m thick) with underlying clay (0.50 m thick).

The palynological and ^{14}C data (Fig. 2; Table 2) suggest that the sediments formed during the Preboreal–Subatlantic (PB–SA). During the first half of the Preboreal (PB-1), the shrub (*Betula sect. Fruticosae*) and dwarf birch (*Betula nana*) formation was widespread (27%–34%) in lowland areas, and the willow percentages were significant (to 7%). The more elevated land was occupied by the restricted areas of single trees, partly by sparse, small pine-birch-spruce-alder forests (*Pinus* 10%–15%, *Picea* 3%–7%) with a moss covering. Steppe taxa such as *Artemisia* (22%–25%) and Chenopodiaceae (18%–22%) were widespread. During the second half of the Preboreal (PB-2), arborescent birch began its expansion: sparse birch and pine forests began to develop and elm and hazel (in undergrowth) appeared. The share of xerophytes in the landscape diminished sharply; they were replaced by a gramineous-*Carex* association.

At the beginning of the Boreal (BO-1), birch forests (*Betula* to 90%) with a small proportion of pine spread everywhere. Among the broad-leaved species, oak and linden appeared after elm. During the

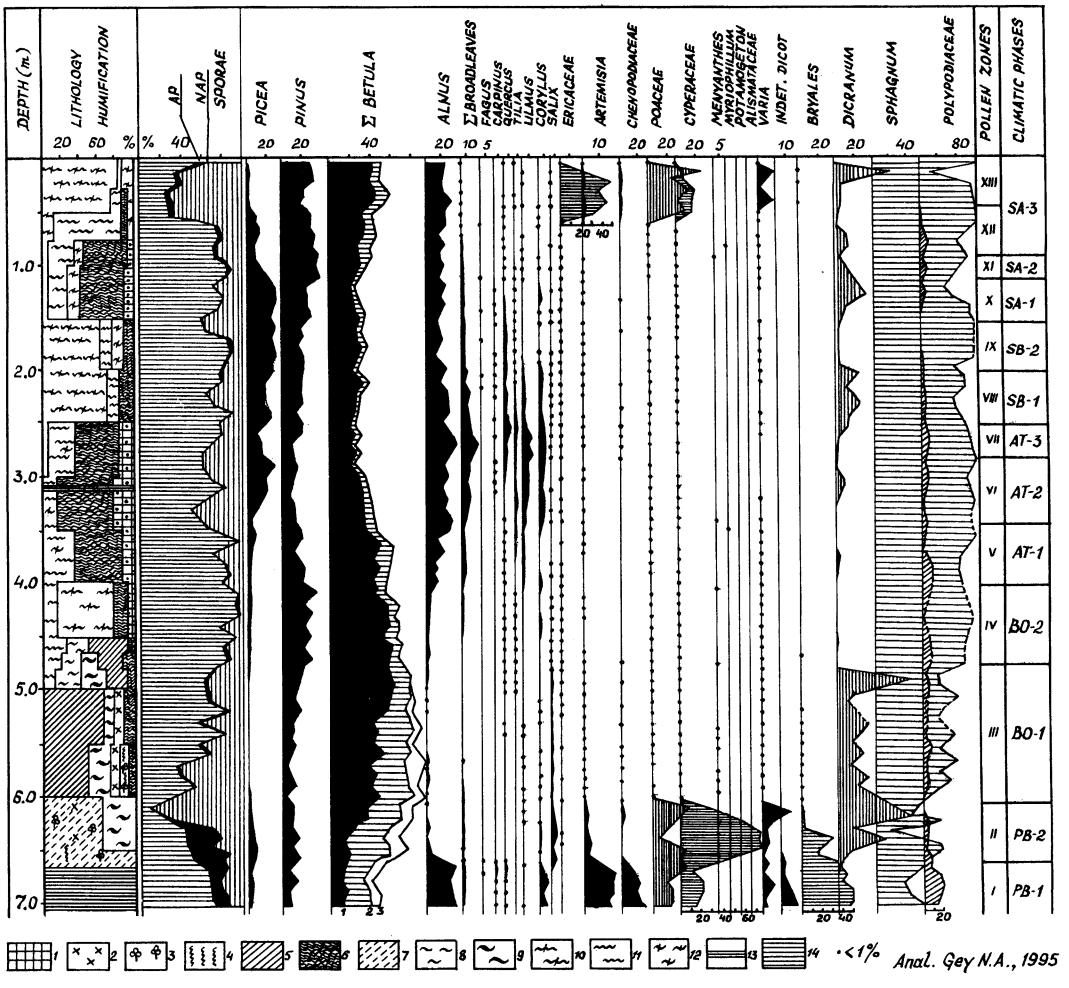

Figure 2 Chrono-palynological diagram of the Shirinsky Mokh raised bog sediments. Symbols: 1. *Pinus* peat; 2. *Equisetum* peat; 3. *Menyanthes*; 4. *Phragmites* peat; 5. *Carex* peat; 6. *Eriophorum* peat; 7. *Scorpigium*; 8. *Sphagnum sect. cuspidata*; 9. *S. subsecundum*; 10. *S. fuscum*; 11. *S. magellanicum*; 12. *S. angustifolium*; 13. charred layer of peat; 14. clay.

second half of the Boreal (BO-2), pine percentages began to rise (21%–34%) and pine-birch forests became dominant. Some broad-leaved species (such as elm, oak, and linden) were present constantly. Alder and spruce were no longer present in the forests. The spore-pollen spectra characteristic for the Atlantic and the development of vegetation during this period are similar to those of the Nikolsko-Lutinskoye bog section (Figs. 1, 2). Beginning in the Subboreal, the territory was part of the dark coniferous taiga zone. Early in the period (SB-1) birch was the relatively dominant species in the forest. In pollen zone SB-2, spruce was expanding intensively in birch-pine forests and gradually became a dominant species (21%–27%). The share of broad-leaved species decreased (to 3%–6%) and beech replaced oak.

The dominant and subdominant vegetation and spore-pollen spectra of the Subatlantic (SA) are similar to those of the Nikolsko-Lutinskoye bog section, except for the first phase (SA-1). The proportion of spruce was much higher in this section (Figs. 1, 2).

Table 2 ^{14}C dates of the Shirinsky Mokh raised bog sediments

Depth (cm)	Lab code	$\delta^{14}C$ (‰) or ^{14}C age (yr BP)[a]	Calibrated age AD/BC (1σ)
0–2	LU-3312	*68.9 ± 10.6*	1989 AD–1993 AD
2–4	LU-3313	*139.5 ± 8.6*	1985 AD–1989 AD
4–6	LU-3314	*176.3 ± 9.9*	1980 AD–1985 AD
6–8	LU-3401	*244.4 ± 8.8*	1976 AD–1980 AD
8–10	LU-3399	*320.7 ± 9.1*	1972 AD–1976 AD
10–12	LU-3315	*345.7 ± 10.5*	1968 AD–1972 AD
12–14	LU-3400	*464.7 ± 9.4*	1963 AD–1968 AD
14–16	LU-3402	*211.7 ± 9.8*	1959 AD–1963 AD
16–18	LU-3316	*23.1 ± 9.7*	1955 AD–1959 AD
22–24	LU-3317	60 ± 50	1750 AD–1959 AD
28–30	LU-3318	180 ± 80	1750 AD–1959 AD
34–36	LU-3319	30 ± 60	1750 AD–1959 AD
40–42	LU-3320	30 ± 50	1750 AD–1959 AD
46–48	LU-3321	100 ± 40	1750 AD–1959 AD
70–80	LU-3325	240 ± 50	1534 AD–1936 AD
80–90	LU-3326	410 ± 50	1440 AD–1620 AD
90–100	LU-3327	480 ± 60	1404 AD–1472 AD
100–110	LU-3328	980 ± 40	1014 AD–1158 AD
110–120	LU-3329	1320 ± 50	664 AD–770 AD
120–130	LU-3330	1600 ± 60	416 AD–540 AD
130–140	LU-3331	1820 ± 40	142 AD–246 AD
140–150	LU-3332	2010 ± 30	36 BC–54 AD
150–160	LU-3333	2380 ± 90	760 BC–370 BC
160–170	LU-3334	2460 ± 60	760 BC–412 BC
170–180	LU-3335	2430 ± 60	756 BC–402 BC
180–190	LU-3336	2600 ± 60	826 BC–554 BC
190–200	LU-3337	2820 ± 60	1036 BC–854 BC
210–220	LU-3339	3230 ± 70	1600 BC–1414 BC
220–230	LU-3340	3800 ± 90	2398 BC–2044 BC
230–240	LU-3341	4030 ± 70	2848 BC–2460 BC
240–250	LU-3342	4090 ± 60	2862 BC–2500 BC
250–260	LU-3343	4250 ± 70	2920 BC–2694 BC
260–270	LU-3344	4590 ± 80	3500 BC–3106 BC
270–280	LU-3345	5030 ± 90	3946 BC–3714 BC
280–290	LU-3346	5050 ± 70	3948 BC–3782 BC
290–300	LU-3347	5230 ± 80	4220 BC–3964 BC
300–310	LU-3348	5500 ± 100	4460 BC–4250 BC
310–320	LU-3349	6120 ± 100	5210 BC–4920 BC
330–340	LU-3351	6640 ± 80	5579 BC–5450 BC
340–350	LU-3352	7030 ± 110	5960 BC–5750 BC
350–360	LU-3353	6980 ± 90	5940 BC–5726 BC
360–370	LU-3354	7310 ± 100	6190 BC–6000 BC
370–380	LU-3355	7540 ± 70	6422 BC–6240 BC
400–410	LU-3358	7630 ± 70	6532 BC–6376 BC
410–420	LU-3359	7960 ± 70	7000 BC–6708 BC
420–430	LU-3360	7890 ± 60	6994 BC–6602 BC
440–450	LU-3362	8240 ± 80	7416 BC–7052 BC

Table 2 (Continued)

Depth (cm)	Lab code	^{14}C age (yr BP)	Calibrated age AD/BC (1σ)
450–460	LU-3363	8190 ± 80	7264 BC–7046 BC
460–470	LU-3365	8230 ± 70	7410 BC–7050 BC
470–480	LU-3366	8160 ± 80	7262 BC–7038 BC
480–490	LU-3367	8400 ± 60	7498 BC–7324 BC
490–500	LU-3368	8580 ± 50	7588 BC–7504 BC
500–510	LU-3369	8400 ± 70	7502 BC–7314 BC
510–520	LU-3370	8360 ± 50	7486 BC–7312 BC
520–530	LU-3371	8590 ± 70	7692 BC–7504 BC
530–540	LU-3372	8720 ± 80	7890 BC–7594 BC
540–550	LU-3373	8790 ± 80	7935 BC–7702 BC
560–570	LU-3375	8980 ± 70	8046 BC–7962 BC
580–590	LU-3377	9080 ± 60	8122 BC–8028 BC
590–600	LU-3378	8960 ± 80	8046 BC–7935 BC
600–610	LU-3379	9140 ± 130	8340 BC–8040 BC
610–620	LU-3380	9360 ± 80	8518 BC–8262 BC
640–650	LU-3383	9380 ± 110	8840 BC–8260 BC
650–660	LU-3384	9410 ± 90	8832 BC–8278 BC
660–670	LU-3385	9850 ± 100	9380 BC–8980 BC

[a]δ^{14}C measurements in *italics*.

Lammin-Suo Bog

The Lammin-Suo bog is located on the Karelian Isthmus near the settlement of Iljichovo, 12 km north of the town of Zelenogorsk. A section of peat 4.0 m thick was obtained by drilling to a depth of 4.1 m; there was sand at the bottom, and a layer of strongly decomposed peat (0.2 m thick) was found at depths of 2.5–2.7 m. These sediments formed during the Boreal–Subatlantic (BO-SA-3).

The palynological and ^{14}C data (Fig. 3; Table 3) show that the predominant forest formation during the Boreal was pine-birch forest (*Betula* 60–75%, *Pinus* 18–32%). Alder and spruce were not among the forest-forming species and the only thermophyl species was elm (but this appeared only sporadically) and hazel was in the undergrowth. The gramineous-*Carex* community dominated in the herbaceous cover. The climatic change in pollen zone AT gave rise to a number of broad-leaved species in forests—in AT-1 the pine-birch forests with some elm; linden and oak occurred sporadically (pollen of broad-leaved species contributed up to 3%); in AT-2 mixed broad-leaved forests in which the frequency of linden along with elm was significant, and beech appeared as well (broad-leaved species 6–11%). During the whole period, alder forests were widespread on the outlying sides of the bog (*Alnus* 10–15%). Spruce began to expand to the end of pollen zone AT-2. Sediments of the final phase of AT were absent.

The spore-pollen spectra of the Subboreal are similar to those of the Shirinsky Mokh section for the same period (Figs. 2, 3). The sporae-pollen spectra of the Subatlantic (SA), which show the development of vegetation during the period, bear a close resemblance to those of the Nikolsko-Lutinskoye bog section (Figs. 1, 3).

Vishnevskoye Lake

Vishnevskoye Lake (Table 4) is located on the lacustrine-glacial plain to the north of the central highland of Karelian Isthmus (15 m asl). It is a shallow basin with an average depth of about 2 m and

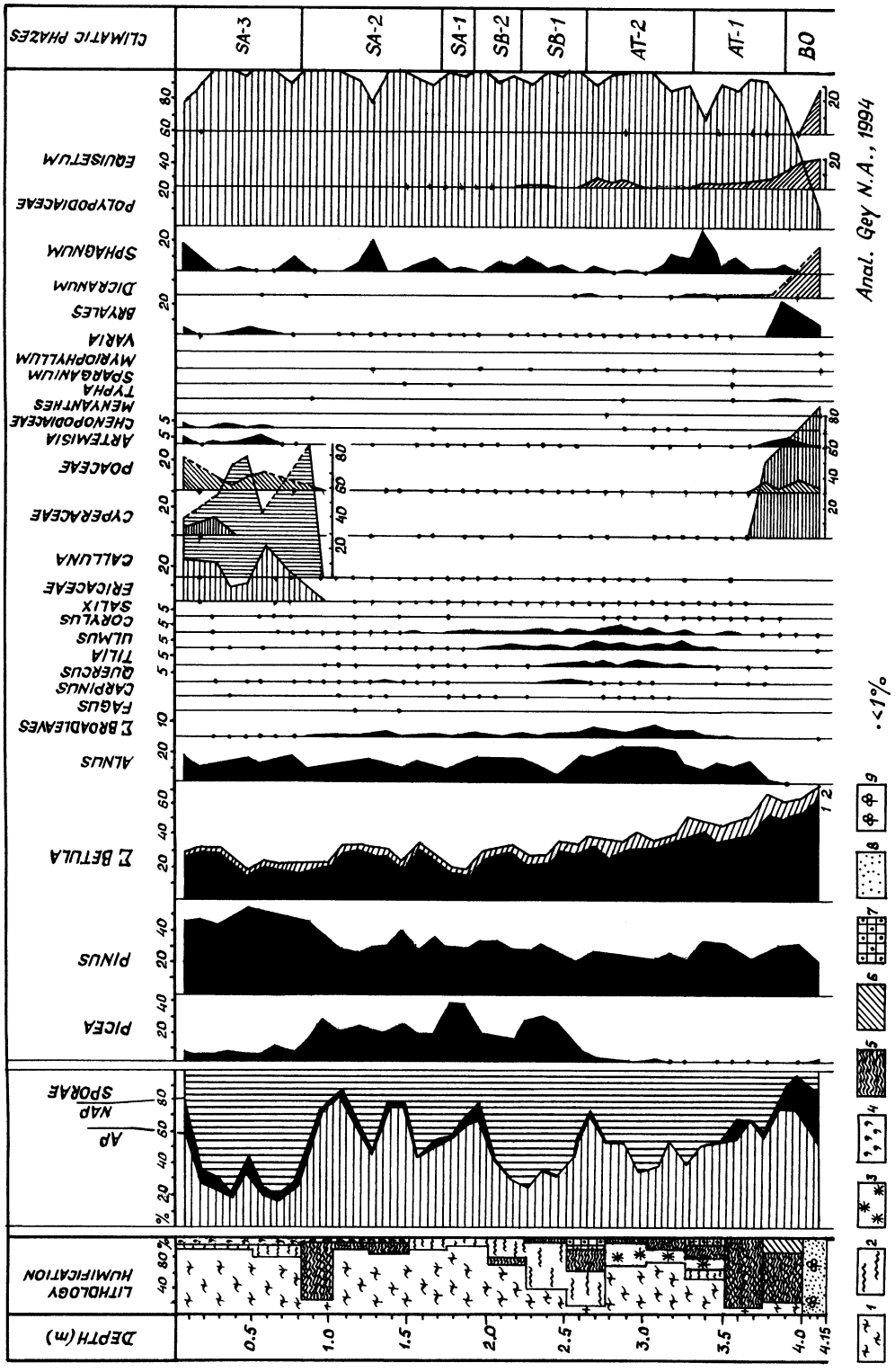

Figure 3 Chrono-palynological diagram of the Lammin-Suo raised bog sediments. Symbols: 1. *Sphagnum fuscum*; 2. *S. magellanicum*; 3. *S. terres* 4. small shrubs; 5. *Eriophorum* peat; 6. *Carex* peat; 7. *Pinus* peat; 8. sand; 9. plant remains.

TABLE 3. ^{14}C Dates of the Lammin-Suo Raised Bog Sediments

Depth (cm)	Lab code	$\delta^{14}C$ (‰) or ^{14}C age (yr BP)[a]	Calibrated age AD/BC (1σ)
0–10	LU-3080	*113.2 ± 8.6*	1978 AD–1993 AD
10–15	LU-3081	*271.6 ± 7.9*	1967 AD–1978 AD
15–20	LU-3082	*390.4 ± 9.1*	1956 AD–1967 AD
20–25	LU-3083	*17.5 ± 7.2*	1945 AD–1956 AD
25–30	LU-3084	*18.7 ± 8.6*	1750 AD–1956 AD
30–35	LU-3085	*–2.1 ± 7.8*	1750 AD–1956 AD
35–40	LU-3086	*–9.7 ± 8.5*	1750 AD–1956 AD
40–45	LU-3087	*5.4 ± 7.7*	1750 AD–1956 AD
45–50	LU-3088	*0.7 ± 7.5*	1750 AD–1956 AD
50–60	LU-3063	*6.3 ± 9.4*	1750 AD–1956 AD
70–80	LU-3064	490 ± 60	1402 AD–1469 AD
90–100	LU-3065	650 ± 80	1292 AD–1396 AD
100–110	LU-3168	1410 ± 50	610 AD–668 AD
110–120	LU-3066	1800 ± 40	144 AD–324 AD
120–130	LU-3169	1940 ± 50	18 AD–124 AD
150–160	LU-3068	1950 ± 50	14 AD–120 AD
170–180	LU-3069	2230 ± 70	372 BC–200 BC
180–190	LU-3171	2370 ± 60	752 BC–376 BC
200–210	LU-3172	2800 ± 60	1004 BC–848 BC
210–220	LU-3071	2790 ± 60	996 BC–846 BC
220–230	LU-3173	3080 ± 50	1400 BC–1268 BC
240–250	LU-3174	3210 ± 60	1520 BC–1416 BC
250–260	LU-3073	3780 ± 40	2278 BC–2062 BC
260–270	LU-3175	5610 ± 70	4500 BC–4358 BC
270–280	LU-3074	6320 ± 50	5314 BC–5222 BC
280–290	LU-3176	6590 ± 60	5564 BC–5444 BC
310–320	LU-3076	6860 ± 60	5738 BC–5628 BC
330–340	LU-3077	7170 ± 70	6108 BC–5892 BC
350–360	LU-3078	7490 ± 90	6388 BC–6214 BC
370–380	LU-3079	7770 ± 50	6598 BC–6484 BC

[a]$\delta^{14}C$ measurements in *italics*.

maximum depth of about 3.5 m. The thickness of lake sediments extracted was 10 m (sapropel, 8.6 m; clayey sapropel, 0.8 m; clay, 0.8 m [Fig. 4]). Sediment accumulation began in the lake since the Younger Dryas (Table 4). Palynological data show that the ratio between the main components of the sporae-pollen spectra is almost identical to that of the Nikolsko-Lutinskoye bog section for the same period (Figs. 1, 4).

During the Preboreal, arborescent birch and pine expanded rapidly (*Betula sect. Albae* 30–60%, *Pinus* 10–50%); however, during the first half of the pollen zone PB-1 period, sparse birch forests with some shrub and dwarf birch and willow persisted. At the beginning of pollen zone PB-2, pine-birch forests predominated (*Betula sect. Albae* 25–65%, *Pinus* 20–45%); at the end of the period, alder and the broad-leaved species appeared (elm was first). The herbaceous cover was characterized by dominance of graminoides.

During the Boreal, pine-birch forests were replaced by pine forests (*Pinus* 45%–80%) when birch (*Betula sect. Albae* 25%–35%) and alder (*Alnus* 5%–15%) and broad-leaved species appeared. The proportion of herbs was sharply reduced.

During the first half of the Atlantic (AT-1), pine forests with an admixture of birch and alder continued to dominate, but the share of the broad-leaved species increased (5%–11%, mostly *Ulmus* 3%–7%). In the Mid-Atlantic (AT-2) the share of the broad-leaved species in the forests decreased (2%–6%) and spruce began to expand (*Picea* 10–20%). Spruce-pine and birch-pine forests (*Pinus* 35%–45%, *Betula sect. Albae* 17%) with an admixture of thermophilous plants (elm, linden, oak, beech, and hazel) were spreading then. At the end of the Atlantic (AT-3), the share of broad-leaved species began to rise again (to 8%) and this phase was characterized by dominance of spruce-birch-pine forests with a noticeable proportion of broad-leaved species (hazel and alder).

At the beginning of the Subboreal (SB-1), pine and spruce became the forest-forming species (*Pinus* 60% max, *Picea* 24% max). Spruce-pine forests with an admixture of birch (*Betula sect. Albae* max 7%) and alder (*Alnus* ca. 4%) developed but the contribution of the broad-leaved species remained rather small (ca. 5%).

In the middle of pollen zone SB (SB-2) the maximal expansion of spruce took place (*Picea* 32%). Pine (*Pinus* 45%) and spruce forests with birch (*Betula sect. Albae* 10–13%) were widespread but spruce was replaced by alder in moist areas (*Alnus* 4%–7%). Toward the end of the Subboreal (SB-3) the share of spruce decreased (*Picea* 18%–25%) and spruce-pine and birch-pine forests became common.

By and large, the spore-pollen spectra characteristics for the Subatlantic (SA) are identical to those of the Nikolsko-Lutinskoye bog section (Figs. 1, 4).

Sakkala Bog

The Sakkala bog is located in the northeastern part of the Karelian Isthmus, near the Gromovo railway station. The peat bed consists of highbog (0–2 m), with carex peat in between (2.0–2.5 m) and fen arboreal-carex, carex, arboreal, and arboreal-grass peat (2.5–4.35 m) below this (Fig. 5). Peat accumulation began during the middle of the Atlantic.

Based on the palynological and ^{14}C data, we recognize several vegetational changes (Fig. 5; Table 5): in the middle of the Atlantic (AT-2), alder-birch forests with some pine (*Betula sect. Albae* 14%–36%, *Alnus* 8%–65%, *Pinus* 8%–48%) were developed in the region and broad-leaved species (not <4%) and hazel (*Corylus* ca. 2%) were present as an admixture. Toward the end of the phase, spruce began to expand in the forests. Toward the end of the Atlantic, birch and pine became the forest-forming species (*Betula sect. Albae* 30%–45%, *Pinus sylvestris* to 30%) while alder occupied the low-lying and moister areas (*Alnus* 15–30%). Broad-leaved species were also important, such as elm and linden with some oak and hazel (max 9.6%), but the share of spruce was insignificant (*Picea* 5% max).

At the beginning of the Subboreal (SB-1), pine-birch forests dominated (*Betula sect. Albae* 30%–50%, *Pinus* 25–35%) with an admixture of spruce (*Picea* 10%–20%) and broad-leaved species (4%–8%); alder occupied the damp areas. During the second part of the Subboreal (SB-2) spruce began to predominate (*Picea* 30% max) and pine-spruce (*Pinus* 30%–35%) and birch-spruce (*Betula sect. Albae* 20%–30%) forests developed.

Changes in the sporae-pollen spectra suggest that during the Subatlantic vegetation changes occurred here the same way as in the Nikolsko-Lutinskoye bog section (Figs. 1, 5).

Suo Bog

The Suo bog is 2 km to the south of Suuri Lake, near the settlement of Kuznechnoye in Priozersk region of Leningrad province. The peat is 6.3 m at maximum thickness, and it documents all stages

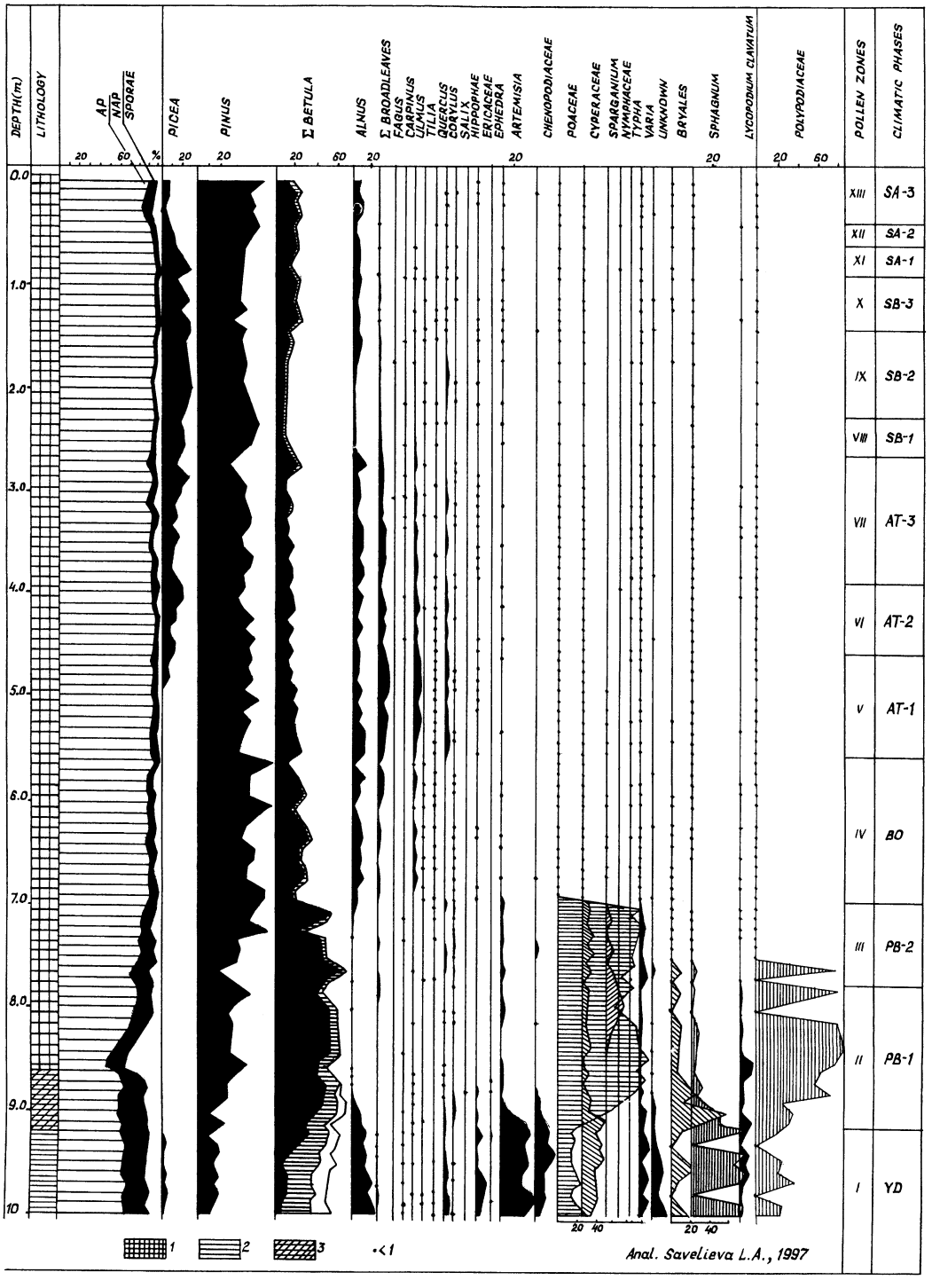

Figure 4 Chrono-palynological diagram of the Vishnevskoye Lake sediments. Symbols: 1. sapropel (gyttja); 2. clay; 3. clayey sapropel (gyttja).

Table 4 ^{14}C dates of the Vishnevskoye Lake sediments

Depth (cm)	Lab code	^{14}C age (yr BP)	Calibrated age AD/BC (1σ)
30–40	LU-3763	1600 ± 80	392 AD–590 AD
50–60	LU-3764	1670 ± 100	250 AD–530 AD
90–100	LU-3766	2580 ± 150	840 BC–420 BC
110–120	LU-3767	2990 ± 140	1390 BC–1030 BC
130–140	LU-3768	4270 ± 160	3090 BC–2610 BC
150–160	LU-3769	4100 ± 170	2890 BC–2410 BC
170–180	LU-3770	3840 ± 140	2470 BC–2040 BC
190–200	LU-3771	3710 ± 120	2280 BC–1930 BC
210–220	LU-3772	4150 ± 80	2872 BC–2616 BC
230–240	LU-3773	3930 ± 90	2564 BC–2214 BC
250–260	LU-3774	4420 ± 90	3298 BC–2918 BC
270–280	LU-3775	4610 ± 90	3508 BC–3108 BC
290–300	LU-3776	4730 ± 130	3650 BC–3350 BC
310–320	LU-3777	4940 ± 90	3902 BC–3640 BC
330–340	LU-3778	4990 ± 170	3980 BC–3550 BC
350–360	LU-3779	5450 ± 110	4450 BC–4100 BC
370–380	LU-3780	5600 ± 100	5440 BC–4340 BC
410–420	LU-3782	5560 ± 170	4660 BC–4170 BC
430–440	LU-3783	6310 ± 150	5430 BC–5070 BC
450–460	LU-3784	6570 ± 210	5600 BC–5290 BC
470–480	LU-3785	7030 ± 330	6180 BC–5530 BC
530–540	LU-3788	7690 ± 190	6710 BC–6230 BC
590–600	LU-3791	8270 ± 260	7540 BC–6780 BC
610–620	LU-3792	8260 ± 190	7490 BC–7040 BC
670–680	LU-3795	8680 ± 240	7980 BC–7490 BC
690–700	LU-3796	8860 ± 180	8040 BC–7620 BC
700–720	LU-3868	9170 ± 170	8390 BC–8030 BC
720–740	LU-3969	9510 ± 180	8490 BC–8420 BC
740–760	LU-3870	9710 ± 210	9130 BC–8480 BC
760–780	LU-3871	10,940 ± 180	11,075 BC–10,725 BC
800–820	LU-3873	10,290 ± 220	10,500 BC–9270 BC
840–860	LU-3875	10,580 ± 390	11,075 BC–9390 BC

of bog evolution: lake, fen, intermediate, and raised bogs. The oligotrophic stage of the bog took place at the boundary of pollen zones SB-1 and SB-2 (3980 ± 120 BP).

The palynological and geochronological data (Chernova et al. 1997) indicate that xerophytic herbs (*Artemisia,* Chenopodiaceae) and low shrubs dominated here during the Younger Dryas. Sparse birch and pine forests were also found in the area.

In the Preboreal, sparse pine-birch forests developed, and thickets of dwarf birch, willow, and shrub heath were widespread. We dated the Younger Dryas/Preboreal boundary at around 10,520 BP.

During the Boreal, the forest-forming species were birch and pine. The broad-leaved species (elm and hazel first of all) found their way in, but their share of the forest composition was not significant. Sedges and graminoides dominated among the herbs. In the diagram, the upper boundary of the Boreal is defined by the important rise in pollen of the broad-leaved species. It was dated at 8120 ± 220 BP.

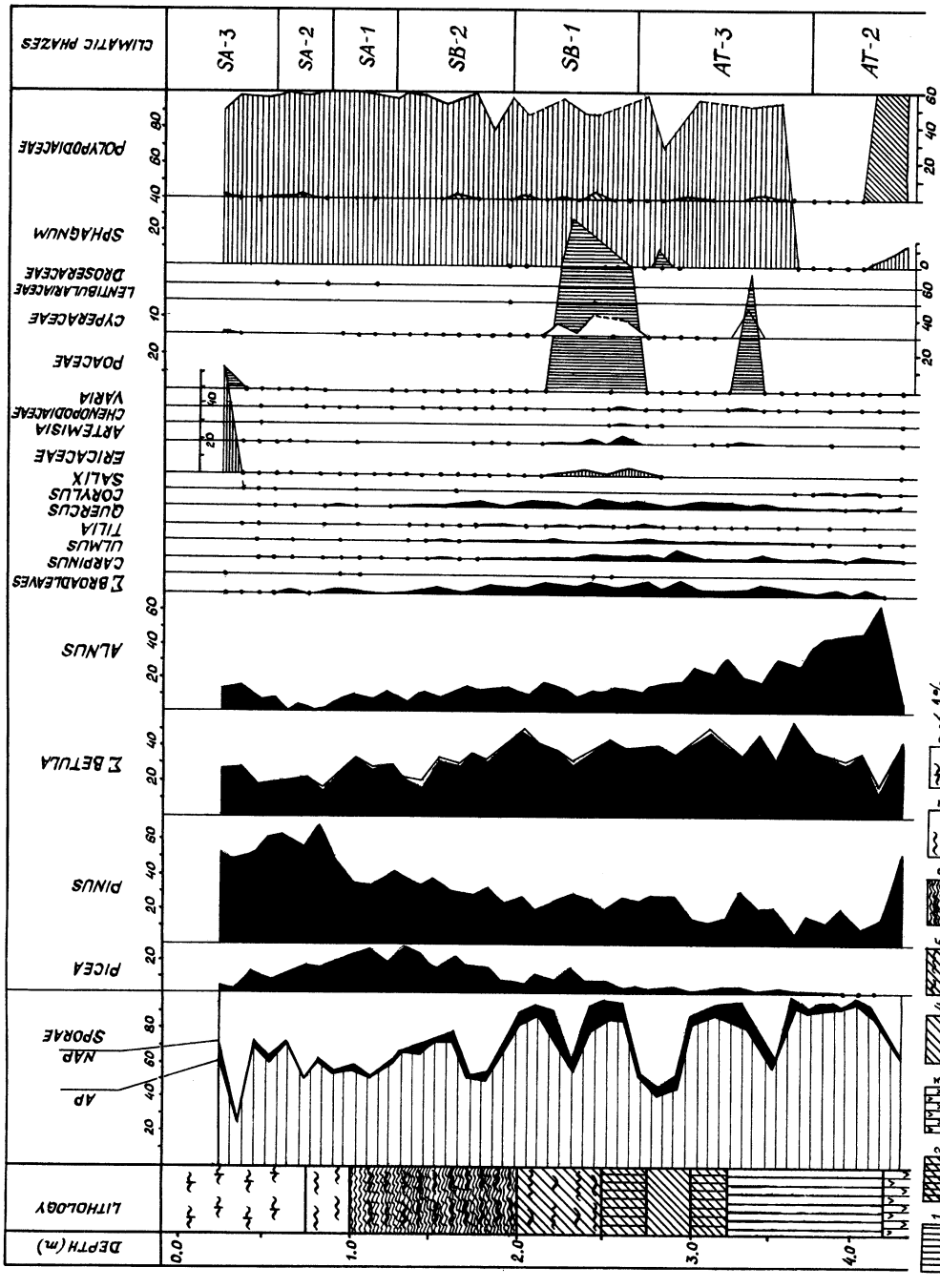

Figure 5 Chrono-palynological diagram of the Sakkala raised bog sediments. Symbols: 1. woody fen peat; 2. woody *Carex* fen peat; 3. woody grass fen peat; 4. *Carex* fen peat; 5. *Carex transitiona* peat; 6. *Eriophorum - Sphagnum* highbog peat; 7. *magellanicum* peat; 8. *foscum* peat.

TABLE 5. ^{14}C Dates of the Sakkala raised bog sediments

Depth (cm)	Lab code	^{14}C age (yr BP)	Calibrated age AD/BC (1σ)
20–30	LU-3718	270 ± 60	1514 AD–1802 AD
40–50	LU-3719	730 ± 50	1248 AD–1376 AD
70–80	LU-3754	1170 ± 60	792 AD–961 AD
80–90	LU-3721	1440 ± 70	554 AD–664 AD
90–100	LU-3798	1430 ± 70	554 AD–668 AD
110–120	LU-3799	1570 ± 80	422 AD–594 AD
120–130	LU-3723	2150 ± 60	350 BC–60 BC
140–150	LU-3724	2430 ± 100	760 BC– 400 BC
150–160	LU-3755	2650 ± 50	890 BC–790 BC
170–180	LU-3800	3430 ± 70	1872 BC–1626 BC
180–190	LU-3726	3360 ± 80	1736 BC–1526 BC
200–210	LU-3727	3830 ± 80	2450 BC–2142 BC
220–230	LU-3728	3880 ± 40	2452 BC–2292 BC
240–250	LU-3729	4150 ± 50	2870 BC–2618 BC
260–270	LU-3730	4330 ± 60	3032 BC–2884 BC
270–280	LU-3801	4490 ± 100	3340 BC–3040 BC
290–300	LU-3802	4790 ± 90	3658 BC–3380 BC
300–310	LU-3732	5380 ± 50	4326 BC–4102 BC
340–350	LU-3734	5170 ± 50	4038 BC–3822 BC
350–360	LU-3803	5720 ± 70	4674 BC–4470 BC
360–370	LU-3735	5840 ± 50	4780 BC–4620 BC
380–390	LU-3736	5950 ± 50	4904 BC–4784 BC
400–410	LU-3737	6130 ± 40	5196 BC–4960 BC
410–420	LU-3810	6320 ± 100	5420 BC–5080 BC
420–426	LU-3738	6370 ± 60	5422 BC–5258 BC

The damp and warm climate of the Atlantic was responsible for expansion of pine-birch forests with an admixture of broad-leaved species (elm, linden, and oak) and dark alder forests (*Alnus*, max 20% in AT-2). The upper boundary of the Atlantic was synchronous with the time of decreased pollen percentage of the broad-leaved species and also with increasing spruce pollen frequencies. Pollen zone AT-3 was characterized by the maximum percentage of broad-leaved pollen, including oak and beech (7%–9%).

During the Subboreal the contribution of broad-leaved species gradually reduced; however, in pollen zone SB-1 (as well as in AT-3) mixed broad-leaved forests were still widespread. Their share in the vegetation cover of the area declined in pollen zone SB-2; *Ulmus* pollen appeared first on the diagram but disappeared last (ca. 1140 ± 40 BP). The expansion of dark coniferous forests caused by increasing climatic moisture took place during pollen zone SB-2, SB-3, and most of the Subatlantic (SA-1 and SA-2), that is, within the age range of 3200–1000 BP.

During the Subatlantic, pine and birch-pine forests were widespread and the share of spruce gradually decreased. The percentage of spruce in the pollen spectra reached 40% within the time period ca. 3200–3000 BP, 20% within the limit ca. 2200–1100 BP, and did not exceed 4–5% from ca. 850 ± 40 BP to the present.

DISCUSSION

The arboreal (AP), herb (NAP), and spore (Sporae)-curves throughout the Holocene were compared for all the diagrams (Figs. 1–5). In pollen zone SA-3, the abrupt reduction in pollen percentages of arboreal species (AP) and increase of *Sphagnum* spores (with the exception of the Vishnevskoye Lake section) was clear-cut. All sections had similar *Picea*-curves including clear maxima in pollen percentages during the Subboreal. Toward the end of pollen zone SA-3 the frequency of spruce pollen decreases sharply (to 2–5%). The *Pinus*-curve was continuous throughout the entire Holocene with a noticeable increase of *Pinus* pollen value in the Subatlantic. The percentages of *Pinus* pollen in the bog sediments studied was less (on average) than in the Vishnevskoye Lake ones, where its percentages varied from 30% to 65% during the Holocene. This makes the reconstruction of forest composition using palynological data of these lake sediments difficult. The *Betula* curve was also unbroken throughout the Late Glacial and Holocene. The maximum amount of *Betula sect. Albae* pollen was noted in PB and BO and a relatively smaller maximum of it in SA. The maximum amount of *Betula sect. Fruticosae* pollen was observed in the Late Glacial, with smaller (except for one) in the Subatlantic sediments (see the Nikolsko-Lutinskoye and Sirinsky Mokh sections). The maximal amount of *Betula nana*-pollen was found in Late Glacial sediments.

All diagrams showed similarities in the *Alnus* curves and time-transgressive changes from alder on a north-south axis (Table 6). The appearance of alder in the southernmost section, Nikolsko-Lutinskoye, was dated at 9650 ± 240 BP and in the more northern Suo at 7770 ± 50 BP.

The beginning of the continuous curve for pollen of the broad-leaved species occurred in the BO. The distinct time-transgressive change in representation of the thermophilous flora from south to north and then its disappearance from the forests after the end of SB is notable (Table 6). The maximal total amount of the broad-leaved and hazel pollen corresponds to the end of the Atlantic (AT-3) in all bog sediments studied and to the beginning of AT (AT-1) in the lake sediments (the section from Vishnevskoye Lake).

The palynozones indicated on chrono-palynological diagrams (Figs. 1–5) were related to the ^{14}C scale by dating of nearly every 10 cm layer of sediments (Tables 1–5).

About 300 dates were obtained for 6 sections located in Leningrad and Novgorod provinces (Tables 1–5) and for 2 in Karelia (the results from the last 2 sections were published in Elina et al. (1996)). Such detailed investigations were carried out for the first time in this area. As a whole, we found that the palynological zones conformed with natural events equated to the climatic periods of the Blytt-Sernander scheme and subperiods (phases) according to Khotinsky (1977). Consideration of all the data obtained makes it possible to define the chronological boundaries between palynozones and the climatic phases (Table 7).

We used information-statistical methods (Klimanov 1976) to reconstruct the quantitative characteristics of the Late Glacial and Holocene climates. This method is based on the statistical correlation between data from recent spore-pollen spectra and recent climatic conditions; the average statistical error in determining the mean temperature for July and per year is ±0.6 °C, the mean for January is ±1 °C, and the average annual precipitation is ± 25 mm.

Paleoclimatic reconstructions were made for all 6 sections. The paleoclimatic curves show that they complement each other: for example, the Little Ice Age is reflected in more detail by the Lamin-Suo and Shirinsky Mokh sections, and the Subboreal by the Suo section. Figure 6 shows the correlation between the average annual paleotemperatures for all the sections studied and the time scale.

Table 6 Dynamics of the indicator arboreal species and alder during the Holocene in the area of modern Leningrad and Novgorod provinces

Section names	*Picea*		*Alnus*	Broad-leaved species						*Corylus*	
				Total pollen sum			*Ulnus*	*Tilia*	*Quersus*		
	EB[a]	Abrupt reduction	EB	EB	Maximum	Abrupt reduction	EB	EB	EB	EB	Abrupt reduction
Nikolsko-Lutinskoye	9040 ± 250	Between 600 ± 50 and 720 ± 170	Between 9650 ± 240 and 10,360 ± 140	9040 ± 160	Between 4320 ± 60 and 4350 ± 80	780 ± 70	9040 ± 160	7060 ± 80	6450 ± 90	9040 ± 250	2320 ± 80
Shirinsky Mokh	8400 ± 50	Between 100 ± 40 and 240 ± 60	8230 ± 70	Between 8400 ± 70 and 8590 ± 70	Between 4590 ± 60 and 5030 ± 90	980 ± 40	Between 8400 ± 70 and 8590 ± 70	7630 ± 70	Between 6120 ± 100 and 6640 ± 80	8580 ± 50	2820 ± 60
Lammin-Suo	Between 6590 ± 60 and 6860 ± 60	Between 490 ± 60 and 650 ± 80	7770 ± 50	7770 ± 50	5610 ± 70	Between 1410 ± 50 and 650 ± 80	7770 ± 50	7170 ± 70	Between 6590 ± 60 and 6860 ± 60	7490 ± 90	3120 ± 60
Vishnevskoye Lake	Between 7690 ± 190 and 8270 ± 260	<1600 ± 80	9170 ± 170	9170 ± 170	Between 7030 ± 330 and 7690 ± 190	Between 2580 ± 150 and 2990 ± 110	9170 ± 170	Between 7690 ± 190 and 8270 ± 260	Between 5560 ± 170 and 5600 ± 100	9670 ± 200	Between 4610 ± 90 and 4730 ± 130
Sakkala	5950 ± 50	<730 ± 50	—	—	4490 ± 1000	2650 ± 50	—	5840 ± 50	5170 ± 50	—	3830 ± 80
Suo	Between 4620 ± 160 and 6110 ± 60	850 ± 40	Between 6770 ± 180 and 9000 ± 230	Between 6780 ± 180 and 9000 ± 230	Between 4620 ± 160 and 6110 ± 220	3210 ± 80	Between 6780 ± 180 and 9000 ± 230	Between 4620 ± 160 and 6110 ± 220	Between 4140 ± 120 and 4250 ± 90	Between 6780 ± 180 and 9000 ± 230	Between 4140 ± 130 and 425 ± 90

[a]The empirical boundary (EB) is a level after which pollen of a particular species occurs constantly (Neustadt 1965).

The values of annual precipitation could not be averaged because there was no clear correlation between precipitation and temperatures in different sections and the data only show local changes.

In the graph, the changes of paleotemperatures ($\Delta t°_a$) are represented as variations from recent temperature values (Fig. 6). Recent climatic parameters (Climatic Atlas 1990) for the sections under study were, on average, as follows: mean July temperatures around 17–18 °C, mean January temperatures 8–9 °C, average annual temperature 3–5 °C and average precipitation of 600 mm per year.

We will not discuss here the quantitative characteristics of $\Delta t°_a$ because they are shown in the figures. We shall consider the time of extremes of climatic deterioration and amelioration. The oldest ^{14}C date (ca. 11,270 BP) obtained for the section Nikolsko-Lutinskoye delineated the maximum of the Allerød climatic amelioration. The date of ca. 10,680 BP registers the maximum of the climatic deterioration in DR-3, a date very close to the those for climatic deterioration in other regions of Northern Eurasia (ca. 10,500 BP). It should be noted that during all periods of the Late Glacial, there was less precipitation than now; when the natural conditions changed to cold ones, the quantity of precipitation was reduced, and vice versa. During the Preboreal we noted 2 climatic ameliorations (ca. 10,000 and 9400 BP) and 2 deteriorations (ca. 9600 and 9100 BP). In the Boreal we recorded 3 climatic ameliorations and 3 deteriorations with one average maximal climatic amelioration, which took place in the territory of Northern Eurasia around 8500 BP.

One more climatic deterioration was noted at the boundary of BO and AT. It was dated at ca. 8200 BP. After that, the temperatures did not fall below recent values during the entire Atlantic; this fact had been observed earlier in Karelia (Elina et al. 1996). A number of climatic ameliorations separated by deteriorations have been reconstructed for the Atlantic (see Fig. 6). As a whole, their ^{14}C dates are very similar for all sections and have been found to be in good agreement with dates obtained earlier for other regions of Northern Eurasia. We recorded a climatic deterioration at the boundary of the AT and SB dated at ca. 4500 BP. In the Subboreal, a number of climatic ameliorations with a maximum ca. 3500 BP was noted. At the boundary of SB and SA, the climatic deterioration was dated 2500 BP. During the Subatlantic, a number of climatic ameliorations are clearly evident in Figure 1 of the Nikolsko-Lutinskoye section. The little climatic optimum of the Middle Ages and the Little Ice Age are well expressed here; during the Little Ice Age, climatic ameliorations and deteriorations were repeated again and the maximal deterioration was dated at ca. 200 BP.

Thus, this meticulous study of the sections, both palynologically and using the ^{14}C method, enables us to trace the detailed dynamics of climatic changes during the Holocene. It is evident from the paleoclimatic curves that the trend was towards warmer natural conditions from the Late Glacial to the Holocene optimum (ca. 5000–6000 BP) and then toward colder ones. The trend toward climatic deterioration during the Little Ice Age is very clear. The amplitudes of changes in winter temperatures were greater than those of summer ones. As a whole, the ^{14}C dates of climatic ameliorations and deteriorations (within the limits of the method's error) confirm each other well, with both the data of the sections under study and those studied earlier (Klimanov 1989; Elina et al. 1996); thus, they support the hypothesis that large climatic changes (above all, temperatures) were synchronous in the past. As for precipitation, there is no distinctive correlation for different regions and different periods, but it can be said that in the region under study, climatic ameliorations were followed by increased precipitation, and vice versa, decreased precipitation followed the deteriorations.

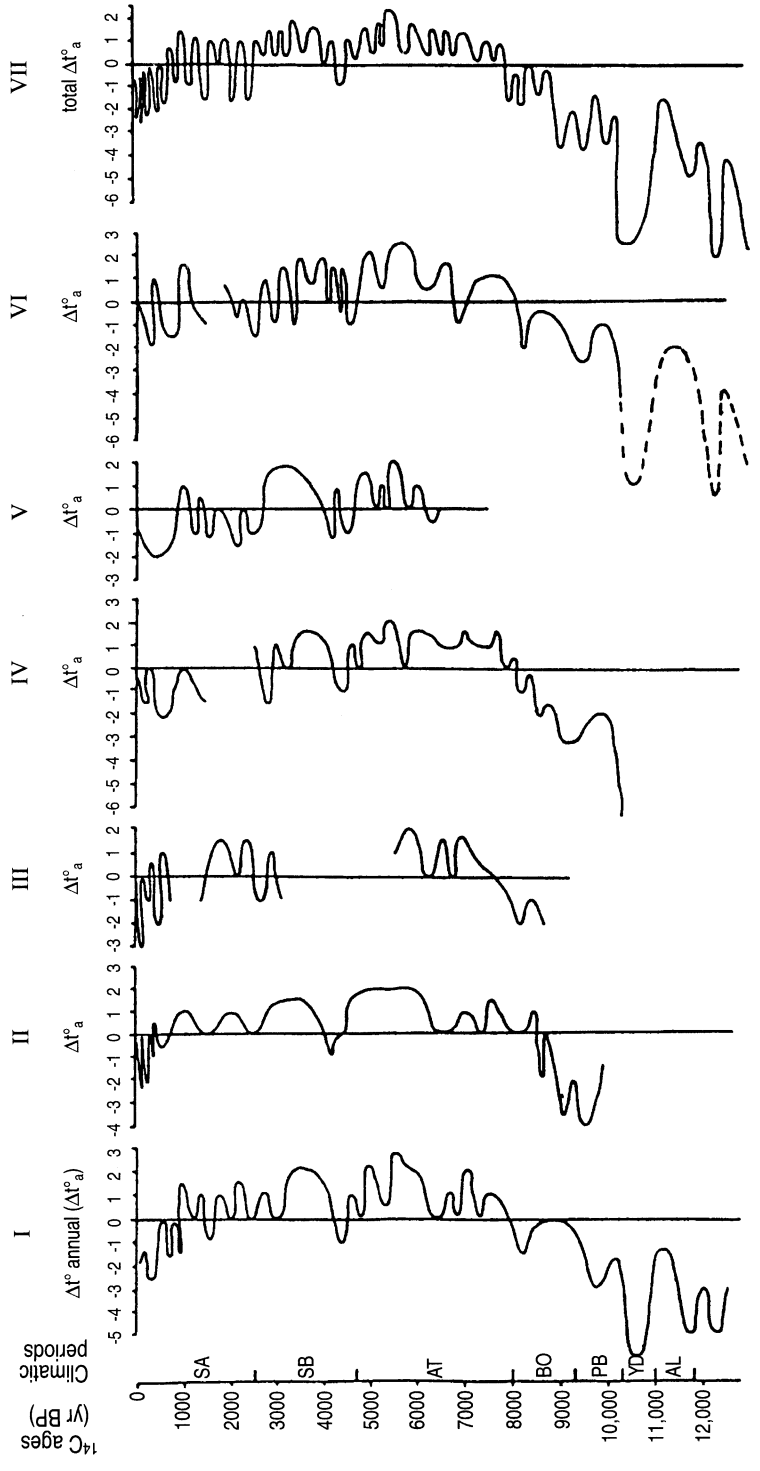

Figure 6 Deviations of the average annual temperatures ($\Delta t°_a$) from the recent temperature values during the Late Glacial and Holocene in Northwestern Russia reconstructed on the basis of chrono-palynological data of the bog and lake sediments studied. I. Nikolsko-Lutinskoye bog section; II. Shirinsky Mokh bog section; III. Lammin-Suo bog section; IV. Vishnevskoye Lake section; V. Sakkala bog section; VI. Suo bog section; VII. Total curve of annual temperature deviations.

Table 7 ^{14}C Chronology of Holocene climatic periods and subperiods (phases) in northwestern Russia[a]

Climatic period	Climatic phase	^{14}C age (yr BP)
Preboreal	PB-1	10,000–9800
	PB-2	9800–9300
Boreal	BO-1	9300–9000
	BO-2	9000–8500
	BO-3	8500–8000
Atlantic	AT-1	8000–7000
	AT-2	7000–6000
	AT-3	6000–4700
Subboreal	SB-1	4700–4200
	SB-2	4200–3100
	SB-3	3100–2500
Subatlantic	SA-1	2500–1700
	SA-2	1700–800
	SA-3	800–0

[a]As new data become available, this scale will be made more precise.

CONCLUSION

For the first time, detailed palynological and geochronological studies have been made of sections of continuous bog and lake sediments of northwestern Russia to mark out palynological zones, date them by the ^{14}C method, and correlate them with climatic periods and phases. The data obtained enable us to reconstruct a vegetation history and to monitor the forest dynamics of northwestern Russia as well as the gradual appearance of the indicator species of trees from the Preboreal onwards. We have set up a ^{14}C chronology for the stages of vegetation development and paleoclimate changes during the Holocene.

ACKNOWLEDGMENTS

We are grateful to Fedor Maksimov, Elena Makarova, and Valentina Andrutskaya for the chemical treatment of samples, for dating, and for palynological analysis. This work was supported by the Russian Foundation of Fundamental Research (Grants N 94-05-17670 and N 96-05-6167).

REFERENCES

Arslanov KhA, Davydova NN, Subetto DA, Khomutova VI. 1992. Lake history of the Northern part of the East European Lowland: Karelian Isthmus. In: Davydova NN, Kabaylene MV, Raukas AV and Jakushko OF, editors. *Lake history of the East European lowland.* St Petersburg: Nauka Publishing House. p 50–77 (in Russian).

Arslanov KhA, Tertychnaya TV, Chernov SB. 1993. Problems and methods of dating low activity samples by liquid scintillation counting. *Radiocarbon* 35(3): 393–8.

Arslanov KhA, Cook GT, Gulliksen S, Harkness DD, Kankainen T, Scott EM, Vartanyan S, Zaitseva G. 1998. Consensus dating of mammoth remains from Wrangel Island. *Radiocarbon* 40(1):289–294.

Broecker WS and Walton A. 1959. ^{14}C from nuclear tests. *Science* 130(3371):309.

Chernova GM, Arslanov KhA, Denisenkov VP, Sevastjanov DB, Tertychnaya TV, Okuneva EJu and Chernov SB. 1997. Paleoecology and the biological variety of vegetation of the northwestern Lake Ladoga area during the Holocene. *Vestnik of St. Petersburg University Ser.* 7; 4:128–37 (in Russian).

Climatic Atlas of the USSR. 1990. Vol 1.

Elina GA, Arslanov KhA, Klimanov VA. 1996. Development stages of Holocene vegetation in Southern and

Eastern Karelia. *Botanical Journal* 81(3):1–17 (in Russian).

Khomutova VI. 1995. The significance of zonal, regional and local vegetation elements in lacustrine pollen spectra. *Granna* 34:246–50.

Khotinsky NA. 1977. *The Holocene of northern Eurasia*. Moscow: Nauka Publishing House. 200 p (in Russian).

Klimanov VA. 1976. On the procedure of reconstruction of quantitative climatic characteristics of the past. *Vestnik of Moscow State University Geographical Series* 2:92–8 (in Russian).

Klimanov VA. 1989. *Cyclic recurrence and quasiperiodicity of climatic changes during the Holocene*. Moscow: 100 p (in Russian).

Kuzmin GF, Dzyba OF, Kleymenova GI. 1985. Dynamics of peat accumulation of the raised bog system. *Vestnik of Leningrad University Geographical Series* 28(4):103–112 (in Russian).

Levin I, Munnich KO, Weiss W. 1980. The effect of anthropogenic CO_2 and ^{14}C sources on the distribution of ^{14}C in the atmosphere. *Radiocarbon* 22(2):379–91.

McNeely R. 1994. Long-term environmental monitoring of ^{14}C levels in the Ottawa region. *Environment International* 20(5):675–9.

Neustadt MI. 1965. On the methods of Holocene sediment study and the terms applied. In: Neustadt M, editor. *Paleogeography and chronology of the late Pleistocene and Holocene*. Moscow: Publishing House of Academy of Sciences. p 66–9 (in Russian).

Nilsson T. 1964. Standardpollendiagramme und C^{14}-datierungen aus dem Ageröds mosse im mittleren Schonen. *Lunds Universitets Årsskrift* 59(7):1–52.

Scott M, Harkness D, Cook G. 1997. *TIRI: report on the Third International Radiocarbon Intercomparison*. University of Glasgow technical report.

RADIOCARBON, Vol 41, Nr 1, 1999, p 47–50

THE MAUNDER MINIMUM: AN INTERLABORATORY COMPARISON OF $\Delta^{14}C$ FROM AD 1688 TO AD 1710

Paul E Damon • Christopher J Eastoe

Department of Geosciences, PO Box 210077, University of Arizona, Tucson, Arizona 85721 USA

Irina B Mikheeva

AF Ioffe Institute of Physics and Technology, Russian Academy of Science, St Petersburg, Russia

ABSTRACT. Measurements on same-age tree-ring samples from proximal Ural Mountain trees by the Ioffe Institute research group and at the University of Arizona demonstrate a variance corresponding to a standard deviation of ±5.1‰ for Ioffe compared to ±2.1‰ for Tucson. There is also a calibration difference of 4.3 ± 1.2 $\bar{\sigma}$‰. Comparison of the same years measured in Seattle on wood from the Pacific Northwest shows an offset of 2.2 ± 0.5 $\bar{\sigma}$‰. This is not a calibration error, but rather is expected from the well-documented evidence for divergence and upwelling of ^{14}C-depleted CO_2 along the west coast of North America.

INTRODUCTION

Professor Grant Kocharov, head of the Astrophysics Section of the Ioffe Institute in St Petersburg, Russia, realized early the importance of radiocarbon research in obtaining information concerning paleosolar physics. Consequently, he encouraged and helped support the dendrochronological research of Professor Bitvinskas in Lithuania and a ^{14}C laboratory in Georgia. His research group also built a ^{14}C laboratory at the Ioffe Physical Technical Institute in Leningrad. Unfortunately, because they were isolated from the mainstream of ^{14}C geophysics research in the West, they were unable to participate in workshops and intercalibration studies that helped workers in the United States and Europe achieve the high precision and accuracy required in paleosolar physics research. Accordingly, Professor Kocharov supplied us with tree-ring samples from the relatively flat ^{14}C maximum resulting from the Maunder Minimum of solar activity (AD 1688–1710) for an intercomparison. The tree-ring samples from the Ural Mountains were dendrochronologically dated by Dr T T Bitvinskas of the Institute of Botany in Kaunas, Lithuania and they are the same samples measured for $\Delta^{14}C$ by Kocharov's research group (Galli et al. 1987).

RESULTS AND EVALUATION

$\Delta^{14}C$ values measured in the Laboratory of Isotope Geochemistry, the University of Arizona, are presented in Table 1 and plotted in Figure 1 along with the measurements published in Galli *et al.* (1987) and data determined at the University of Washington, Seattle, on single-year Douglas-fir tree rings (Stuiver and Braziunas 1993). Table 2 presents an intercomparison of these measurements.

We ascribe the 2.2 ± 0.5 $\bar{\sigma}$ ‰ offset between Tucson and Seattle to the west coast regional effect due to upwelling and atmospheric exchange of ^{14}C-depleted oceanic CO_2 at the divergent margin produced by the Ekman spiral (Kennett 1982; Damon et al. 1989; McCormac et al. 1995; Damon 1995; Southon and Baumgartner 1996; Stuiver and Braziunas 1998). No significant calibration offset is apparent between the Tucson and Seattle laboratories (Kalin et al. 1995; Damon et al. 1998). The 4.3 ± 1.2 $\bar{\sigma}$ ‰ offset between Ioffe and Tucson does reveal a calibration offset. The difference between the variance for both the Seattle and Tucson results ($\sigma_m^2 - \sigma_p^2$) yields a standard deviation (σ_s) of 1‰. This 1‰ σ_s is an approximation of the real variance of the signal independent of the measurement error; it may be compared to the estimate of an average amplitude of the approximately 11-yr cycle of 1.40 ± 0.16‰ for the period of time from AD 1510 to AD 1945 (Stuiver and Braziunas 1993). For the 22 yr at the flat minimum preceding the Maunder Minimum from AD 1619 to AD 1640, we obtained a variance of 3.24 yielding a σ_s of about 1.8‰ from the Stuiver and Bra-

Table 1 Results of $\Delta^{14}C$ measurements on dendrochronologically dated tree rings from AD 1688 to 1710

Year	$\Delta^{14}C$ (‰)	$\delta^{13}C$ (‰)
1688	16.1 ± 1.9	−22.7
1690	14.4 ± 1.9	−22.2
1691	16.9 ± 1.9	−22.5
1692	15.6 ± 1.8	−22.2
1693	16.7 ± 1.8	−21.9
1694	15.9 ± 1.8	−22.2
1695	14.0 ± 1.7	−22.1
1696	18.6 ± 1.8	−22.1
1697	16.8 ± 1.8	−22.5
1698	15.1 ± 1.8	−22.2
1699	19.9 ± 2.0	−22.7
1701	19.8 ± 1.7	−22.7
1702	18.7 ± 1.8	−22.3
1703	16.9 ± 1.7	−23.0
1704	20.4 ± 1.8	−22.8
1705	17.0 ± 2.0	−21.8
1706	20.0 ± 1.7	−22.0
1707	19.4 ± 2.1	−22.2
1708	18.3 ± 1.8	−22.3
1710	13.8 ± 1.8	−21.8

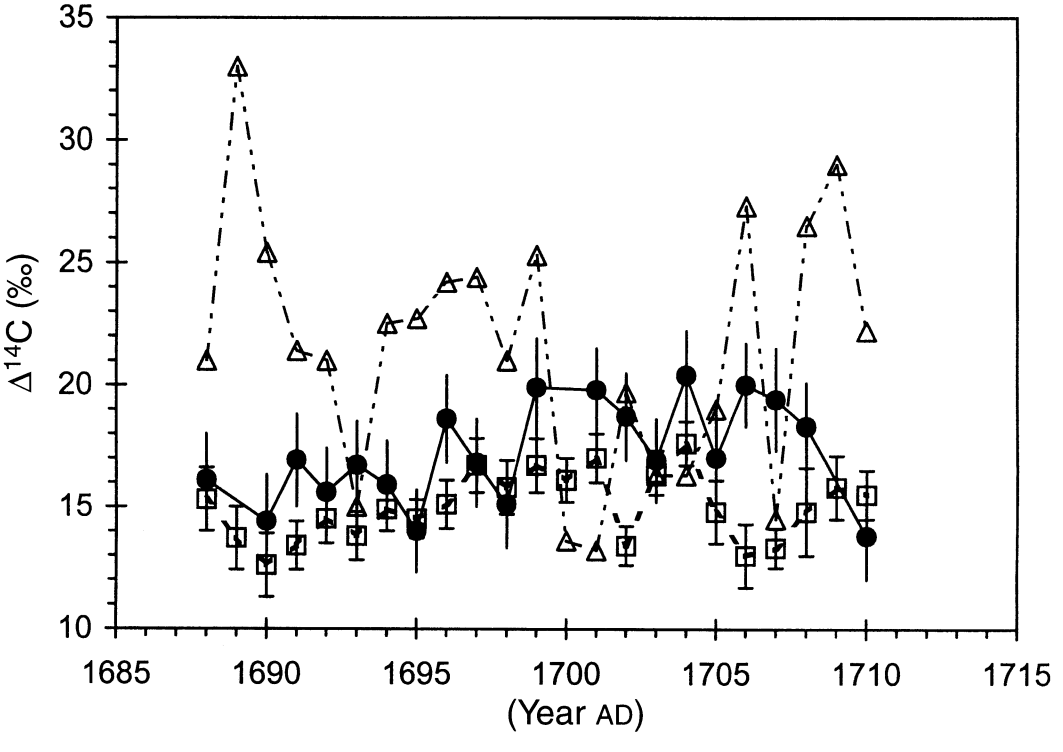

Figure 1 The results of $\Delta^{14}C$ measurements in tree-rings of 1688–1700 AD according to the present work (●); Stuiver and Braziunas (1993) (□); Galli et al. (1987) (△).

Table 2 Intercomparison of measurements on single-year tree rings for the interval AD 1688–1710

	Ioffe (1) (‰)	Tucson (2) (‰)	Seattle (3) (‰)
$\bar{\chi}$	21.5	17.2	15.0
σ_m	5.1	2.1	1.4
σ_p	?	1.8	1.1

$\bar{\chi}$ = mean value; σ_m = measured; σ_p = average Poisson counting precision
(1) Galli *et al* 1987; (2) this paper; (3) Stuiver and Braziunas 1993

ziunas (1993) data. The lower σ_s during the Maunder Minimum is compatible with the presence of the 22-yr cycle and suppression of the 11-yr cycle (Peristykh and Damon 1998) as suggested by Vasiliev and Kocharov (1983).

CONCLUSION

$\Delta^{14}C$ measurements on same-age samples measured under the direction of Professor Kocharov and also measured at the University of Arizona demonstrate a greater variance for the Ioffe Institute results, corresponding to a standard deviation of ±5.1‰ (σ_m) compared to the Tucson results of ±2.1‰ (σ_m). Konstantinov et al. (1997) also concluded, in explaining the differences in data series, that the experimental errors of the Soviet data are much greater than ±3‰. The Tucson–Ioffe calibration offset is 4.3 ± 1.2 $\bar{\sigma}$ ‰. We ascribe an offset between Tucson measurements and Seattle measurements of 2.2 ± 0.5 $\bar{\sigma}$ ‰ to divergence and upwelling of ^{14}C-depleted CO_2 along the west coast of North America. This divergence is caused by the wind-driven Ekman Transport and ocean currents diverted by coriolis force that result in the Ekman Spiral and west coast divergence and upwelling. The high-precision results from Seattle and Tucson also demonstrate a flat $\Delta^{14}C$ maximum corresponding to the Maunder Minimum, with variance and standard deviation around ±1‰.

ACKNOWLEDGMENTS

We greatly appreciate Professor Grant Kocharov of the Ioffe Institute in St Petersburg for making available the Ural Mountain tree rings that made this study possible. This work was supported by NSF Grant ATM-9520135 and the state of Arizona.

REFERENCES

Damon PE. 1995. A note concerning "Location-dependent differences in the ^{14}C content of wood" by McCormac et al. *Radiocarbon* 37(2):829–30.

Damon PE, Cheng S, Linick TW. 1989. Fine and hyperfine structure in the spectrum of secular variations of atmospheric ^{14}C. *Radiocarbon* 31(3):704–18.

Damon PE, Eastoe CJ, Hughes MK, Kalin RM, Long A, Peristykh AN. 1998. Secular variation of $\Delta^{14}C$ during the Medieval Solar Maximum: a progress report. *Radiocarbon* 40(1):343–350.

Galli M, Castagnoli CC, Attolini MR, Cechini S, Nanni T, Kocharov GE, Mikheeva IB, Bitvinskas TT, Konstantinov AN, Metskhvarishvili RYa. 1987. A 400-year ^{14}C record: 11-year and longer cycles. In: Chudakov E, editor. *Proceedings of the 20th International Cosmic Ray Conference, Moscow;* Vol 4. Moscow: Nauka. p 280–3.

Kalin RM, McCormac FG, Damon PE, Eastoe CJ, Long A. 1995. Intercomparison of high-precision ^{14}C measurements at the University of Arizona radiocarbon laboratory. *Radiocarbon* 37(1):33–8.

Kennett JP. 1982. *Marine geology.* Englewood Cliffs (NJ): Prentice Hall. 813 p.

Konstantinov AN, Krasiljschikov AM, Lazarev VE, Mikheeva IB. 1997. On the variation of ^{14}C in the Earth's atmosphere in the last 400 years. *Izvestiia Akademii Nauk, seriia fizicheskaia* 61(6):1242–8 (in Russian).

McCormac FG, Baillie MGL, Pilcher JR, Kalin RM. 1995. Location-dependent differences in the ^{14}C content of wood. *Radiocarbon* 37(2):395–407.

Peristykh AN, Damon PE. 1998. Modulation of atmo-

spheric ^{14}C concentration by the solar wind and irradiance components of the Hale and Schwabe solar cycles. *Solar Physics* 177(1/2):343–55.

Southon JR, Baumgartner TA. 1996. A long-term record of upwelling from the Santa Barbara basin, Southern California. *Radiocarbon* 38(1):114.

Stuiver M, Braziunas TF. 1993. Sun, ocean, climate and atmospheric CO_2: an evaluation of causal and spectral relationships: *Holocene* 3(4):289–305.

Stuiver M, Braziunas TF. 1998. Anthropogenic and solar components of hemispheric ^{14}C. *Geophysical Research Letters* 25(3): 329–32.

Vasiliev VA and Kocharov GE. 1983. On the solar activity dynamics during the Maunder Minimum. In: Kocharov GE, editor. *Trudy XIII Leningradskogo Seminara po Kosmofizike* (Proceedings of the XIII Leningrad Seminar on Space Physics). Leningrad: Nauka. p 75–100 (in Russian).

RADIOCARBON, Vol 41, Nr 1, 1999, p 51–73

OCEANIC RADIOCARBON BETWEEN ANTARCTICA AND SOUTH AFRICA ALONG WOCE SECTION I6 AT 30°E

Viviane Leboucher[1] • James Orr[2] • Philippe Jean-Baptiste[2] • Maurice Arnold[1] • Patrick Monfray[1]
Nadine Tisnerat-Laborde[1] • Alain Poisson[3] • Jean-Claude Duplessy[1]

ABSTRACT. Accelerator mass spectrometry (AMS) radiocarbon measurements were made on 120 samples collected between Antarctica and South Africa along 30°E during the WOCE-France CIVA1 campaign in February 1993. Our principal objective was to complement the Southern Ocean's sparse existing data set in order to improve the ^{14}C benchmark used for validating ocean carbon-cycle models, which disagree considerably in this region. Measured ^{14}C is consistent with the θ-S characteristics of CIVA1. Antarctic Intermediate Water (AAIW) forming north of the Polar Front (PF) is rich in ^{14}C, whereas surface waters south of the PF are depleted in ^{14}C. A distinct old ^{14}C signal was found for the contribution of the Pacific Deep Water (PDW) to the return flow of Circumpolar Deep Waters (CDW). Comparison to previous measurements shows a ^{14}C decrease in surface waters, consistent with northward displacement of surface waters, replacement by old deep waters upwelled at the Antarctic Divergence, and atmospheric decline in ^{14}C. Conversely, an increase was found in deeper layers, in the AAIW. Large uncertainties, associated with previous methods for separating natural and bomb ^{14}C when in the Southern Ocean south of 45°S, motivated us to develop a new approach that relies on a simple mixing model and on chlorofluorocarbon (CFC) measurements also taken during CIVA1. This approach leads to inventories for CIVA1 that are equal to or higher than those calculated with previous methods. Differences between old and new methods are especially high south of approximately 55°S, where bomb ^{14}C inventories are relatively modest.

INTRODUCTION

The Southern Ocean extends south to Antarctica and north to the Subtropical Front (STF), which meanders between 40°S and 50°S. As such, the Southern Ocean covers about 21% of the world's ocean surface. Within the Southern Ocean, large vertical exchanges take place between water masses. Important processes include ventilation of deep waters at the Antarctic Divergence Zone (ADZ, ca. 65°S), production of ventilated bottom waters in the Weddell Sea and around the Antarctic continental slope, and formation of Antarctic Intermediate Water (AAIW) within the Polar Frontal Zone (PFZ) between the Polar Front (PF) and the Subantarctic Front (SAF).

The Southern Ocean is considered to be a major sink for anthropogenic CO_2 (Sarmiento et al. 1992). However, for this region, there is substantial disagreement between carbon-cycle simulations from different ocean general circulation models (OGCMs), which offer the only means to estimate future oceanic CO_2 uptake (Orr 1996). Radiocarbon is routinely used to evaluate the performance of such models (Toggweiler et al. 1989a, 1989b; Maier-Reimer 1993; Taylor 1995; Orr 1996). However, few ^{14}C data are available in the remote Southern Ocean, where both the spatial and temporal changes in ^{14}C are important. Here, we provide ^{14}C data to complement the sparse established dataset. Previous ^{14}C measurements include those from GEOSECS (Geochemical Ocean Sections Study) during 1973–1978 (Östlund and Stuiver 1980; Stuiver and Östlund 1980; Stuiver et al. 1981), from the Winter Weddell Sea Experiment (WWSP) in 1986 (Schlosser et al. 1994), and from INDIGO (Indian Gas Ocean project) in 1985–1987 (Östlund and Grall 1988). The ^{14}C data presented here were collected during CIVA1 (Circulation et Ventilation dans l'Antarctique) of WOCE-France taken in February–March 1993. Measurements of ^{14}C were made by AMS in Gif-sur-Yvette, France.

[1]Laboratoire des Sciences du Climat et de l'Environnement (LSCE), Avenue de la Terrasse, F-91198 Gif-sur-Yvette Cedex, France
[2]Laboratoire des Sciences du Climat et de l'Environnement (LSCE), DSM/CEN Saclay/CEA, L'Orme, Bât. 709, F-91191 Gif-sur-Yvette Cedex, France
[3]Laboratoire de Physique et Chimie Marines (LPCM), Université Pierre et Marie Curie, 4, place Jussieu, F-75252 Paris Cedex 05, France

Oceanic ^{14}C must be separated into its natural and anthropogenic components if it is to be useful for model validation. Natural ^{14}C is produced by cosmic radiation and can be considered at present to be in steady state with respect to the vertical turnover time of the ocean (ca. 1000 yr). Bomb ^{14}C was injected in the atmosphere nearly exclusively by atmospheric thermonuclear weapons tests during the 1950s and 1960s. At its peak in 1963, the nuclear contribution nearly doubled prenuclear atmospheric levels of ^{14}C. Since then, atmospheric ^{14}C has decreased. At present, levels are roughly 10% higher than in the prenuclear period. Both ^{14}C components are transferred to the ocean by air-sea gas exchange as $^{14}CO_2$. With its steady-state production and 5730 yr half-life, the natural component of ^{14}C is useful for evaluating modeled deep-ocean circulation fields. Bomb ^{14}C has had much less time to invade the ocean. Because its boundary conditions have changed rapidly since the late 1950s, bomb ^{14}C is useful for evaluating near-surface circulation fields predicted by ocean models.

To separate natural and bomb ^{14}C, we first applied the method developed by Broecker et al. (1995), which relies on the near linear correlation between natural $\Delta^{14}C$ and dissolved silica throughout much of the ocean. However, for the stations situated south of 45°S (~90% of samples collected here), uncertainties associated with Broecker et al.'s method are large. Since the GEOSECS campaign in the 1970s, it has become less certain that deep waters remain uncontaminated with bomb ^{14}C, as supposed by Broecker et al. (1995) for GEOSECS era samples. To take this possibility into account, we modified the bomb versus natural separation methodology for our samples taken south of 45°S. Our new method takes advantage of CFC-11 and CFC-12 measured during CIVA1 and uses a simple ventilation model, similar to that used in previous tracer studies (Jenkins 1980; Andrié et al. 1986; Haine 1996).

METHODS

The ^{14}C data (Table 1) were obtained following the procedure described by Bard et al. (1987) and Arnold et al. (1987). Seawater was collected in 12-L Niskins. Once aboard ship, seawater was transferred to 250 mL borosilicate bottles and poisoned with 1 mL of saturated $HgCl_2$ solution. The borosilicate bottles were then sealed. Back in the laboratory, CO_2 was extracted by adding 2 mL of 15N H_3PO_4 to a 100 mL seawater aliquot in a vacuum-tight system sparged by He gas (flow rate 80 mL min^{-1}). Extraction required 1 h. Water was removed by traps at −80°C; CO_2 was trapped at −180°C. Subsequently, CO_2 was reduced to graphite using hydrogen in the presence of iron powder (6–8 h). The carbon-iron mixture was divided into 3 parts, then pressed into an aluminum target for accelerator mass spectrometry (AMS) analysis. Usually, 2 or 3 targets per sample were analyzed to obtain a precision close to ±5‰. The 3 isotopes, ^{12}C, ^{13}C and ^{14}C, were measured directly in the AMS system to calculate $\Delta^{14}C$ normalized to a $\delta^{13}C$ of −25‰. The data are expressed as $\Delta^{14}C$ in per mil (Stuiver and Polach 1977).

RESULTS

To establish the level of agreement of our ^{14}C CIVA1 measurements with previous data, Figure 1 provides ^{14}C profiles from station 442 of GEOSECS (1978) and from station 1 of JADE1 (Java Australia Dynamic Experiment 1989) cruise, both taken at the same location (1°S, 91°E) in the equatorial Indian Ocean. The ^{14}C measurements from JADE1 were made in Gif-sur-Yvette by AMS just prior to those of CIVA1. JADE1 and CIVA1 samples received identical processing. The deep portions of GEOSECS and JADE1 profiles, where bomb ^{14}C has not penetrated, agree to within the precision of the measurements. Therefore, our ^{14}C measurements by AMS are consistent with those from GEOSECS, determined by β-counting. Furthermore, the methodology used at Gif-sur-Yvette has been previously checked by directly comparing β-counting and AMS measurements performed on the same samples from INDIGO (Bard et al. 1988).

Table 1 Data for the stations occupied during the CIVA1 cruise

Depth (m)	Potential temp. (°C)	Salinity (S, psu)	Sig 0	SiO_2 (μmol kg^{-1})	SCO_2 (mmol kg^{-1})	CFC-11 (pmol kg^{-1})	CFC-12 (pmol kg^{-1})	Num. of meas.	$\Delta^{14}C$ (‰)	Nat. $\Delta^{14}C$ (‰)	Bomb $\Delta^{14}C$ (‰)
Station 6	*68°S, 30°E*										
10.2	0.2009	33.915	27.218	62.25	2149	6.76	2.92	2	−97 ± 4	−132	35
19.9	0.1145	33.919	27.225	62.25	2152	6.72	2.93	2	−97 ± 4	−132	36
40	−0.1182	33.933	27.249	63.06	2160	6.7	2.86	2	−98 ± 4	−133	35
100.6	−1.7636	34.35	27.651	68.77	2217	5.68	2.47	2	−114 ± 4	−139	25
150.5	−1.6967	34.371	27.665	70	2210	5.59	2.45	2	−117 ± 4	−140	23
199.7	−0.5536	34.468	27.708	83.5	2240	3.59	1.52	2	−141 ± 4	−154	13
324.4	0.7518	34.642	27.773	99.93	2247	1.14	0.46	2	−165 ± 4	−176	11
698.8	0.7136	34.693	27.816	115.4	2254	0.58	0.23	2	−157 ± 4	−163	6
998.8	0.4484	34.687	27.829	124.7	2266	0.46	0.18	2	−157 ± 4	−162	5
1198.8	0.2899	34.683	27.833	130.9	2264	0.41	0.17	2	−164 ± 4	−168	4
2247.1	−0.2104	34.666	27.847	136.3	2260	0.56	0.21	2	−158 ± 4	−163	6
2497.6	−0.2729	—	27.848	135.6	2258	0.64	0.24	2	−153 ± 4	−159	6
2997.6	−0.378	34.665	27.851	136.3	2253	0.91	0.36	3	−145 ± 7	−153	9
3495.9	−0.4769	34.655	27.852	137.1	2254	1	0.41	2	−157 ± 4	−167	10
3681.3	−0.5667	34.655	27.855	137.1	—	0.99	0.4	2	−162 ± 4	−171	10
Station 8	*67°S, 30°E*										
10.6	0.646	33.866	27.155	60	2158	6.58	2.89	2	−97 ± 4	−130	33
20.2	0.6406	33.869	27.155	60	2164	6.57	2.84	2	−97 ± 5	−130	33
40	−1.505	34.249	27.568	60.77	2197	5.7	2.46	2	−104 ± 4	−131	27
80.8	−1.7041	34.356	27.653	65.5	2216	5.43	2.36	2	−103 ± 4	−136	33
124.7	−1.142	34.412	27.682	71.02	2228	4.62	1.95	2	−111 ± 4	−141	30
175.9	0.4412	34.564	27.729	86.01	2255	2	0.85	2	−130 ± 5	−156	26
322.1	1.1479	34.679	27.778	92.69	2266	0.74	0.29	2	−155 ± 5	−162	7
598.4	1.0146	34.708	27.812	102.5	2263	0.39	0.15	2	−148 ± 4	−152	4
795	0.7838	34.704	27.823	110.1	2267	0.32	0.13	2	−179 ± 5	−182	4
997.1	0.5854	34.697	27.83	115.4	2250	0.27	0.09	2	−175 ± 4	−175	0
1195.8	0.3901	34.687	27.834	118.4	2267	0.33	0.12	2	−154 ± 4	−157	3
1795.5	0.0023	34.672	27.841	124.8	2270	0.53	0.12	2	−154 ± 5	−159	4
2242.4	−0.1795	34.667	27.846	128.6	2263	—	—	2	−154 ± 4	−160	6
2740.9	−0.3279	34.663	27.85	127.8	2260	0.69	0.28	3	−166 ± 8	−173	7
3193.9	−0.4247	34.659	27.851	126.3	2258	0.94	0.39	2	−160 ± 4	−169	9
3697.2	−0.5206	34.656	27.853	127.1	2260	0.98	0.42	2	−167 ± 4	−176	10
4065.7	−0.6255	34.652	27.855	129.3	2247	0.91	0.36	2	−150 ± 4	−159	9
4065.9	−0.6265	34.653	27.856	130.9	2253	0.94	0.36	2	−154 ± 4	−163	9
Station 12	*65°S, 30°E*										
10.6	1.004	33.829	27.1	54.24	2164	6.45	2.79	2	−117 ± 5	−125	8
20.1	1.0006	33.829	27.1	53.44	2155	6.44	2.79	2	−97 ± 4	−123	26
39.4	0.6738	33.842	27.15	54.24	2168	6.46	2.81	2	−97 ± 5	−124	27
99.8	−0.9583	34.411	27.673	70.95	2225	4.37	1.87	2	−125 ± 5	−141	16
149.7	0.6731	34.57	27.721	85.3	2259	1.84	0.75	2	−140 ± 4	−155	16
200.1	0.9763	34.615	27.74	89.28	2261	1.29	0.49	2	−144 ± 4	−159	15
324.5	1.2006	34.675	27.772	95.66	2255	0.72	0.26	2	−148 ± 4	−155	7
499.8	1.2749	34.715	27.799	102	2264	0.3	0.07	2	−152 ± 4	−152	0
698.9	1.0755	34.718	27.813	—	2266	0.24	0.05	2	−158 ± 4	−158	0
998	0.749	34.706	27.827	113.2	2257	0.2	0.04	2	−152 ± 4	−152	0
1197.1	0.5752	34.699	27.831	116.4	2259	0.2	0.03	2	−161 ± 4	−161	0
2000	—	34.674	—	—	2264	0.23	0.04	2	−164 ± 5	−164	0
3000	—	34.663	—	—	2261	0.4	0.11	2	−155 ± 4	−158	4
4495.9	-0.6169	34.652	27.856	129.2	2253	0.63	0.22	2	−164 ± 4	−170	6
Station 18	*61°S, 30°E*										
11.3	1.7759	33.686	26.938	44.3	2136	6.32	2.83	2	−74 ± 5	−114	40
20.9	1.6254	33.721	26.973	44.72	2140	6.33	2.85	2	−85 ± 5	−114	30
40.7	−0.0172	33.891	27.211	45.56	2152	6.41	2.85	2	−80 ± 5	−116	36
80	−1.62	34.122	27.463	50.6	2176	6.11	2.74	2	−87 ± 5	−121	34
126.5	−1.213	34.198	27.509	57.35	2196	5.56	2.44	2	−91 ± 5	−127	36
175.2	0.7429	34.482	27.646	82.22	2243	—	—	2	−124 ± 5	−152	28
252.1	1.4748	34.635	27.72	90.64	2250	0.85	0.33	2	−146 ± 5	−155	8
599.1	1.2922	34.718	27.799	100.3	—	0.36	0.15	2	−143 ± 6	−146	4
799.7	1.0488	34.714	27.812	107.1	—	0.31	0.11	2	−166 ± 5	−169	3
998.9	0.8452	34.709	27.823	112.1	—	0.24	0.1	2	−164 ± 5	−164	0
1197.6	0.6426	34.7	27.828	116.4	—	0.21	0.09	2	−162 ± 5	−162	0
2244.5	0.0032	34.673	27.843	127.3	—	0.22	0.07	2	−156 ± 5	−156	0
2995.5	−0.2888	34.664	27.849	127.3	—	0.24	0.1	2	−157 ± 5	−157	0
4495.7	−0.6071	34.655	27.857	129	2260	0.26	0.09	2	−154 ± 5	−154	0
Station 24	*57°S, 30°E*										
10.4	2.2178	33.626	26.853	40.6	2131	6.27	2.84	2	−83 ± 5	−111	27
19.8	2.2133	33.625	26.853	40.6	2139	6.27	2.82	2	−77 ± 5	−111	33
40.7	2.2012	33.633	26.862	40.6	2140	6.26	2.84	2	−74 ± 5	−111	37
99	−0.7262	33.92	27.267	50.32	—	6.91	3.06	2	−81 ± 5	−120	39
150.5	−1.6046	34.141	27.476	68.97	2202	6.62	2.91	2	−87 ± 5	−139	52
199.3	−1.4569	34.234	27.549	73.03	2209	6.08	2.68	2	−92 ± 5	−143	51
320.7	0.5166	34.596	27.751	99.78	2256	1.6	0.7	2	−141 ± 5	−157	15

Table 1 Data for the stations occupied during the CIVA1 cruise *(Continued)*

Depth (m)	Potential temp. (°C)	Salinity (S, psu)	Sig 0	SiO_2 (μmol kg^{-1})	SCO_2 (mmol kg^{-1})	CFC-11 (pmol kg^{-1})	CFC-12 (pmol kg^{-1})	Num. of meas.	$\Delta^{14}C$ (‰)	Nat. $\Delta^{14}C$ (‰)	Bomb $\Delta^{14}C$ (‰)
496.9	0.9574	34.695	27.803	108.3	2263	0.45	0.18	2	−153 ± 5	−157	5
696.1	0.7337	34.695	27.818	114.4	2267	0.38	0.15	2	−151 ± 5	−155	4
997.1	0.5577	34.695	27.829	120.9	2268	—	—	2	−151 ± 5	−153	3
1195.8	0.4318	34.69	27.833	125.3	2268	0.23	0.11	2	−175 ± 5	−177	3
1992.9	0.0367	34.675	27.842	129	—	0.19	0.07	2	−177 ± 5	−177	0
2995.3	−0.3072	34.663	27.85	130.6	—	0.22	0.08	2	−171 ± 4	−171	0
4495.2	−0.6165	34.654	27.856	129.4	2258	0.23	0.09	2	−156 ± 4	−156	0
5422.2	−0.7349	34.65	27.858	129	2256	0.28	0.11	2	−150 ± 4	−153	3
Station 28	*54.3°S, 30°E*										
10.9	2.8814	33.876	26.998	26.37	2147	5.91	2.72	2	−69 ± 6	−96	28
19.9	2.8829	33.877	26.998	26.37	2147	5.1	2.53	2	−81 ± 5	−96	16
39.5	2.7778	33.952	27.066	29.66	2155	5.94	2.72	2	−83 ± 5	−100	17
101.2	0.0656	34.096	27.378	48.6	2190	5.85	2.67	2	−97 ± 5	−119	21
151.1	0.6092	34.294	27.456	55.18	2210	4.81	2.09	2	−80 ± 5	−125	45
197.2	1.3819	34.366	27.511	65.07	2239	2.54	1.08	2	−109 ± 5	−135	26
323.1	1.9407	34.572	27.632	78.23	2262	0.81	0.33	2	−142 ± 5	−148	7
496.7	1.8816	34.658	27.707	85.23	2262	0.47	0.17	2	−150 ± 5	−155	5
701.6	1.6213	34.689	27.752	91.4	2263	0.49	0.21	2	−153 ± 5	−158	5
995.2	1.5408	34.737	27.795	91.81	2257	0.25	0.08	2	−147 ± 4	−147	0
1399.7	1.0201	—	27.823	105.4	2261	0.22	0.09	2	−156 ± 4	−156	0
2494.4	0.1553	34.68	27.841	126.4	2261	0.25	0.07	2	−164 ± 5	−164	0
3993.7	−0.4818	34.658	27.853	130.1	2262	0.21	0.08	2	−164 ± 4	−164	0
4996.3	−0.621	34.657	27.858	129.7	—	0.21	0.09	2	−156 ± 4	−156	0
5455.9	−0.6523	34.653	27.858	128.4	2260	0.19	0.08	2	−151 ± 4	−151	0
Station 38	*49.7°S, 30°E*										
9.3	4.5363	33.874	26.835	3.03	2121	5.29	2.95	2	−52 ± 5	−73	22
18.8	4.5366	33.874	26.836	3.89	2120	5.33	2.89	2	−50 ± 5	−74	24
38.2	4.5302	33.876	26.836	5.19	2119	5.3	2.88	2	−47 ± 5	−75	29
79	3.139	33.982	27.061	15.12	2150	5.3	2.84	2	−27 ± 5	−85	58
125.9	2.6988	34.011	27.123	18.15	2154	5.12	2.74	2	−45 ± 5	−88	43
172.9	3.169	34.125	27.173	20.31	2162	4.11	2.2	2	−31 ± 6	−90	59
325.4	2.6227	34.199	27.28	34.17	2188	2.96	1.56	2	−61 ± 6	−104	43
576.9	2.3437	34.36	27.433	56.5	2233	1.34	0.67	2	−100 ± 5	−127	26
795.4	2.4431	34.525	27.556	70.07	2254	0.51	0.26	2	−130 ± 5	−140	10
998	2.3759	34.613	27.632	75.32	2258	0.23	0.09	1	−141 ± 8	−141	0
1198	2.3707	34.685	27.691	75.31	2255	0.16	0	2	−131 ± 5	−131	0
2498.4	1.1142	34.735	27.825	105.6	2272	0.08	0	2	−158 ± 5	−158	0
3994.5	−0.1069	34.672	27.848	132.2	2257	0.25	0.12	2	−156 ± 5	−156	0
5183.5	−0.4829	34.656	27.853	135.2	—	0.21	0.08	2	−153 ± 5	−153	0
Station 52	*44°S, 30°E*										
9.8	12.315	34.475	26.125	1.96	—	3.45	1.82	2	43 ± 5	−72	115
19.4	12.297	34.472	26.128	1.96	2061	3.41	1.87	2	49 ± 5	−72	121
39.7	12.045	34.45	26.156	1.96	2058	3.47	1.95	2	53 ± 5	−72	125
100.5	9.2985	34.596	26.756	7.34	2116	3.62	1.89	2	55 ± 5	−77	132
142.6	8.7958	34.594	26.835	8.31	2123	3.43	1.79	2	34 ± 5	−78	112
197.4	7.916	34.497	26.892	9.78	2135	3.36	1.75	2	33 ± 5	−80	113
323.3	6.3703	34.341	26.983	13.71	2143	3.29	1.62	2	11 ± 5	−84	94
499	5.1576	34.3	27.128	23.19	2180	2.2	1.09	2	−29 ± 5	−93	65
698.7	4.0819	34.329	27.244	35.84	2196	1.62	0.8	2	−61 ± 5	−106	45
1001.2	3.0136	34.421	27.423	58.5	2239	0.73	0.32	2	−125 ± 5	−125	0
1198.1	2.7672	34.53	27.532	68.5	2251	0.28	0.16	2	−142 ± 4	−142	0
2244.9	2.2081	34.793	27.789	72.65	2236	0	0	2	−137 ± 4	−137	0
3496.4	1.0783	34.753	27.841	104.5	2267	0.04	0	2	−153 ± 4	−153	0
4497.9	0.1862	34.69	27.846	132	—	0.13	0.1	2	−160 ± 4	−160	0

Figure 2 shows a map including the WOCE/CIVA1 transect between 68°S and 44°S along 30°E, where ^{14}C samples were collected. Also indicated are other stations in the same area where ^{14}C has been measured on previous campaigns: GEOSECS, WWSP, and INDIGO.

The θ and S along the CIVA1 transect (Fig. 3A,B)[4] exhibit signatures of the major fronts that characterize the Southern Ocean: the Antarctic Divergence Zone (ADZ) between 63°S and 67°S, the Weddell Gyre Front (WF) at 57°S, the Polar Front (PF) at 52°S, and the Subantarctic Front (SAF) at 48°S (Gordon 1971; Whitworth and Nowlin 1987; Orsi et al. 1993, 1995; Archambeau et al. 1998). The

[4]*Note:* Color versions of Figs. 3, 4, 7 and 9 are available at http://www.radiocarbon.org/Journal/v41n1/Leboucher/

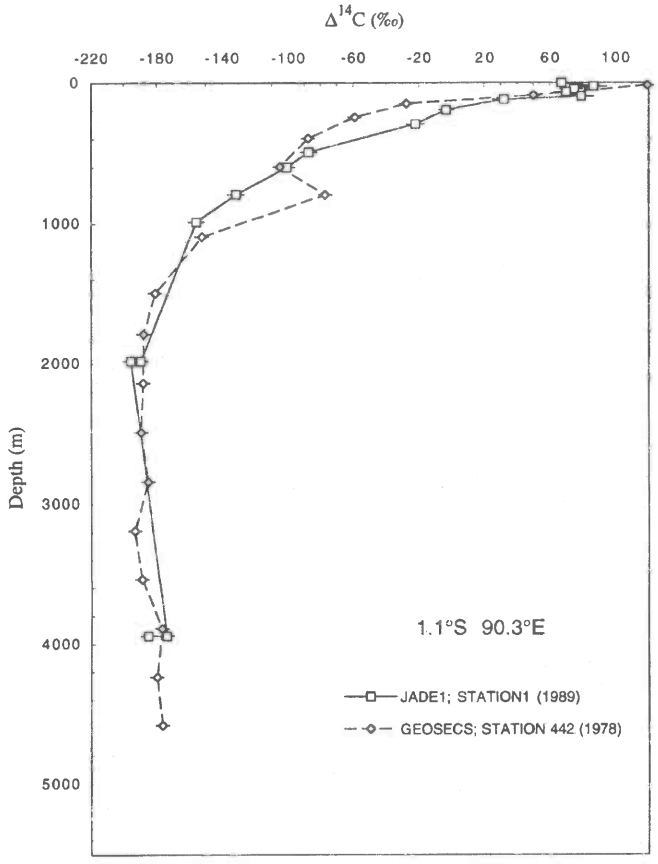

Figure 1 Profiles of measured $\Delta^{14}C$ from GEOSECS station 442 and JADE1 station 1

principal water masses are likewise apparent. From the Antarctic continent to the PF, the Summer Surface Water (SSW) overlies the near freezing Winter Water (WW). Below the WW lies a massive amount of Circumpolar Deep Water (CDW), which is relatively warm (>0.1 °C) and old (with respect to ventilation by contact with the surface). Beneath the CDW and along the bottom is found the Antarctic Bottom Water (AABW). In the AABW, one can trace the influence of the Weddell Sea Bottom Water (WSBW), which at its origin (the Weddell Sea) has a temperature <–0.7 °C. Another water mass, the Subantarctic Surface Water (SASW), lies between the PF and the SAF. The SASW has higher temperatures and salinities than the more southern surface waters and is remarkable for its south-to-north downward tilt in θ and S isolines, where AAIW is formed. In this northern part of the CIVA1 section, intermediate level CDW bears a high salinity signature (maximum 34.8 psu) from its contact with North Atlantic Deep Water (NADW). AABW north of the Atlantic-Indian ridge is warmer and less dense than AABW to the south, which is closer to the source of the cold WSBW. Further description of CIVA1 hydrography can be found in Archambeau et al. (1998).

Table 1 provides the CIVA1 ^{14}C measurements. These data are presented as a composite latitude versus depth section (Fig. 4A) as well as individual profiles (Fig. 5A,B). The former reveals that the distribution of the measured ^{14}C roughly follows CIVA1 hydrography. A striking contrast is found across the PF: north of the PF, surface waters are enriched in ^{14}C (levels reach 55‰); south of the PF, the upper 200 m are depleted in ^{14}C (levels from –70‰ to –140‰). The Southern depletion is principally due to old CDW upwelling in the Antarctic Divergence Zone between 63°S and 67°S (Toggweiler and Wallace 1995). However, winter ice cover limits gas exchange and thus may play

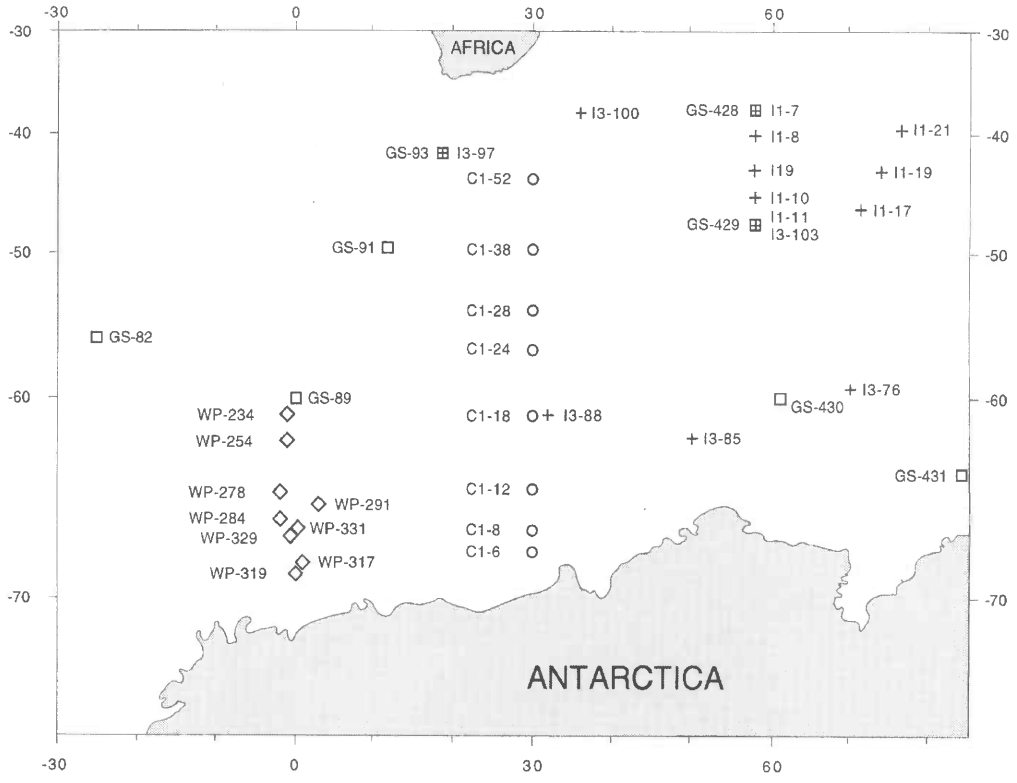

Figure 2 Stations occupied to collect samples for ^{14}C during CIVA1 (C1) as well as adjacent ^{14}C stations from GEOSECS (GS), WWSP (WP), INDIGO (I1 and I3)

some role (Weiss et al. 1979; Poisson and Chen 1987). North of the PF, ^{14}C-enriched surface waters sink below warmer subantarctic water and move toward the north along downward sloping isopycnal surfaces, where AAIW is formed.

A core of old water ($\Delta^{14}C$ less than $-170‰$) is located near 57°S between 1000 and 2000 m (station 24). This corresponds to the oldest CDW. A shallow extension of old CDW is found near 66°S (station 8) with the oldest values (less than $-175‰$) between 800 m and 1000 m.

End members for and mixing between intermediate, deep, and bottom waters ($\sigma_\theta < 27.7$) are more easily seen on CIVA1's θ-S diagram (Fig. 6A). The core of the CDW is identifiable by its salinity maximum induced by the contribution of NADW. Another influential water mass is the AABW, which forces most of the data points on the θ-S plot to lie on a straight line between the CDW and AABW end-member. The ^{14}C data are helpful to pinpoint a third water mass component. Points from stations 8 and 24 reveal that the most ^{14}C-depleted waters have slightly different θ-S characteristics (Figs. 6B, 6C). These tendencies point to the older ^{14}C-depleted Pacific Deep Water (PDW) as an important contributor. The same trend was found from measurements of ^{3}He in the Southern Ocean (Jean-Baptiste et al. 1991). The contribution of PDW to the CDW is also consistent with the return Pacific flow scheme described by Toggweiler and Samuels (1993) based on Pacific-Antarctic $\Delta^{14}C$ difference, on the silica distribution in sediments of the Pacific sector of the Southern Ocean (Worthington 1977), and on previous inverse model results (Wunsch et al. 1983). The WOCE sec-

tion P6 along 32°S in the Pacific Ocean shows a substantially older ^{14}C signal for this return flow (Key et al. 1996).

Figure 4A further shows that AABW has higher levels of ^{14}C ($\Delta^{14}C = -150‰$ to $-160‰$) than does CDW. The reason is that AABW originates principally in the Weddell Sea via mixing of newly formed WSBW with intermediate depth waters (Foster and Carmack 1976; Carmack and Foster 1977; Weiss et al. 1979; Mensch et al. 1996). The recent ventilation of the WSBW is clearly indicated by steady-state and transient tracer measurements (^{14}C, ^{3}H, CFC-11, CFC-12, ^{39}Ar, ^{18}O and helium isotopes) in the Weddell Sea (Bayer and Schlosser 1991; Schlosser et al. 1991; Mensch et al. 1996; Wepperning et al. 1996). GEOSECS ^{14}C data provide further evidence of such formation and indicate an eastward spreading of recently ventilated bottom waters (enriched in ^{14}C) from the Weddell Sea (Fig. 7).

DISCUSSION

Observed Change in Oceanic ^{14}C

Few previously collected ^{14}C data are available for ^{14}C in the same region (Fig. 2). Those that are available include measurements from GEOSECS (1973–1978), ANTV in the Weddell Sea (1986) and INDIGO (1985–1987). Figure 8 provides details of the measured change of surface ocean ^{14}C with time. Unfortunately, south of 65°S as well as between 55°S and 50°S, no adjacent GEOSECS era data exist. Between about 65°S and 55°S, surface ocean ^{14}C decreased progressively from 1973–

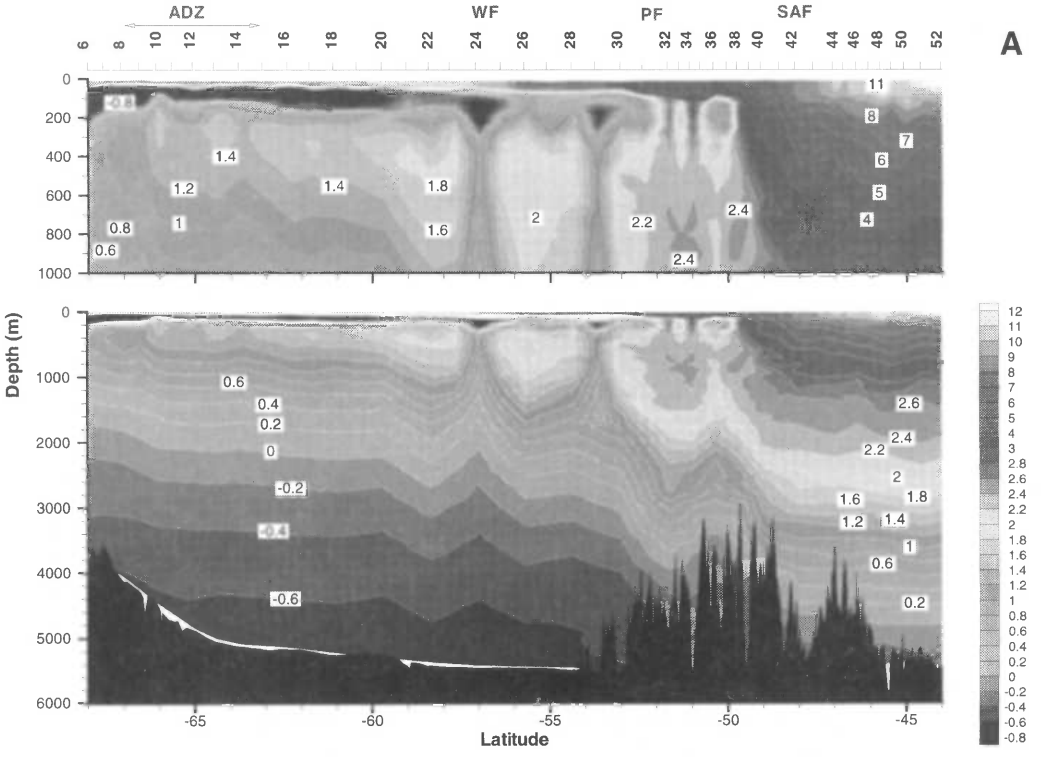

Figure 3 (A) Potential temperature θ, (B) salinity S, and (C) CFC-12 concentrations along the CIVA1 section. Also indicated are frontal zones mentioned in the text (ADZ, WF, PF and SAF).

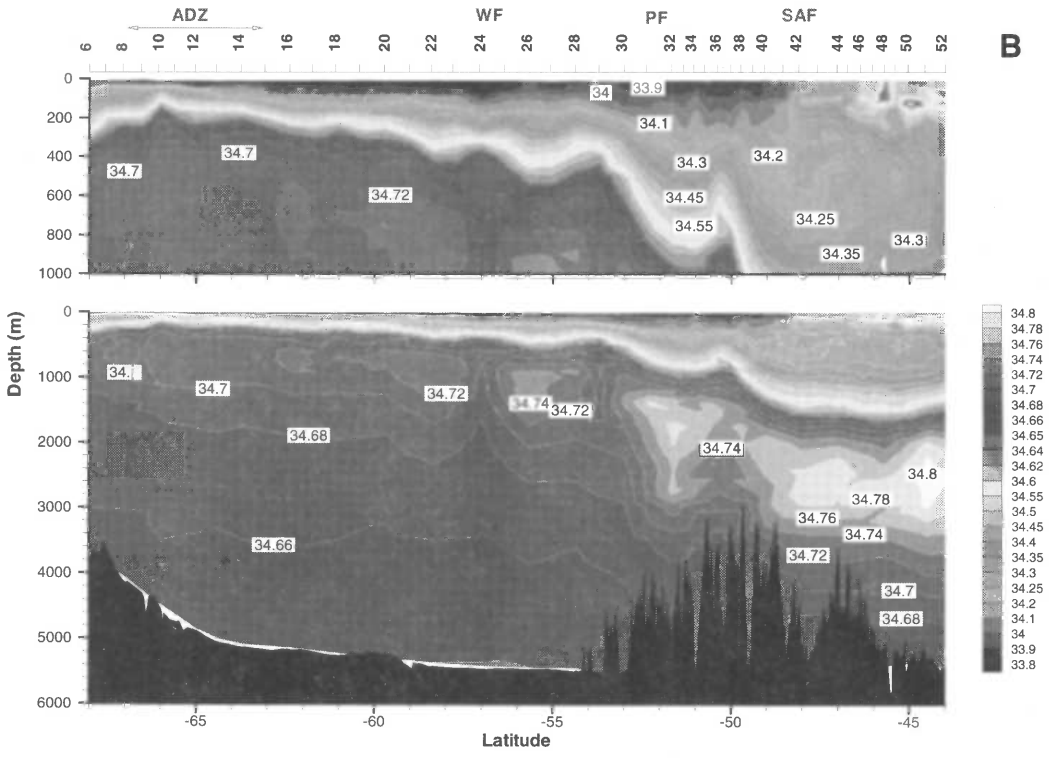

Figure 3B (See Fig. 3A)

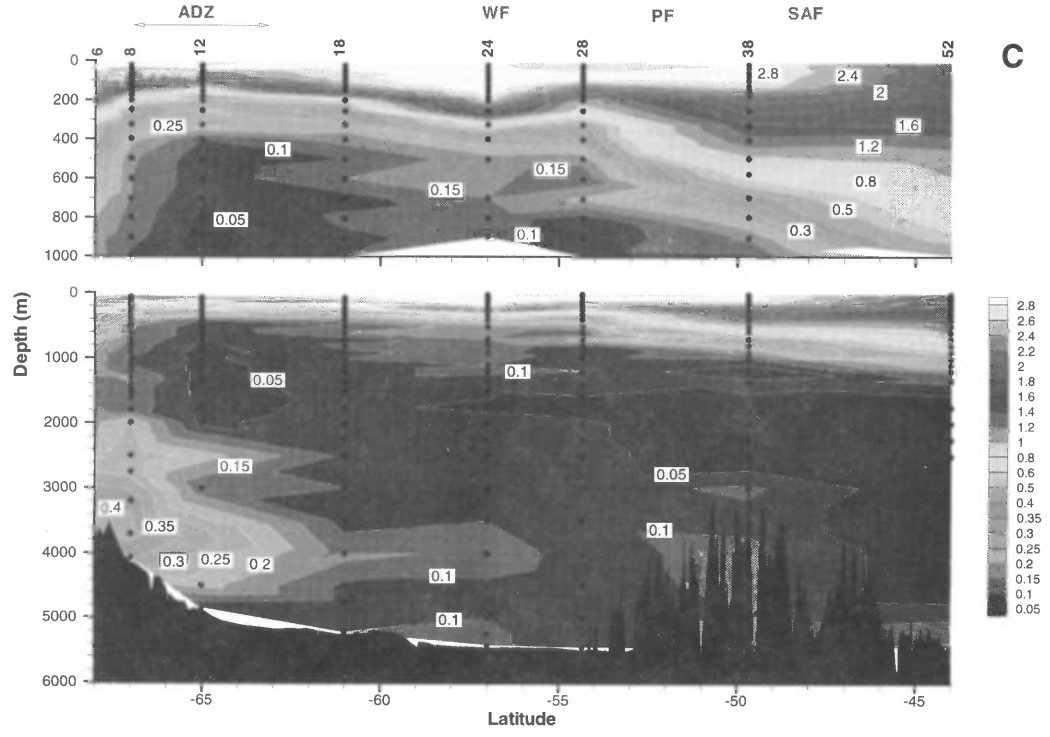

Figure 3C (See Fig. 3A)

1978 to 1993. This decreasing trend results from the decline in atmospheric ^{14}C and the replacement of the surface waters south of the Polar Front with upwelled CDW, which remains largely uncontaminated by bomb ^{14}C (Toggweiler and Wallace 1995). From 50°S to 44°S, there also appears to be a reduction with time, assuming a linear spatial trend between those 2 CIVA data points.

Figure 9 provides a more in-depth look at the CIVA1 minus GEOSECS temporal change. The GEOSECS data in the Southern Ocean are sparse but were selected based on the proximity to the CIVA1 section. However, many of the chosen GEOSECS stations are far from the CIVA1 section, leading to substantial uncertainty about our calculated CIVA1-GEOSECS section. Nevertheless, natural variability must be substantially smaller than the large temporal changes in near-surface ^{14}C that have occurred since GEOSECS. Within the upper 200 m, ^{14}C has decreased substantially since GEOSECS. Just below, ^{14}C has increased. The increase extends deeper in the north than in the south. North of the CIVA1 Polar Front, the large subsurface increase in ^{14}C since GEOSECS (up to +80‰) tags the formation of AAIW. The CDW remains largely uncontaminated by bomb ^{14}C, a result that is consistent with the CIVA1 CFC data (Archambeau et al. 1998), which likewise reveal no significant recent contamination of the core of the CDW (Fig. 3C). Conversely, the AABW has been recently ventilated according to both the CIVA1-GEOSECS ^{14}C difference and the CIVA1 CFC data.

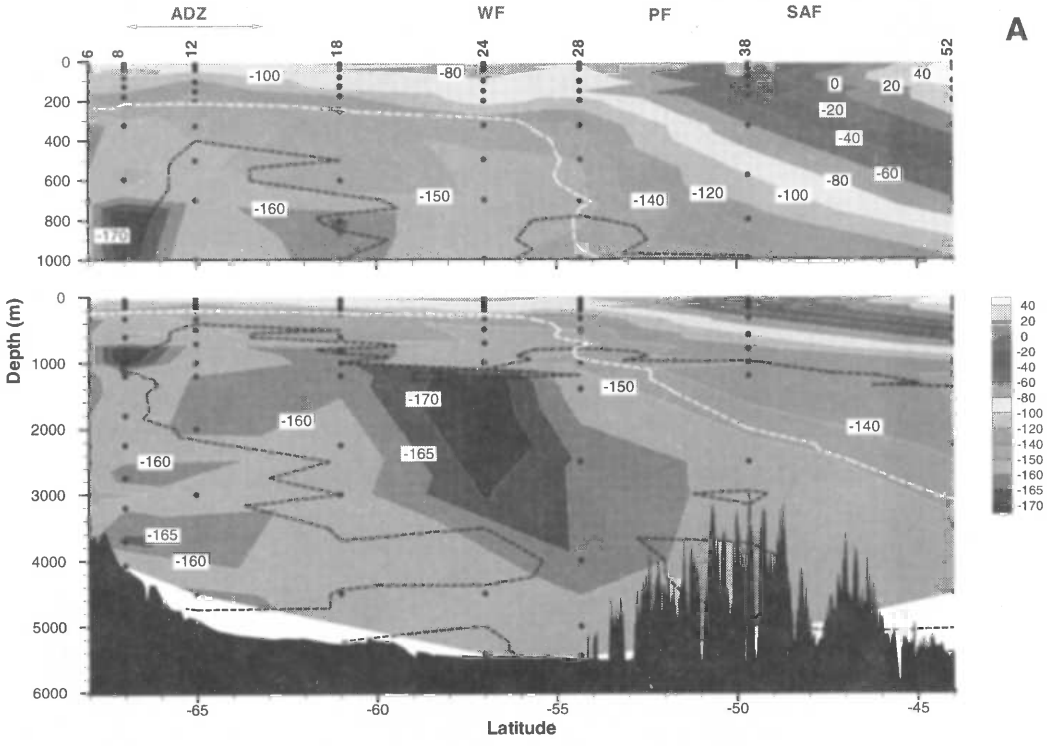

Figure 4 CIVA1 sections for (A) measured ^{14}C as well as (B) natural ^{14}C and (C) bomb ^{14}C components estimated by our new CAS methodology; SAS was used for station 52 at 44°S. For SAS, the 90 µmol kg^{-1} isoline for dissolved silica (thick dashed line) provides the limit for penetration of bomb ^{14}C. For CAS, that limit is provided by the 0.1 pmol kg^{-1} isoline for CFC-12 (thin dashed line).

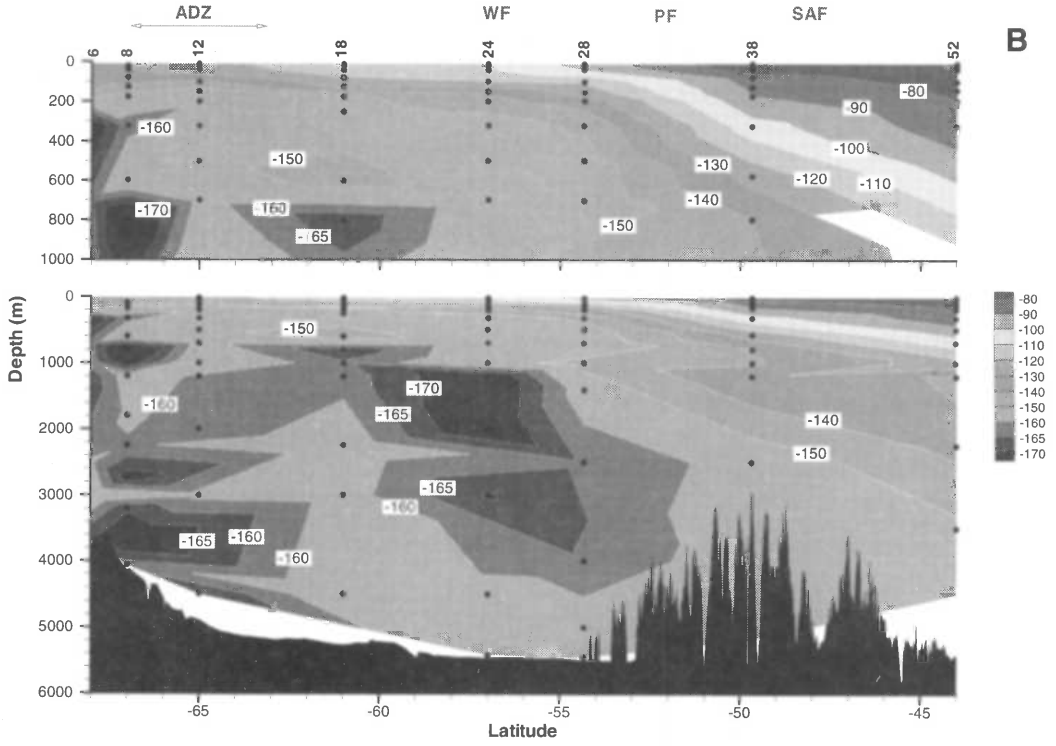

Figure 4B (See Fig. 4A)

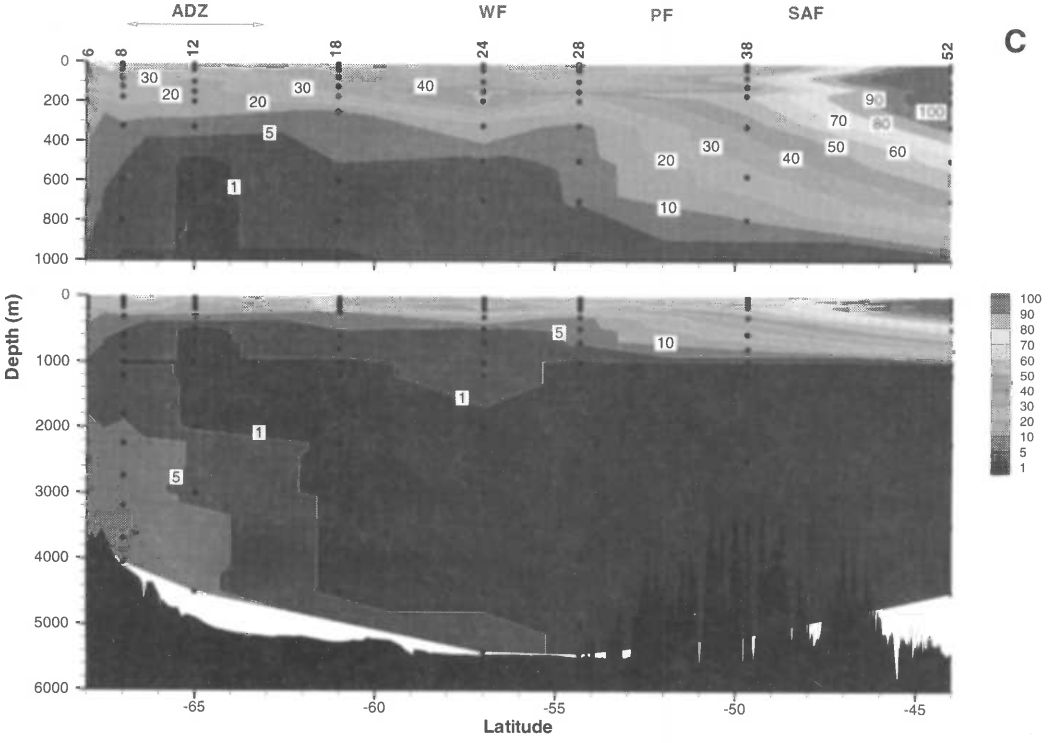

Figure 4C (See Fig. 4A)

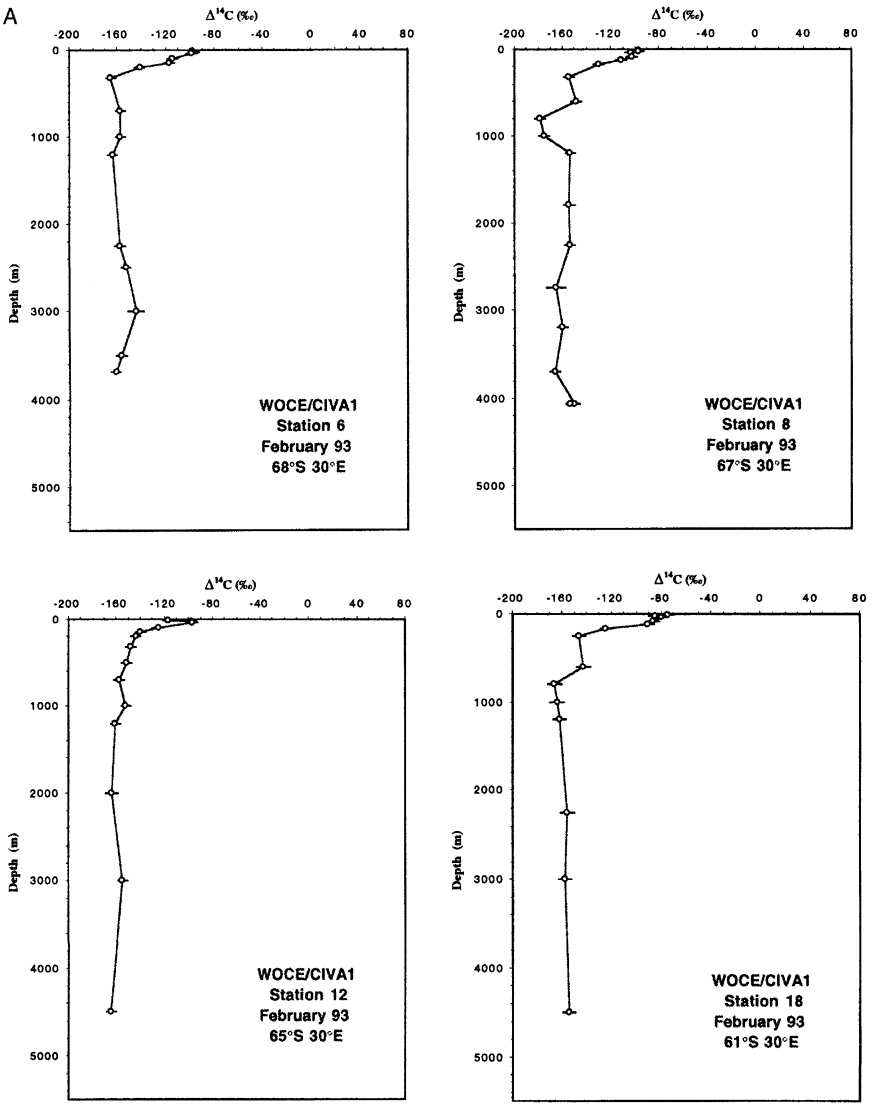

Figure 5A Profiles of measured $\Delta^{14}C$ for CIVA1 stations 6, 8, 12, and 18

Estimating Natural and Bomb ^{14}C

Broecker et al. (1995) developed a general method to reconstruct the distribution of natural ^{14}C in the ocean. They applied their method to the GEOSECS (1972–1978), TTO (1980–1983) and SAVE (1987–1989) data to distinguish natural from bomb ^{14}C. Besides surface prenuclear ^{14}C data, Broecker et al. (1995) used bomb tritium to delimit the penetration depth of bomb ^{14}C, and the relationship between silica and natural ^{14}C to determine the latter in the upper water column. For CIVA1, we employ the same method for our one station that fell north of 45°S (station 52 at 44°S). South of 45°S, Broecker et al. (1995) rely purely on SiO_2. In deep waters ($SiO_2 > 90$ µmol kg^{-1}), Broecker et al.

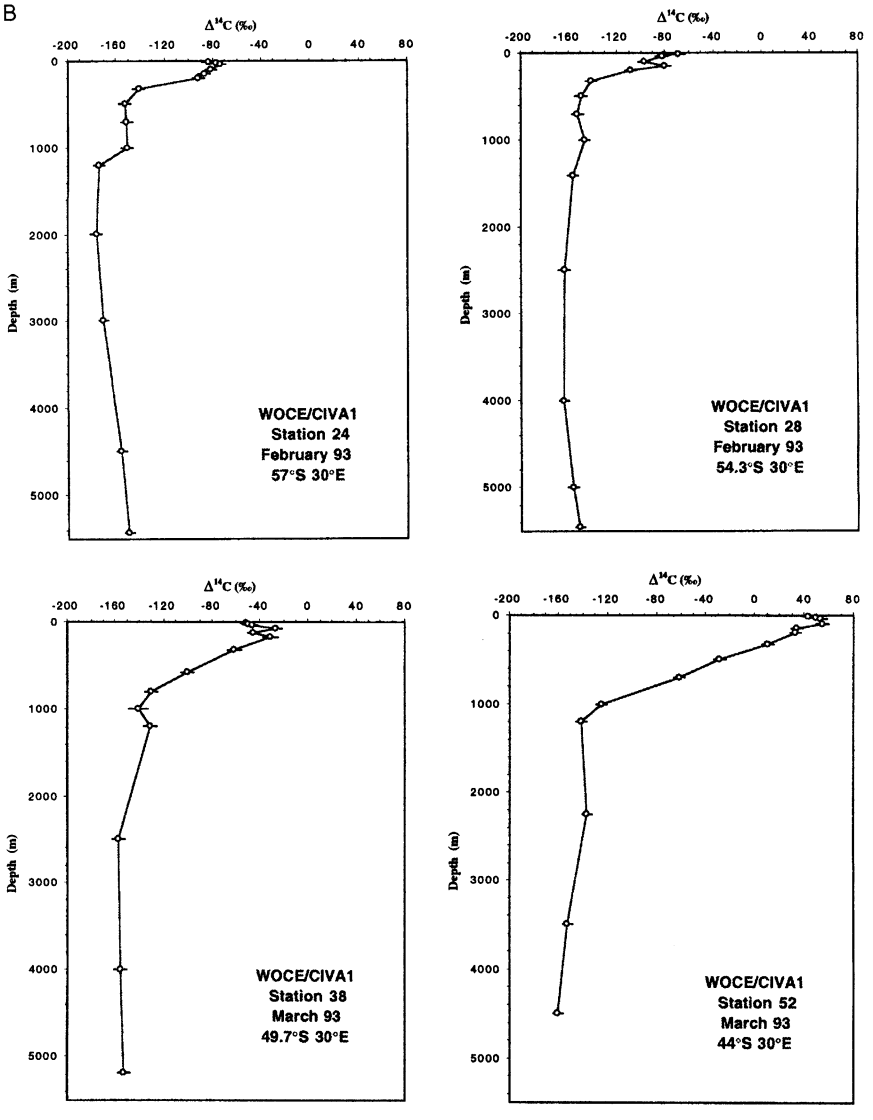

Figure 5B Profiles of measured $\Delta^{14}C$ for CIVA1 stations 24, 28, 38 and 52

(1995) consider that ^{14}C is entirely natural in origin (i.e., that deep waters were entirely free from bomb ^{14}C). Although this is a reasonable approximation for the time of GEOSECS, only about 10 yr after the peak in atmospheric ^{14}C, such appears not to be the case for CIVA1 samples, collected about 20 yr later.

At the time of CIVA1, it is possible that bomb ^{14}C had penetrated into deep waters of the Southern Ocean, where vertical mixing and advection are particularly active. To properly address such a possibility, we were forced to modify the method for the region south of 45°S. For this, we employ a simple ventilation model (see Appendix) that relates deep water concentrations to historical surface values. The ventilation parameters of such a model are calibrated by CFC data, measured during CIVA1,

because such gases have no natural component. Hence, this approach is termed the CFC Analogue Strategy (CAS). Then, with a data-based reconstructed history of surface ocean ^{14}C in the same region, we computed the penetration of bomb ^{14}C.

Silica Analogue Strategy and CFC Analogue Strategy

The Silica Analogue Strategy (SAS) from Broecker et al. (1995) improves on previous methodology (Broecker et al. 1985) to separate natural and bomb ^{14}C in the ocean by exploiting the linear correlation between natural ^{14}C and dissolved silica found to exist in ^{3}H-free waters throughout most of the oceans:

$$\Delta^{14}C_{\text{natural}} = -70 - SiO_2 \tag{1}$$

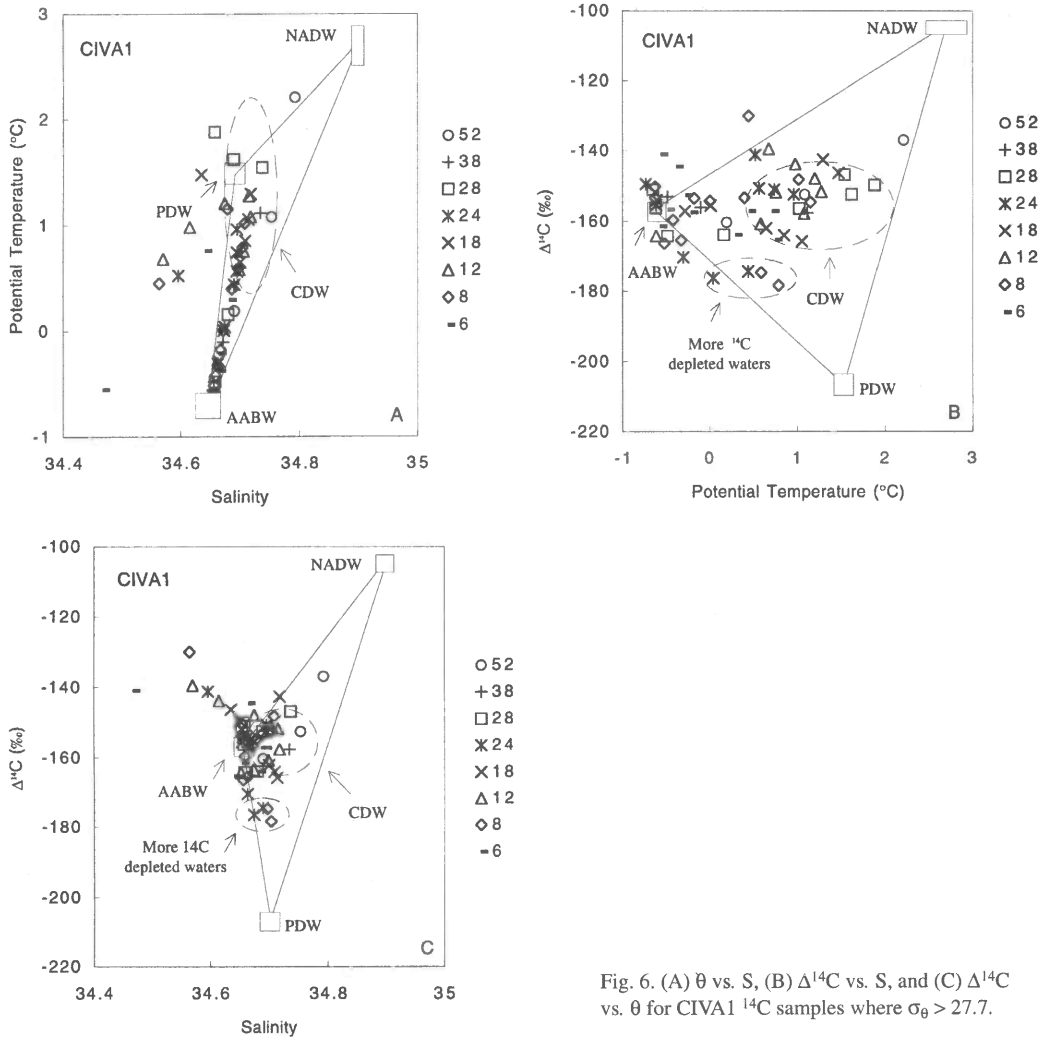

Fig. 6. (A) θ vs. S, (B) $\Delta^{14}C$ vs. S, and (C) $\Delta^{14}C$ vs. θ for CIVA1 ^{14}C samples where $\sigma_\theta > 27.7$.

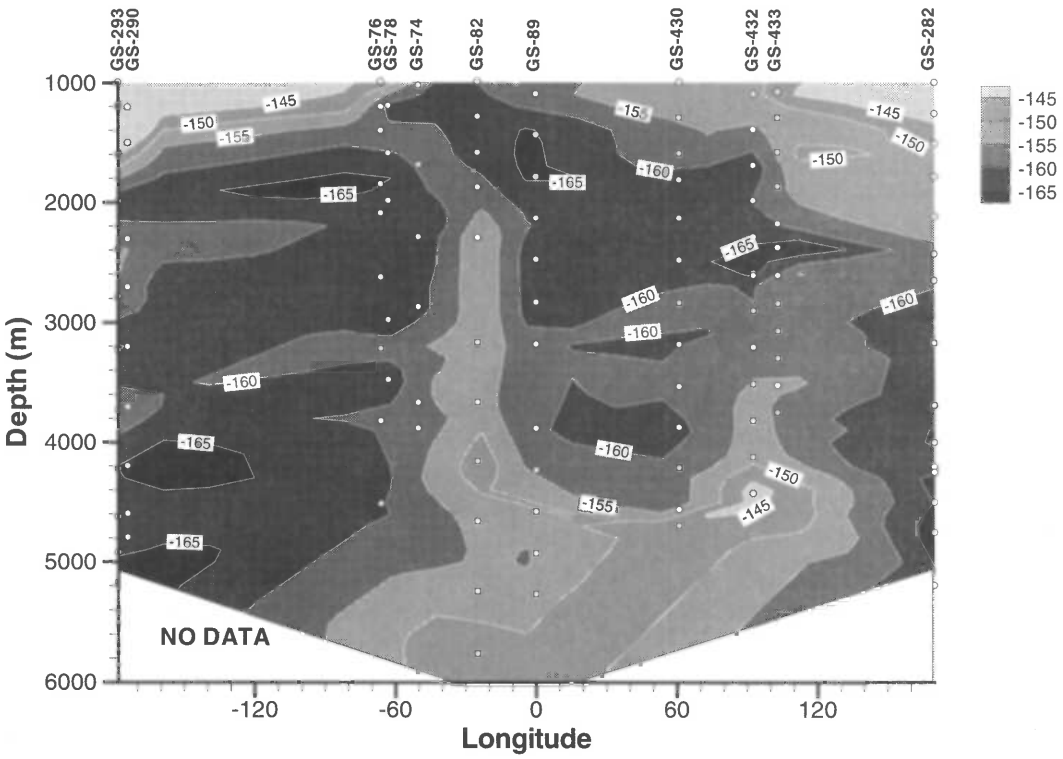

Figure 7 Longitudinal section of measured ^{14}C in the Antarctic Circumpolar Current (ACC) from GEOSECS (1972–1978). Latitudes of stations vary between 52°S and 62°S.

where $\Delta^{14}C$ is in ‰ and SiO_2 is in µmol kg^{-1}. Broecker et al. (1995) estimate the uncertainty of the natural ^{14}C thus calculated as ±10‰. Figure 10 is a plot of ^{14}C versus silica for GEOSECS, INDIGO3, and CIVA1 data from the Southern Ocean south of 50°S. Also given is the linear regression from equation (1). For waters south of 45°S, Broecker et al. (1995) apply equation (1) when $SiO_2 < 90$ µmol kg^{-1}. They assume that waters with $SiO_2 > 90$ µmol kg^{-1} are uncontaminated with bomb ^{14}C. However, south of 45°S, contamination of deep waters by bomb ^{14}C is much more likely for CIVA1-era samples. Figure 10 suggests that bomb ^{14}C has invaded deep waters since GEOSECS: for waters with SiO_2 between 90 and 100 µmol kg^{-1}, ^{14}C is greater during CIVA1 than during GEOSECS. Thus, for CIVA1, one cannot use the SAS method alone, which assumes that measured variability in deep water ^{14}C is due to natural variation. Instead, south of 45°S, we modified the technique in defining 3 separate regions (Fig. 4A):

1. In the waters where $SiO_2 < 90$ µmol kg^{-1}, natural ^{14}C is deduced from Broecker et al.'s (1995) SAS methodology.
2. In the core of the CDW, where $\Delta^{14}C$ values are the lowest and have not changed since the time of GEOSECS, we consider the ^{14}C to be entirely prenuclear in origin. Arbitrarily, we choose the weak CFC-12 concentrations of 0.1 pmol kg^{-1} as a limit to any anthropogenic contamination. We are unable to employ the CFC-11/CFC-12 dating method near the surface, nor in deep waters. Indeed, the ratio CFC-11/CFC-12 is not usable to date young near-surface waters in CIVA1 because since the mid-1970s, growth rates of atmospheric CFC-11 and CFC-12 have

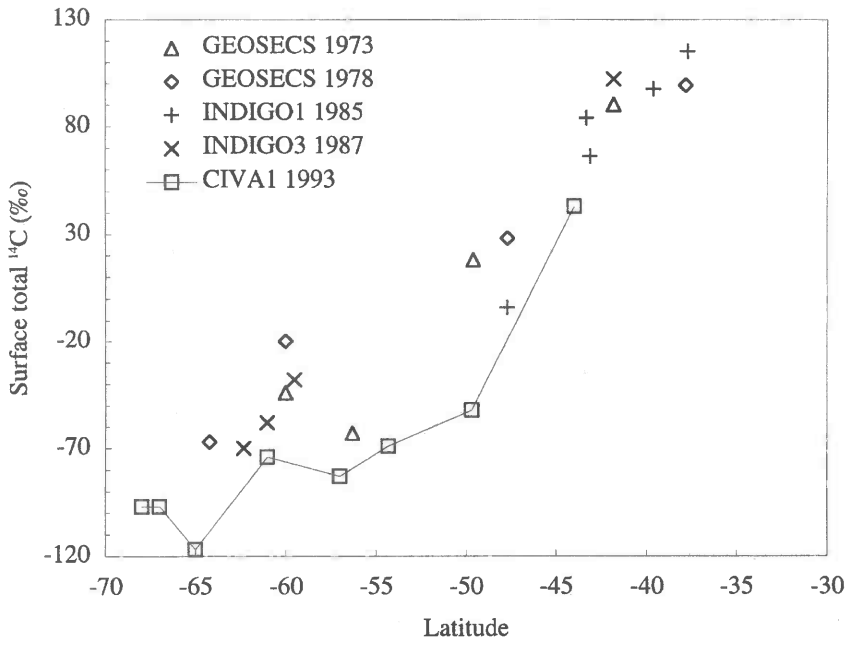

Figure 8 Measured surface ocean ^{14}C from GEOSECS, INDIGO and CIVA1 as a function of latitude for the region between 25°W to 85°E and 70°S to 30°S.

been the same. Furthermore, in CIVA's deep waters where the CFC concentrations are very low, uncertainty in the CFC-11/CFC-12 ratio is too large to be of any use.

3. Elsewhere (i.e., mainly in the ventilated southernmost part of the section), our vertical mixing model and CFCs from CIVA1 are used to calculate the annual ventilation rate of any water parcel, and subsequently, the bomb ^{14}C contribution based on a reconstructed history of surface bomb ^{14}C. By dealing directly with surface ocean concentrations, we avoid problems due to the roughly 100-fold difference in the time required for ^{14}C versus CFCs to equilibrate between the atmosphere and surface ocean (Broecker and Peng 1974).

Natural Versus Bomb ^{14}C

Figure 4B shows the computed natural ^{14}C. Surface values of natural ^{14}C increase from south to north from −132‰ to −72‰. Our lowest surface values in the far south are consistent with the rare existing data set (Broecker et al. 1985; Bard 1988; Toggweiler and Samuels 1993; Berkman and Forman 1996), especially considering the uncertainties from analysis, the Suess effect (5‰ to 12‰ [Berkman and Forman 1996]), the silica-natural ^{14}C relationship (±10‰), and natural spatial variability. Waters north of the PF, where AAIW forms, have higher natural ^{14}C, largely because they rest longer at the surface and thus equilibrate more extensively with the atmosphere; also circulation patterns transport natural ^{14}C to the north as described previously. South of the PF, a large portion of the intermediate and deep waters have natural ^{14}C values lower than −160‰, which is the average value of the waters of the Antarctic Circumpolar Current (Broecker et al. 1995).

The bomb ^{14}C results (Fig. 4C) are consistent with the observed trends of the total $\Delta^{14}C$ values: waters are poor in bomb ^{14}C south of the PF and richer in the north; intermediate, deep, and bottom

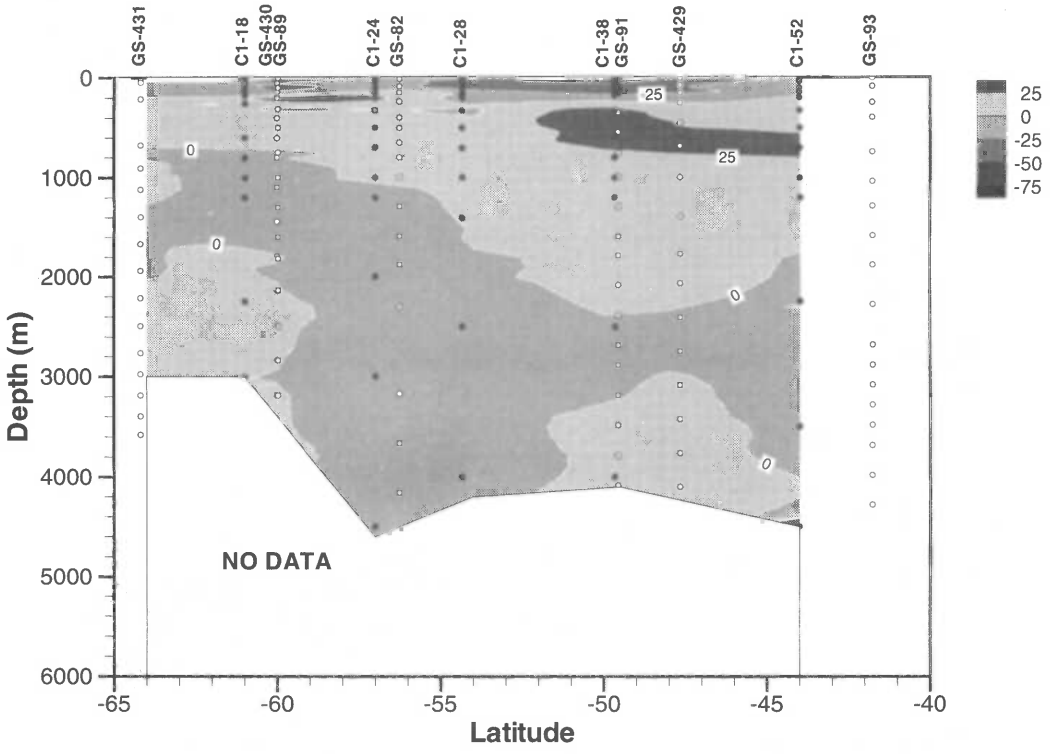

Figure 9 Section of the measured change in ^{14}C between GEOSECS and CIVA1. GEOSECS stations are taken from longitudes between 25°W and 85°E. GEOSECS and CIVA1 station data were triangulated then interpolated to the same 1-degree latitudinal grid before taking differences.

waters contain little if any bomb ^{14}C. The only exception is where substantial bomb ^{14}C is detected between 2000 and 5000 m in the far south along the continental slope. Deep and bottom waters in the northern portion of the section contain insignificant levels.

Bomb ^{14}C Inventories

Following Broecker et al. (1985), we calculated the vertical integral of bomb ^{14}C (also known as the inventory) as the area between bomb and natural ^{14}C profiles (Table 2, Fig. 11). With our method, inventories range from 1.7 to 10.9×10^9 atoms cm^{-2}. Inventories are larger north of the PF (stations 38 and 52) as well as in the far south, at stations 6 and 8. North of 45°S (station 52), the bomb ^{14}C inventory is highest ($10.9 \pm 1.6 \times 10^9$ atoms cm^{-2}) and its uncertainty is lowest: both the SAS and CAS methods give the same inventory. We were able to properly apply the SAS method at station 52, because our measured CIVA1 ^3H (not shown) was well above background levels. Figure 11 compares CIVA1 bomb ^{14}C inventories to those from GEOSECS and INDIGO. The temporal change is similar in structure to that seen for surface concentrations (Fig. 8). Around 60°S, the differences between inventories during CIVA1 (CAS) and GEOSECS (SAS) tend towards zero: the ^{14}C loss near the surface is compensated by buildup at depth (Fig. 4C). Around 60°S, when the SAS methodology is used, CIVA1 inventories are only 20% to 50% of those determined using CAS. Further south, stations at 67°S and 68°S exhibit the largest differences between the SAS and CAS methods.

Uncertainties concerning the Southern Ocean's bomb ^{14}C inventories are large but their magnitude is relatively small compared to the inventories throughout most of the rest of the ocean (Broecker et

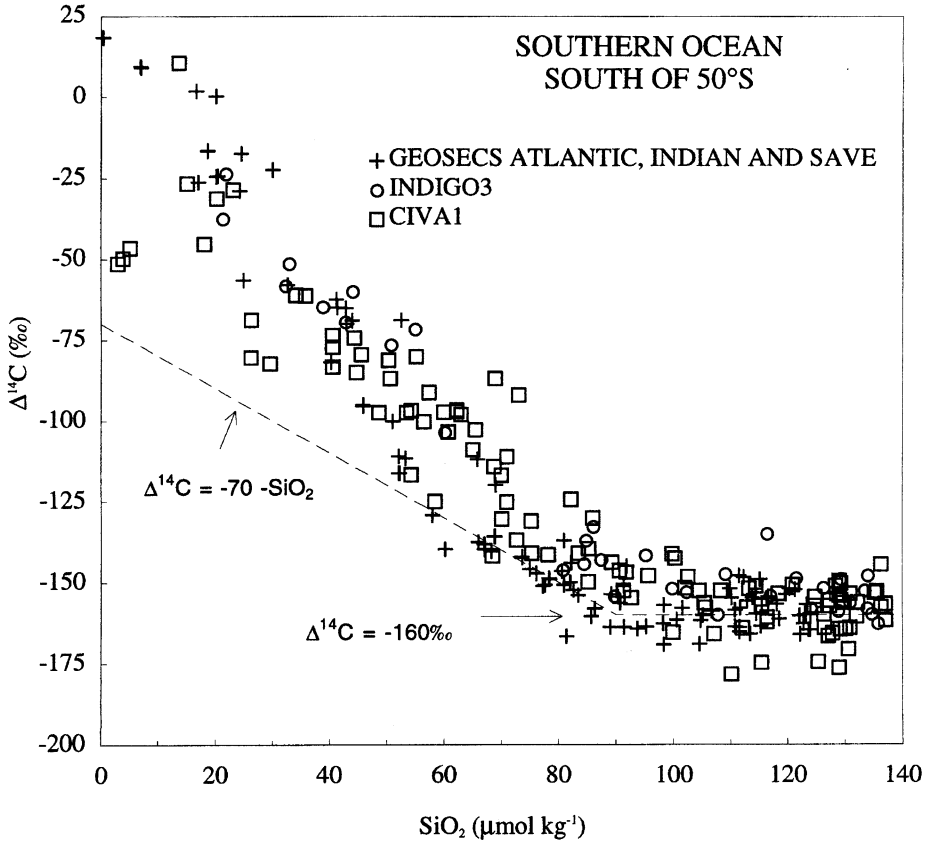

Figure 10 ^{14}C versus dissolved SiO_2 for stations taken south of 50°S from the GEOSECS, INDIGO3, and CIVA1 expeditions. Also provided is the linear correlation between the natural $\Delta^{14}C$ and silica for tritium-free waters (Broecker et al. 1995).

al. 1995). Thus, uncertainties in this region do not substantially alter estimates of the global ocean inventory of bomb ^{14}C. Regional patterns of bomb ^{14}C inventories are generally useful to help evaluate the behavior of OGCMs (Toggweiler et al. 1989b). However, they are less useful in the Southern Ocean, due to the large uncertainties there. On the other hand, levels of bomb ^{14}C near the surface in this same region have much smaller uncertainties than do corresponding horizontal and vertical gradients, and are thus more useful for model validation.

CONCLUSION

To complement the sparse ^{14}C data set in the Southern Ocean, AMS ^{14}C measurements were made on recently collected samples taken along the CIVA1 cruise track. The measured ^{14}C distribution reveals a dramatic contrast between samples taken south and north of the PF. Surface waters in the south are depleted due to upwelling of old CDW at the ADZ, which drives transport to the north; northern surface waters are rich in ^{14}C due to transport from south to north and their more extensive equilibration with the atmospheric ^{14}C. The oldest deep waters are found in the CDW ($< -170‰$) and derive from the PDW.

Table 2 CIVA1 bomb ^{14}C inventories

Station	Surface total ^{14}C (‰)	Bomb ^{14}C inventories[a]	10^9 atoms per cm^{2b}
6	−97	1	4.9
8	−97	1.2	5.1
12	−117	0.8	2.4
18	−74	1.1	1.7
24	−83	1.8	3.1
28	−69	1.5	1.7
38	−52	4.7	4.7
52	43	10.9	—

[a]Following the Broecker et al. (1995) method
[b]Following the chlorofluorocarbon analogue strategy

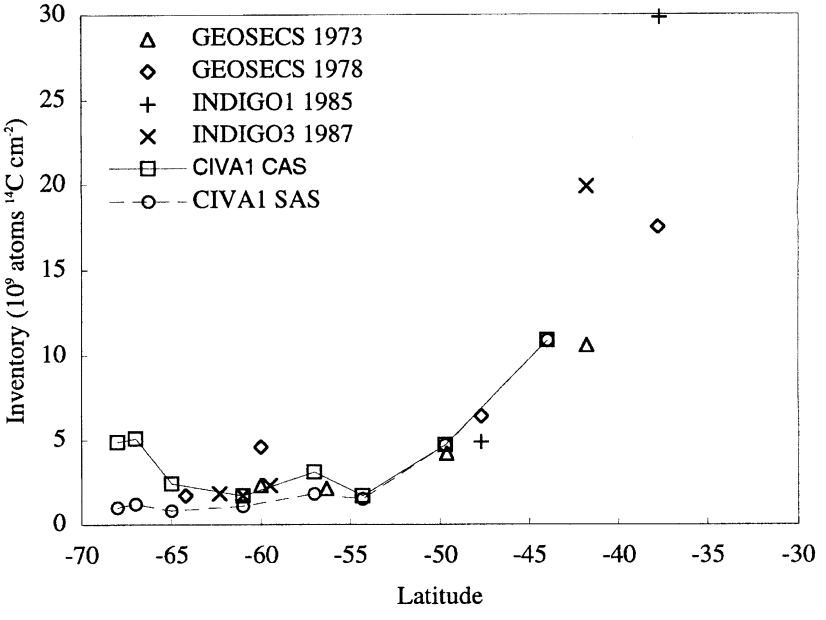

Figure 11 Bomb ^{14}C inventory versus latitude for GEOSECS, INDIGO3 and CIVA1 stations within 25°W–85°E and 70°S–30°S.

Bomb ^{14}C has contaminated deep waters in the far south based on differences in measured ^{14}C between CIVA1 and GEOSECS and the CIVA1 distribution of CFC-11 and CFC-12. Our new CAS method relies on measured CFCs, a simple mixing model, and the established history of surface ocean ^{14}C. A previously developed method, SAS from Broecker et al. (1995), relies on the assumption that all deep waters of the Southern Ocean are free of bomb ^{14}C. For CIVA1 as well as other WOCE-era samples, such an assumption is invalid. In terms of bomb ^{14}C inventories, our new CAS methodology yields estimates identical to the SAS method for stations north of the PF, but substantially greater than SAS results when south of the PF (up to 5 times more when south of the ADZ). Although CAS offers an improvement for determining inventories south of PF, uncertainties remain high and are not ideal for validating ocean carbon-cycle models. CAS estimates in deep waters south of the PF would be improved if the history of surface ocean ^{14}C there were better constrained. South

of the PF, we recommend that ocean modelers not concern themselves with inventories but rather with bomb and natural ^{14}C distributions (Fig. 4B,C), weighing errors accordingly. For CIVA1 north of the PF, bomb ^{14}C is found in surface and intermediate layers; in the far south, bomb ^{14}C is found throughout the water column. Since GEOSECS, ^{14}C has decreased in surface waters (roughly the upper 200 m) and has increased below, to as deep as 2000 m north of the PF.

The CIVA1 section began near Antarctica and was aborted prematurely at 44°S due to an emergency medical evacuation. Fortunately, the repeat section CIVA2 (February–March 1996) will allow the northern gap (where ^{14}C inventories should be greatest) to be filled in, once ^{14}C measurements are completed. The CIVA section along with other new WOCE ^{14}C data will greatly improve coverage in the Southern Ocean, a key area for ocean CO_2 uptake. However, care will have to be exercised when estimating natural and bomb ^{14}C components so that ocean modelers will be able to take full advantage of this unique data set.

ACKNOWLEDGMENTS

For the variety of analyses required for this study, we thank E. Kaltnecker for help in measuring ^{14}C, A. Dapoigny for help with ^{3}H, D. Thouron at the Groupe de Recherche en Geodésie Spatiale (GRGS) for providing the CIVA1 SiO_2 data, and J.-F. Tannau for help in building the degassing system. The CIVA1 cruise was supported by the Institut Français pour la Recherche et la Technologie Polaire (IFRTP). AMS ^{14}C measurements were supported by the CEA and CNRS. The contribution of JCO was supported by the Environment and Climate Programme of the EC (Contract ENV-CT95-0132). This is LSCE Contribution N° 110.

REFERENCES

Andrié C, Jean-Baptiste P, Merlivat L. 1986. Tritium and Helium-3 in the northeastern Atlantic Ocean during the 1983 topogulf cruise. *Journal of Geophysical Research* 93:12511–24.

Archambeau A-S, Pierre C, Poisson A, Schauer B. 1998. Distributions of oxygen and carbon stable isotopes and CFC-12 in the water masses of the Southern Ocean at 30°E from South Africa to Antarctica: results of the CIVA1 cruise. *Journal of Marine Systems* 17:25–38.

Arnold M, Bard E, Maurice P, Duplessy J-C. 1987. ^{14}C dating with the Gif-Sur-Yvette Tandetron Accelerator: status report. *Nuclear Instruments and Methods in Physics Research* B29:120–3.

Bard E. 1988. Correction of AMS ^{14}C ages measured in planktonic foraminifera: paleoceanographic implications. *Paleoceanography* 3:635–45.

Bard E, Arnold M, Maurice P, Duplessy J-C 1987 Measurements of bomb radiocarbon in the ocean by means of accelerator mass spectrometry: technical aspects. *Nuclear Instruments and Methods in Physics Research* B29:297–301.

Bard E, Arnold M, Östlund HG, Maurice P, Monfray P, Duplessy J-C. 1988. Penetration of bomb radiocarbon in the tropical Indian Ocean measured by means of accelerator mass spectrometry. *Earth and Planetary Science Letters* 87:379–89.

Bayer R, Schlosser P. 1991. Tritium profiles in the Weddell Sea. *Marine Chemistry* 35:123–36.

Berkman PA, Forman SL. 1996. Pre-bomb radiocarbon and the reservoir correction for calcareous marine species in the Southern Ocean. *Geophysical Research Letters* 23:363–6.

Broecker WS, Peng TH. 1974. Gas exchange rates between air and sea. *Tellus* 26:21–35.

Broecker WS, Peng T-H, Östlund G, Stuiver M. 1985. The distribution of bomb radiocarbon in the ocean. *Journal of Geophysical Research* 90:6953–70.

Broecker WS, Sutherland S, Smethie W, Peng TH, Östlund G. 1995. Oceanic radiocarbon: separation of the natural and bomb components. *Global Biogeochemical Cycles* 9:263–88.

Carmack EC, Foster TD. 1977. Water masses and circulation in the Weddell Sea. In: Dunbar MJ, editor. *Polar oceans*. Calgary: Arctic Institute of North America. p 151–65.

Foster TD, Carmack EC. 1976. Frontal zone mixing and Antarctic bottom water formation in the southern Weddell Sea. *Deep-Sea Research* 23:301–17.

Gordon AL. 1971. Antarctic polar front zone. In: Reid JL, editor. *Antarctic Oceanology I, Antarctic research series*. Washington: American Geophysical Union. p 205–21.

Haine TWN. 1996. Combining passive tracer observations with ocean circulation models. *International WOCE Newsletter* 23:3–5.

Jean-Baptiste P, Mantisi F, Mémery L, Jamous D. 1991.

^{3}He and chlorofluorocarbons (CFC) in the Southern Ocean: tracers of water masses. *Marine Chemistry* 35:137–50.

Jenkins WJ. 1980. Tritium and ^{3}He in the Sargasso Sea. *Journal of Marine Research* 38: 533–69.

Key RM, Quay PD, Jones GA, McNichol AP, Von Reden KF, Schneider RJ. 1996. WOCE AMS Radiocarbon I: Pacific Ocean results (P6, P16, P17). *Radiocarbon* 38(3):425–518.

Maier-Reimer E. 1993. Geochemical cycles in an ocean general circulation model preindustrial tracer distributions. *Global Biogeochemical Cycles* 7:645–77.

Mensch M, Bayer R, Bullister JL, Schlosser P, Weiss RF. 1996. The distribution of tritium and CFCs in the Weddell Sea during the mid-1980s. *Progress in Oceanography* 38:377–415.

Orr JC. 1996. The ocean carbon-cycle model intercomparison project of IGBP/GAIM. In: Ormerod B, editor. *International Energy Agency, ocean storage of CO_2 workshop 3: international links and concerns* (ISBN 1 89 83 73 04 3). Southampton, England.

Orsi AH, Nowlin WD, Whitworth T III. 1993. On the circulation and stratification on the Weddell Gyre. *Deep-Sea Research* 40:169–203.

Orsi AH, Whitworth T III, Nowlin WD. 1995. On the meridional extent and fronts of the Antarctic Circumpolar Current. *Deep-Sea Research* 42:641–73.

Östlund HG, Grall C. 1988. *INDIGO 1985–1987 Indian Ocean radiocarbon: tritium laboratory data report.* University of Miami: Rosenstiel School of Marine and Atmospheric Science.

Östlund HG, Stuiver M. 1980. GEOSECS Pacific radiocarbon. *Radiocarbon* 22(1):25–53.

Poisson A, Chen C-TA. 1987. Why is there little anthropogenic CO_2 in the Antarctic bottom water? *Deep-Sea Research* 34:1255–75.

Sarmiento JL, Orr JC, Siegenthaler U. 1992. A perturbation simulation of CO_2 uptake in an ocean general circulation model. *Journal of Geophysical Research* 97: 3621–45.

Schlosser P, Bullister JL, Bayer R. 1991. Studies of deep water formation and circulation in the Weddell Sea using natural and anthropogenic tracers. *Marine Chemistry* 35:97–122.

Schlosser P, Kromer B, Weppernig R, Loosli HH, Bayer R, Bonani G, Suter M. 1994. The distribution of ^{14}C and ^{39}Ar in the Weddell Sea. *Journal of Geophysical Research* 99:10275–87.

Stuiver M, Östlund HG. 1980. GEOSECS Atlantic radiocarbon. *Radiocarbon* 22:1–24.

Stuiver M, Östlund HG. 1983. GEOSECS Indian Ocean and Mediterranean radiocarbon. *Radiocarbon* 25(1): 1–29.

Stuiver M, Östlund HG, McConnauqhey TA. 1981. GEOSECS Atlantic and Pacific ^{14}C distribution. In: Bolin B, editor. *Carbon cycle modeling*. New York: John Wiley & Sons. p. 201–9.

Stuiver M, Polach HA. 1977. Reporting of ^{14}C data. *Radiocarbon* 19(3):355–63.

Taylor NK. 1995. Seasonal uptake of anthropogenic CO_2 in a ocean general circulation model. *Tellus* 47B:145–69.

Toggweiler JR, Dixon K, Bryan K. 1989a. Simulations of radiocarbon in a coarse-resolution world ocean model. 1. Steady state prebomb distributions. *Journal of Geophysical Research* 94:8217–42.

Toggweiler JR, Dixon K, Bryan K. 1989b. Simulations of radiocarbon in a coarse-resolution world ocean model. 2. Distributions of bomb-produced carbon 14. *Journal of Geophysical Research* 94:8243–64.

Toggweiler JR, Samuels B. 1993. New radiocarbon constraints on the upwelling of abyssal water to the ocean's surface. In: Heimann, M, editor. *The global carbon cycle*. Berlin: NATO ASI Series. p 333–66.

Toggweiler JR, Wallace D. 1995. Transport capacity for passive tracers. *US WOCE Report 1995*. p 36–8.

Warner MJ, Weiss RF. 1985. Solubilities of chlorofluorocarbons 11 and 12 in water and seawater. *Deep-Sea Research* 32:1485–97.

Weiss RF, Östlund HG, Craig H. 1979. Geochemical studies of the Weddell Sea. *Deep-Sea Research* 26A: 1093–120.

Weppernig R, Schlosser P, Khatiwala S, Fairbanks RG. 1996. Isotope data from Ice Station Weddell: implications for deep water formation in the Weddell Sea. *Journal of Geophysical Research* 101:25723–39.

Whitworth T III, Nowlin WD. 1987. Water masses and currents of the southern ocean at the Greenwich Meridian. *Journal of Geophysical Research* 92:6462–76.

Worthington LV. 1977. The case for near-zero production of Antarctic bottom water. *Geochimica Cosmochima Acta* 41:1001–6.

Wunsch C, Hu DX, Grant B. 1983. Mass, heat, salt, and nutrients fluxes in the South Pacific Ocean. *Journal of Physical Oceanography* 13: 725–753.

APPENDIX: VENTILATION MODEL

Our ventilation model is inspired by Jenkins (1980) who used such a model to explain the penetration of ^3H in the North Atlantic and to study the $^3H/^3He$ relationship. At any time t, our model determines the annual ventilation rate η, which is defined as the fraction of water at depth z replaced by water originating from the surface during the timestep Δt. A time-lag τ is defined to correspond to the travel time of a water parcel moving from the surface to depth z. Thus, at depth z

$$C_{z,t+1} = C_{z,t} + \eta \times [C_{0,(t-\tau)} - C_{z,t}] \quad \text{(A1)}$$

where $C_{0,(t-\tau)}$ is the surface concentration at time $(t-\tau)$ and $C_{z,t}$, $C_{z,t+1}$ are the concentrations at depth z in years t and t+1.

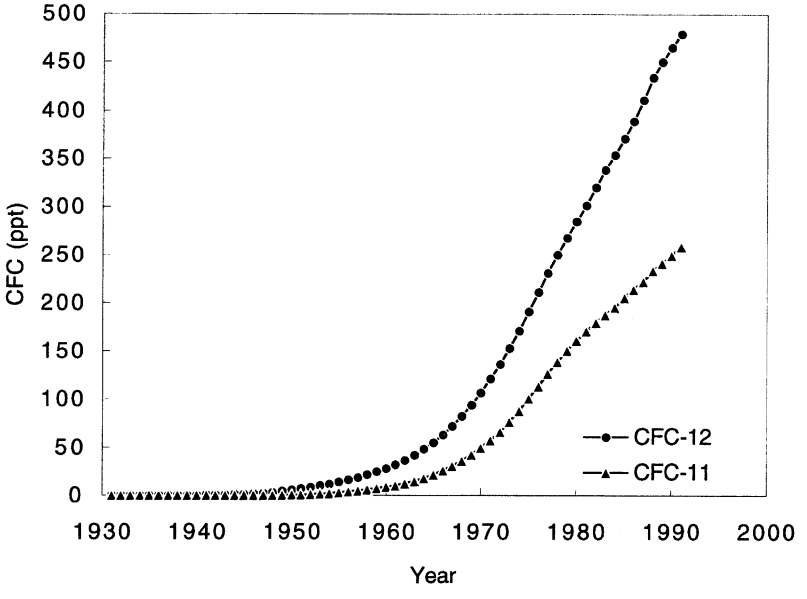

Figure A1 Partial pressure of atmospheric CFC-11 and CFC-12 in the Southern Hemisphere versus time (Walker, Salameh, and Weiss, personal communication 1995).

First, the annual ventilation rate and the transit time are adjusted using both CFC-11 and CFC-12 to match the measured concentrations at the time of CIVA1 (1993). For our calculations, we used the time evolution of atmospheric CFC-11 and CFC-12 concentrations (Fig. A1) given by Walker, Salameh, and Weiss (personal communication 1995) as well as solubilities from Warner and Weiss (1985). This simple method gives the best result when a transit time τ of < 1 yr is chosen. Results are essentially identical whether using CFC-11 or CFC-12. With our method (Δt = 1 yr), this means that τ is set to zero.

Second, we used the same model, now with the known η and τ from the CFC calibration, and a reconstructed ^{14}C input function shown in Figure A2, to determine the evolution of the total ^{14}C until the time of CIVA1 (see an example of the method in Fig. A3). For this, we again used equation (A1), where C is now ^{14}C. The reconstructed ^{14}C input function has large uncertainties due to the scatter of available data (Fig. A3). We have arbitrarily drawn minimum and maximum curves. We favor the lowest curve because it allows a close agreement around the transition at 90 μmol kg^{-1}

between the CAS and SAS methods; SAS is applied for waters where SiO_2 lies between 0 and 90 µmol kg^{-1}.

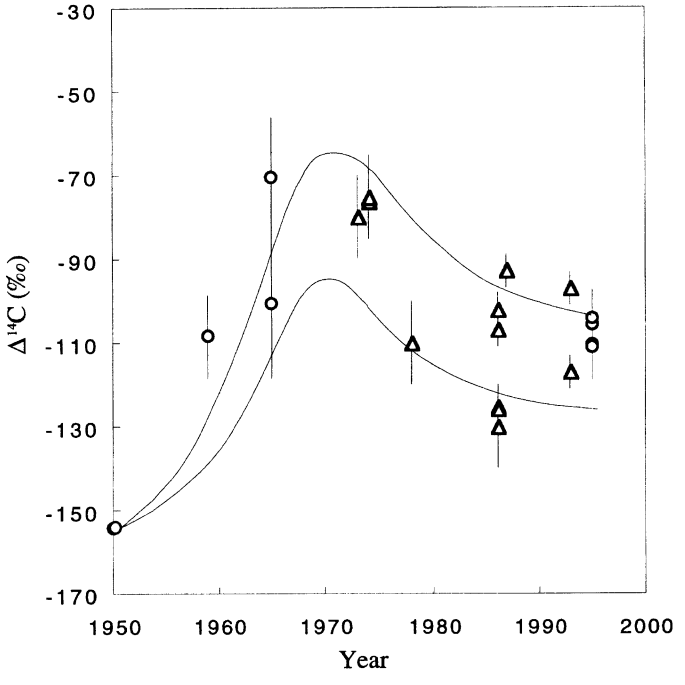

Figure A2 Time evolution of the surface ocean $\Delta^{14}C$ compiled from the ^{14}C record from marine molluscs, brachiopods, echinoderms and foraminifera (○) collected near the Antarctica (Berkman and Forman 1996), and ^{14}C measurements on surface samples from GEOSECS, INDIGO3 and CIVA1 stations (△) near Antarctica (Östlund and Stuiver 1980; Stuiver and Östlund 1980, 1983; Stuiver et al. 1981; Schlosser et al. 1994; Östlund and Grall 1988). Predicted prenuclear surface $\Delta^{14}C$ is ca. −150‰ (Berkman and Forman 1996). Minima and maxima curves are drawn arbitrarily. We chose the lower curve for our CAS methodology because with it CAS and SAS methods agree for waters where SiO_2 <90 µmol kg^{-1}.

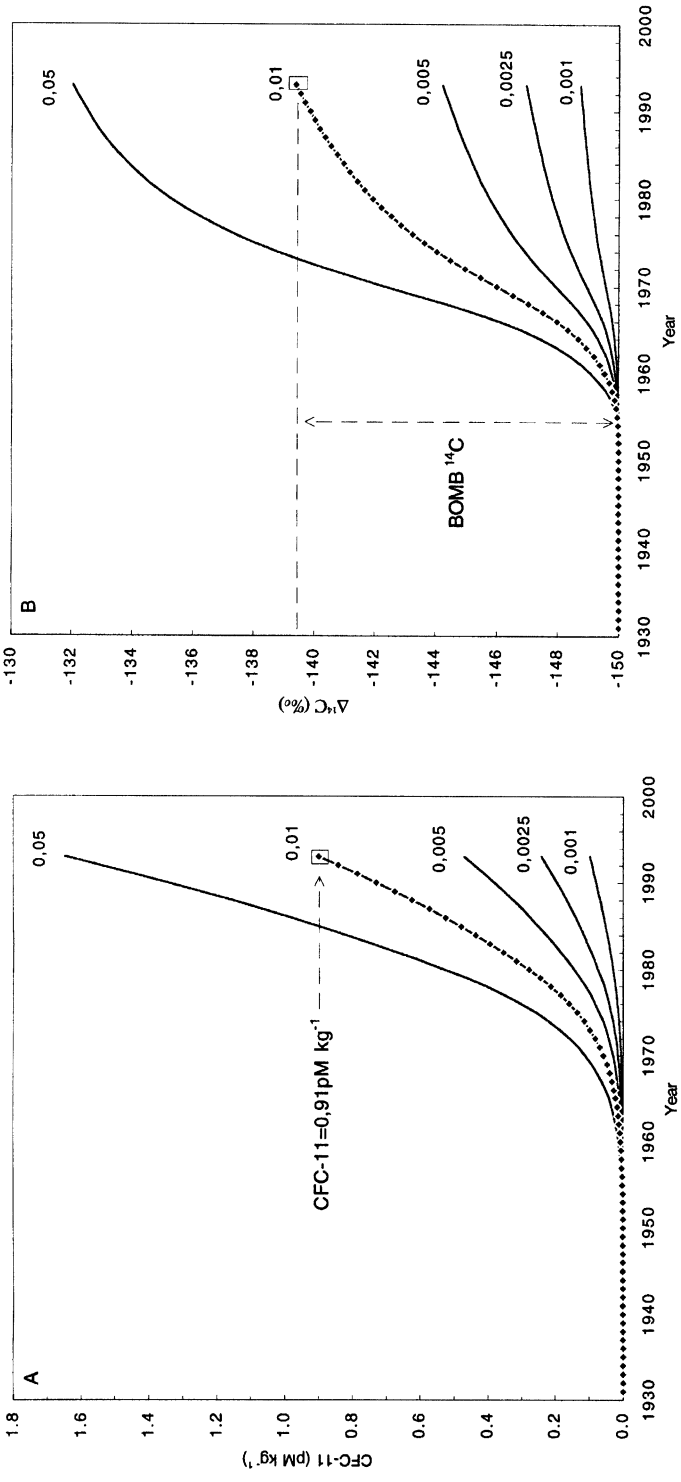

Figure A3 Illustration of our use of the mixing model to determine the bomb ^{14}C component for the sample at 4065 m from CIVA1 station 8. With the known CFC-11 input function and a transit time set to zero, several dilution rates are shown for ventilation from the surface. For this sample, the dilution rate of 0.01 is appropriate since it produces the measured CIVA1 CFC-11 concentration in 1993 (0.91 pmol kg^{-1}). With that dilution rate, the surface ocean record of bomb ^{14}C (Fig. A2), and equation (A1), we calculate the corresponding contribution of bomb ^{14}C (10‰). The same operation repeated for the same sample with the CFC-12 gives consistent results. For our final bomb ^{14}C estimates we average results obtained when using CFC-11 and CFC-12.

RADIOCARBON, Vol 41, Nr 1, 1999, p 75–79

RADIOCARBON DISTRIBUTION IN NORTHWEST BELARUS NEAR THE IGNALINA NUCLEAR POWER PLANT

Nikolaj D Mikhajlov • Vladimir M Kolkovsky • Iren D Pavlova

Institute of Geological Sciences of the National Academy of Sciences of Belarus, Kuprevich Street 7, Minsk, 220141 Republic of Belarus

ABSTRACT. Since 1994, the Institute of Geological Sciences has undertaken an environmental monitoring program to measure radiocarbon levels in territory adjacent to active nuclear power plants (NPP). We determined ^{14}C concentrations in natural objects from areas contiguous to Ignalina NPP as well as ^{14}C background concentration in areas remote from the NPP. In the environs of the Ignalina station comparatively elevated levels of ^{14}C were observed in vegetation and waters of Lake Drisvyaty. This appears to be a consequence of release of carbon radioisotope into the atmosphere and probably into waters of the lake during operation of the nuclear reactor.

INTRODUCTION

The accident at the Chernobyl Nuclear Power Plant (NPP) in the Ukraine raised questions in Belarus concerning the reliability of operational cycles of the NPPs surrounding the territory of our country. Some answers can be obtained by studying the distribution of radiocarbon as one of the components of environmental radiocontamination. For this purpose we chose as an object of research the area in northwestern Belarus where the Ignalina NPP (INPP), in Lithuania (55°37′N, 26°36′E), is situated most closely to Belarus. The INPP, located on Lake Drisvyaty (Fig. 1), is equipped with Chernobyl-type reactors; 2 units operate there.

^{14}C can be formed in the active zone of nuclear reactors of any type, where flows of neutrons can interact with reactor components, coolant, the nuclear fuel moderator or impurities contained in these. The rate of ^{14}C formation in the fuel depends mainly on concentrations of nitrogen admixtures. What distinguishes the INPP reactor, which uses boiling water under pressure as a coolant (heat-carrier) and graphite as a moderator, is the presence of abundant nitrogen in an active zone used in a mixture with helium for cooling and a large mass of carbon in the moderator. This results in a significant rate of ^{14}C generation, approximately an order of magnitude greater than in reactors of other types (Ryblevsky et al. 1979). ^{14}C formed in the coolant and moderator is released partially or completely into the environment as a gas-aerosol complex, and also from reactor fuel in the form of radioactive waste.

METHODS

^{14}C concentrations were measured at some experimental sites selected on the basis of their location with respect to the nuclear plant. The INPP premises are characterized in general by increased technogenic load on the landscape and by destruction of the soil/vegetation cover. Two canals designed for water intake for cooling the reactor and for dumping coolant into a reservoir extend from the NPP to Lake Drisvyaty, and a thermal anomaly has been recorded within the lake (Novikov et al. 1994).

A water-controlled area of Lake Naroch, a hydrological post in Belovezhskaya Pushcha, and some sites in the Dokshitsy District of the Vitebsk Region (Berezinsky Reserve) and the Gorki and Dubrovno Districts of the Mogilev Region were chosen as control regions, presumably not exposed to the NPP influence (Table 1).

Measurement of ^{14}C activity was performed at the Institute of Geological Sciences using liquid scintillation counting (LSC). Benzene synthesis from samples of vegetation, surface water, and mollusk

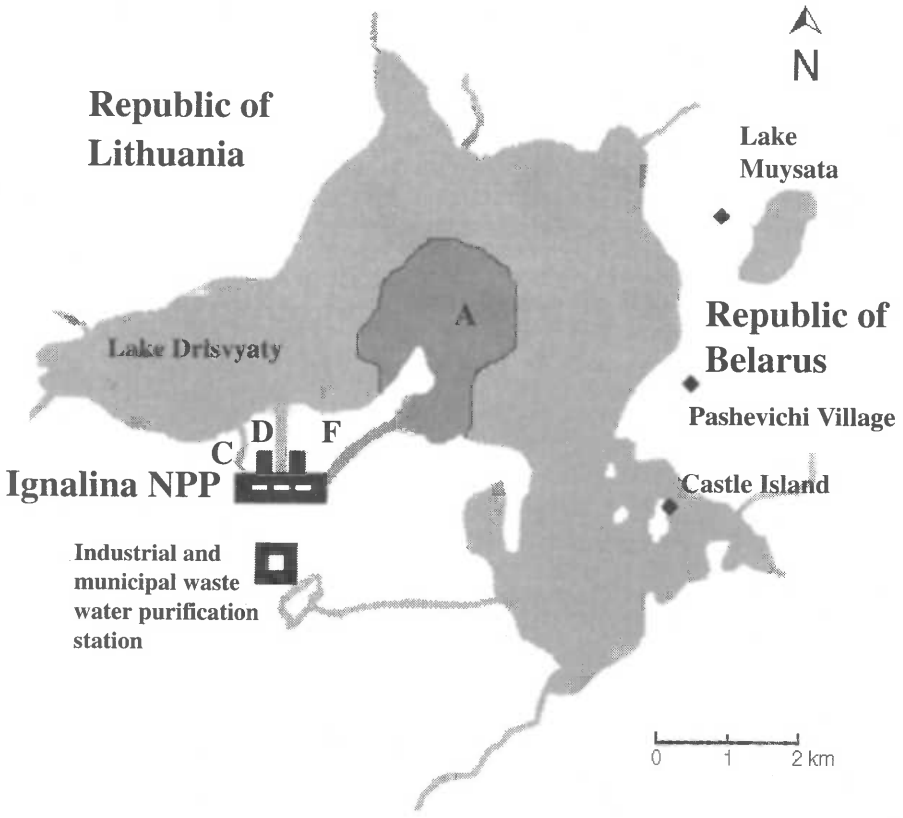

Figure 1 Environs of Ignalina NPP and sample sites. **A** = heat anomaly of the lake; **C** = INPP industrial and rainwater sewer; **D** = INPP water intake canal; **F** = INPP heated water outflow canal; ♦ = sample selection sites.

shells was performed using a synthesis installation (Skripkin and Kovaliukh 1994; Skripkin and Kovaliukh 1998) that enables production of highly purified benzene in sufficient amounts for counting. β-counting was done using a Tri-Carb® TR-2500 AB and an LKB 1211 Rackbeta. The results of ^{14}C activity are expressed as a percentage of the modern standard.

RESULTS

As shown by the results of ^{14}C measurement (Table 2), the region of Belarus contiguous with the INPP is distinguished by an increase in ^{14}C concentrations in vegetation of up to 120%–150% relative to the present level in undisturbed areas. Bulrush sampled near Castle Island in Lake Drisvyaty and 2-yr-old pine cones growing on the lakeside close to Pashevichi Village exhibit the maximum ^{14}C accumulation. Relatively high ^{14}C values were observed directly in water from Lake Drisvyaty, connected by canals with the INPP.

At the same time, water from the closed Lake Muysata does not manifest the NPP influence in every year observed. ^{14}C concentrations vary from the current level (102 pMC) up to a comparatively increased one (132 pMC). Similar ^{14}C contents (120–150 pMC) are also observed in carbonate of mollusk shells (*Anadonta*, *Unio,* and *Dreisena*) collected along lake shores. ^{14}C release from INPP

Table 1 Radiocarbon concentration in natural objects from Belarus, far from any NPP

Sample type	Collection site	Year dated	Lab code	^{14}C content (pMC)
Cowberry leaves	Brest region	1994	IGSB-76	102
Moss	Brest region	1994	IGSB-77	107
Oak leaves	Brest region	1996	IGSB-255	104
Oak leaves	Gorki region	1994	IGSB-54	101
Annual grasses	Gorki region	1994	IGSB-41	98
Carbonate from water	Vitebsk region, Medsozol Lake	1994	IGSB-385	128
Birch leaves	Vitebsk region, Medsozol Lake	1994	IGSB-26	115
Atmospheric carbonate	Minsk	1994	IGSB-9	94
Moss	Minsk region	1994	IGSB-15	126
Pine needles	Mogilev region	1994	IGSB-56	86
Birch leaves	Mogilev region	1994	IGSB-57	92
Atmospheric carbonate	Naroch lake	1994	IGSB-80	103
Moss	Naroch lake	1996	IGSB-257	99
Annual rings of pine (1984)	Vitebsk region	1987	IGSB-6	105
Annual rings of pine (1985)	Vitebsk region	1987	IGSB-7	105
Annual rings of pine (1986)	Vitebsk region	1987	IGSB-8	102
Carbonate of mollusk shells (*Anadonta, Unio,* and *Dreisena)*	Vitebsk region, Losvido Lake	1997	IGSB-413	127

operation was revealed as well in eggshell carbonate from hens whose food consisted of cereals grown near the NPP (Pashevichi Village, 152 pMC).

The analysis of ^{14}C in annual rings of trees (Fig. 2) shows the tendency of ^{14}C distribution during the period 1979–1994 and is closely comparable to determinations of ^{14}C concentrations in water from Lake Drisvyaty made by Banis (1988), who found that they varied from 115 to 150 pMC during 1978–1986.

In comparison with 1994 values, our 1996 measurements showed a reduction in ^{14}C concentrations in plants. This phenomenon seems to be associated with the fact that in 1996 the Ignalina NPP was repeatedly subjected to preventive maintenance.

CONCLUSION

Our determinations of ^{14}C concentration in the atmosphere, surface waters, and vegetation are essentially the first ones for the Belarus area. They characterize both ^{14}C background concentrations (without penetration of technogenic radioisotopes) and ^{14}C values in the region adjoining the Ignalina NPP. Obvious variations in the distribution of ^{14}C concentrations are associated with penetration into surrounding air and surface water of "surplus" ^{14}C from the nuclear power plant operating in its standard regime. The data obtained point to the value of including ^{14}C measurement in a radioisotope monitoring system.

Table 2 Radiocarbon concentrations in natural objects from areas contiguous to Ignalina NPP

Sample type	Collection site	Year dated	Lab code	^{14}C content (pMC)
Atmospheric carbonate	Lake Drisvyaty	1994	IGSB-65	96
Atmospheric carbonate	Lake Drisvyaty	1995	IGSB-175	110
Atmospheric carbonate	Lake Drisvyaty	1996	IGSB-380	106
Carbonate from water	Lake Drisvyaty	1994	IGSB-384	144
Carbonate from water	Lake Muysata	1995	IGSB-382	132
Carbonate from water	Lake Drisvyaty	1996	IGSB-383	154
Algaes	Lake Drisvyaty	1994	IGSB-39	105
Algaes	Lake Drisvyaty	1995	IGSB-179	111
Barley	Shore of Lake Drisvyaty	1996	IGSB-210	117
Bulrush	Lake Drisvyaty, Castle Island	1994	IGSB-22	150
Bulrush	Lake Drisvyaty, Castle Island	1995	IGSB-176	143
Bulrush	Lake Drisvyaty, Castle Island	1996	IGSB-191	119
Flax	Shore of Lake Muysata	1996	IGSB-206	104
Oats	Shore of Lake Volosovo	1996	IGSB-192	111
Alder leaves	Lake Drisvyaty, Castle Island	1994	IGSB-38	107
Alder leaves	Lake Drisvyaty, Castle Island	1995	IGSB-174	117
Alder leaves	Lake Drisvyaty Castle Island	1996	IGSB-199	115
Alder leaves	Shore of Lake Drisvyaty	1994	IGSB-42	112
Alder leaves	Shore of Lake Drisvyaty	1995	IGSB-172	110
Young pine cone	Shore of Lake Drisvyaty	1995	IGSB-182	119
Young pine cone	Shore of Lake Drisvyaty	1996	IGSB-215	115
2-yr-old pine cones	Shore of Lake Drisvyaty	1994	IGSB-31	190
2-yr-old pine cones	Shore of Lake Drisvyaty	1995	IGSB-167	138
2-yr-old pine cones	Shore of Lake Drisvyaty	1996	IGSB-214	118
Carbonate from mollusk shells – *Anadonta Unio*	Lake Muysata	1996	IGSB-314	133
Carbonate from mollusk shells – *Anadonta Unio*	Lake Muysata	1996	IGSB-315	135
Carbonate from mollusk shells – *Dreisena*	Lake Drisvyaty	1996	IGSB-313	124
Mollusk soft tissue – *Anadonta Unio*	Lake Muysata	1996	IGSB-280	123
Soft tissue of mollusk – *Dreisena*	Lake Drisvyaty	1996	IGSB-281	124
Eggshell from household hens	Stankevichi Village (Lake Muysata)	1997	IGSB-393	137
Eggshell from household hens	Pashevichi Village	1997	IGSB-394	152

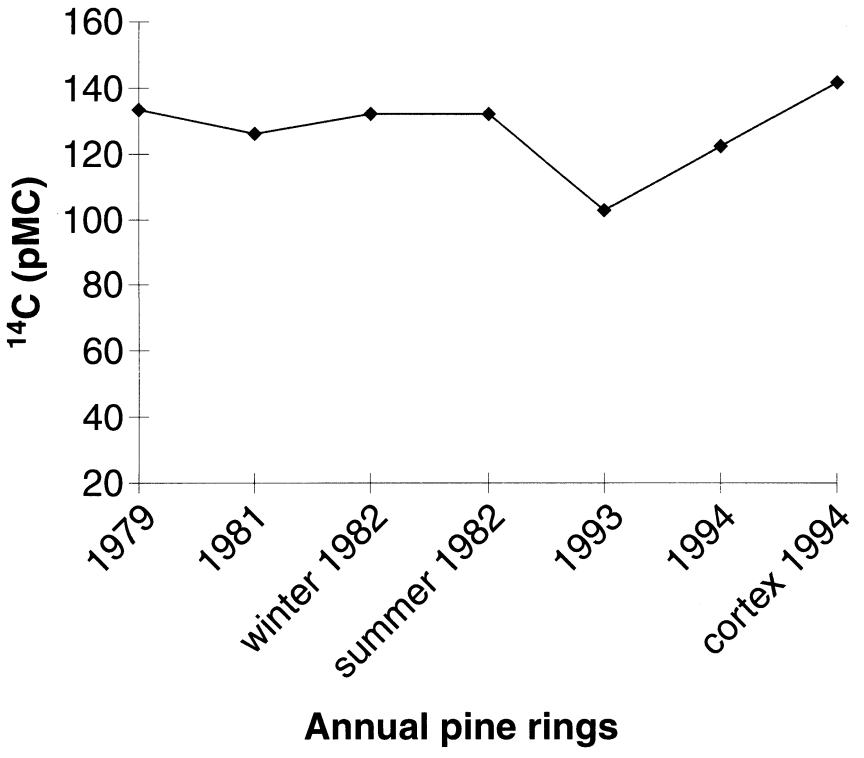

Figure 2 ^{14}C concentrations in annual rings of pine growing along the Lake Drisvyaty shoreline

REFERENCES

Banys J. 1988. Isotope hydrogeochemical investigation in the region of Ignalina APS. *Isotope Geochemical Research in Baltic Countries and Belarus (Tallinn)*: 5–15 (in Russian).

Novikov G, Romanov V, Kapelchikov N. 1994. Influence of Ignalina NPP on conditions of Drisvyaty Lake. Byelorussian State University Bulletin, Series 2: *Chemical, Biological, and Geographical Sciences* 1: 63–6 (in Russian).

Ryblevsky V, Golenetsky S, Kirdin G. 1979. *Radioactive carbon in the biosphere*. Moscow: AtomIzdat. 196 p (in Russian).

Skripkin V, Kovaliukh N. 1994. A universal technology for oxidation of carbon-containing materials for radiocarbon dating. Conference of Geochronology and Dendrochronology of Ancient Towns and Radiocarbon Dating of Archeological Finds. 1994 Oct 31–Nov 4; Vilnius, Lithuania. Abstracts and Papers. Vilnius: Vilnius University Press. p 37–42.

Skripkin V, Kovaliukh N. 1998. Recent developments in the procedures used at the SSCER laboratory for the routine preparation of lithium carbide. *Radiocarbon* 40(1):211–4.

RADIOCARBON, Vol 41, Nr 1, 1999, p 81–97

VARIATIONS OF ISOTOPIC COMPOSITION OF CARBON IN THE KARST ENVIRONMENT FROM SOUTHERN POLAND, PRESENT AND PAST

Anna Pazdur[1] • Tomasz Goslar[1] • Mirosława Pawlyta[1] • Helena Hercman[2] • Michał Gradziński[3]

ABSTRACT. We describe a comprehensive study of carbon isotopes in several karst springs and their environs in a contemporary karst environment in the region of the Cracow-Wieluń Upland and Western Tatra Mountains, Southern Poland. We collected samples of water, plants and carbonate deposited on aquatic plants, and obtained ^{13}C values and ^{14}C concentrations. We also investigated a group of the youngest calcium carbonates from caves where deposition is still being observed or ceased no more than a few hundred years ago. The determination of a ^{14}C dilution factor (q) in these carbonates allows us to determine the "true" radiocarbon ages of old speleothems from caves in the area under investigation and enables the use of old speleothems as suitable material for extending the ^{14}C calibration time scale, the "Absolute" age having been determined by U/Th or amino acid racemization (AAR) dating methods. Measurements of $\delta^{13}C$ and ^{14}C concentrations were made on dissolved inorganic carbon (DIC) extracted from water samples. Calculated values of q range from 0.55 to 0.68 and $\delta^{13}C$ values range from −10‰ to −13‰ versus VPDB with mean values equal to 0.65 and −12‰, respectively. Results indicate that the dissolution process of limestone bedrock is a closed system with the dominating contributor being biogenic carbon dioxide.

Isotopic composition of carbon in contemporary plants collected at the karstic springs at 3 localities is highly diverse, with different species distinctly varying in both q and $\delta^{13}C$ values. Extremely light values of ^{13}C (under −40‰), observed in Algae and *Hyloconium splendens*, are correlated with ^{14}C concentrations that are much lower than 100 pMC. Small systematic changes of isotopic composition were found in plants of the same species collected along streams at various distances from the spring. The youngest calcium carbonates from different caves show a relatively high scatter of both $\delta^{13}C$ values and ^{14}C concentration. The lower reservoir effect for ^{14}C is observed in samples with higher value of $\delta^{13}C$, indicating equilibrium conditions in the sedimentation of carbonate. Pazdur et al. (1995b) presented ^{14}C dating results and paleoclimatic interpretation of 170 ^{14}C analyses of 89 speleothems from 41 caves obtained through 1994. Investigations continued until early 1997, during which time a speleothem, JWi2, was dated by ^{14}C, U/Th and AAR dating methods, and its stable isotope composition ($\delta^{13}C$ and $\delta^{18}O$) analyzed in detail (reported here). Carbon isotope analyses indicate very large differences among results obtained by U/Th, AAR, and ^{14}C dating methods.

INTRODUCTION

It is widely recognized that isotopic studies of carbon and oxygen of freshwater calcite precipitates in the temperate zone have the potential to reconstruct certain parameters of environmental conditions that existed during sedimentation. The isotopic compositions of carbon, oxygen, uranium, and thorium in freshwater carbonates deposited in speleothems (Geyh and Hennig 1986; Geyh and Schleicher 1990; Gascoyne 1992; Harmon et al. 1978; Hennig et al. 1983, Hercman 1991; Pazdur et al. 1995b; Baker et al. 1993; Schwarcz 1986), calcareous tufas (Pazdur et al. 1988; Srdoč et al. 1983; Turi 1986; Usdowski et al. 1979) and lake sediments (Digerfeldt 1988; Goslar et al. 1995; Magny 1992, 1993; Pazdur et al. 1995a) enable reconstruction of the time scale of sedimentary processes and their climatic conditions. Measurement of radiocarbon in carbonates enables us to determine the ^{14}C age of sediments, that is, the time of deposition on the ^{14}C time scale, but with a substantial error that depends on the geochemical cycle of carbon in the investigated area (e.g., "reservoir effect"). The U/Th dating method allows calendar ages to be determined back to about 300 ka but with relatively low precision, particularly for younger sediments. Measured values of the stable isotopes of carbon and oxygen ($\delta^{13}C$ and $\delta^{18}O$) in carbonate are indicative of temperature and humidity during the deposition processes.

The isotopic composition of calcareous precipitates under the same thermal conditions is characteristic of the sedimentary environment (caves, springs, lakes), geographical region (altitude, longi-

[1]Institute of Physics, Silesian Technical University, Krzywoustego 2, PL-44-100 Gliwice, Poland
[2]Polish Academy of Science, Institute of Geological Sciences, Twarda 51/55, PL-00-818 Warszawa, Poland
[3]Jagiellonian University, Institute of Geological Sciences, Oleandry 2a, PL-30-063 Cracow, Poland

tude), type of bedrock in the karst area or carbonate in the soil and source of water infiltrating bedrock (meteoric water, groundwater from different depths), source of CO_2 dissolving the bedrock (atmospheric, biogenic, metamorphic) and type of vegetation covering the study area; incorporation of CO_2 from decomposing plants generally predominates.

Differing conditions during precipitation of freshwater carbonate determine the seasonal changes of carbon isotope composition. These are induced by changes in the isotopic composition of atmospheric CO_2, dissolved inorganic carbon (DIC) in water, and the photosynthetic pathways in plants (Willkom and Erlenkeuser 1973; Horvatinčić et al. 1989; Marcenko et al. 1989; Shore et al. 1995). To try to answer the many questions associated with studies of isotope composition in the environment, the research must continue over several years and isotopic analyses must be performed on all parts of the ecosystem that may be relevant to the geochemical cycle of carbon in the study area.

Simple geochemical models describing the cycle of carbon isotopes in the environment and the isotopic composition of DIC in water (Pearson and Hanshaw 1970; Vogel 1970) predict that the concentration of ^{13}C and ^{14}C isotopes is determined by carbon from different sources and that the ^{14}C concentration at the time of precipitation of carbonates is <100 pMC. This so-called "reservoir effect" is important in the ^{14}C dating of groundwater (Eichinger 1983; Mook 1976, 1980; Mook et al. 1974), speleothems (Geyh and Schleicher 1990; Schwarcz 1986), tufas (Pazdur 1988; Pazdur et al. 1988, Srdoč et al. 1983) and lake sediments (Olsson 1986; Pazdur et al. 1995a). Measurements of carbon isotope composition in different parts of the contemporary environment in the karst area enable one to infer the magnitude of the "reservoir correction" for ^{14}C ages of carbonates from the region of interest. This reservoir correction can then be used to determine the "true conventional radiocarbon age" of a single layer of calcium carbonate in a speleothem. The possibility of U/Th dating the same layer provides the relationship between conventional ^{14}C ages and calendar ages (U/Th method), that is, the possibility of extending the calibration of the ^{14}C time scale to around 50 ka BP (Goslar et al. 1997). A few uncertainties in extending back into the past glacial period are inherent in inferring the ^{14}C age of groundwater, thus of cave carbonates (Pearson 1992).

THE STUDY AREA

The main study area is the Cracow-Wieluń Upland of Southern Poland (Fig. 1; Pazdur et al. 1995b), the largest and best explored karst region in Poland. The Cracow-Wieluń Upland consists of Upper Jurassic limestones and covers about 2900 km^2. Stable isotope data for the bedrock ($\delta^{13}C$ and $\delta^{18}O$, see Table 1) are comparable with results for Jurassic limestones from other regions throughout the world (Keith and Weber 1964; Morse and Mackenzie 1990). Three sites chosen for the study of the contemporary environment were 1) a karst spring and its environs in Będkowska Valley, 2) karst Zygmunt Springs, and 3) several small karst springs and their environs in Zdów. Chochołowska Cave is located in the Western Tatra Mountains; the bedrocks of this karst area consist of Mesozoic limestones and dolomites.

MATERIALS AND METHODS

Contemporary Environment

The research included different parts of the local karst ecosystems of the sites of interest. A Pazdur, M F Pazdur and H Hercman collected water samples from karst springs from October 1991 to June 1993 (Table 2). M Gradziński collected samples from Chochołowska Cave. During 1992–1993, recent carbonates deposited on algae, mosses growing in karst springs (Table 3) and some water samples were collected. A Pazdur, M F Pazdur and H Hercman collected plant samples from Octo-

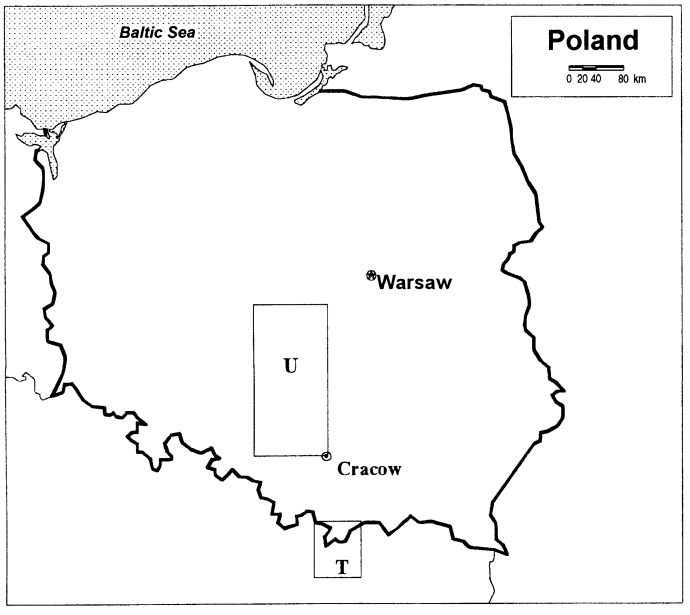

Figure 1 Map of Poland and investigated karst areas. U = Cracow-Wielún Upland, T = Tatra Mountains.

Table 1 $\delta^{13}C$ and $\delta^{18}O$ values in limestones

Sample	$\delta^{13}C$ (‰, VPDB)	$\delta^{18}O$ (‰, VSMOW)	Site
Cracow-Wieluń Upland, Cave			
JM0	+2.53	26.66	Mamutowa
JMd0	+1.16	26.09	Mydlnicka
JD0	+2.95	27.69	Dziewicza
JC0	+2.32	26.40	Ciemna
STG0	+4.24	28.95	Tomaszówki Górne
DB0/2	+3.25	29.22	Będkowska Valley
DB/4	+2.33	34.08	Będkowska Valley
DB0/8	3.33	30.85	Będkowska Valley
JZł0	−0.5	23.40	Złodziejska
"Cracow"	−2.3	26.00	Limestones near Cracow
Western Tatra Mountains, Cave			
JCh0/1	−1.4	23.6	Chochołowska
JCh0/2	−1.0	24.2	Chochołowska
JCh0/3	−4.5	24.0	Chochołowska

ber 1991 to June 1993 (Table 4). J Baryła, botanist at the Jagiellonian University, and T Goslar identified plants.

Most of the plant samples were collected in spring and early summer during the time of intensive growth. One sample series was collected in late autumn (October 1991 and December 1992) from the spring in the Będkowska Valley and along the stream course (Fig. 6). All plants except one moss sample (*Hyloconium splendens* and *Pleurozium schreberi*; Table 4) grew in an aquatic environment in springs with differing rates of water flow, the strongest flow being in the Zygmunt Springs, weaker in

Table 2 Isotopic composition of carbon in DIC of water samples from karst springs under different caves, Chochołowska Cave and atmospheric CO_2 from Dziewicza Cave

Lab nr Gd-	Sample name	Collection date	^{14}C (pMC)	$\delta^{13}C$ (‰, VPDB)	Site
4759	BWW1/91	91.10.01	61.9 ± 0.9	−12.03	Będkowska Valley (main outflow); Caves: Nad Źródłem, Na Tomaszówkach, Łabajowa, Kawiory
4886	BWW1/92	92.09.10	55.7 ± 0.7	−12.94	Będkowska Valley (main outflow); Caves: Nad Źródłem, Na Tomaszówkach, Łabajowa, Kawiory
4921	BWW2/92	92.12.03	58.4 ± 0.8	−11.63	Będkowska Valley (main outflow); Caves: Nad Źródłem, Na Tomaszówkach, Łabajowa, Kawiory
4889	DBW2/92	92.09.10	70.0 ± 1.4	−9.66	Będkowska Valley; Dziewicza Cave
4882	BDzW1/92	92.09.10	70.0 ± 1.2	−11.84	Będkowska Valley Cave; Dziewicza Cave
4836	WWW1/92	92.04.30	63.1 ± 0.8	−11.95	Kluczwody Valley (main outflow); Wierzchowska Cave
4866	WWW2/92	92.06.28	61.5 ± 1.0	−10.11	Kluczwody Valley (main outflow); Wierzchowska Cave
6670	DPnSSW1/92	92.05.27	50.6 ± 0.7	−12.32	Prądnik Valley, outflow below Stokowa Skała; Łykowiec Cave
4880	WSW1/92	92.06.01	67.4 ± 0.8	−13.16	Sąspowska Valley, spring in Sąspów
4847	JCHW1/92	92.04.01	82.2 ± 1.8	−4.90	Chochołowska Cave, outflow inside of cave
9010	ZZWW1/93	93.05.01	66.1 ± 0.8	−12.60	Zygmunt Springs; Wierna Cave
9030	ZDWW1/93	93.06.12	72.8 ± 0.9	−12.00	Springs in Zdów; no clear connection with caves
6577	JD-ATM1/91	91.10.11	112.6 ±1.5	−27.88	Dziewicza Cave; atmospheric CO_2

Table 3 $\delta^{13}C$ and $\delta^{18}O$ in carbonates deposited on aquatic plants growing in different springs

Sample name	$\delta^{13}C$ (‰, VPDB)	$\delta^{18}O$ (‰, VSMOW)	Plant	Site
ZDRW 4/93/C	−0.9	21.9	Alga	Spring in Zdów
ZDRW 7/93/C	−1.0	23.5	Alga	Spring in Zdów
ZRW 1/93A/C	0.0	22.7	Moss	Zygmunt Springs
ZRW 6/93/C	−2.5	23.0	Alga	Zygmunt Springs
ZRW 7/93B/C	−3.0	22.2	Alga	Zygmunt Springs
ZRW 14/93/C	−2.9	21.8	Alga	Zygmunt Springs
DBIM 8/92/C	−3.8	26.1	Moss	Będkowska Valley
DBIM 2/92/C	−0.9	25.7	Moss	Będkowska Valley

the spring in the Będkowska Valley, and very slow flow or almost stagnant water in Zdów. Two characteristic groups of aquatic plants were investigated: submerged and semi-submerged in water.

Caves

The youngest calcium carbonates (moonmilk, soda straw stalactite, and outer layers of stalagmite) from different caves in the Cracow-Wieluń Upland and Western Tatra Mountains (Table 5) were col-

Table 4 Isotopic composition of carbon (^{14}C and $\delta^{13}C$) in aquatic plants from the Karst area of the Cracow-Wieluń Upland

Collection date	Lab nr. Gd-	Sample	Plant	^{14}C (pMC)	$\delta^{13}C$ (‰, VPDB)
Będkowska Valley					
91.10.18	7131	DBRW1/91	*Campylium elodes*	55.5 ± 0.3	–48.70
91.10.18	6674	DBRW2/91	*Bryophyta*	64.8 ± 0.7	–42.15
92.12.03	6766	DBRW1/92	*Ranunculus scleratus* L.	61.3 ± 0.8	–39.20
92.12.03	6770	DBRW2/92	*Hyloconium splendens* L.	66.8 ± 0.7	–47.14
92.12.03	4945	DBRW3/92	*Mysotis palustris* Nath.	60.0 ± 0.9	[a]
92.12.03	6800	DBRW4/92	*Hyloconium splendens* Helw.	60.5 ± 0.8	[a]
92.12.03	4939	DBRW5/92	*Veronica beccabunga* L.	87.8 ± 0.9	–34.40
92.12.03	6789	DBRW6/92	*Hyloconium splendens* Helw.	69.4 ± 0.8	–43.49
92.12.03	4938	DBRW7/92	Algae	76.7 ± 1.2	–44.30
92.12.03	6794	DBRW8/92T	Graminae	100.2 ± 1.0	–35.55
92.12.03	4942	DBRW8/92M	*Hyloconium splendens* Helw.	57.0 ± 1.0	–47.00
93.05.20	6939	DBRW1/93	*Crateneuron filicinum* Helw.	67.3 ± 0.9	–43.10
93.05.20	9136	DBRW3/93	*Hyloconium splendens* L.	53.9 ± 1.3	–39.20
93.05.20	9119	DBRW6/93	*Ranunculus scleratus* L.	70.8 ± 2.6	–33.70
93.05.20	9137	DBRW7/93	*Ranunculus scleratus* L.	63.6 ± 1.4	–34.40
93.05.20	9140	DBRW9/93	*Hyloconium splendens* L.	63.2 ± 1.6	–39.30
93.05.20	6932	DBRW11/93	*Pleurozium schreberi* (and *Hyloconium splendens*)	118.6 ± 0.6	–26.70
Zygmunt Springs					
93.05.01	9118	ZRW4/93A	*Cardamine amara* L.	116.5 ± 2.5	–29.00
93.05.01	9135	ZRW9/93A	Algae	70.5 ± 1.5	–44.20
93.05.01	9125	ZRW11/93	*Mentha aquatica* L.	118.5 ± 1.8	–39.60
Springs in Zdów					
92.07.12	6682	ZDRW1/92	*Ranunculus scleratus* L.	73.8 ± 0.7	–33.95
92.07.12	6683	ZDRW2/93	*Hyloconium splendens* L.	78.9 ± 1.0	–33.24
93.05.01	9123	ZDRW2/93	*Brachythecium rivulsre* B.S.G.	86.6 ± 2.2	–36.80
93.05.01	9139	ZDRW6/93	*Brachythecium rivulsre* B.S.G.	62.4 ± 1.9	–35.20
93.05.01	9122	ZDRW9/93	*Cratoneuron filicinum* Helw.	72.8 ± 2.3	–33.40
93.05.01	9124	ZDRW11/93A	*Eur. rip.* (Helw.) Richs.[b]	62.6 ± 2.7	–43.80
93.06.12	6909	ZDRW13/93	(?)	93.5 ± 0.9	–25.00
93.06.12	6100	ZDRW14/93	*Mentha longifolia* (L.) Huds.	111.8 ± 1.4	–25.00

[a]Assumed value of $\delta^{13}C = -30.0$‰; [b]*Eurh. Rip.* = *Eurchynhium riparioides* (Helw.) Richs.

lected during cave explorations by M. Gradziński and A. Górny, from the Geological Museum, Academy of Mining and Metallurgy, Cracow.

A stalagmite (JWi2) approximately 30 cm long, found in Wierna Cave, underwent U/Th and AAR dating at the Institute of Geochemistry and Physics of Minerals, Ukrainian Academy of Sciences, Kiev (Pazdur et al. 1995c) and ^{14}C dating at the Gliwice Radiocarbon Laboratory.

METHODS

All samples were analyzed for ^{14}C content, using gas (CO_2) proportional counters at the Gliwice Radiocarbon Laboratory. Plant samples, prior to combustion, were treated with 2% HCl, washed and dried. Calcium carbonate samples were treated with HCl to create CO_2. The pretreatment of water samples was carried out prior to determination of ^{14}C and $\delta^{13}C$ concentration in DIC according to standard IAEA Vienna procedure. The precipitated $BaCO_3$ was reacted with HCl in a sealed reaction vessel connected to a vacuum line and the CO_2 collected.

Table 5. Isotopic composition of carbon (^{14}C and $\delta^{13}C$) in the youngest calcium carbonate from different caves of the Cracow-Wieluń Upland and western Tatra Mountains (Chochołowska Cave)

Lab nr. Gd-	Sediment	Sample[a]	^{14}C (pMC)	$\delta^{13}C$ (‰, VPDB)	Cave
5912	Moonmilk (?)	JD2/2	80.5 ± 0.6	−2.48[b]	Dziewicza
7126	Moonmilk	JŁd1	53.1 ± 0.4	−5.12[b]	Ładna
7129	Moonmilk	JŁd2	47.0 ± 0.4	−8.24[b]	Ładna
4850	Soda straw stalactite	JM3	84.0 ± 1.5	−8.00[b]	Mamutowa
7105	Moonmilk	JM4	37.4 ± 0.5	−5.43[b]	Mamutowa
7026	Moonmilk (flowstone)	JSA1/1	47.1 ± 0.5	−6.00[b]	Szeroki Awen
3549	Moonmilk (?)	Schr.Ic37/1	83.6 ± 0.6	−2.67	Schron IIC37
7027	Moonmilk (flowstone)	JSnM1/1	82.6 ± 0.7	−2.15	Schron Nad Młynami
6668	Moonmilk (flowstone)	SWJ1	84.2 ± 1.0	([b])	Schronisko w Wąwozie Jamki
5920	Outer layer of stalagmite	JT1/1	73.5 ± 0.5	−3.67[b]	Towarna
5921	Outer layer of stalagmite	JT1/2	87.9 ± 0.5	([b])	Towarna
5926	Outer layer of stalagmite	JT1/3	88.1 ± 0.5	([b])	Towarna
3562	Moonmilk (flowstone)	JZg1	44.7 ± 0.8	−1.34[b]	Zegar
7154	Moonmilk	JZg2	44.5 ± 0.4	−6.14[b]	Zegar
7128	Moonmilk	JzK1	48.0 ± 0.4	−0.01[b]	z Kominem
7125	Furry moonmilk	JZł1	60.5 ± 0.4	−0.58[b]	Złodziejska
	Furry moonmilk	JZł2	—	−2.3	Złodziejska
4837	Moonmilk (?)	JCh-MW-1/92	54.9 ± 1.0	([b])	Chochołowska
4846	Moonmilk (?)	JCh-MW-2/92	58.7 ± 1.5	−0.7	Chochołowska
Kiev	Felt moonmilk	JCh-MW-1/93/C	78.9 ± 0.9	−0.1	Chochołowska
		JCh-MW-1/93/ORG	—	−30.4	Chochołowska
Kiev	Furry moonmilk (outer part)	JCh-MW-2/93/C	78.3 ± 0.7	0.5	Chochołowska
Kiev		JCh-MW-2/93/ORG	83.2 ± 0.6	−29.4	Chochołowska
Kiev	Furry moonmilk (inner part)	JCh-MW-3/93/C	70.0 ± 0.8	1.7	Chochołowska
Kiev		JCh-MW-3/93/ORG	72.9 ± 0.6	−29.7	Chochołowska

[a]C = carbonate fractions of sample; ORG = organic fractions

[b] = assumed values of $\delta^{13}C$ in samples to correct ^{14}C (pMC) values: −2‰ for SWJ1, −3.5‰ for JT1/2 and JT1/3, −1‰ for JChMW2/92.

Results of the ^{14}C measurements are presented in the tables and figures as percent of ^{14}C concentration in an undisturbed atmosphere (pMC; Stuiver and Polach 1977). The international ^{14}C dating standard, HOxII, was used as the modern reference material. The $\delta^{13}C$ measurements were carried out at the Mass Spectrometry Laboratory in Lublin UMCS University and at the Institute of Geochemistry and Physics of Minerals, Ukrainian Academy of Science, Kiev.

RESULTS AND DISCUSSION

DIC in Water

Table 2 and Figures 2 and 3 show the ^{14}C content and $\delta^{13}C$ of DIC in karst spring waters from the Cracow-Wieluń Upland and Chochołowska Cave. The carbon isotope composition of DIC from Będkowska Valley, Zygmunt Springs and springs in Zdów ranges from 55.7 ± 0.7 pMC to 72.8 ± 0.9 pMC for ^{14}C concentration and from −12.94‰ to −9.66‰ for $\delta^{13}C$. The weighted means are 61.8 ± 2.1 pMC and −11.8 ± 1.0‰ (Table 6). These results agree with the model of dissolution of limestone with zero pMC for the ^{14}C concentration and close to zero $\delta^{13}C$ from H_2CO_3 derived from microbial degradation of plant detritus in topsoils (A = 110–120 pMC and $\delta^{13}C$ = −25‰) and the subsequent

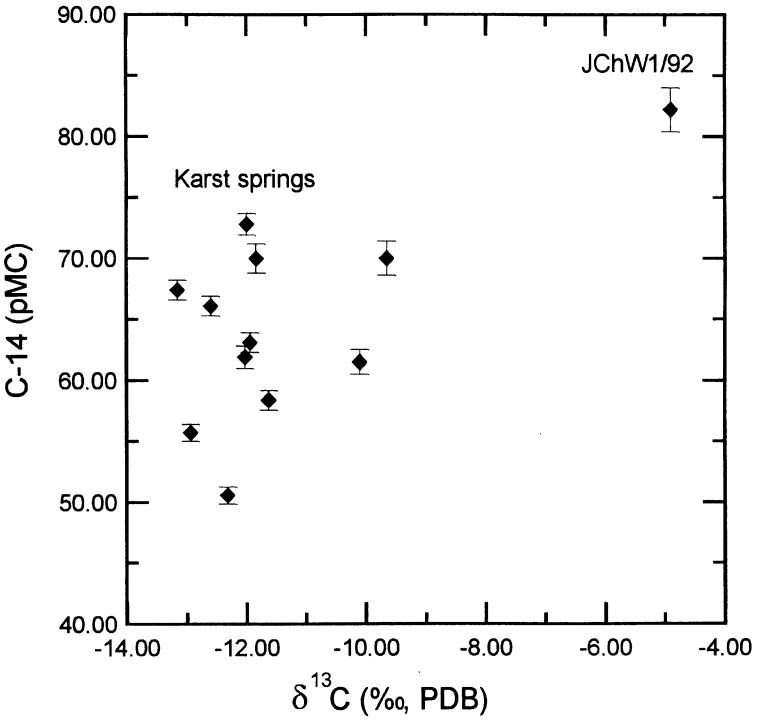

Figure 2 Results of ^{14}C and $\delta^{13}C$ measurements in DIC of waters from different karst springs and from Chochołowska Cave

Table 6 Weighted means of ^{14}C and $\delta^{13}C$ in waters, carbonates and different groups of plants

Sample	$<^{14}C>^a$ (pMC)	Nr of samples	$<\delta^{13}C>$ (‰,VPDB)	No. of samples
Waters	61.8 ± 2.10	11	−11.8 ± 1.0	11
Carbonates on plants	62.6 ± 8.5	3	−2.37 ± 2.2	10
Graminae and others	107.4 ± 4.4	4	−32.3 ± 5.7	4
Other plants	71.2 ± 4.0	7	−34.1 ± 2.5	7
Hyloconium	64.7 ± 1.7	11	−40.5 ± 5.2	11
Algae	74.3 ± 3.0	2	−44.3 ± 0.1	2

[a] < > = weighted means

process of exchange between liquid and gaseous phases (Mook et al. 1974; Mook 1976). Similar results of ^{14}C and $\delta^{13}C$ measurements in DIC in water were obtained by Marcenko et al. (1989) in waters from the karst region in northwest Yugoslavia.

^{14}C and $\delta^{13}C$ values are slightly higher in samples BDzW1/92 taken from stagnant water in Dziewicza Cave and in sample ZdWW1/93 taken from low water flow in Zdów (Table 2). Relatively high values of ^{14}C and $\delta^{13}C$ are observed in DIC from Chochołowska Cave; the water sample was collected as drops falling from the cave ceiling during a 2-week period; exchange of carbon between liquid phase and atmospheric CO_2 cannot be excluded in this sample. There is no significant corre-

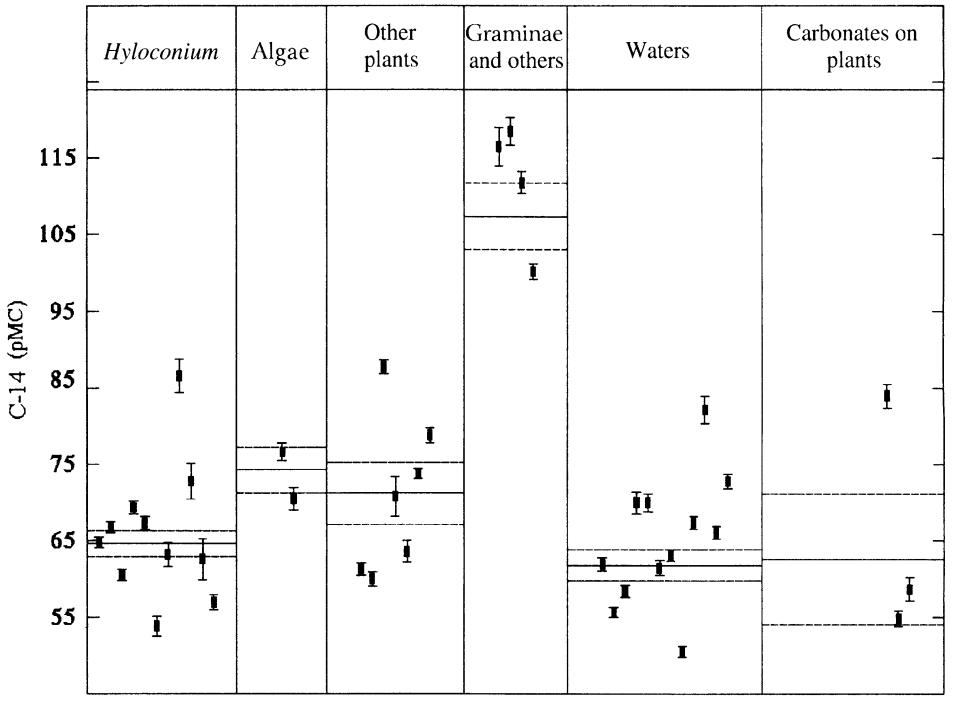

Figure 3 ^{14}C in different groups of aquatic plants. Straight lines indicate weighted means of ^{14}C. Dashed lines indicate ranges of one standard error.

lation between ^{14}C and $\delta^{13}C$ (Fig. 2) in water from Cracow-Wieluń Upland. One sample of atmospheric CO_2 was collected by absorption of CO_2 in a saturated NaOH solution at Dziewicza Cave. A ^{14}C concentration of 112.6 ± 1.5 pMC was measured (Table 2, sample JD-ATM 1/91).

Carbonates on Plants

Some algae and mosses growing in springs were heavily encrusted with calcium carbonate. These carbonate samples were usually too small for ^{14}C measurements; therefore we found only $\delta^{13}C$ and $\delta^{18}O$ values (Table 3; Figs. 3–4). The mean ^{14}C for 3 samples is 62.6 ± 8.5 pMC, which is the same as the mean ^{14}C in DIC of water (61.8 ± 2.1 pMC). The $\delta^{13}C$ values in all samples are relatively lower, compared to values of $\delta^{13}C$ observed in limestones (Table 1), and $\delta^{18}O$ values in these samples are much lower than similar values in bedrock. These results indicate that carbonate samples are indeed calcium encrustations on plants and not the grains of detrital carbonates.

^{14}C and $\delta^{13}C$ in Plants

The results of measurements of ^{14}C concentration and $\delta^{13}C$ values are listed in Table 4 and presented in Figures 3–5. Plants are grouped by species and photosynthetic pathways. In aquatic plants, such as submerged *Hyloconium* and Algae species and the group named "other plants", which contains partly submerged and semi-submerged plants (*Campylium elodes, Crateneuron falicinum, Mysotis palustris, Ranunculus scleratus, Veronica beccabunga,* etc.; Table 4), the concentration of ^{14}C is much lower than 100 pMC. We also found values of $\delta^{13}C$. The mean ^{14}C and $\delta^{13}C$ values are: 64.7 ± 1.7 pMC and −40.5 ± 5.2‰ in *Hyloconium,* 74.3 ± 3.0 pMC and −44.3 ± 0.1‰ in Algae, and 71.2 ± 4.0 pMC and −34.1 ± 2.5‰ in the group "other plants" (Table 6). Similarly, Marcenko et al. (1989)

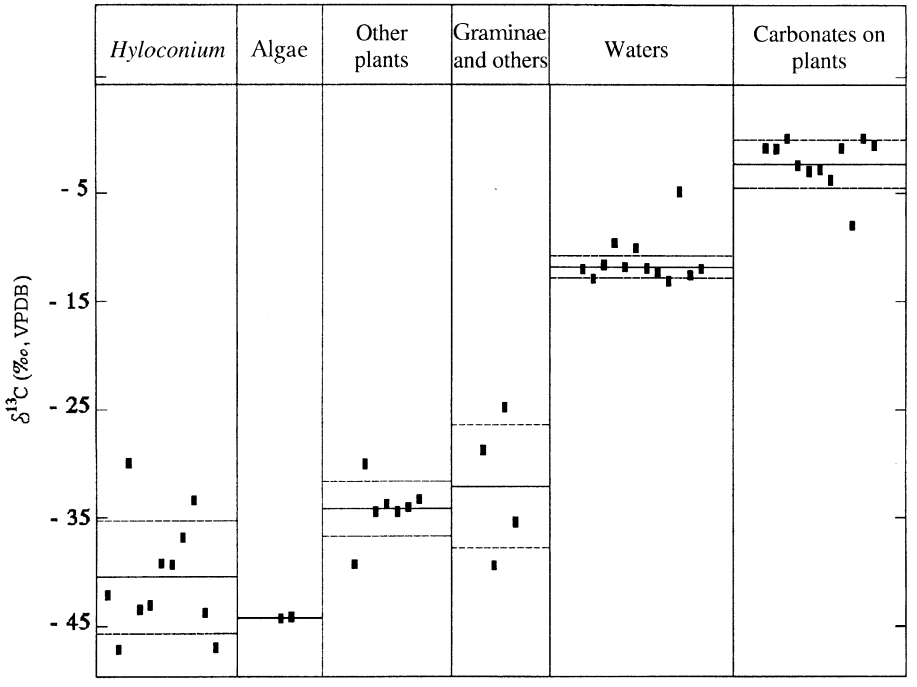

Figure 4 $\delta^{13}C$ values in different groups of aquatic plants. Straight lines indicate weighted means of $\delta^{13}C$. Dashed lines indicate ranges of one standard error.

found low ^{14}C concentrations and $\delta^{13}C$ values were observed for aquatic plants that photosynthesize carbon from freshwater DIC and atmospheric CO_2.

The group "Graminae and others" in Figures 3 and 4 contains plants terrestrial mosses as well as partly and semi-submerged plants (Graminae, *Cardamine amara).* The mean values of ^{14}C concentration and $\delta^{13}C$ for these plants are higher than for the plants from the groups discussed above (107.4 ± 4.4 pMC and -32.3 ± 5.7‰; Table 6). In all groups of plants there is no clear correlation between concentration of ^{14}C and $\delta^{13}C$ value (Fig. 5). Figure 6 shows ^{14}C and $\delta^{13}C$ in different species of plants along the stream course in the Będkowska Valley. ^{14}C pMC and $\delta^{13}C$ values are weakly correlated with distance from point of water discharge.

The Youngest Calcium Carbonate from Caves

Many samples of calcium carbonate in the group of the youngest sediments, taken from different caves, have been identified by M Gradziński as "moonmilk" (Table 5). They were deposited on the walls or found on the floor of caves in the form of flowstones. Moonmilk is white, amorphous crystal, mainly calcite or aragonite. It is suggested that it is of bacterial origin. The crystals usually display needle, branched or helicoidal forms and can be found in 2 shapes, as "furry" and "felt" moonmilk. One sample found was "soda-straw" stalactite, which is a fundamental form of stalactite. It is a single sheath of crystal enclosing a feedwater canal. Growth occurs at the tip, and the c-axis is oriented down the form (Ford and Williams 1994; Ford and Cullingford 1976). Other samples listed in Table 5 are the outermost layers of speleothems. Samples from Chochołowska Cave, where sedimentation is still occurring, were identified as furry moonmilk and felt moonmilk, deposited in the presence of unidentified species of microorganics which grew in the cave (Gradziński et al. 1997). For these sam-

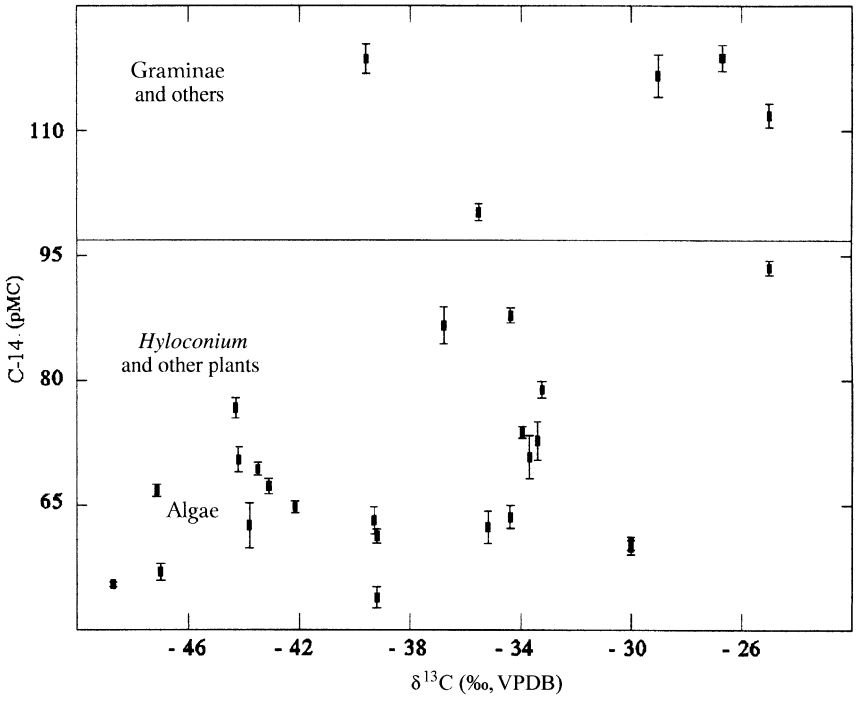

Figure 5 ^{14}C and $\delta^{13}C$ values in different groups of aquatic plants

ples, ^{14}C concentrations and $\delta^{13}C$ values in both carbonate and organic fractions were measured. On the basis of sedimentological observations (soft, porous and white calcium carbonate), other samples belong to the group of youngest sediments.

If we assume the model of the sedimentation of calcium carbonate in caves, with carbon sources from limestone and biogenic CO_2, the ^{14}C concentration in contemporary carbonates should be ca. 85 pMC (Geyh and Schleicher 1990; Schwarcz 1986), that is, an apparent age of 1350 yr. Observed values of ^{14}C concentration are much lower than 85 pMC in a group of 10 samples (Table 5), lower than 50% in 6 samples and slightly higher than 50% in 4 samples. Therefore, samples JŁd1, JŁd2, JM4, JSA1/1, JZg1, JZg2, JZK1 and JZł1 are much "older" than other samples from Cracow-Wieluń Upland (Table 5). The conventional ^{14}C age of the "youngest" sample in this group (JZł1) is ca. 4000 BP and the age of the "oldest" sample (JM4) is ca. 7900 BP. The ^{14}C concentration in the second group of samples from Cracow-Wieluń Upland caves ranged from ca. 73 (JT1/1 sample) to ca. 88 pMC (JT1/2 and JT1/3 samples); apparent ages of these samples are 2470 and 1020 BP.

Low ^{14}C concentrations occur in 2 samples from Chochołowska Cave (Table 5): JChMW 1/92 (ca. 55pMC) and JChMW 2/92 (ca. 58.7 pMC), whereas the samples of felt and furry moonmilk from the same cave have much higher ^{14}C concentrations. In both carbonate and organic fractions of furry moonmilk and in carbonate of felt moonmilk, ^{14}C concentration ranges from ca. 70 to ca. 83 pMC. Notable is the correctly higher value of ^{14}C in the outer part, and the lower value in the inner part of the furry moonmilk sample (Table 5).

The $\delta^{13}C$ values are relatively high and scattered, with the lightest being −8.24‰ and the heaviest ca. 0‰. The higher values of $\delta^{13}C$ indicate precipitation of carbonate from DIC in equilibrium with atmospheric CO_2 (Mook 1976). A correlation between ^{14}C concentration and $\delta^{13}C$ values is not

Będkowska Valley

Series: DBRW ()/91 collected in October 1991
DBRW /92 collected in December 1992

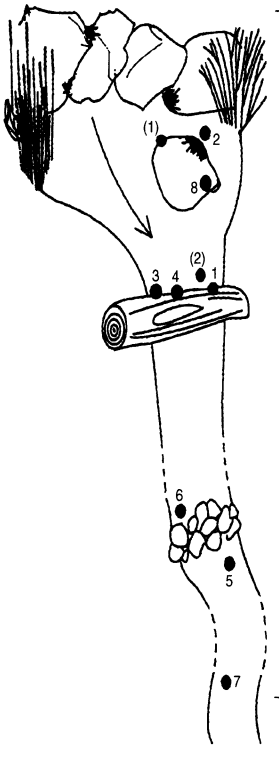

Distance	Sample	Plant	^{14}C (pMC)	$\delta^{13}C$ (‰)
ca. 1 m	(1)/91	Moss	55.0 ± 0.3	−48.70
	2/92	Moss	66.8 ± 0.7	−47.14
	8/92	Moss	57.0 ± 1.0	—
	8/92T	Grass	100.2 ± 1.0	−35.55
ca. 6 m	(2)/91	Moss	64.8 ± 0.7	−42.15
	4/92	Moss	60.5 ± 0.8	—
	1/92	*Ranunculus*	61.3 ± 0.8	−39.20
	3/92	*Mysotis*	60.0 ± 0.9	—
ca. 20 m	6/92	Moss	69.4 ± 0.8	−43.49
	5/92	*Veronica*	87.8 ± 0.9	−34.40
ca. 50 m	7/92	Alga	76.7 ± 1.2	−44.30

Figure 6 Changes of ^{14}C and $\delta^{13}C$ values in aquatic plants along the stream course in Będkowska Valley

observed (Fig. 7). It should be noted that "bomb" ^{14}C may affect the calibration of contemporaneously deposited (zero-age) ^{14}C levels. Moonmilk and soda-straw stalactite might contain post-1950 carbon. This could be confirmed by tritium measurements on the water presumed to be currently depositing $CaCO_3$. These investigations have not been made.

The Oldest Speleothems

Detailed studies of isotopic changes recorded in selected speleothems is an effective tool for reconstructing subtle climate changes in the moderate zone (Gascoyne 1992; Harmon et al. 1978). Eighty-9 speleothems from 41 caves in the Cracow-Wieluń Upland were investigated before 1994 and 170 ^{14}C dates obtained (Pazdur et al. 1995b); 45 of these samples yielded infinite dates. One of the speleothems, JWi2, was dated by the U/Th and amino acid racemization (AAR) methods at the Institute of Geochemistry and Physics of Minerals of the Ukrainian Academy of Sciences in Kiev. AAR results were based on experimentally determined relationships between stable and unstable amino acids, Thr/Leu and Thr/Glu (Julg et al. 1987; McCoy 1987). Pazdur et al. (1995b) measured stable isotopes ($\delta^{13}C$ and $\delta^{18}O$) along the growth line and observed a strong correlation between $\delta^{13}C$ and $\delta^{18}O$. Table 7 shows ^{14}C dates on several samples of JWi2 speleothem recently made in the Gliwice Radiocarbon Laboratory.

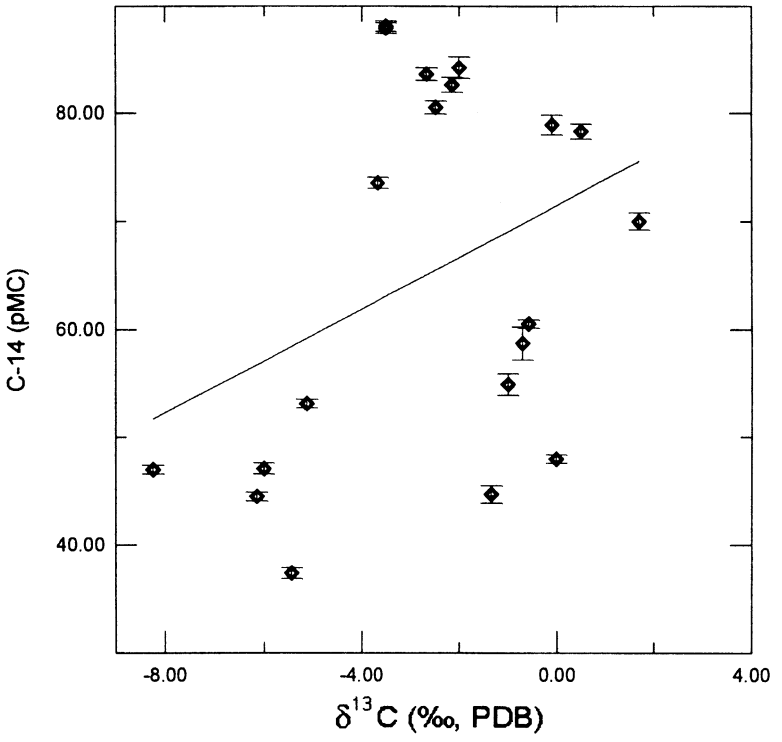

Figure 7 ^{14}C and $\delta^{13}C$ values in the youngest calcium carbonate (moonmilks, soda straw stalactite, outer layers of speleothems) from different caves. Straight line is linear approximation of results by the least squares method.

Table 7 ^{14}C dating results for speleothem JWi2

Lab no. Gd-	Distance (cm)	Age (ka BP)	$\delta^{13}C$ (‰, VPDB)
6736	0.5 ± 0.5	25.7 ± 0.2	−9.29
7871	8.2 ± 4.8	47.2 +4.3 / −2.8	−8.50
7873		>45.9	−9.30
10558	16.0 ± 3.0	>46.7	−8.50
10573	20.5 ± 1.0	40.2 +2.6 / −2.0	−7.80
7874	25.5 ± 3.4	>46.9	−9.06
7870	32.5 ± 3.5	41.2 +3.1 / −2.3	−9.10
10560(?)	36.5 ± 0.5	34.1 +2.3 / −1.9	−9.80
6735	37.0 ± 0.2	23.7 ± 0.2	−10.15

The cone-shaped stalagmite JWi2, 35 cm high, was examined and sedimentological analysis revealed it to be composed of 3 parts. The lower part contains many detrital components (i.e., quartz grains, Fe and Al oxides and hydroxides, and small bones), indicating that the crystallization of this part of the stalagmite occurred in wet conditions. The central part consists of a number of large calcite crystals with some brown laminae resulting from clastic or organic impurities. Competitive growth of crystals is visible and inclusions are abundant, characteristics that indicate the stalagmite grew in favorable conditions. Its upper part contains smaller and irregularly shaped calcite crystals with numerous brown laminae, indicating that the upper part of the stalagmite grew in unstable conditions.

The first ^{14}C measurements of speleothem JWi2 were to determine the time of its initiation and the end of calcium carbonate sedimentation (Pazdur et al. 1995b). The ^{14}C age (25,730 ± 200 BP) obtained from the bottom of the speleothem (the beginning of the sedimentation) was much younger than the U/Th and AAR ages (Table 8). The ^{14}C date on the outer layer at the top of the speleothem (23,700 ± 200 BP) is much older, by about 4 ka, than U/Th and AAR ages. Dates on several layers between the bottom and top of speleothem JWi2 indicated much older ^{14}C ages, both in comparison to the earlier ^{14}C dates and the U/Th and AAR dates. The first ^{14}C dates received from the top and bottom of the speleothem are probably too young because of contamination of speleothem outer layers by younger carbon (Srdoč et al. 1986); they are excluded from discussion and presentation in Figure 8.

Table 8 Results of U/Th and AAR dating and calculated ^{14}C ages of speleothem JWi2

Distance (cm)	Method	AAR or U/Th (ka)	^{14}C age (ka BP)
0.5 ± 0.5	U/Th	28.4 ± 1.1	49.5 ± 4.1
0.5 ± 0.5	U/Th	29.0 ± 1.0	49.5 ± 4.1
0.5 ± 0.5	AAR	33.7 ± 2.2	49.5 ± 4.1
2.0 ± 0.5	AAR	31.0 ± 1.8	49.0 ± 4.1
3.4 ± 0.4	U/Th	27.0 ± 1.1	48.5 ± 4.2
11.5 ± 1.5	U/Th	25.6 ± 1.0	45.5 ± 4.5
20.3 ± 1.7	AAR	28.6 ± 1.0	42.2 ± 5.2
21.3 ± 0.7	AAR	28.6 ± 1.0	41.9 ± 5.3
21.3 ± 0.7	AAR	25.5 ± 0.8	41.9 ± 5.3
20.9 ± 0.4	U/Th	22.9 ± 0.9	42.0 ± 5.2
23.7 ± 0.3	U/Th	24.2 ± 1.0	41.0 ± 5.5
25.6 ± 0.7	U/Th	24.2 ± 1.0	40.3 ± 5.7
25.6 ± 0.7	AAR	23.0 ± 0.8	40.3 ± 5.7
35.7 ± 0.5	U/Th	20.2 ± 0.8	36.6 ± 6.9
36.0 ± 0.5	AAR	18.0 ± 0.7	36.4 ± 6.9
36.0 ± 0.5	U/Th	18.9 ± 0.8	36.4 ± 6.9
36.0 ± 0.5	U/Th	19.5 ± 0.8	36.4 ± 6.9
36.5 ± 0.5	U/Th	19.5 ± 0.8	23.7 ± 0.5

Dating results are presented in Figure 8. It is worth noting that the least-squares lines fitted to ^{14}C data and AAR results, as a function of the sample distance from the bottom of speleothem, are parallel (see line equations in Fig. 8). On the basis of the linear relation between measured ^{14}C conventional ages (excluding the first 2 values) and distance, the ^{14}C conventional ages were calculated for all layers dated by AAR and U/Th methods. These results are shown in Table 8 and Figure 9.

If we assume that AAR ages obtained from the organic fractions of the samples are "true, calendar ages" of dated layers, the reservoir effect can be estimated as apparent age (T_{app}) of calcium carbonate sample dated by ^{14}C (Pazdur 1988). Apparent ages of dated samples as differences between conventional ^{14}C ages and AAR ages are 15.9 ka at the bottom (x=0) and 16.3 ka at the top (x=35 cm) of the speleothem. The dilution factors (q) calculated on the basis of relation

$$T_{app} = -8033 \ln q \quad (1)$$

are q = 0.14 at the bottom and q = 0.13 at the top, in other words the same along the whole growth line. Similarly, T_{app} and q values estimated on the basis of comparing ^{14}C conventional ages and U/Th ages

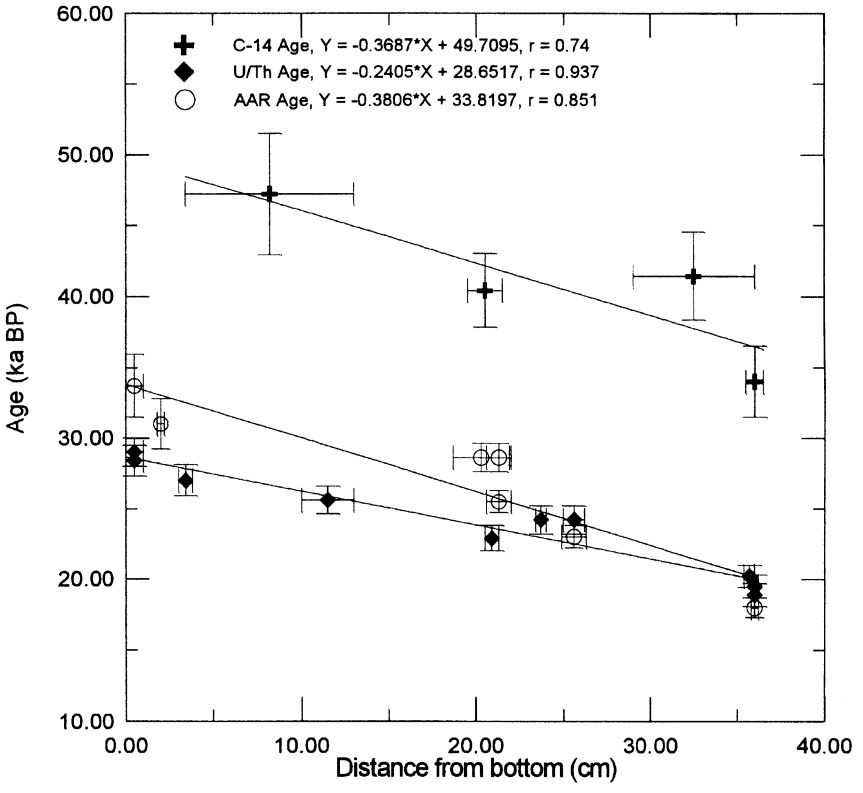

Figure 8 Results of ^{14}C, U/Th, and AAR dating of speleothem JWi2. Samples were taken from different distances from the bottom. Straight lines are linear approximations of results by the least squares method (note the equation lines).

are: 21.1 ka and 0.07 for x = 0 and 16.5 ka and 0.13 for x = 35 cm. The estimated values of apparent ages are extremely high and dilution factors extremely low. In the above estimations, changes of ^{14}C concentration in the past are neglected.

The relation between ^{14}C and U/Th ages (Fig. 9) is the reverse of that reported by Goslar et al. (forthcoming) for the long series of ^{14}C and U/Th dates in the interval 20–60 ka, obtained for speleothems from other caves in Europe. In relation to U/Th ages, the ^{14}C dates are younger by ca. 5 ka for 20 ka U/Th age and ca. 15 ka for 60 ka U/Th age with a plateau in the range 30–50 ka of U/Th ages.

In the light of these observations, comparison of the results of ^{14}C and U/Th and AAR dating for speleothem JWi2 requires additional explanation. The observed low value of the dilution factor indicates a significant contribution of old ^{14}C-free carbon in the calcium carbonate of the speleothem. The source of old carbon may have been old bedrocks if the speleothem was subject to diagenesis or redeposition, or both processes. Another possible cause for the incorporation of old carbon is the presence of ^{14}C-free metamorphic CO_2 during dissolution of limestone. This process should be excluded as the only cause of the sedimentation of calcium carbonate of speleothem JWi2, with low values of $\delta^{13}C$, which change from ca. −7 to ca. −11‰ in different layers.

Measurements of carbon isotope composition in the youngest (contemporary) calcium carbonate from caves, in DIC of water, and in aquatic plants are background for measurements of radiocarbon

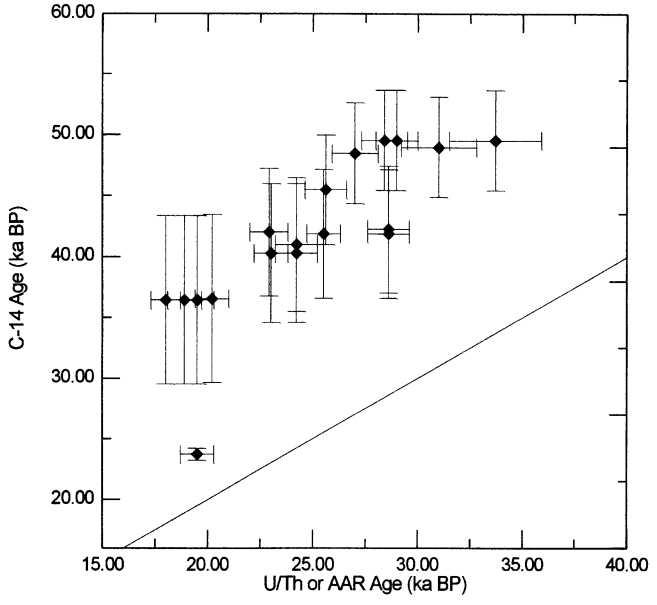

Figure 9 Comparison of calculated ^{14}C and U/Th and AAR ages. The conventional ^{14}C ages were calculated using the relation between measured ^{14}C ages and distance of the dated samples from the bottom of the speleothem. Straight line is described by equation Y=X.

content in the speleothem from the Wierna cave (stalagmite JWi2). The highest observed value of apparent age of the contemporary calcium carbonate is 7.89 ka (Table 5) from moonmilk sample JM4 with 37.4 pMC of ^{14}C content. The results of ^{14}C and $\delta^{13}C$ in DIC of water (Table 2) indicate a closed system of the carbon cycle in the study area.

We assume that, in the karst area, processes of the bedrock dissolution and precipitation of $CaCO_3$ occurred in the presence of the biogenic CO_2 and strong kinetic isotope effect. Suppose that, as a result, $CaCO_3$ with ca. 37 pMC of ^{14}C and $\delta^{13}C$ of ca. –9.5‰ (i.e., 37% of –25‰ in biogenic CO_2) was formed. The second step of the geochemical process was dissolution of deposited calcium carbonate in the presence of old metamorphic CO_2 with $\delta^{13}C$ ca. –8‰ and the same dissolution factor for ^{14}C isotope, q ca. 0.37. Successive precipitation of $CaCO_3$ from that solution would result in calcium carbonate with a dissolution factor ca. 0.14 and almost the same value of $\delta^{13}C$.

The above simple considerations give a ^{14}C isotope content consistent with the estimated value of the dilution factor for speleothem JWi2, obtained on the basis of the comparison of ^{14}C and AAR ages. The estimated $\delta^{13}C$ value is consistent with measured values of different layers (Pazdur et al. 1995b).

CONCLUSION

Measurements of carbon isotope values in the contemporary karst environment of Southern Poland proved that the karst area of Cracow-Wieluń Upland establishes a closed geochemical system for carbon. The $\delta^{13}C$ values in most species of aquatic plants reflect C_3 photosynthetic carbon pathways. The reservoir effect determined for recent calcium carbonate from caves may help in estimating the apparent ages of speleothems dated by the ^{14}C method.

The determination of a ^{14}C dilution factor in carbonaceous deposits is necessary to study speleothems as a suitable material for extending the ^{14}C calibration time scale. The possible use of old speleothems requires both the absolute age and the "true" ^{14}C age of the sample. But, in turn, the "true" ^{14}C age of the speleothems is possible only if the dilution factor is known and must be determined independently, in this case by using the measurements of contemporary carbonates.

Observed results of ^{14}C, AAR and U/Th datings for speleothem JWi2 indicate the possibility of errors in the application of dates from speleothems in order to calibrate the ^{14}C time scale and the need to select speleothems to solve the problem. If our considerations are correct, we may assume that on the Cracow-Wieluń Upland, in the period of 20–30 ka BP (AAR or U/Th time scale), geophysical processes resulted in the evolution of metamorphic CO_2.

ACKNOWLEDGMENTS

This study was financially supported by grants BW 707/RMF 1/92, BW 327/RMF 1/93, and BK 213/RMF 1/97 from the Silesian Technical University and by grants No. 6 P04E 026 10 and No. 0586/P04/95/09 from the Committee for Scientific Research, Poland. M. Gradziński was supported by the Foundation for Polish Science in 1997.

REFERENCES

Baker A, Smart PL, Ford DC. 1993. Northwest European palaeoclimate as indicated by growth frequency variations of secondary calcite deposits. *Palaeogeography, Palaeoclimatology, Palaeoecology* 100:291–301.

Digerfeldt G. 1988. Reconstruction and regional correlation of Holocene lake-level fluctuations in Lake Bysjon, South Sweden. *Boreas* 17:165–82.

Eichinger L. 1983. A contribution to the interpretation of ^{14}C groundwater ages considering the example of a partially confined aquifer. *Radiocarbon* 25(2):347–56.

Ford TD, Cullingford CHD. 1976. *The science of speleology.* London: Academic Press. p 593, 302.

Ford D, Williams P. 1994. *Karst geomorphology and hydrology.* London: Chapman and Hal. p 338, 340.

Gascoyne M. 1992. Palaeoclimate determination from cave calcite deposits. *Quaternary Sciences Reviews* 11:609–23.

Geyh MA, Hennig GJ. 1986. Multiple dating of a long flowstone profile. *Radiocarbon* 28(2A): 503–9.

Geyh MA, Schleicher H. 1990. *Absolute age determination: physical and chemical dating methods and their applications.* Berlin-Heidelberg: Springer-Verlag. p 162–80.

Goslar T, Arnold M, Bard E, Kuc T, Pazdur MF, Ralska-Jasiewiczowa M, Różański K, Tisnert N, Walanus A, Wicik B, Więckowski K. 1995. High concentration of atmospheric ^{14}C during the Younger Dryas cold episode. *Nature* 377: 414–7.

Goslar T, Hercman H, Lauritzen SE, Pazdur A. 1997. Comparison of radiocarbon and U/Th dates of speleothems. Manuscript.

Gradziński M, Szulc J, Smyk B. 1997. Microbial agents of moonmilk calcification. In: Jeannin PY, editor. *Proceedings of the 12th international congress of speleology 1997.* p 275–8.

Harmon RS, Thompson P, Schwarcz HP, Ford DC. 1978. Late Pleistocene palaeoclimate of North America as inferred from stable isotope studies of speleothems. *Quaternary Research* 9:54–70.

Hennig GJ, Grun R, Brunnacker K. 1983. Speleothems, travertines and palaeoclimate. *Quaternary Research* 20:1–29.

Hercman H. 1991. Reconstruction of geological environment of the Western Tatra Mts based on isotopic dating of speleothems. Zeszyty Naukowe Politechniki Śląskiej, Seria Matematyka-Fizyka, Z. 66. *Geochronometria* 8:1–139.

Horvatinčić N, Srdoč D, Solar J, Tvrdikova H. 1989. Comparison of the ^{14}C activity of groundwater and recent tufa from karst areas in Yugoslavia and Czechoslovakia. *Radiocarbon* 31(3):884–92.

Julg A, Lafont R, Perinet G. 1987. Mechanism of collagen racemization in fossil bones: application to absolute dating. *Quaternary Science Reviews* 6(1):25–8.

Keith ML, Weber JN. 1964. Carbon and oxygen isotope composition of selected limestones and fossils. *Geochimica et Cosmochimica Acta* 28:1787–816.

Magny M. 1992. Holocene lake-level fluctuations in Jura and the northern subalpine ranges, France. *Boreas* 21:319–34.

Magny M. 1993. Solar influences on Holocene climatic changes illustrated by correlations between past lake-level fluctuations and atmospheric ^{14}C record. *Quaternary Research* 40:1–9.

Marcenko E, Srdoč D, Golubic S, Pezdic J, Head MJ. 1989. Carbon uptake in aquatic plants deduced from their natural ^{13}C and ^{14}C content. *Radiocarbon*

31(3):785–94.

McCoy WD. 1987. The precision of amino acid geochronology and paleothermometry. *Quaternary Science Reviews* 6(1): 43–54.

Mook WG. 1976. *The dissolution-exchange model for dating groundwater with ^{14}C. Interpretation of environmental and isotope data in groundwater hydrology.* Vienna: IAEA. p 213–25.

Mook WG. 1980. Carbon-14 in hydrogeological studies. In: Fritz P, Fontes J-C, editors. *Handbook of environmental isotope geochemistry, the terrestrial environment.* A. Vol 1. Amsterdam: Elsevier. p 49–74.

Mook WG, Bommerson JC, Staverman WH. 1974. Carbon isotope fractionation between dissolved bicarbonates and gaseous carbon-dioxide. *Earth and Planetary Science Letters* 22: 169–76.

Morse JW, Mackenzie FT. 1990. Carbonates as sedimentary rocks in subsurface processes. In: Morse JW, Mackenzie FT, editors. *Geochemistry of sedimentary carbonates.* Amsterdam: Elsevier. p 373–446.

Olsson IU. 1986. Radiometric methods. In: Berglund B, editor. *Handbook of Holocene palaeoecology and palaeohydrology.* Chichester: John Wiley & Sons. p 273–312.

Pazdur A. 1988. The relations between carbon isotope composition and apparent age of freshwater tufaceous sediments. *Radiocarbon* 30(1):7–18.

Pazdur A, Fontugne MR, Goslar T, Pazdur MF. 1995. Lateglacial and Holocene water-level changes of the Gośiąż Lake, Central Poland, derived from carbon isotopes studies of laminated sediment. *Quaternary Science Reviews* 14:125–35.

Pazdur A, Pazdur MF, Pawlyta J, Górny A, Olszewski M. 1995b. Palaeoclimatic implications of radiocarbon dating of speleothems from the Cracow-Wieluń Upland, Southern Poland. *Radiocarbon* 37(2):103–10.

Pazdur A, Pazdur MF, Starkel L, Szulc J. 1988. Stable isotopes of the Holocene calcareous tufa from southern Poland as palaeoclimatic indicator. *Quaternary Research* 30:177–89.

Pearson FJ Jr, Hanshaw BB. 1970. Sources of dissolved carbonate species in groundwater and their effects on carbon-14 dating. *Isotope Hydrology.* Vienna: IAEA. p 271–86.

Pearson FJ Jr. 1992. Effects of parameter uncertainty in modelling ^{14}C in groundwater. In: Taylor RE, Long A, Kra RS, editors. *Radiocarbon after four decades: an interdisciplinary perspective.* New York: Springer-Verlag. p 262–75.

Schwarcz HP. 1986. Geochronology and isotope geochemistry of speleothems. In: Fritz P, Fontes J-C, editors. *Handbook of environmental isotope geochemistry, the terrestrial environment.* B. Vol 2. Amsterdam: Elsevier. p 271–304.

Shore JS, Cook GT, Dougmore AJ. 1995. The ^{14}C content of modern vegetation samples from the flanks of the Katla Volcano, southern Iceland. *Radiocarbon* 37(2):525–9.

Srdoč D, Horvatinčić N, Obelić B, Krajcar-Bronić I, O'Malley P. 1986. The effects of contamination of calcareous sediments on their radiocarbon ages. *Radiocarbon* 28(2A):510–4.

Srdoč D, Horvatinčić N, Obelić B, Sliepcevic A. 1983. Radiocarbon dating of tufa in palaeoclimatic studies. *Radiocarbon* 25(2):421–7.

Stuiver M, Polach H. 1977. Discussion: reporting of ^{14}C data. *Radiocarbon* 19(3):355–63.

Turi B. 1986. Stable isotope geochemistry of travertines. In: Fritz P, Fontes J-C, editors. *Handbook of environmental isotope geochemistry, the terrestrial environment.* B. Vol 2. Amsterdam: Elsevier. p 207–38.

Usdowski E, Hoefs J, Menschel G. 1979. Relationship between ^{13}C and ^{18}O fractionation and changes in major element composition in a recent calcite-depositing spring: a model of chemical variations with inorganic $CaCO_3$ precipitation. *Earth and Planetary Science Letters* 42:267–76.

Vogel JC. 1970. Carbon-14 dating of groundwater. *Isotope Hydrology.* Vienna: IAEA. p 225–39.

Willkom H, Erlenkeuser H. 1973. ^{14}C measurements on water plants and sediments of lakes. Proceedings of the 8th International Conference on Radiocarbon Dating, Wellington, New Zealand. p 312–23.

RADIOCARBON, Vol 41, Nr 1, 1999, p 99–101

A ΔR CORRECTION VALUE FOR SAMOA FROM KNOWN-AGE MARINE SHELLS

Matthew B Phelan

Radiocarbon Dating Laboratory, School of Science and Technology, University of Waikato, Private Bag 3105, Hamilton, New Zealand

ABSTRACT. A first-order ΔR correction value for marine samples is presented based on 3 radiocarbon determinations of known-age marine shells from Samoa.

INTRODUCTION

The modeled marine calibration curves (Stuiver et al. 1986; Stuiver and Braziunas 1993) present a global average of the world ocean response lag to atmospheric variation through time of radiocarbon. Local and regional deviations from this global average complicate the precise calibration of marine samples and, particularly, the chronometric comparison of such samples with terrestrial samples and with marine samples from different regions. A correction value (ΔR) can be calculated to account for such regional deviations from the modeled marine curve. This may be based on differences between the ^{14}C activity of stratigraphically paired samples of terrestrial and marine origin or on the ^{14}C activity of marine shell samples of known age.

For the central Pacific generally there are very few known ΔR values. Stuiver et al. (1986: Table 1) publish 3 values: for Eniwetok, Tahiti, and Hawai'i. This study provides a 4th ΔR value for the central Pacific from the Samoan archipelago based on the ^{14}C activity of 3 known-age marine shell samples. These samples were collected by Captain Zembsch, the German Imperial Consul-General in Samoa between 1879 and 1883 (Masterman 1934) and were provided by the Museum für Naturkunde in Berlin. The museum labels attached to the shells note that they were collected between 1881 and 1883 and on this basis calculations are made on a known calendar age of 1882 AD. Although unclear from the information provided, it would seem likely that they were collected from the island of 'Upolu (13°50′S, 172°W). The mollusc species involved, *Turbo petholatus, Strombus pacificus,* and *Strombus lentiginosus*, are all gastropods and coral reef dwellers, preferring shallow intertidal coral sands and rocks (Dance 1992; Cernohorsky 1972).

METHODS

Samples were washed in an ultrasonic bath and then acid washed (2M HCl) for 100 s to remove the outer shell surface and any possible contaminants. Samples were then hydrolyzed and converted to benzene and ^{14}C activity was determined by liquid scintillation counting (LSC). All samples are reported according to conventions outlined in Stuiver and Polach (1977). The Waikato Laboratory reports ^{14}C results based upon the HOxII reference standard and the ANU sucrose secondary standard. Ages are reported as conventional ^{14}C ages BP based on the Libby half-life and include a lab error multiplier (K) of 1.22 (Higham and Hogg 1997).

RESULTS

Samoan known-age marine shell, collected live in 1882, from the collection of the Museum für Naturkunde, Berlin.

Wk 6383 **550 ± 40**
Marine Shell (*Turbo petholatus*) $\delta^{13}C = +2.0‰$
$\Delta R = +70 \pm 40$

Wk 6384 **500 ± 40**
Marine Shell (*Strombus pacificus*) $\delta^{13}C = +2.1‰$
$\Delta R = +20 \pm 40$

Wk 6385 **560 ± 40**
Marine Shell (*Strombus lentiginosus*) $\delta^{13}C = +3.2‰$
$\Delta R = +80 \pm 40$

These 3 age determinations are statistically indistinguishable and give an error-weighted mean of 537 ± 23 BP (Ward and Wilson 1978). Stuiver et al. (1986) provide the formula $\Delta R = P–Q$, where P = the ^{14}C age of a known-age sample and Q = the ^{14}C age of the model mixed-ocean layer for the calendar year (AD) of the known-age sample. In other words, ΔR is the difference between the modeled ^{14}C age of surface water and the known ^{14}C age of surface water represented by the marine shell sample. In this case Q = 480 BP (Stuiver and Braziunas 1993) and P = 537 ± 23 BP. Therefore, $\Delta R = +57 \pm 23$ ^{14}C yr. This figure remains the same if a ΔR value is calculated based on the individual determinations and a weighted mean is calculated on these individual results although the standard error using this method is ± 18 ^{14}C yr. Stuiver and Braziunas (1993) recommend the use of the larger standard error and therefore the standard error of ± 23 ^{14}C yr is used.

DISCUSSION

A number of studies have recently pointed to the distortion of ^{14}C determinations on marine shell caused by hardwater influx into lagoonal and estuarine environments (Dye 1994; Ingram 1998). In general, the geology of 'Upolu and the Samoan archipelago is of entirely volcanic origin and the only geological carbonates available are Holocene beach sands (Keating 1992; Fox and Cumberland 1962). As all 3 samples are of grazing gastropods it may be possible that some calcium carbonates from the sands are ingested during browsing (Dye 1994). Studies of *Strombus gigas* from the Bahamas show sand comprising between 58% and 99% of gut contents (Stoner and Waite 1991) and, importantly, they note that the "[i]sotope signatures of juvenile conch [*Strombus gigas*] suggest that the sediments may provide an important source of carbon and nitrogen". Tanaka, Monaghan and Rye (1986) estimate that about 50% of carbon in mollusc shell derives from metabolic carbon rather than dissolved inorganic carbon (DIC) from the surrounding seawater. The difficulty lies in determining what, if any, fraction of the ingested substrate material might be metabolized. This problem is currently the subject of a doctoral research project. At present, the possibility that Holocene sands may be providing a source of ^{14}C-depleted carbon to the samples cannot be excluded with confidence.

Stuiver and Braziunas (1993) note that ΔR values represent differences both in regional atmospheric ^{14}C activity and in marine ^{14}C activity due to regional oceanic processes. The data presented here cannot account for variation through time of these variables and as such they provide a first-order ΔR value for Samoa. To account for changes in either regional atmospheric ^{14}C activity or changes through time in oceanic processes, a stratigraphic sequence of paired terrestrial/marine samples needs to be analyzed. One paired sample can be found in the archaeological literature. Beta 35603, 2600 ±170 BP ($\delta^{13}C = –28.4‰$, charcoal) and Beta 35604, 2770 ± 80 BP ($\delta^{13}C = +1.7‰$, *Tridacna maxima*) are from the To'aga archaeological site in the Manu'a group of American (eastern) Samoa (Kirch 1993) (A Southern Hemisphere correction value has not been applied, as Manu'a is only 14° south of the equator). These samples yield ΔR= –230 (Stuiver and Braziunas 1993). This is a number of magnitudes different from the value derived from the known-age samples and indicates either 1) differences between western and eastern Samoa in surface ocean ^{14}C activity, 2) change in regional oceanic processes through time, or 3) some problem of association between these 2 determinations. Choosing among these possible explanations is currently a matter of speculation. How-

ever, the latter option seems the most likely as the Manu'a group is only ca. 100 km from Western Samoa, a distance over which large-scale oceanic differences in ^{14}C activity are unlikely to vary. In relation to temporal changes in surface ocean ^{14}C activity, independent data relevant to the surface ocean ^{14}C activity at about 2600 BP are not available.

CONCLUSION

A 1st-order ΔR correction value for the Samoan archipelago is calculated at +57 ± 23 ^{14}C yr. This result is part of an ongoing research effort aimed at improving the utility of marine shell as a ^{14}C-dating medium for the South Pacific region. Other factors pertinent to the development of reliable and accurate ΔR correction values are the effects of 4 independent variables: regional oceanic processes, local environmental conditions, individual species relationship to the carbon cycle, and temporal variation in these factors. The manner in which variation occurs in each of these variables needs to be understood if archaeologists are to develop reliable Pacific chronologies using marine shell as a sample type for ^{14}C dating.

ACKNOWLEDGMENTS

Thanks go to Dr Matthias Glaubrecht, Museum für Naturkunde, Berlin, for supplying the shells; Dr Tom Higham, University of Waikato Radiocarbon Dating Lab, for comments on the draft manuscript; and Dr Tom Dye, International Archaeological Research Institute, Inc., Hawai'i, for review comments. This research has been supported by a University of Waikato Postgraduate Scholarship.

REFERENCES

Cernohorsky WO. 1972. *Marine shells of the Pacific.* Vol 2. Sydney: Pacific Publications. 411 p.

Dance SP. 1992. *Shells.* London: Harper Collins Publishers. 256 p.

Dye T. 1994. Apparent ages of marine shells: implications for archaeological dating in Hawai'i. *Radiocarbon* 36(1):51–7.

Fox JW, Cumberland KB. 1962. *Western Samoa: land, life and agriculture in tropical Polynesia.* Christchurch: Whitcomb and Tombs Ltd. 337 p.

Higham TFG, Hogg AG. 1997. Evidence for late Polynesian colonization of New Zealand: University of Waikato radiocarbon measurements. *Radiocarbon* 39(2):149–92.

Ingram BL. 1998. Differences in radiocarbon age between shell and charcoal from a Holocene shell mound in Northern California. *Quaternary Research* 49:102–10.

Keating BH. 1992. Geology of the Samoan Islands. In: Keating BH, Bolton BR, editors. *Geology and offshore mineral resources of the Central Pacific Basin.* New York: Springer-Verlag. p 127–78.

Kirch PV. 1993. Radiocarbon chronology of the To'aga site. In: Kirch PV, Hunt TL, editors. *The To'aga site: three millennia of Polynesian occupation in the Manu'a Islands, American Samoa.* Contributions of the University of California Archaeological Research Facility, nr 51. Berkeley: Archaeological Research Facility. p 85–92.

Masterman S. 1934. *The origins of international rivalry in Samoa, 1845–1884.* London: George Allen and Unwin, Ltd. 233 p.

Stoner AW, Waite JM. 1991. Trophic biology of *Strombus gigas* in nursery habitats: diets and food sources in seagrass meadows. *Journal of Molluscan Studies* 57(4):451–61.

Stuiver M, Braziunas TF. 1993. Modeling atmospheric ^{14}C influences and ^{14}C ages of marine samples to 10,000 BC. *Radiocarbon* 35(1):137–89.

Stuiver M, Polach HA. 1977. Discussion: reporting of ^{14}C data. *Radiocarbon* 19(3):355–63.

Stuiver M, Pearson GW, Braziunas T. 1986. Radiocarbon age calibration of marine samples back to 9000 cal yr BP. *Radiocarbon* 28(2B):980–1021.

Tanaka N, Monaghan MC, Rye DM. 1986. Contribution of metabolic carbon to mollusc and barnacle shell carbonate. *Nature* 320:520–3.

Ward GK, Wilson SR. 1978. Procedures for comparing and combining radiocarbon age determinations: a critique. *Archaeometry* 20(1):19–31.

RADIOCARBON, Vol 41, Nr 1, 1999, p 103–110

RADIOCARBON DATES FROM NORTHERN MONGOLIA

Mark Hall[1] • Zagd Batsaikhan[2] • William Honeychurch[3]

ABSTRACT. Since 1996, the Mongolian-American Expedition to Northern Mongolia has been excavating in the Egiin Gol Valley. The goal of this research has been to examine the competing hypotheses explaining the emergence of pastoral nomadism and the evolution of nomadic complexity. The chronological placement of burials and sites in the survey area has been a key facet of this research. At present, these investigations have generated 10 radiocarbon dates from archaeological contexts. Presented here are the previoulsy unpublished ^{14}C dates and some comments on their significance.

INTRODUCTION

The Egiin Gol Valley (ca. 49.5°N, 103.5°E) is in northern Mongolia just south of the Russian border and Lake Baikal (Fig. 1). The lower Egiin Gol Valley is the scene of intensive, multinational archaeological work due to its proposed flooding by a hydroelectric dam project. Within a salvage archaeology context, the Mongolian-American Expedition to Northern Mongolia is researching the emergence of pastoral nomadism and the evolution of nomadic complexity. The chronological placement of burials and sites is a key facet of this research.

While numerous excavations have been conducted in Mongolia over the past 50 years, an absolute chronology for Mongolia still needs to be established. Most of the chronological schemes for Mongolian prehistory are currently based on similarities in artifact styles to those in use in China or western Siberia (Askarov et al. 1992; Martynov 1991). In many cases, the artifacts being used as the basis for the chronology are not absolutely dated themselves. Furthermore, chronologies based on the similarities of artifact styles are plagued by uncertainties about where styles originated, how quickly they spread, and how long they stayed in use (Deetz and Dethlefsen 1965).

Mongolia is a crossroads between the steppe cultures of Siberia and the sedentary cultures of China; without an absolute chronology, scholars will continue to argue over the direction of cultural influences in the region. Our purpose here is to present 10 radiocarbon determinations from several archaeological sites in the Egiin Gol Valley of northern Mongolia.

METHODS

The ^{14}C determinations presented here were made at 3 different ^{14}C laboratories. The wood and charcoal samples prefixed with Beta were run at Beta Analytic Inc., while those with TX prefixes were run at the Radiocarbon Laboratory, University of Texas at Austin. Dating at both laboratories was performed using the liquid scintillation counting (LSC) method. The single bone sample was run at the accelerator mass spectrometry (AMS) facility at the University of Arizona. All ^{14}C determinations presented here are based on a 5568-yr half-life and are corrected for carbon fractionation.

All subsequent calibrations and mathematical operations were done using the program OxCal, Version 2.18. OxCal is a Bayesian calibration program that allows the user to incorporate archaeological, historical and stratigraphic information into the calibration procedure. Details on the mathematics and algorithms used in the program can be found in Bronk Ramsey (1995a, 1995b). The 1993 bidecadal calibration curve of Stuiver and others (Stuiver et al. 1993) was used for the calibration.

[1]Archaeology Department, National Museum of Japanese History, 117 Jonai-cho, Sakura-shi, Chiba 285, Japan
[2]Department of Anthropology, Mongolian State University, Ulan Bataar, Mongolia
[3]Museum of Anthropology, University of Michigan, Ann Arbor, Michigan 48105 USA

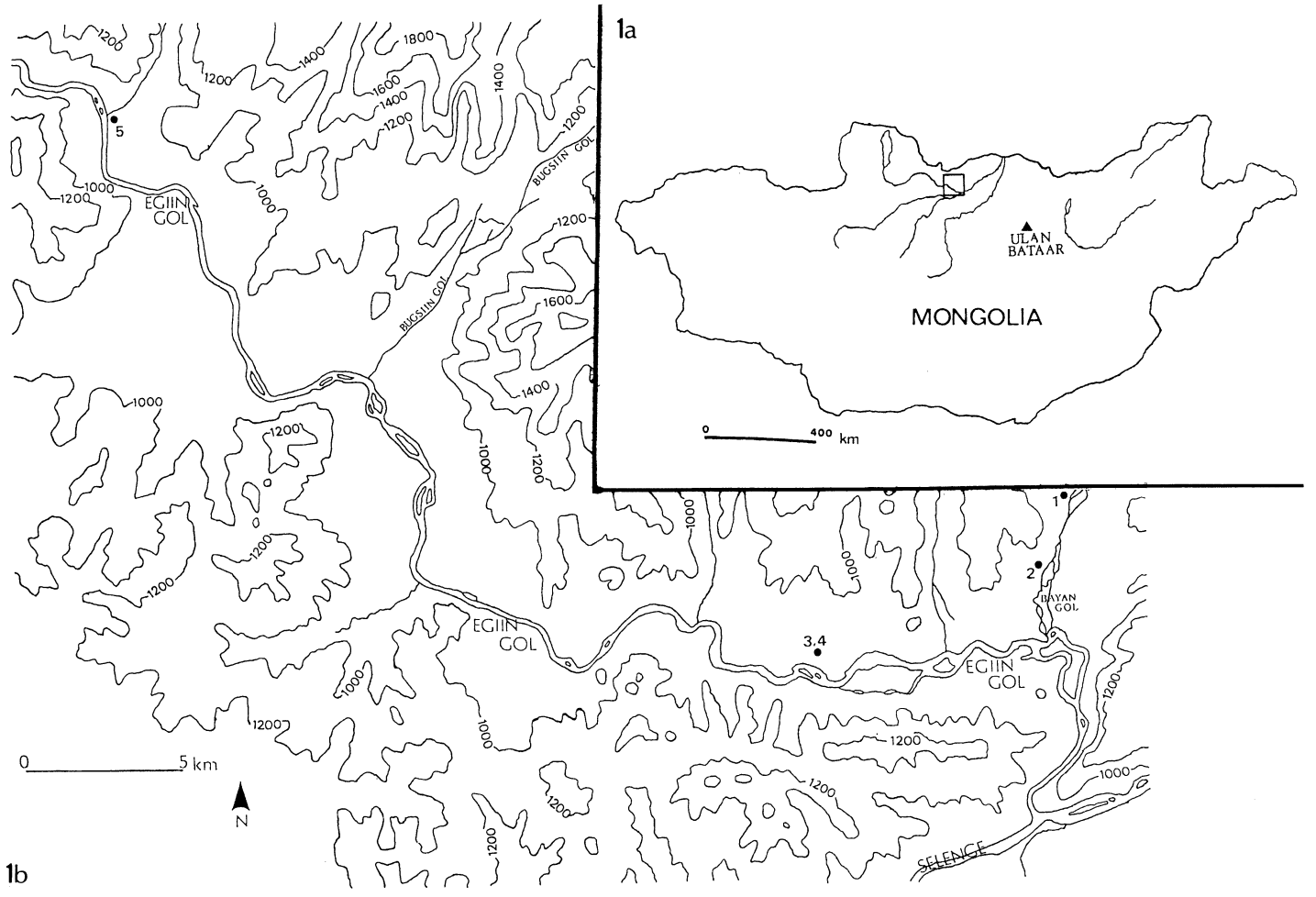

Figure 1 Map of the sites. Figure 1a is a map of Mongolia showing the general survey and excavation area. Figure 1b is a map of the Egiin Gol Valley. The key for the sites are: 1. Bayan Gol kheregsur sites; 2. Mukhtagiin Am cemetery; 3. Burkhan Tolgoi; 4. Borkhustyn Enger; and 5. Khailantiin Gol kheregsur field.

To correct for a possible "old wood" effect with the charcoal and wood samples, all calibrated ^{14}C determinations are offset by 50 ± 50 calendar years. Two considerations support using this correction instead of a larger one. First, large parts of the Eurasian steppe have been dominated by grasses with stands of birch (*Betula*), larch (*Larix*), pine (*Pinus*), and poplar (*Populus*) in the river valleys since 3500 BP (Khotinskii 1984; Sun and Chen 1991). Birches, larches, and poplars seldom live for more than 100 yr (Dallimore and Jackson 1948; Schweingruber 1993). Second, a review of the age of the wood utilized in the construction of the celebrated burial mounds of Pazyryk showed that the timbers ranged in age from 41 to 138 calendar years (Hall 1997).

DISCUSSION

Three of the ^{14}C samples are associated with *kheregsur* complexes. Kheregsurs are large stone mounds, usually surrounded by linear or circular features made of stone, that are scattered throughout the countryside in northern and western Mongolia. There is no consensus as to the date when kheregsurs were built and in use in Mongolia. Novgorodova (1989) and Okladnikov (1990) favored a date in the 2nd millennium BC, while others (Askarov et al. 1992; Erdélyi et al. 1967; Volkov 1995) have argued for a date in the 1st millennium BC. Published excavations of these structures suggest they were used as both tombs and ceremonial structures (Erdélyi 1967).

Excavations were conducted on stone features at the kheregsur sites of Bayan Gol and Khailantiin Gol. In both areas, not only are the khergsurs surrounded by stone fences, but numerous small circular and rectangular stone-built features are found near the monuments. The calibrated dates for the features associated with the kheregsurs at Bayan Gol and Khailantiin Gol are considerably younger than one would generally expect. The cattle remains recovered from Bayan Gol date to the time of the Turkic confederacy (ca. AD 550–740) or Uighir Empire (ca. AD 740–840) in Mongolia. One of the features from Khailantiin Gol dates from the Manchu period down to the present day, and the other feature is clearly modern. It is possible that these 3 dates could be discrepant; alternatively, it is also possible that the use of these sites has continued since their construction. There is no reason to suspect that the kheregsurs were used solely by a single cultural group or in a single time period.

Three burials and one feature at the "Xiong-nu cemetery" of Burkhan Tolgoi were excavated by the Mongolian-American Expedition in 1996. Over 100 stone-marked grave pits are present at the site; the cemetery is assigned to the historical Xiong-nu period, about 200 BC to AD 155 (Barfield 1989; Minyaev 1996; Yü 1990), due to the presence of bronze mirror fragments, lacquerware, and silk found in a few of the burials by previous expeditions to the valley. In addition, one ^{14}C determination from tomb 15 was found to date to 1845 ± 45 BP (Ly-6857) (Crubézy et al. 1996). It should be stressed, though, that nothing at the cemetery definitively links it to the ethnic Xiong-nu. Burkhan Tolgoi could well have been a cemetery used by the Ting-ling or other nomadic groups participating in the Xiong-nu confederacy (Barfield 1989; Mori 1985) or could date to before or after the time of the Xiong-nu confederacy.

The 5 ^{14}C determinations from Burkhan Tolgoi were calibrated with the constraints placed on them that they date between 200 BC and AD 155. The mathematical model and OxCal code for this is presented in the Appendix. Except for the ^{14}C determination from Tomb 44 (TX-9316), all the calibrated determinations support the hypothesis that the cemetery at Burkhan Tolgoi dates to the historically attested Xiong-nu confederacy. While based on only 4 dates (including Ly-6857), the summed probability distributions indicate that Burkhan Tolgoi was in use for most of the span of the historical Xiong-nu confederacy (Fig. 2). There is only a 0.1% probability that the ^{14}C determination from Tomb 44 dates between 200 BC and AD 155. Further research is needed to establish whether this

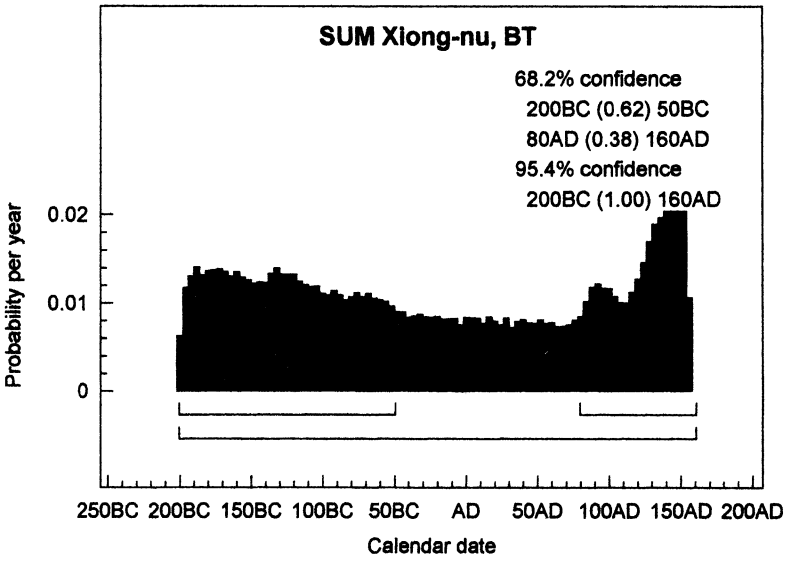

Figure 2 Summed probability distribution of the calibrated ^{14}C determinations for Burkhan Tolgoi. Only the dates satisfying the Bayesian model are used in this diagram. The calibrated dates cover the entire time span of the historical Xiong-nu confederacy.

determination is discrepant or whether the burial actually predates the Xiong-nu confederacy. It is hoped that the continuing French-Mongolian excavations at Burkhan Tolgoi will also produce more ^{14}C determinations.

Three burials believed to date from the Medieval period of Mongolia have also been excavated. Borkhustyn Enger was a single, small, low stone mound to the north of Burkhan Tolgoi. The shape was semicircular and considered to be typical of Mongol burials from the 12th through 14th centuries AD. The archaeology and ^{14}C determination are in good agreement with one another for this burial. Mukhtagiin Am in the Bayan Gol drainage contains over 30 burials of various shapes and sizes. Tomb 2 at Mukhtagiin Am dates to a 300-yr time span that saw the Khitans, Mongols, Tatars, and Turkic-speaking tribes vying for control of the Mongolian plateau (Barfield 1989; Okada 1985). Further comparative study needs to be done on the arrowheads and horse gear found in this burial for clues to the ethnic origin of the individual. Tomb 7 from Mukhtagiin Am dates from the later years of the Mongol Empire to the formation of the northern Yüan dynasty in Mongolia. The size and shape of this burial was typical for the Mongol Empire period.

CONCLUSION

While the ^{14}C determinations from Bayan Gol and Khailantiin Gol do not provide evidence for when the kheregsurs themselves were built, they do provide evidence for the continued use of these monuments. Like the megalithic monuments of the British Isles (Barrett 1994), the kheregsur complexes of Mongolia were probably built through time and used by successive generations.

The ^{14}C determinations from Burkhan Tolgoi point to the cemetery's use for nearly 2/3 of the historical Xiong-nu confederacy. The ^{14}C dates in combination with the pottery from these tombs can be used to construct a chronology for the different types of "Xiong-nu" pottery in northern Mongolia. Further research is required to determine if Tomb 44 actually predates the Xiong-nu confederacy.

At both the 1σ and 2σ confidence intervals, tomb 2 at Mukhtagiin Am dates to the time period when a variety of historically known groups were trying to gain control of the Mongolian plateau. Borkhustyn Enger dates to the Mongol Empire period, whereas tomb 7 at Mukhtagiin Am spans from the late Mongol Empire period through the northern Yüan dynasty.

The dates presented in this study are only a start toward developing an absolute chronology for northern Mongolia. More work needs to be done on dating the kheregsurs and tying material finds, such as pottery and arrowheads, to absolute dates. Once this is done, archaeologists, art historians, and historians can then begin to address the nature of cultural contact and interaction across the Eurasian steppe and northern China.

ACKNOWLEDGMENTS

Financial support for this project was provided by a Wenner-Gren International Collaborative Research Grant (grant number ICRG 20). Thanks are in order to the Ministry of Enlightenment of Mongolia and the Institute of History, Mongolian Academy of Sciences, for allowing the ^{14}C samples to be taken from Mongolia. Bill Chu, Shu Takahama, and Henry Wright provided useful comments while this article was being written; Sheelagh Frame provided identification of the animal bone sample; Yumiko Nakanishi provided help on translating the Japanese sources; and Heather Trigg provided identification of the wood samples. Time and financial support for Mark Hall during the writing of this article were provided by the Japanese Society for the Promotion of Science (JSPS) and the National Museum of Japanese History.

ARCHAEOLOGICAL SAMPLES

Egiin Gol Kheregsur Series

AA-24118. Bayan Gol, Kheregsur #2 **1330 ± 50**

$\delta^{13}C = -21.31‰$

The lower limbs and jaw of *Bos* were recovered from underneath a rectangular stone feature forming part of the enclosure surrounding khergsur #2 at Bayan Gol. The above determination was taken from an astragalus (ankle bone) found beneath the stone feature at a depth of 5–10 cm below datum. Calibrated date ranges at 1σ: AD 660–720 (0.69), AD 740–770 (0.31). Calibrated date range at 2σ: AD 630–820 (1.00).

Beta-114601. Khailantiin Gol, Feature 1 **100.6 ± 0.9 pMC**

$\delta^{13}C = -22.8‰$

This determination was obtained from charcoal found beneath a small, circular stone feature in the khergsur complex of Khailantiin Gol. The depth of the sample was 18 cm below datum. The excavation also yielded some corroded iron fragments. The date is modern.

Beta-114602. Khailantiin Gol, Feature 2 **240 ± 60**

$\delta^{13}C = -23.1‰$

This determination was obtained from charcoal discovered beneath a small, rectangular stone feature in the khergsur complex of Khailantiin Gol. The feature also yielded sherds of a coarse, dark-brown earthenware. The sample and artifacts were recovered at a depth of 15 cm below datum. Calibrated dates at 1σ: AD 1710–Present (1.00). Calibrated dates at 2σ: AD 1590–Present (1.00).

Burkhan Tolgoi Series

TX-9315. Burkhan Tolgoi, Tomb 43 **2140 ± 50**

$\delta^{13}C = -27.4‰$

Wood utilized in the construction of the coffin from Tomb 43. The tomb was badly robbed in antiquity; only a few incised pottery sherds and very fragmentary human bones were found in the coffin and stone chamber. The coffin was 2.60 m below datum. 160–10 BC (1.00) at 1σ, 200 BC–AD 50 (1.00) at 2σ.

TX-9316. Burkhan Tolgoi, Tomb 44 **2460 ± 60**

$\delta^{13}C = -24.8‰$

Tomb 44 was also badly robbed in antiquity. The remains of a bow, pottery, a horse, and an adult male were found scattered through the grave shaft and wooden coffin. The ^{14}C determination was obtained from wood utilized in the construction of the coffin. Calibrated date range at 1σ: 680–400 BC (1.00). Calibrated date range at 2σ: 760–310 BC (1.00).

TX-9317. Burkhan Tolgoi, Tomb 45 **2220 ± 130**

$\delta^{13}C = -25.1‰$

Feature 45 was originally thought to be a tomb. There was no evidence of disturbance, but the feature was found to contain only a horse skull and charcoal at a depth of 1.3 m. The ^{14}C determination was obtained from charcoal associated with the horse skull. Extended counting for a total of 45,500 min was performed on this sample due to its small size. 200–20 BC (1.00) at 1σ, 200 BC–AD 100 (1.00) at 2σ.

Beta-103071. Burkhan Tolgoi, Tomb 46 **1990 ± 60**

$\delta^{13}C = -27.4‰$

Wood utilized in the construction of the coffin from Tomb 46. The coffin was 1.5 m below datum. While robbed in antiquity, this female burial yielded a brooch, glass fragments, carved bone sticks (possibly hair pins or eating implements), and numerous iron fragments. Calibrated date range at 1σ: AD 10–150 (1.00). Calibrated date range at 2σ: 90 BC–AD 160 (1.00).

Comment: All but one (TX-9316) of the Burkhan Tolgoi series of ^{14}C determinations were calibrated assuming they date between 200 BC and AD 155. These constraints are reflected in the calibrated date ranges reported above. TX-9316 does not satisfy the Bayesian model and was calibrated as an individual date. It is hoped that dating the human remains and horse bones in Tomb 44 will clarify whether this tomb dates to the time of the Xiong-nu confederacy or earlier.

Medieval Series

Beta-114600. Borkhustyn Enger **860 ± 70**

$\delta^{13}C = -32.0‰$

Charcoal found at a depth of 25–30 cm below datum in the child's burial. There was no evidence of a coffin or wood chamber being utilized in the burial. Extended counting for 4000 min was done on the charcoal. Calibrated date range at 1σ: AD 1130–1330 (1.00). Calibrated date range at 2σ: AD 1050–1390 (1.00).

Beta-114603. Mukhtagiin Am, Tomb 2 **910 ± 60**

$\delta^{13}C = -25.2‰$

This ^{14}C determination was obtained on wood utilized in the construction of the coffin. The wood has been identified as some species of *Pinus*. The coffin was at a depth of 95 cm below datum. Arrowheads, a quiver, and horse gear were all recovered from the burial. Calibrated date range at 1σ: AD 1090–1280 (1.00). Calibrated date range at 2σ: AD 1020–1350 (1.00).

Beta-114604. Mukhtagiin Am, Tomb 7 **680 ± 80**

$\delta^{13}C = -24.4‰$

Wood forming the coffin. The wood, in a poorly preserved condition, has been identified as some species of *Larix*. The depth of the coffin was 79 cm below datum. AD 1310–1470 (1.00) at 1σ, AD 1230–1530 (1.00) at 2σ.

REFERENCES

Askarov A, Volkov V, Ser-Odjav N. 1992. Pastoral and nomadic tribes at the beginning of the first millennium B.C. In: Dani A, Masson V, editors. *History of civilizations of Central Asia.* Vol 1, *Dawn of civilization: earliest times to 700 B.C.* Paris: Unesco. p 459–472.

Barfield T. 1989. *The perilous frontier: nomadic empires and China.* Cambridge (MA): Basil Blackwell. 325 p.

Barrett J. 1994. *Fragments from antiquity: an archaeology of social life in Britain, 2900–1200 BC.* Oxford: Basil Blackwell. 190 p.

Bronk Ramsey C. 1995a. OxCal, version 2.18 [computer program]. http://units.ox.ac.uk/departments/rlaha/oxcal/oxcal_h.html.

Bronk Ramsey C. 1995b. Radiocarbon calibration and analysis of stratigraphy: the OxCal program. *Radiocarbon* 37(2):425–30.

Crubézy E, Martin H, Giscard P-H, Batsaikhan Z, Erdenebaatar D, Maureille B, Verdier J. 1996. Pratiques funéraires et sacrifices d'animaux en Mongolie à la période Proto-Historique. *Paléorient* 22:89–107.

Dallimore W, Jackson AB. 1948. *A handbook of coniferae including Ginkgoaceae.* London: Edward Arnold. 682 p.

Deetz J, Dethlefsen E. 1965. The Doppler effect and archaeology: a consideration of the spatial aspects of seriation. *Southwestern Journal of Anthropology* 21: 196–206.

Erdélyi I, Dorjsüren C, Navan D. 1967. Results of the Mongolian-Hungarian archaeological expeditions 1961–1964. *Acta Archaeologica Academiae Scientiarum Hungaricae* 19:335–70.

Hall M. 1997. Towards an absolute chronology for the iron age of inner Asia. *Antiquity* 71(274):863–74.

Khotinskii, N. 1984 Holocene vegetational history. In: Velichko A, editor. *Late Quaternary environments of the Soviet Union.* Minneapolis: University of Minnesota. p 179–200.

Martynov AI. 1991. *The ancient art of northern Asia.* Urbana: University of Illinois Press. 300 p.

Minyaev S. 1996. *Les Xiongnu.* Dossiers d'Archéologie 212:74–83.

Mori M. 1985. Yuboku kokkano seiritsu to hatten [Formation and development of nomadic states]. In: Mori M, Kanda N, editors. *Kita Ajia Shi* [North Asian history]. 2nd ed. Tokyo: Yamakawa Shuppansha. p 41–80.

Novgorodova E. 1989. *Drevniaia Mongoliia: nekotorye problemy khronologii i etnokulturnoi istorii* [Ancient Mongolia: some problems of chronology and ethnocultural history]. Moscow: Nauka. 381 p.

Okada H. 1985. Mongoru no toitsu [The unification of Mongolia]. In: Mori M, Kanda N, editors. *Kita Ajia Shi* [North Asian history]. 2nd ed. Tokyo: Yamakawa Shuppansha. p 135–68.

Okladnikov A. 1990. Inner Asia at the dawn of history. In: Sinor D, editor. *The Cambridge history of early inner Asia.* Cambridge: Cambridge University Press. p 41–96.

Schweingruber F. 1993. *Trees and wood in dendrochronology.* Berlin: Springer-Verlag. 402 p.

Stuiver M, Long A, Kra RS, editors. 1993. Calibration 1993. *Radiocarbon* 35(1):1–244.

Sun X, Chen Y. 1991. Palynological records of the last 11,000 years in China. *Quaternary Science Reviews* 10:537–544.

Volkov V. 1995. Early nomads of Mongolia. In: Davis-Kimball J, Bashilov V, Yablonsky L, editors. *Nomads of the Eurasian Steppes in the early Iron Age.* Berkeley: Zinat Press. p 319–34.

Yü Y. 1990. The Hsiung-nu. In: Sinor D, editor. *The Cambridge history of early inner Asia.* Cambridge: Cambridge University Press. p 118–50.

APPENDIX: MATHEMATICAL MODEL AND OXCAL CODE

Letting Θ_x be the probability distribution for the calendar dates of the calibrated radiocarbon determination of burial x, and Δ_x the calendar years to offset Θ_x, then Θ_x' is defined as

$$\Theta_x' = \Theta_x + \Delta_x \ . \quad (1)$$

For the overall sequence of ^{14}C determinations from Burkhan Tolgoi, the Bayesian model is

$$200 \text{ BC} > \Theta_{\text{LY-6857}} , \Theta'_{\text{TX-9315}} , \Theta'_{\text{TX-9316}} , \Theta'_{\text{TX-9317}} , \Theta'_{\text{Beta-103071}} > \text{AD } 155 \ . \quad (2)$$

No archaeological, historical, or stratigraphical evidence exists for the relationship between the tombs. ^{14}C determination TX-9316 was found not to satisfy the above constraints. It was calibrated with no constraints in place.

The OxCal code for the calibration of the Burkhan Tolgoi sequence is:

```
SEQ "Xiong-nu"
{
CURVE "C:\OXCAL\CAL20.DTA";
TPQ
{
CAL -200;
};
PHASE "BT"
{
DATE "Ly" 1845 45;
DATE "Tx-9317" 2220 130; OFFSET 50 50;
DATE "Tx-9315" 2140 50; OFFSET 50 50;
DATE "Tx-9316" 2460 60? OFFSET 50 50;
DATE "Beta 103971" 1990 60; OFFSET 50 50;
};
TAQ
{
CAL 150;
};
};
```

RADIOCARBON, Vol 41, Nr 1, 1999, p 111–115

BOOK REVIEW

Claudio Tuniz, John R Bird, David Fink, and Gregory F Herzog. *Accelerator Mass Spectrometry: Ultrasensitive Analysis for Global Science*. Boca Raton, CRC Press, 1998: 371 p. ISBN 0-8493-4538-3. List price $89.95 US (hardcover).

Reviewed by: John S Vogel, Center for Accelerator Mass Spectrometry, Lawrence Livermore National Laboratory, Livermore, California, USA

Longtime readers of this journal know that Accelerator Mass Spectrometry (AMS) has transformed from an exciting curiosity 20 years ago to a current mainstay of applied isotope research, especially of radioisotope geochronology. AMS made possible the quantification of long-lived radioisotopes that could not previously be measured with routine practicality. AMS also radically affected the purview and practice of radiocarbon dating and tracing, the target of perhaps 80% of all AMS measurements. AMS particularly enriches research that is carried out by collaboration among AMS "physicists", experienced practitioners of conventional counting, and isotope geo- or bioscientists.

I attended my first Radiocarbon Conference in Seattle (1982) shortly after abandoning my "planned" career in high-energy cosmic ray astrophysics. There were 20 AMS scientists at the meeting (13% of the 154 attendees), most of us representing some species of experimental nuclear physicist. We were surrounded by the greater number of earth and archaeological scientists who mesmerized us with discussions of lab multipliers, calibration statistics, and box-models. AMS methods then under development were inserted in the last section of the proceedings, and only one research paper in the proceedings presented AMS data from a natural matrix (measuring ^{10}Be, not ^{14}C!). At the 1997 Radiocarbon Conference in Groningen, AMS laboratories sent 20% of the 244 attendees, and AMS was fully integrated into all sessions, with approximately half the papers reporting results based on AMS measurements. Indeed, many of the participants used AMS data exclusively, or as often as expenses permitted. The increased overall attendance at Groningen was due in part to the successful efforts of the organizers to especially attract scientists from Eastern Europe. However, many of the participants, particularly new graduates and young scientists, were drawn to the field by the exciting opportunities that AMS brought to the study of ^{14}C in natural systems.

By the time of the Seattle conference, AMS scientists had also convened informally to discuss technological development (Rochester in 1978 and Argonne in 1981). These meetings evolved into a separate AMS conference series in counter-tempo with the Radiocarbon Conferences. The published proceedings of these Radiocarbon and AMS Conferences have served as the primary archived resource about AMS for the scientific and education communities during the past 2 decades. Unfortunately, such proceedings are not readily available to a large fraction of potentially interested readers, since they appear under the auspices of relatively specialized journals. AMS scientists still spend a significant fraction of our time educating new colleagues about the subjects discussed in these volumes. We often wish for an accessible text that could be cited as an introductory substitute for our personal instruction and our collated collections of *Radiocarbon* and "NIM" (*Nuclear Instruments and Methods in Physics Research*) articles. *Accelerator Mass Spectrometry: Ultrasensitive Analysis for Global Science* by Tuniz et al. has now summarized AMS technology and applications.

It is fitting that a phrase such as "global science" appears in the book title, since AMS studies now advance fields of research as varied as volcanic reemergence of subducted sediments, ocean water mass circulations, geomorphology on many scales, human history and archaeology, chemical and biological tracing, climatic effects of mass and energy reservoirs, nuclear interactions, and atmo-

spheric gas transport (to name just a "few" subjects). Indeed, "global" is insufficient to include the effects due to solar system debris (discoid science?) or galactic cosmic rays (spiral science?), but these effects are pursued using "globally" available reservoirs such as meteorites or ice cores. It is this global reach of AMS applications that presents a formidable barrier to summarizing AMS science in book form. The authors are to be congratulated for their courage.

All the authors have experience in the gritty world of natural sample collection and chemical purification. They also know the torment of bullying the first generation of AMS measurements from accelerator systems that had been designed as sledgehammers for nuclear physics collision research rather than as scalpels for exquisite isotope ratio mass spectrometry. They have remained in the field and experienced the later generation of versatile, high-throughput spectrometers. The authors are familiar with all areas of AMS technology and application but, perforce, maintain particular interests in the research that first led them to AMS. For all 4, this includes the very long-lived isotopes of light (<50 amu) elements in geological matrices and their production by high-energy nuclear interactions.

A glance at the table of contents reveals the inclusion of all topics and subtopics that one could hope for in a general book about AMS. A closer look reveals, however, that many topics and most subtopics are covered in less than a page. Anthropogenic isotope production, including the immensely useful ^{14}C bomb pulse, is covered in one page, while extraterrestrial production merits 18 pages. Oceanography is summarized in 5 pages, but rare nuclear physics interactions are accorded 15 pages. Thus, this is a book of personal science as well as global science. The reader must use this text as a jumping-off point into further literature to find the broader coverage. Readers will find mention of fields already subjected to AMS studies by browsing this book, but they may not find the depth of discussion needed to determine the value of AMS for their particular interests. The authors wisely provide guidance to the reader in the front of the book with a "User's Guide" that diagrams their suggested paths through the material for maximal use of what they offer.

One must first understand what AMS is and how it has been used in order to determine the likelihood of applying it effectively to a research problem. The book's introduction follows this obvious path. There are perhaps 3 starting points for an explanation of AMS techniques and applications: *isotope ratio mass spectrometry (IRMS)*, of which AMS is a type that is done with highly energetic ions; *quantification of radioactive isotopes*, for which AMS is primarily used by the largest number of researchers needing detection efficiency greater than decay counting; and *nuclear physics,* from which discipline the initial technologies and practitioners arose. These authors (prudently, I believe) choose a modified IRMS introduction which reinforces the concept that AMS does not depend on decay properties. The IRMS approach also emphasizes a chief distinction between AMS and decay counting—the incorporation of the elemental abundance directly in the measurement as the denominator of an isotope ratio. This is covered quickly in the Overview of Chapter 1, so quickly that neophytes might not notice the important message. A plot is used to convey the AMS sensitivity advantage over counting radioisotopes, but the simple equation relating activity to the number of isotopes present might have better brought out the inefficiency of decay counting and helped those familiar with counting to see the place of AMS in terms of isotope lifetimes. The Overview also provides a quick introduction to AMS analyses in the scientific fields covered in more detail later. The valuable properties of AMS are further explained in terms of precision, background, contamination, and isobaric interferences at the end of the second chapter. These are "hidden" behind a less interesting, but extensive, listing of the isotopes that have been investigated using AMS, a list that seems to intrude at this introductory position in the text.

The instrumentation of AMS is described in more detail in Chapter 3, but here the detail and broad survey of assorted approaches again buries the message of what exactly makes AMS inherently sensitive. Spectrometer components of AMS are presented as sequential elements, without stressing the aspects that make AMS more sensitive than conventional IRMS. Instead, negative ions are seen to limit the elements amenable to AMS, and electron stripping is described primarily from the physicist's view as a charge-changing approach to higher energies. This chapter could have used a few more diagrams explaining ion behavior for the non-expert whose curiosity desired more than the Overview in Chapter 1 but who is not up to the equations that are so familiar to the physicist. The final introductory chapter, Chapter 4, covers the topic that most needs to be understood by the field scientist as well as the analytical scientist: sample specification and preparation. Again, the coverage is broad but shallow. Section headings at least alert the reader to the types of samples that have been investigated for the various AMS isotopes, and details are available from the copious references, including a serendipitous table that covers most applications of ^{14}C. Comparatively detailed tables of procedures are provided for a number of isotopes extracted from rock matrices. This 4-chapter introduction is gentle enough to lead the dedicated reader into the rest of the book, but does not present a coherent path that is independent of external guidance. Although the authors plainly suggest in their user's guide that "readers interested chiefly in applications should proceed directly from Chapter 1 (Overview) to Chapters 9 to 14 (Applications)", I think that some judicious reading of the other introductory chapters will be needed to make this leap.

This leap over 4 chapters will definitely be the desirable path for most readers, because Chapters 5 through 8 present a dauntingly detailed discussion of the physics of *in situ* radioisotope production and distribution. Having started scientific life a cosmic ray enthusiast, I appreciate the collection of this material into 4 organized chapters, clearly the heart of the book in the authors' view. Exposure dating using *in situ* production of isotopes in rocks is a field that was nearly (totally?) impossible without AMS. This collection of the physics needed to interpret this revitalized research is now usefully in one place for the first time. The section is less essential to the "isotope tracers" in oceanography, atmospherics, climatology, carbon cycling, biology, and organic chronography. However, even the utilitarian tracers amongst us should know the sources of our isotopes, and a discussion of natural and anthropogenic environmental production and distribution (including some simplistic diagrams) could have been isolated from the copious rocky material for their benefit. Certainly sections 7.1 and 7.4 should be read by many readers on their way from the introductory chapters to Chapters 10 (Environmental Applications) and 12 (Archaeological Applications). A different arrangement of the book might have brought some application chapters forward, including some geoscience tracing, and delayed the production and distribution chapters for presentation with Chapter 9 (Extraterrestrial Applications) and some topics in Chapter 11 (Geoscience Applications). Had this been done, some of the repetition in Chapters 9 and 11 of material in Chapters 5–8 would have been more obvious (or eliminated), and most readers could proceed more easily from the introduction to non–*in situ* Applications.

Applications like archaeology, environmental tracing, biology, and material science have become some of the greatest pleasures to AMS physicists, if my understanding of my colleagues has been accurate. When many of us started down a road to experimental nuclear physics and related subjects, we were fulfilling a curiosity about fundamental properties of nature, probably with little thought to later employability. Little did we know that decades later we would be involved in studies with art curators, entomologists, soil chemists, climatologists, lunar prospectors, ocean biologists, and so on. Any description of the applications of AMS is always a pleasant read, and Chapters 9 through 14 of this text are no different. No matter what the research, the sensitivity of AMS provokes amazement

that "that" can actually be quantified and understood—choose your own "that". I would have failed the Ph.D. qualifying exam if I had been asked how to determine the length of time that a meteorite had spent in space since it was blasted from a larger body and *then* to determine the length of time that the same object lay beneath the ice fields of Antarctica. Physicists can now even address biological conferences and actually command respect for data showing the cycling of 35 μg of folic acid in a human over hundreds of days. AMS is still a quiet revolution happening in many fields, and these chapters provide just a taste of the possibilities without exhausting the potentials. We all have our favorite subjects and could quibble with the authors over their choice of topics, but they capture, with varying success, the excitement of AMS in globally diverse research. The least satisfactory description is that of life science applications. I hesitate to criticize it, however, since the authors could complain in turn that those of us who are taking AMS into biology have not published as much as we might have. This subject is farthest from the authors' interests and experiences. Life scientists will not gain enough from this text to begin their own use of AMS. A set of colored plates between Chapters 10 and 11 provides visual hints of the scientific fun to be had in applying AMS around the globe, despite the serious look of Dr. Tuniz in one photo that is also on the cover (shown holding a 2000-yr-old Madagascan elephant bird egg dated at ANSTO).

The 4 appendixes provide 2 lists and 2 text sections. Appendix 1 is a very handy form of the "Middleton Bible", which simply is the starting point for all considerations of producing negative ions required for AMS. Appendix 3 attempts to list all the AMS facilities that had operated at the time of writing, including the sadly high fraction that produced only a demonstration of some AMS capability and those that have been discontinued at nuclear research centers. Appendices 2 and 4 provide the equations and explanations of 2 concepts that are so central to the use of AMS that their appearance only as appendices mystifies me. The interaction of energetic ions with matter (Appendix 2) forms the basis of both molecular destruction through electron removal and particle identification through energy loss that are fundamental to the advance of AMS over low-energy MS and decay counting. All students of AMS need *some* understanding of this material, while fewer users need understand the detailed production of isotopes that is accorded lengthy explication in the main text. The situation appears even more extreme in the case of Appendix 4, "Data Reduction and Interpretation". One pedagogical approach to AMS would set forth the fundamental properties of decay counting (a subject not found in a single coherent form in this book) with a following contrast to the information derived from an isotope ratio or concentration. Some of this contrast is only suggested in this appendix and sparsely in other parts of the text. Many people come to AMS with prior experience in decay counting, and their success with AMS seems proportional to their ability to distinguish the reduction and interpretation of isotope ratios from counting data. This contrast affects the designs of all experimental use of AMS, whether the samples contain "natural" radioisotopes or tracer levels of applied isotopes. The sketchy view in this appendix mentions most of the relevant factors: fractionation, production, contamination, efficiency, comparison to standards, calibration, reservoir effects. Missing is a discussion of isotope dilution, equivalent to the carrier addition that is mentioned in passing in the various recipes for sample preparation. The authors hint at the importance of these appendices by including them in a prominent place in "A User's Guide" at the start of the book. At least 2 of them were worthy of a chapter among the introductory material.

Following the appendices is a glossary of about a hundred words or phrases that the student will find useful, as may the curious specialist who uses the text to wander into a chapter far from his or her expertise. The definitions seem superficial, however, and define either words that are fundamental to isotopic studies or concepts that are so specialized as to appear only once in the whole text. In either case, they could have been well defined in the relevant introductory passages or at the time of

their single use, with lookup access through the index. The index itself is broad but lacking some discipline, with even cursory uses of a phrase sometimes indexed when they offer little additional information on the indexed topic.

The 1200 references are drawn heavily (about 50%) from the 2 journals that have been the mainstay of AMS publications, *Radiocarbon* and *Nuclear Instruments and Methods in Physics Research.* References are predominantly (about 2/3) to applications of AMS. The references thus form a strong base for more detailed reading about the use of AMS in diverse fields. They include meeting abstracts, which are less useful for archival recovery. The references, as well as the text itself, seem to be complete up to about 1994, or just after the Sixth International AMS Conference, whose proceedings were coedited by 2 of the book's authors. References beyond that date are decidedly more spotty, but journal databases available through the Internet can be used by the interested reader to fill in the recent work performed by authors referenced here. Confirming the proper link from a citation to a listed reference is not an enjoyable task in authoring papers, let alone in a book of this breadth. Unfortunately, it appears that there are at least a few misconnections, or that the authors were specifically loose with publications of this reviewer. The most egregious one noticed, under Figure 14.2, mistakenly credits the Zurich laboratory with biochemical kinetic studies at least 8 years before we obtained the data shown in the figure.

This volume will be comfortable territory for the physicist versed in nuclear or particle science. It will not be as readily absorbed by applied scientists or students from distant fields seeking to understand the capabilities, processes and limitations of AMS in their areas of research. While trying to capture the "global" impact of the AMS technique, the authors were tempted by too broad an approach. On the whole, the book fails to impart a truly global view of the moving body of AMS work. Some attention to a grander synthesis of isotope science and the underlying conceptual foundations of AMS would have more lasting value. This text is a good AMS reference that allows the reader to avoid many trips to a library in search of *Radiocarbon* or *NIM*, but it is an insufficient guide to the growing power of AMS in some fields. A knowledgeable instructor could construct a graduate geophysics course around this text. As the only purposely composed book (excluding proceedings volumes) about AMS, it is a useful reference for the AMS student, and partially serves the serious scientist approaching AMS for isotope quantification.

Work on this review was performed under the auspices of the U.S. Department of Energy at Lawrence Livermore National Laboratory under contract W-7405-ENG-48.

RADIOCARBON UPDATES

Obituary

As many of our readers know, Hans Oeschger of the University of Bern died on 25 December 1998. A former Associate Editor of *RADIOCARBON,* Professor Oeschger was a pioneer in radiocarbon measuring technology and one of the world's foremost researchers in climate studies. We have scheduled for our next issue an obituary and memorial with an emphasis on Professor Oeschger's contributions to radiocarbon work, written by his Bern colleagues. In the meantime, we join with the scientific community in expressing our sadness at his passing and honoring his contributions to our field.

Awards

NERC Grant Award to Dr Gerry McCormac, The Queen's University of Belfast: "Inter-Hemispheric C-14 Offsets: Temporal Variations"

A previous study funded by the Natural Environment Research Council (NERC ref: GR9/02597 to Dr Gerry McCormac) of the United Kingdom and the New Zealand Foundation for Research, Science and Technology (ref: UOW-508 to Drs Alan Hogg and Tom Higham) to investigate the hemispheric offset in ^{14}C using tree-ring dated wood from the British Isles and New Zealand demonstrated that a hemispheric offset exists and that there are temporal variations in its magnitude. The initial study funded by NERC covered the 200-yr period AD 1720 to AD 1940 and used paired samples of oak and cedar from the British Isles and New Zealand, respectively.

Recently the NERC have awarded a grant (GR3/11941) for £123,328 to the group at Queen's University, Belfast, led by Dr Gerry McCormac to extend the period of measurements back to AD 1000. These measurements and measurements made by the group from Waikato University will create a Southern Hemisphere calibration curve that is linked to the Northern Hemisphere dataset and will determine the extent to which hemispheric offsets alter with time.

Change of Address

Paula Reimer has left the University of Washington in Seattle to take up a postdoctoral fellowship in the Belfast Radiocarbon Laboratory where she will be working with Dr Gerry McCormac on the abovementioned interhemispheric ^{14}C offsets and reservoir corrections. She is also involved in a stable isotope project on sediment cores from Lough Neagh, Northern Ireland. The radiocarbon calibration program CALIB will continue to be supported and is available from the University of Washington webpage <URL:http://depts.washington.edu/qil>.

New address:

Radiocarbon Lab
Dept. of Archaeology & Palaeoecology
Queen's University of Belfast
Belfast BT7 1NN, Northern Ireland
Phone: +44 1232 273980
Fax: +44 1232 315779
Email: p.j.reimer@qub.ac.uk

New Laboratory Listing

We recently received notice of a second radiocarbon laboratory at the National Centre for Scientific Research "Demokritos" near Athens, Greece. It has been performing dating using liquid scintillation counting since 1994. The new laboratory listing is:

LIH Dr. Nicolaos Zouridakis
Laboratory of Isotope Hydrology
Institute of Physical Chemistry
National Centre for Scientific Research "Demokritos"
153 10 Aghia Paraskevi Attikis
POB 60228
Greece
Tel: +30 1 6503969; Fax: +30 1 6511766

Associate Editor Retirement

As part of his (very) gradual transition to retirement from academic duties, Doug Harkness of the NERC Radiocarbon Laboratory in East Kilbride is stepping down from his duties as an Associate Editor of *RADIOCARBON*. During his period of service he co-edited both the Proceedings of the 15th International Radiocarbon Conference and our special-topic issue on ^{14}C and Soil Dynamics. We thank Doug for his assistance and good sense he has provided us over the past few years.

Jerusalem 2000 ירושלים

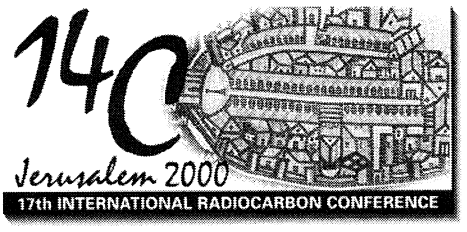

17th International Radiocarbon Conference

It is our great pleasure to invite you to participate in the 17th International Radiocarbon Conference, scheduled for June 18–23, 2000, in Israel.

The Conference will be held at a beautiful location, in the rural setting of Kibbutz Ma'ale Hachamisha in the Judean Hills, just west of Jerusalem. The Kibbutz offers an attractive self-contained arrangement of excellent accommodation and conference facilities, which will enable a high degree of interaction between conference participants. The City of Jerusalem with its unique history and tourist attractions is a short drive away and is easily reached by bus or taxi.

The first ^{14}C Conference at the dawn of a new millennium will undoubtedly include exciting new scientific developments. Keeping the tradition of past Radiocarbon conferences, the scientific program will include a wide variety of topics. Sessions will be devoted to:

- Archaeology – with a special session on ^{14}C data of historical periods in the Near East
- Calibration of the ^{14}C time scale
- Sample treatment and measurement techniques
- Geophysics and Geochemistry of ^{14}C
- Cosmogenic radionuclides
- Environment past and present
- Global change
- Glaciology
- Hydrology
- Oceanography
- Geology
- Soils

Participants are welcome to indicate their preference for either oral or poster presentation of their papers. However, the final decision regarding form of presentation will be made by the Organizing Committee. Detailed information will be included in the Second Announcement.

The social program of the Conference will include an afternoon walking tour in the Old City of Jerusalem and a one-day tour in the unique Dead Sea area (lowest point on the earth's surface). A floating swim in the Dead Sea – which is seven times saltier than the ocean – is indeed a unique fun experience.

Sincerely, The Organizing Committee:

Israel Carmi, Chairperson, The Weizmann Institute of Science
Elisabetta Boaretto, Secretary, The Weizmann Institute of Science
Hendrik J. Bruins, Ben Gurion University of the Negev
Michael Paul, Hebrew University of Jerusalem
Dror Segal, Hebrew Antiquities Authority
Yoseph Yechieli, Geological Survey of Israel

For further information, please see the Conference website:

http://www.radiocarbon.co.il/

Jerusalem 2000 ירושלים

RADIOCARBON Back Issues
Price Reduction—Save up to 87%

Selected copies just $5 each. Conference proceedings $10.

YEAR	VOLUME	Write in the number of copies desired for each issue					
		NR 1	NR 2	NR 2A	NR 2B	NR 3	NR 4
1980	22		*			*	
1981	23						
1982	24						
1983	25		*				
1984	26						
1985	27						
1986	28						
1987	29						
1988	30						
1989	31					*	
1990	32						
1991	33						
1992	34						

Calculate Payment

Regular issues:

_____ copies × $5 ea. = $_____

*Conference Proceedings issues:

_____ copies × $10 ea. = $_____

Subtotal: $_____

Shipping via surface mail:
(Contact us for other shipping methods)

Add $2 ea. book for US
Add $3 ea. book outside US

_____copies × $____ea. = $_____

Shipping total: $_____

Total due: $_____

Payment & Shipping Address

❑ MasterCard ❑ Visa
❑ Check enclosed ❑ Please bill me

Name:

Address:

Fax: E-mail:

For Credit-Card Orders

Card number: Expiration date:

Signature: Phone:

For online Contents see: `http://www.radiocarbon.org/Pubs/contents.html`

Prices good while supplies last. Mail or fax this form to:

RADIOCARBON, 4717 East Fort Lowell Road, Room 104, Tucson, Arizona 85712-1201 USA
Phone: +1 520 881-0857; Fax: +1 520 881-0554; orders@radiocarbon.org

RADIOCARBON

An International Journal of Cosmogenic Isotope Research

The University of Arizona
Department of Geosciences
4717 E. Ft. Lowell Rd., Rm. 104
Tucson, AZ 85712-1201 USA

Phone +1 520 881-0857
Fax: +1 520 881-0554

E-mail: orders@radiocarbon.org
http://www.radiocarbon.org/

1999 PRICE LIST

Proceedings of the 16th International Radiocarbon Conference (Vol. 40, Nos. 1 and 2, 1998)	$70.00*
INTCAL98 (1998 Calibration issue; Vol. 40, No. 3, 1998)	40.00
Proceedings of the 15th International Radiocarbon Conference (Vol. 37, No. 2, 1995)	50.00
Liquid Scintillation Spectrometry 1994 (ISBN: 0-9638314-3-7; 1996)	20.00
Liquid Scintillation Spectrometry 1992 (ISBN: 0-9638314-0-2; 1993) (ISBN: 0-9638314-0-2; 1993)	10.00
Special offer—**LSC 92** and **LSC 94** package—save $5.00	25.00
Late Quaternary Chronology and Paleoclimates of the Eastern Mediterranean (ISBN: 0-9638314-1-0; 1994)	30.00
Tree Rings, Environment and Humanity (ISBN 0-9638314-2-9; 1996) (Proceedings of the International Tree-Ring Conference, Tucson, Arizona, 1994)	40.00

SUBSCRIPTION RATES VOLUME 41, NOS. 1–3, 1999	
Institution	**120.00**
Individual	**65.00**
Lifetime Subscription—Institutional	2000.00
Lifetime Subscription—Individual	700.00

BACK ISSUES (except conference proceedings and special issues)	Single issue 40.00
VOLUMES 1–9 each volume	40.00
VOLUMES 10–21 each volume	65.00
VOLUMES 22–38 each volume	100.00
Radiocarbon Conference Proceedings	50.00
SPECIAL FULL-SET OFFER—Volumes 1–40 (1959–1998)	800.00

Big savings. Includes 11 out-of-print issues. Take $50.00 off for each additional set.

POSTAGE AND HANDLING CHART

	U.S.	Foreign
Subscription	--	$10.00
Book or Proceedings	$2.75	$5.00
Single back issue	$1.25	$2.00
Full set	$35.00	$75.00

Postage rates are for surface mail. Please contact us for airmail or express delivery rates.

Orders must be prepaid. We accept payments by Visa and MasterCard, or by check or money order payable in $US to *Radiocarbon*.

*Postage will be added; see above chart. Subscription rates and book prices are subject to change.

Radiocarbon dating Services

The test of time

At the Rafter Radiocarbon Laboratory we have been successfully meeting the test of time for more than 45 years.

Athol Rafter established the laboratory in 1952. Today, using Accelerator Mass Spectrometry, we carry on the tradition of excellence that Athol Rafter began.

At Rafter we understand what our clients expect – accurate dating, at competitive rates and superior turnaround times and service.

Recent work undertaken by our team of multi-disciplinary scientists includes:

- improving methods for contaminant removal in textile dating
- refining paleodietary studies
- improving techniques for pollen dating
- overcoming marine shell dating problems.

The Rafter Radiocarbon Laboratory has an international reputation for accurately dating a wide range of organic materials, sediments, textiles, bone, ivory, paper, wood, parchment, charcoal, shell, foraminifera and peat.

We also offer a wide range of archaeometric services that include stable isotope measurements ($\partial^{13}C$, $\partial^{15}N$, $\partial^{18}O$), amino acid profiles, PIXE/PIGME, X-ray diffraction, petrology and palynology.

For accurate dating and analysis results that will stand the test of time, talk with Dr Rodger Sparks at the Rafter Radiocarbon Laboratory about your next project.

RAFTER

RADIOCARBON LABORATORY

Institute of Geological & Nuclear Sciences Limited
PO Box 31 312, Lower Hutt, New Zealand
Telephone: 64 4 570 4671, Facsimile: 64 4 570 4657
Email: r.sparks@gns.cri.nz
http://www.gns.cri.nz/atom/rafter/rafter.htm

Institute of
GEOLOGICAL
& NUCLEAR
SCIENCES
Limited

IGN 7484